VTT PUBLICATIONS 775

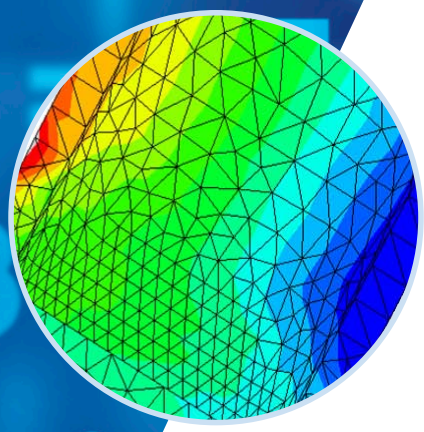

Otso Cronvall

Structural lifetime, reliability and risk analysis approaches for power plant components and systems

VTT PUBLICATIONS 775

Structural lifetime, reliability and risk analysis approaches for power plant components and systems

Otso Cronvall

ISBN 978-951-38-7760-6 (soft back ed.)
ISSN 1235-0621 (soft back ed.)

ISBN 978-951-38-7761-3 (URL: http://www.vtt.fi/publications/index.jsp)
ISSN 1455-0849 (URL: http://www.vtt.fi/publications/index.jsp)

JULKAISIJA – UTGIVARE – PUBLISHER

VTT, Vuorimiehentie 5, PL 1000, 02044 VTT
puh. vaihde 020 722 111, faksi 020 722 4374

VTT, Bergsmansvägen 5, PB 1000, 02044 VTT
tel. växel 020 722 111, fax 020 722 4374

VTT Technical Research Centre of Finland, Vuorimiehentie 5, P.O. Box 1000, FI-02044 VTT, Finland
phone internat. +358 20 722 111, fax + 358 20 722 4374

Technical editing Marika Leppilahti

Kopijyvä Oy, Kuopio 2011

Otso Cronvall. Structural lifetime, reliability and risk analysis approaches for power plant components and systems [Rakenteellisen eliniän, varmuuden ja riskien analysoimisen lähestymistapoja voimalaitosten komponenteille ja järjestelmille]. Espoo 2011. VTT Publications 775. 264 p.

Keywords structural mechanics, fracture mechanics, risk analysis, reliability, PFM, RI-ISI

Abstract

Lifetime, reliability and risk analysis methods and applications for structural systems and components of power plants are discussed in this thesis. These analyses involve many fields of science, such as structural mechanics, fracture mechanics, probability mathematics, material science and fluid mechanics.

An overview of power plant environments and a description of the various degradation mechanisms damaging the power plant systems and components are presented first. This is followed with a description of deterministic structural analysis methods, covering e.g. structural mechanics and fracture mechanics based analysis methods as well as the disadvantages of the deterministic analysis approach. Often, physical probabilistic methods are based on deterministic analysis methods with the modification that one or more of the model parameters are considered as probabilistically distributed. Several probabilistic analysis procedures are presented, e.g. Monte Carlo Simulation (MCS) and importance sampling. Description of probabilistic analysis methods covers both physical and statistical approaches. When the system/component failure probabilities are combined with knowledge of failure consequences, it is possible to assess system/component risks. Several risk analysis methods are presented as well as some limitations and shortcomings concerning to them.

Modelling methods for various degradation (or ageing) mechanisms are presented. These methods are needed in the lifetime analyses of structural systems and components of power plants. In general, the lifetime analyses in question necessitate a thorough knowledge of structural properties, loads, the relevant degradation mechanisms and prevailing environmental conditions. The nature of degradation models of structural systems/components can be deterministic, probabilistic or a combination of these two types. Degradation models of all these kinds are presented here. Some important risk analysis applications are described. These include probabilistic risk/safety assessment (PRA/PSA) and risk informed in-service inspections (RI-ISI).

In practise, lifetime and risk analyses are usually performed with a suitable analysis tool, i.e. with analysis software. A selection of probabilistic system/component degradation and risk analysis software tools is presented in the latter part of this thesis. Computational application of probabilistic failure and lifetime analyses to a representative set of NPP piping components with probabilistic codes VTTBESIT and PIFRAP are presented after that.

The thesis ends with a summary and suggestions for future research.

Otso Cronvall. Structural lifetime, reliability and risk analysis approaches for power plant components and systems [Rakenteellisen eliniän, varmuuden ja riskien analysoimisen lähestymistapoja voimalaitosten komponenteille ja järjestelmille]. Espoo 2011. VTT Publications 775. 264 s.

Avainsanat structural mechanics, fracture mechanics, risk analysis, reliability, PFM, RI-ISI

Tiivistelmä

Tämän lisensiaattityön aiheina ovat voimalaitosten rakennejärjestelmien ja -komponenttien käyttöiän, luotettavuuden ja riskitarkastelujen analyysimenetelmät ja sovellukset. Näihin analyysimenetelmiin liittyy usea tieteen ala, kuten lujuusoppi, murtumismekaniikka, todennäköisyysmatematiikka, materiaalitiede ja virtausmekaniikka.

Ensin esitetään yleiskatsaus voimalaitosympäristöistä sekä kuvaukset erilaisista voimalaitosten rakennejärjestelmiä ja -komponentteja koskevista vaurioitumismekanismeista. Sitten käsitellään deterministiset rakenneanalyysimenetelmät, kuten lujuusopin ja murtumismekaniikan menetelmät, sekä eritellään deterministisen lähestymistavan puutteita. Usein fysikaaliset probabilistiset menetelmät perustuvat deterministisiin vastaaviin sillä muunnelmalla, että yksi tai useampi malliparametri on asetettu probabilistisesti jakaantuneeksi. Työssä esitetään useita probabilistisia analyysimenetelmiä, kuten Monte Carlo -simulaatio ja tärkeysperusteinen otanta. Todennäköisyysperusteisia analyysimenetelmiä koskeva kuvaus kattaa sekä fysikaaliset että tilastolliset lähestymistavat. Kun rakennejärjestelmien/-komponenttien todennäköisyydet yhdistetään tietämykseen seausvaikutuksista, voidaan arvioida vastaavat riskit. Työssä esitetään useita riskianalyysimenetelmiä sekä eräitä niitä koskevia rajoituksia ja puutteellisuuksia.

Työssä esitetään valikoima erilaisia vaurioitumismekanismeja koskevia mallinnusmenetelmiä. Näitä menetelmiä tarvitaan rakennejärjestelmien ja -komponenttien käyttöikäanalyyseissa. Yleisesti ottaen kyseiset käyttöikäanalyysit edellyttävät perusteellisia tietoja rakenteellisista ominaisuuksista, kuormista, merkittävistä vaurioitumismekanismeista sekä vallitsevista olosuhteista. Rakennejärjestelmien/-komponenttien vaurioitumista kuvaavat mallit voivat olla tyypiltään deterministisiä, probabilistisia tai näiden yhdistelmä. Työssä esitetään kaikkiin näihin tyyppeihin lukeutuvia vaurioitumismalleja. Lisäksi esitetään muutamia merkittäviä riskianalyysin sovelluksia. Näihin lukeutuvat todennäköisyyspohjaiset turvallisuus- ja riskianalyysit (PSA ja PRA) ja riskitietoiset tarkastusohjelmat (RI-ISI).

Käytännössä käyttöikä- ja riskianalyysit tehdään yleensä jollakin sopivalla analyysityökalulla eli sovellusohjelmalla. Työn jälkipuoliskolla esitetään valikoima rakennejärjestelmien/-komponenttien vaurioitumisen ja riskien analyysisovelluksia. Sen jälkeen edustavalle valikoimalle ydinvoimalan putkistokomponentteja esitetään analyysiohjelmilla VTTBESIT ja PIFRAP tehdyt todennäköisyysperusteiset vikaantumis- ja käyttöikäanalyysit.

Lopuksi esitetään yhteenveto sekä jatkotutkimusaiheita koskevia ehdotuksia.

Foreword

The author expresses his gratitude to VTT for providing both working quarters and altogether nearly three person work months worth of resource support for the preparation of this licentiate thesis. The author expresses his gratitude to Professor Juha Paavola for supervising the thesis and to DrTech Kaisa Simola for being the inspector for this thesis as well as for valuable advice and comments. The author also expresses his gratitude to DrTech Heli Talja for encouragement and preparing the way for this thesis in its earlier phase, to MSc Jouni Alhainen for computational support and music related discussions, and to Niina for general support and caring understanding, in particular during the completion phase of the thesis. Gratitude is also addressed to many fellow researchers from VTT and certain experts from the domestic energy industry for providing useful technical background information and advice during the preparation of this thesis.

Espoo, December 2011

Author

Contents

List of symbols

Latin symbols

A	event rate parameter before the first event
A	rate coefficient in constitutive equation for creep
a	crack depth
a_0	initial crack depth, initial crack length
a_c	critical value of crack depth
a_{CA}	depth of creep induced cavity/crack
$a_{CA,0}$	threshold depth of creep induced cavity/crack for onset of interaction with fatigue induced crack growth
a_{FA}	depth of fatigue induced crack
a_i	effect of i:th maintenance
a_n	final crack length
a_{11}, a_{12}, a_{22}, a_{33}	coefficients in strain energy density equation
B	geometry factor
b	Burgers vector
b, k	material parameters in *S-N* curves method
c	half of the crack length
c	reduction factor
C	effective corrosion rate in absence of protective coating
$C(t)$	interpolation parameter between small scale creep and extensive creep
C_t	interpolation parameter between small scale creep and extensive creep
$(C_t)_{SSC}$	is separately computed small scale creep limit for interpolation parameter between small scale creep and extensive creep
C, C_F, C_S, C_J	coefficient characterising material and environment in fatigue crack growth rate equation
C	coefficient characterising material and environment in stress corrosion crack growth rate equation
C_0, C_1	stress corrosion crack growth rate equation coefficients
C1, C2	constants in equation for nominal environmental fatigue correction factor

C_β	coefficient in probabilistic equation for aspect ratio of fabrication cracks
CF	radiation embrittlement coefficient
C_i	consequence
C_p	retardation parameter
C^*	C^* integral
C, n, p, q	parameters in fatigue crack growth rate equation
d	critical strength level
D	total accumulated damage
D	outer pipe diameter
D	matrix, which contains the detection probabilities of cracks
D_I	total accumulated damage for crack initiation phase
D_{II}	total accumulated damage for crack propagation phase
D_0, ϕ	material constants in creep crack growth rate equation
$d(t)$	general corrosion propagation depth
E	elastic modulus, Young's modulus
f	loading frequency
F	Faraday's constant
F	renewal process
f	neutron fluence
$f(t)$	time dependent probability density function of component failure
$F(t)$	time dependent renewal process, i.e. a sequence of independent, identically distributed non-negative random variables, of which not all are zero
$f_x(x)$	depth probability for existing manufacturing crack
f_{alloy}	material type dependent coefficient in stress corrosion cracking rate equation
F_{en}	environmental fatigue correction factor
$F_{en,i}$	nominal environmental fatigue correction factor for the stress cycle i
$F_{en,nom}$	nominal environmental fatigue correction factor
f_{i0}	occurrence rate of stress corrosion cracking
f_{ij}	dimensionless function of angular coordinate of the polar system having origin at the crack tip
F_I, F_{II}	crack geometry factors for fracture modes I and II
$f_{\text{orientation}}$	crack propagation direction dependent coefficient in stress corrosion cracking rate equation

$f_x(x)$	probability density function of random variable X, PDF
$F_x(x)$	cumulative distribution function of random variable X, CDF
$f_{xy}(x, y)$	joint probability density function of random variables X and Y
g	performance function, limit state function
G	shear modulus
h	pipe wall thickness
I_n	integration constant
i_0	initial dissolution current density at bare metal surface
i_0	initial value of decay curve of electric current on newly exposed surface
$I_1(x)$	modified Bessel function of order 1
J	J-integral, the strain energy rate
J_1	Bessel function of first kind and of order 1
J_{IC}	mode I fracture toughness
J_R	fracture energy, fracture toughness
k	constant
K	General expression for stress intensity factor
K_I	mode I stress intensity factor
K_{II}	mode II stress intensity factor
K_{III}	mode III stress intensity factor
K_I^{mean}	mode I stress intensity factor corresponding to mean stress
K_{II}^{mean}	mode II stress intensity factor corresponding to mean stress
K_{III}^{mean}	mode III stress intensity factor corresponding to mean stress
K_{Ia}	lower bound crack arrest value for stress intensity factor
K_{IC}	mode I fracture toughness
$K_{I,max}$	Maximum value of mode I stress intensity factor
$K_{I,min}$	Minimum value of mode I stress intensity factor
K_{th}	crack propagation threshold value for stress intensity factor
K^*	strain hardening coefficient determined near failure
L_r, K_r	non-dimensional variables in failure assessment diagram approach
l_0	initial crack length
m	total number of cells in stratified sampling
m	decay constant of current at newly exposed material surface
m	dimensionless constant that is approximately 1.0 for plane stress and 2.0 for plane strain

m, m_y	exponent characterising material and environment in fatigue crack growth rate equation
M	atomic weight of the metal
$M(t)$	time dependent renewal function
$m1$	shaping exponent
M, N	material dependent factors
N	sample size, number of load cycles
n	strain hardening exponent
n	exponent characterising material and environment in stress corrosion crack growth rate equation
n	power law exponent for non-linear behaviour in general corrosion
n	dimensionless work hardening exponent in Ramberg-Osgood equation
n	numerical constant correlated with the degree of sensitisation, water conductivity, corrosion potential
n	exponent in constitutive equation for creep
n	total number of strain increments
$N\left(a \geq a_{FS,i}\right)$	the number of times Monte Carlo simulations have reached or exceeded the selected degradation/failure state in terms of crack depth a
$N(t)$	time dependent point process describing the occurrence of shocks
N_I	number of load cycles for crack initiation phase
N_{II}	number of load cycles for crack propagation phase
$\mathrm{N_{air,RT}}$	fatigue life in air at room temperature
n_d	number of dislocations contributing to formation of slip band
N_f	number of failures, number of load cycles to failure
n_i	number of cycles of operation under certain stress amplitude
N_i	total number of cycles that would produce a failure at certain stress level
N_j	number of samples taken from the j:th cell in stratified sampling
N_i'	modified life at some considered loading level
N_Σ	total accumulated life
N_{slip}	number of active slip bands
$\mathrm{N_{water}}$	fatigue life in water at service temperature
n^*	cyclic strain hardening exponent determined near failure
O^*	transformed level of dissolved oxygen
$\mathbf{P}$	transition probability matrix
p	internal pressure

P, P_i	probability
P_f	failure probability
p_f	rupture failure probability for pipe section
p_{f0}	conditional fracture probability for a given crack length
$p_{FS,i,tj}(t)$	failure probability corresponding to selected degradation/failure state
p_i	initial probabilities of various damage states
P_j	probability that an initial crack exists in the j:th cell in stratified sampling
P_{LM}	Larson-Miller parameter
Q_g	thermal activation energy for crack growth
R	total risk
R	reliability
R	stress ratio
R	universal gas constant
R	strength
r	polar coordinate with origin at the crack tip
$R(t)$	time dependent component reliability
R_{eff}	effective stress ratio
R_i	individual risk
R_i	inner radius
R_{max}	maximum allowable stress ratio
RT_{NDT}	reference nil-ductility temperature of the material
RT_{NDT_0}	initial NDT temperature for unirradiated material
R_y	extent of current yield zone
S	stress level, remote stress resulting from the applied load
S	stress
S	strain energy density factor
S^*	transformed sulphur content
t	wall thickness, plate thickness
t	time in service since start of operation, time since start of corrosion process
T	temperature
T	expected total time in service
t	time in general
t_0	short time constant

t_0	time constant in pitting corrosion model
t_0	starting time of current decay at newly exposed material surface
t_1	transition time from short time to long time behaviour
t_2	transition time from primary to secondary creep
t_F	time of rupture
t_i	time spent at condition *i*
T_i	components of traction vector
T_k	maintenance times
t_r	time to rupture
t_{ri}	time to rupture at condition *i*
T_{ref}	absolute reference temperature used to normalise data
T^*	transformed temperature
$TK_{41\text{J}}$	41 J impact energy transition temperature
$TK_{56\text{J}}$	56 J impact energy transition temperature
$TK_{0.9\text{mm}}$	0.9 mm lateral expansion transition temperature
T, *C*, *G*, *k*2, *k*3, *s*	material parameters which are function of temperature, environment and the metallurgical state of the material
U	factor depending primarily on the stress ratio
$\mathrm{U_{en}}$	cumulative fatigue usage factor
u_i	components of displacement vector
$\mathrm{U_i}$	partial fatigue usage factor
$\dot{u}_i$	displacement rate components
V	pitting corrosion propagation rate
V_0	initial pitting corrosion propagation rate
w	strain density
$\dot{w}$	stress work rate (power) density
x	certain value of the random variable
x	relative initial crack depth, relative initial crack length
$\tilde{X}$	Median value
$X(t)$	time dependent applied stress
X, Y	random variable
X_c	continuous load
x_i	exponent parameter related to considered loading level
y	constant value for strength
$Y(t)$	time dependent strength of a component

Z	response function
z	number of electrons involved in reaction rate
z	charge change at electrolysis
Z_0	limiting value of response function
Z_{OL}	plastic zone diameter

Greek symbols

α	ageing acceleration rate
α	dimensionless constant
α	crack growth rate coefficient
α	Parameter describing the degree of interaction between fatigue induced crack growth and creep induced cavity growth
β	first-order reliability index, geometrical reliability index, Hasofer-Lind reliability index
β	cyclic hardening rate
β_i	frequency of load cycles at some considered loading level
β	exponent in stress corrosion cracking rate equation
β	aspect ratio of fabrication crack
β, λ	dimensionless constants in stress corrosion cracking rate equation
δ	crack tip opening displacement
$\dot{\Delta}$	total displacement rate
$\dot{\Delta}_t$	time dependent creep displacement
$\Delta\varepsilon$	strain range
$\Delta\varepsilon_p$	Parameter related to plastic strain
$\Delta\varepsilon_p$	current value of plastic strain
$\dot{\varepsilon}_p$	absolute value of plastic strain rate
$\Delta\gamma$	shear strain range
Δ_i	damage fraction
ΔJ	cyclic J-integral range
ΔK_{eff}	effective stress intensity factor range
ΔK_{eq}	equivalent stress intensity factor range
ΔK_{th}	fatigue threshold in terms of stress intensity factor range
$\Delta K_I(\varepsilon)$	strain intensity factor range
ΔRT_{NDT}	shift in reference nil-ductility temperature of the material

ΔS	cyclic strain energy density factor range
$\Delta\sigma$	stress range
$\Delta TK_{41\mathrm{J}}$	shift in 41 J impact energy transition temperature
$\Delta TK_{56\mathrm{J}}$	shift in 56 J impact energy transition temperature
$\Delta TK_{0.9\mathrm{mm}}$	shift in 0.9 mm lateral expansion transition temperature
$\dot{\varepsilon}$	strain rate
$\dot{\varepsilon}_{ct}$	crack tip strain rate
ε_f	strain caused by break of protective film at crack tip
ε_f^*	failure strain as a fraction
ε_i	strain accrued at condition *i*
$\varepsilon_{\max}$	maximum strain
$\varepsilon_{\min}$	minimum strain
ε_{ri}	rupture strain at condition *i*
$\dot{\varepsilon}^*$	transformed strain rate
$\tilde{\varepsilon}_{ij}$	dimensionless function of work hardening exponent and angular coordinate around crack tip
Φ	acceleration factor for fatigue induced crack growth rate equation
$\Phi(u)$	standard normal distribution function
Γ	contour around crack tip
κ_i	principal curvatures of the limit state at the minimum distance point
λ, β_m	coefficients in probabilistic equation for aspect ratio of fabrication cracks
$\lambda(t)$	time dependent component failure rate
λ_0	constant random failure rate
$\Lambda(t)$	time dependent integral of the intensity, cumulative failure function
μ_i	mean value point
μ	general mean value
μ_y	scale parameter
ν	Poisson's coefficient
π_0	initial crack degradation/size state
π_k	crack degradation/size state at time *k*
θ	location parameter, angular coordinate around crack tip
θ	angle between the direction of the slip plane and tensile stress

θ	inclination angle of the crack
θ_0	inclination angle of the crack at the direction of minimum strain energy density
ρ	material density
ρ_d	dislocation density
ρ_m	density of the metal
σ	standard deviation
σ_0	reference stress (most often yield strength)
σ_{AXIAL}	axial membrane stress
σ_{ij}	components of stress tensor/matrix
$\tilde{\sigma}_{ij}$	dimensionless function of work hardening exponent and angular coordinate around crack tip
σ_y	yield strength, average local yield strength
σ_y	shape parameter
$\overline{\sigma}_y$	local yield strength

List of abbreviations

AGR	advanced gas-cooled reactor
AIS	adaptive importance sampling
AMV	advanced mean value method
ASME	American Society of Mechanical Engineers
BWR	boiling water reactor
CANDU	Canadian deuterium uranium reactor
CCDP	conditional core damage probability
CCF	common cause failure
CDF	conditional core damage
CDF	crack driving force
CLERP	conditional large early release probability
CTOD	crack tip opening displacement
DFM	deterministic fracture mechanics
DNV	Det Norske Veritas
EAC	environmentally assisted cracking
EDF	Electricité de France
ENIQ	European Network for Inspection and Qualification
EPFM	elastic-plastic fracture mechanics
EPRI	Electric Power Research Institute
ETA	event tree analysis
FAC	flow accelerated corrosion
FAD	failure assessment diagram
FBR	fast breeder reactor
FEM	finite element method
FITNET	European Fitness For Service Network
FMEA	failure mode and effect analysis
FMECA	failure mode effect and criticality analysis
FORM	first-order second-moment method
FPI	fast probability integration
FTA	fault tree analysis
GCR	gas cooled reactor
GUI	graphical user interface
HAZ	heat affected zone

HAZOP	hazard and operability study
HIDA	HIgh temperature Defect Assessment procedure
HSE	Health and Safety Executive
HWR	heavy water reactor
IAEA	International Atomic Energy Agency
IASCC	irradiation assisted stress corrosion cracking
IGSCC	intergranular stress corrosion cracking
INEEL	Idaho National Engineering and Environmental Laboratory
IS	importance sampling
ISI	in-service inspection
IWM	Fraunhofer-Institut für Werkstoffmechanik
JRC	Joint Research Centre
JSME	Japan Society of Mechanical Engineers
LEFM	linear-elastic fracture mechanics
LHS	Latin hypercube simulation
LLNL	Lawrence Livermore National Laboratory
LOCA	loss of coolant accident
LWR	light water reactor
MCS	Monte Carlo simulation
MIC	microbiologically influenced corrosion
MPP	most probable point
MV	mean value method
NDE	non-destructive examination
NDT	non-destructive testing
NDT	nil-ductility temperature
NPP	nuclear power plant
OECD	Organisation for Economic Co-operation and Development
OPDE	OECD Piping Failure Data Exchange
ORNL	Oak Ridge National Laboratory
PDF	probability density function
PFM	probabilistic fracture mechanics
POD	probability of detection
PRA	Probabilistic Risk Assessment
PSA	Probabilistic Safety Assessment
PTS	pressurised thermal shock

PWR	pressurised water reactor
PWROG	Pressurized-Water Reactor Owners Group
PWSCC	primary water stress corrosion cracking
QRA	quantitative risk analysis
RAW	risk achievement worth
RBI	risk based inspection
RCM	reliability centered maintenance
RDF	risk reduction factor
RIF	risk increase factor
RI-ISI	risk informed in-service inspection
RPV	reactor pressure vessel
RRW	risk reduction worth
RSM	response surface method
SA	sensitivity analysis
SAIC	Science Applications International Corporation
SCC	stress corrosion cracking
SINTAP	Structural Integrity Assessment Procedures for European Industry
SKI	Swedish Nuclear Inspectorate
SMAW	shielded metal arc welding
SORM	second-order reliability method
SSC	systems, structures and components
SSM	Swedish Radiation Safety Authority
STUK	The Finnish Radiation and Nuclear Safety Authority
SwRI	Southwest Research Institute
TGSCC	transgranular stress corrosion cracking
TVO	Teollisuuden Voima Oyj
USNRC	U.S. Nuclear Regulatory Commission
VTT	Technical Research Centre of Finland
WRS	weld residual stress
WWER	water-cooled water-moderated energy reactor

1. Objective of the thesis

Several objectives were set for this thesis. One objective is to collect both the methods and background theories for evaluation of operational lifetime, reliability and risk of structural systems and components of power plants. This was pursued by making an extensive literature survey. Another objective is to collect information concerning the relevant existing probabilistic degradation and risk analysis tools, with which one can assess the remaining lifetime and structural integrity of systems/components of power plants. The scope and characteristics of these tools are described. The last objective is to provide an application example. This was carried out by making a failure probability analysis to a representative set of nuclear power plant piping components.

2. Introduction

Structural lifetime, reliability and risk analysis methods and applications for structural systems and components of conventional and nuclear power plants are considered in this thesis. The emphasis here is on the latter power plant type. Lifetime analyses of structural systems and components necessitate a thorough knowledge of their structural properties, loads, supports, the relevant ageing mechanisms and prevailing environmental conditions. Due to distributed nature of many of these properties or phenomena, probabilistic modelling methods are deemed suitable for the lifetime analyses. Failure probabilities combined with knowledge of system or component failure consequences allow performing risk analyses.

An overview of conventional and nuclear power plant environments and a description of the various degradation mechanisms damaging the power plant systems and components are presented first, see Chapter 3. Ageing degradation mechanisms may be divided into two groups based on the resulting failure modes: (1) those that may cause rupture, and (2) those that may cause cracking. Low-cycle fatigue, high-cycle thermal fatigue, and stress corrosion cracking (SCC) of components may cause cracking. Radiation embrittlement, thermal ageing of cast stainless steel components and vibration fatigue of small diameter piping may cause rupture. The mechanisms that have potential to cause rupture are likely to have significantly more risk impact [1].

A description of deterministic structural analysis methods, where the emphasis is on structural mechanics and fracture mechanics based analysis methods, is presented in Chapter 4. Other associated fields of science are material science, chemistry and radiation physics. The disadvantages of the deterministic analysis methods are discussed.

Probabilistic analysis methods are dealt with after that, see Chapter 5. The probabilistic analysis methods are often based on deterministic analysis methods

with the modification that one or more of the model parameters are considered as probabilistically distributed. The presented probabilistic analysis procedures include first-order second moment (FORM) methods, second-order reliability methods (SORM), mean value methods, Monte Carlo simulation (MCS) and importance sampling.

A brief description of risk analysis methods is presented then, see Chapter 6. The engineering definition of risk is now accepted as being the product of the likelihood and the consequence of an event [2]. There exist nowadays a number of risk analysis procedures. The considered risk analysis procedures include failure mode and effect analysis (FMEA), fault tree analysis (FTA), event tree analysis (ETA) and expert opinion. Risk based regulations and standards as well as concerns related to risk assessment are considered also. The trend towards a risk based approach in power plants, and especially in nuclear power plants (NPPs), is being supported by extensive plant operating experience, improved understanding of material degradation mechanisms and the availability of fitness-for-service assessment procedures [3]. At the same time, developments in non-destructive testing (NDT) technology have increased the scope and efficiency of examinations that can be undertaken. Inspection trials have produced a greater appreciation of the limits of NDT performance and reliability.

Deterministic and probabilistic computational modelling methods for various ageing degradation mechanisms damaging power plant components are presented after this, see Chapters 7 and 8. These methods are needed in the lifetime analyses of structural systems and components of power plants. In general, the lifetime analyses necessitate a thorough knowledge of structural properties, loads, supports, the relevant degradation mechanisms and prevailing environmental conditions. The nature of degradation models of structural systems/components can be deterministic, probabilistic or a combination of these two types. Degradation models of all these kinds are presented. Deterministic fracture mechanics is an example of deterministic ageing modelling approaches. Statistic failure models, which are based on observed failure statistics, are an example of probabilistic ageing modelling approach. Probabilistic fracture mechanics, which is discussed in more detail, is a modelling approach which combines both deterministic and probabilistic features. In practise, the degradation analyses are usually performed with suitable analysis tools, i.e. with analysis codes.

A brief description of some important risk analysis applications is presented in Chapter 9. This includes e.g. probabilistic risk/safety assessment (PRA/PSA)

and risk informed in-service inspection (RI-ISI). In addition to the energy industry, PRA/PSA has emerged as an increasingly popular analysis tool in several other industries as well, especially during the last two decades [1]. PRA/PSA is a systematic and comprehensive methodology to evaluate risks associated with every life-cycle aspect of a complex engineered technological entity or component from concept definition, through design, construction and operation, and up to removal from service. In most countries, the method is referred to as PSA. In the United States, the method is referred to as PRA. Recently The Finnish Radiation and Nuclear Safety Authority (STUK) has adviced/announced that also in Finland this method should be referred to as PRA. Despite having two names, the technique is practically the same. RI-ISI involves the planning of an inspection on the basis of the information obtained from a risk analysis of the equipment. The purpose of the risk analysis is to identify the potential degradation mechanisms and threats to the integrity of the equipment and to assess the consequences and risks of failure. The inspection plan can then target the high risk equipment and be designed to detect potential degradation before fitness-for-service could be threatened [3].

Component ageing analyses are discussed after this, see Chapter 10. Ageing of various systems, structures and components (SSCs) affect the safety of power plants. The objective of component ageing analyses is to identify the degradation mechanisms of components and the increase in failure occurrences, to assess the remaining lifetime of components and to find suitable means to prevent or mitigate the effects of ageing.

A selection of various probabilistic system/component degradation and risk analysis tools is presented then, see Chapter 11. These are divided into component and system analysis applications. Another difference in approaches of these programs is that one part of them contains models of one or more specific degradation mechanisms, while the other part consists of general structural reliability analysis codes.

Computational application of probabilistic failure and lifetime analyses to a relatively small but representative set of NPP piping components is presented after that, see Chapter 12. In addition to data concerning structural properties, primary and secondary loads, supports and environment, also data concerning relevant degradation mechanisms and failure modes are needed in the probabilistic failure and lifetime analyses of NPP piping components. Essential sources for piping degradation and failure data are international and plant specific databases. In the probabilistic failure analysis computations two analysis codes were used,

those being probabilistic VTTBESIT, developed by VTT and Fraunhofer-Institut für Werkstoffmechanik (IWM, Germany), and PIFRAP developed by Det Norske Veritas (DNV), respectively.

The thesis ends with a summary and suggestions for further research.

3. Degradation mechanisms concerning power plant components

3.1 Introduction

Ageing degradation in power plants should be managed by ensuring that the design functions remain available throughout the service life of the plant. From the safety perspective, this implies that ageing degradation of SSCs important to safety remains within acceptable limits, and that procedures and personnel training remain adapted. Unchecked, ageing degradation has the potential to reduce the safety of operating power plants.

The technical definition of ageing given by the International Atomic Energy Agency (IAEA) is the following [4]: Ageing is the continuous time dependent degradation of materials due to normal service conditions, which include normal operation and transient conditions. In this thesis degradation is used as an equivalent expression to material ageing.

Ageing degradation can be observed in a variety of changes in physical properties of metals, concrete and other materials in a power plant. These materials may undergo changes in their dimensions, ductility, fatigue capacity and mechanical or dielectric strength. Ageing degradation is caused by a variety of ageing mechanisms, physical or chemical processes such as fatigue, cracking, embrittlement, wear, erosion, corrosion and oxidation. These ageing mechanisms act on SSCs due to a challenging environment with relatively high heat and pressure, radiation, reactive chemicals and synergistic effects. Some operating practices, such as power plant cycling (i.e., changing power output) and equipment testing, can also create stresses for plant SSCs [5]. Some degradation mechanisms can also act simultaneously, like for example fatigue and creep.

There is a fairly limited set of degradation mechanisms, a large commonality in used materials, and fairly similar operating conditions. However, due to the

diversity in plant design, construction and used materials, operating conditions and histories as well as maintenance practices, the specific effects of ageing, although similar, are unique for each plant. Even near twin units at the same site can have substantial differences in the remaining life of major SSCs, based on subtle design or material differences and operating histories [5].

In general, ageing in power plants can be taken to mean evolution of personnel and procedure adequacy and evolution of material or equipment properties, which, after a certain time may not be compatible with the required safety margins, or with an economic functioning of the plant. Repair or replacement of components, as well as change in service conditions for a better compatibility with component reduced capacities are possible [6].

In parallel, safety requirements may increase with time, following the evolution of the public acceptance, and costs of other energy sources may decrease, limiting as a result the economic interest of continued operation. The plant life will then be the result of the consideration of ageing in a changing regulatory, political, technical and economic context.

In the context of stable safety requirements, the evolution of the safety margins for a given component can be illustrated as shown in Figure 3.1-1. This figure, which is given for illustrative purpose only and does not take into account the possibility of component replacement, shows that a better evaluation of the applied loading, as well as a better knowledge of component performance can result in a modification of the demonstrated safety margin, and consequently of the potential component life. A reduction of the applied loading or an increase of component performance would result in an increase of the safety margin. Figure 3.1-2 illustrates the combined influence of the above considerations with a possible evolution of safety requirements.

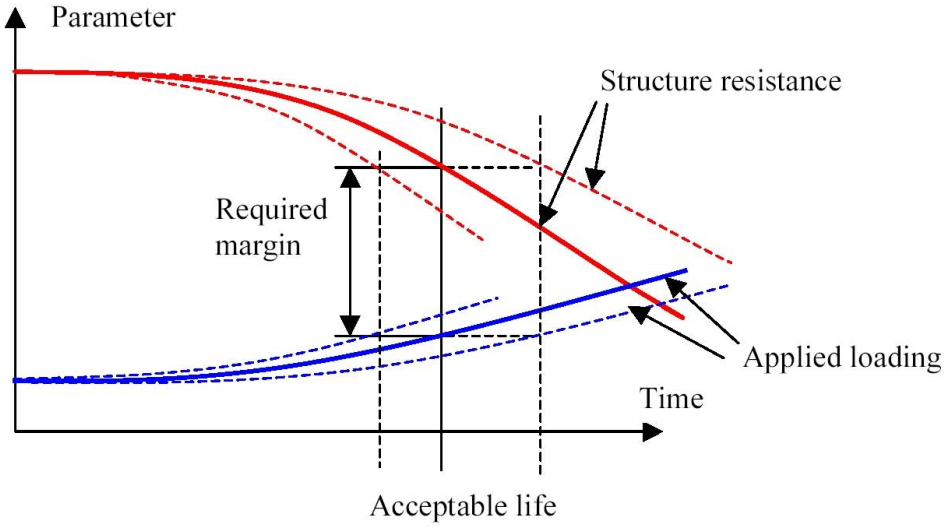

Figure 3.1-1. Illustration of possible component margin evolution during service, from ref. [8].

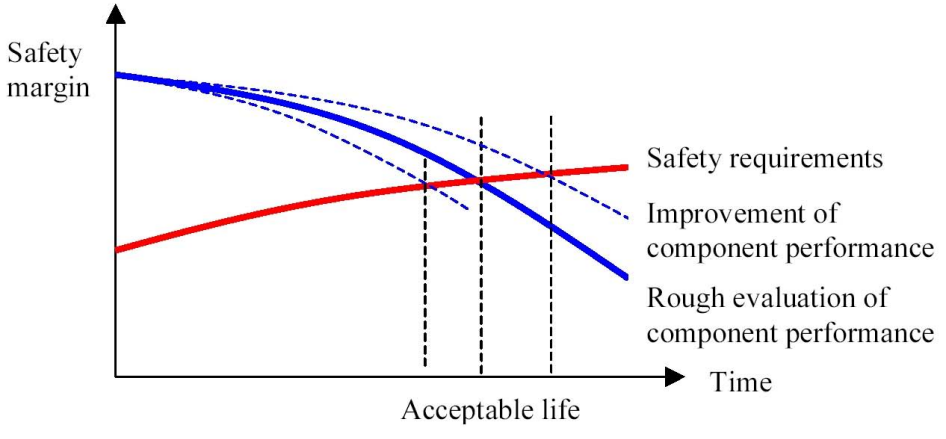

Figure 3.1-2. Illustration of combined evolution of component margins and safety requirements, from ref. [9].

As shown in Figures 3.1-1 and 3.1-2, lifetime extension is not only obtainable through repair or replacement of components, but also through a better use and a better evaluation of the real evolution of component performance, for example a better prediction of material properties evolution, a better evaluation of existing

defects and mechanical behaviour of real defects, or a better knowledge of operating conditions.

Power plant structures generally have substantial safety margins when properly designed and constructed. However, the available margins for degraded structures are not well known. In addition, age related degradation may affect the dynamic properties, structural response, structural resistance/capacity, failure mode and location of failure initiation. A better understanding of the effect of ageing degradation on structures and components, especially passive components, is needed to ensure that the current licensing basis is maintained under all loading conditions [10].

This thesis considers mainly the ageing degradation of metallic SSCs. Depending of the metal or alloy in question and the intensity of the external loading as well as environmental impact, there may be a high potential for the degradation. The processes of degradation can result in material and geometry changes of which the most important are [4]:

- reduced toughness (embrittlement),
- cracking,
- swelling,
- thinning,
- denting and
- pitting.

3.2 Overview of conventional and nuclear power plant environments

The principal route for producing electricity in power plants is the conversion of mechanical energy of rotation into electrical energy using a generator. The large generators used by electric utilities employ a shaft comprising the magnetic field (rotor) which rotates inside a stationary electric field containing conducting wires (stator). Rotation of the shaft is achieved by coupling it to a turbine in which the kinetic energy of a moving fluid is converted into mechanical energy of rotation. The working fluid can be wind, water, steam or combustion gases. The most common turbine type is steam turbine, which employs steam produced from burning fossil fuels in a boiler or from the heat produced by atomic reactions inside a nuclear reactor [11].

Due to the nature and requirements of the energy production methods, the power plant environments are characterised by high system temperatures and

pressures. Many power plant components are also exposed to large temperature and pressure variations, which can in certain cases occur quite quickly. The chemistry of the working fluid can affect the structural integrity of the power plant components as well. Besides the operational conditions, the power plants are shutdown at specific intervals for maintenance and inspection outages, after which the operation is started again. During shutdown the system temperature and pressure are lowered, usually to atmospheric conditions, and during start-up they are correspondingly raised to the operational level. Besides the planned and usually yearly outages, the power plants have to be shutdown when certain accidents, e.g. malfunctions or structural failures, take place. These accidents are, however, relatively rare, and the power plants are also designed to sustain their safety in the case of their occurrence, e.g. with several auxiliary systems.

The pressure, temperature and specific volume of the steam at various stages in coal fired power plants are illustrated in Figure 3.2-1. In general the temperatures in conventional power plants vary from atmospheric conditions during shutdown to nearly 1000 °C in the combustion bed of some boiler types under operational conditions.

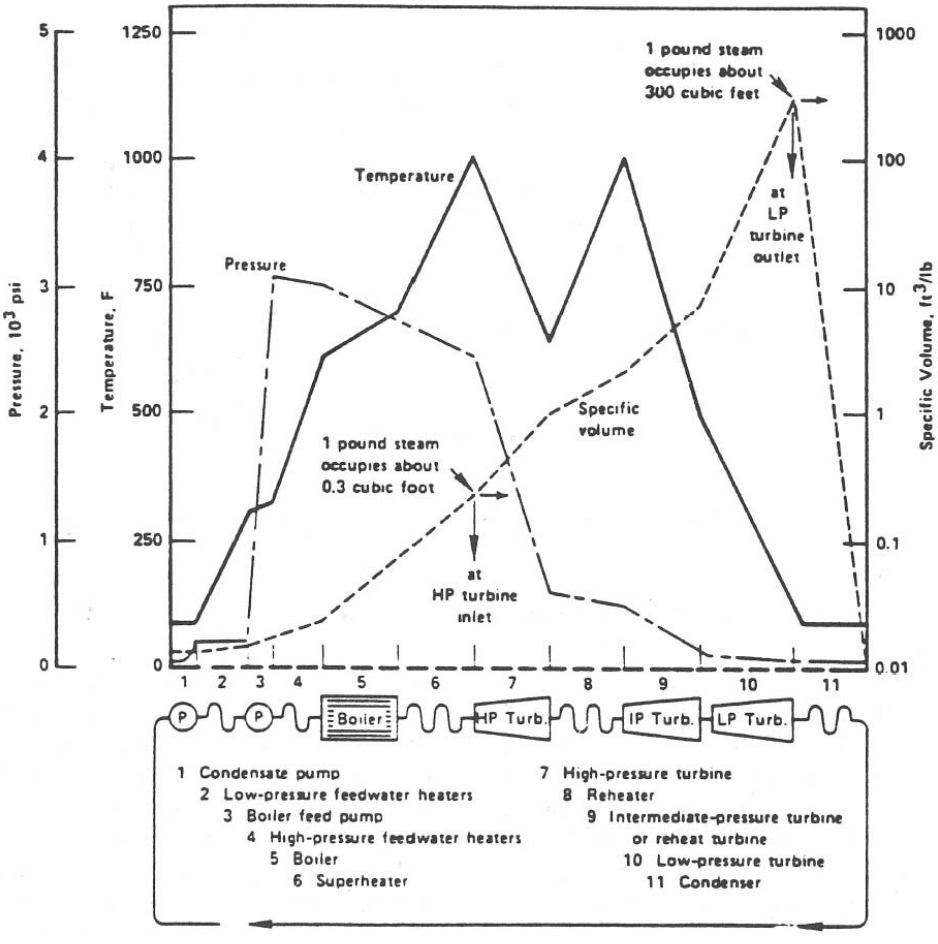

Figure 3.2-1. Relationships between steam pressure, temperature and specific volume in the various components of a large steam power plant, from ref. [13]. 1000 ksi corresponds to approximately 7 MPa and 1000 °F to approximately 540 °C.

Two major factors that influence the temperature and pressure levels in conventional power plants are the boiler type and used fuel. The most common boiler types of conventional power plants are [12]:

- grate-fired furnace,
- bubbling fluidised bed combustion,
- circulating fluidised bed combustion.

Some typical fuels used in conventional power plants are [12]: coal, oil, gas, waste (industrial, municipal), black liquor, peat, biomass and a combination of biomass and e.g. coal, oil or peat.

In grate-fired boilers, the fuel is loaded on the fire grate and combustion air is fed from below the grate to the primary combustion chamber. In the secondary chamber gases evaporated from the fuel bed are incinerated. Pyrolysis of volatile matters starts at 150–200 °C, is fastest at 250–500 °C and finishes around 800 °C [12].

In fluidised bed combustion, the bed is a mixture of inert material, like sand, and coarse fuel particles. A continuous stream of air is fed through the bed to produce turbulence in the bed due to which particles in the bed start to move and the bed becomes fluidised. In bubbling fluidised bed furnaces the fluidising particles remain under a defined level. The bed temperature is maintained relatively low, between 800–900 °C, in order to keep the ash solid and the bed material in the fluidised state. In the circulating system higher gas stream and finer fluidised particles are used and solid fluidised particles drift throughout the combustor with the gas stream. Cyclone is used to separate flue gas from escaped particles, which are continuously circulated back to the bed. Fuel is normally mixed with matter returning from a cyclone [12].

The quality of the working fluid in conventional power plants is monitored and it is attempted to maintain such that the concentrations of various impurities stay low enough. Iron and copper concentrations in the water/steam are an indicator of the efficiency of conditioning. Their values give information about the corrosion/deposition processes in the water/steam cycle, and respectively in the boiler and turbine. Silica concentrations in some boilers may not exceed certain values due to the specification for turbine operation. When operating with fully demineralized water, the silica content will be far below the specified level [14].

The typical pressure boundary materials in conventional power plants are ferritic, martensitic, austenitic and Ni-based alloys. For instance, the material of the steam tubes is typically austenitic stainless steel [11].

Most NPPs use steam cycles that differ little from those of conventional power plants except for the source of heat for the steam generator and for steam supply conditions [18].

According to the reactor type the NPPs are divided to two categories:

- light water reactor (LWR),
- heavy water reactor (HWR).

The LWRs are further divided to the following categories [21]:

- advanced gas-cooled reactor (AGR),
- boiling water reactor (BWR),
- fast breeder reactor (FBR),
- gas cooled reactor (GCR),
- pressurised water reactor (PWR),
- water-cooled water-moderated energy reactor (WWER).

The LWRs are designed so that the core is both moderated and cooled by highly purified water and the fuel is enriched uranium that fissions with thermal neutrons [18]. The most common LWR types are the BWR and PWR.

The BWRs operate at a pressure that allows boiling of the coolant water adjacent to the fuel elements inside the reactor core, producing slightly radioactive steam that passes directly to the steam turbines. The radioactivity in the steam, however, has a half-life of only a few seconds. The propagation of radioactivity to the turbine-feedwater system is virtually non-existent [18]. BWR plant operating pressures are typically from 6.90 to 7.24 MPa (1000 to 1050 psi), whereas the operating temperatures range from 282 to 288 °C (540 to 550 °F), respectively [19].

The PWR is currently the predominant nuclear reactor type in the world. The water in the PWR is in slightly higher temperature as in the BWR but is at a higher pressure, so that the reactor coolant remains liquid through the entire reactor coolant loop. Another difference between these two reactor types is that PWRs have an additional separate water loop that isolates the turbine steam loop from the reactor coolant [18].

The Table 3.2-1 are shows typical operational temperatures and pressures for common PWR plant types.

Table 3.2-1. Typical operational temperatures for common PWR plant types, from ref. [20].

Parameter/ Reactor type	**Westinghouse (4-loop plant)**	**Framatome**	**Siemens**	**WWER 440**	**WWER 1000**	**EPR**
Cold leg temperature, °C	292.5	292	291.3	270	290	295.5
Hot leg temperature, °C	325.5	329.5	326.1	300	325	328
Primary circuit pressure, MPa	15.51	15.51	15.2–15.8	12.2–12.5	15.7	15.5

The best known HWR is the Canadian Deuterium Uranium (CANDU) reactor. It utilises natural uranium as a fuel and heavy water as a moderator and coolant. These reactors produce a substantial saving due to the absence of fuel enrichment costs, but a large chemical plant is required to supply the quantities of heavy water required [18].

As the vast majority of the operating NPPs are LWRs, the description of further details of HWRs is omitted here.

As for local loads, one important issue is welding process induced residual stresses. They are locally confined to the weld regions and can be relatively high, e.g. of the scale of yield stress in tension on and near the inner surface. Thus they have to be taken into account in the structural integrity/safety analyses. The resulting residual stress state in a welded component is determined by welding related parameters, material properties and geometrical constraints. The first issue refers to the local shrinkage, quench and phase transformations caused by the localised thermal cycle. While the latter issue concerns the constraining effect of the surrounding structure, and in case of dissimilar metal welds the unbalance in material properties. It is generally known that there are three primary sources for weld residual stress redistribution or relaxation, which are the following [22]: transient mechanical loads, thermal treatments and irradiation exposure. Mainly weld residual stresses have to be taken into account in NPP environments, whereas due to relatively high operational temperatures of conventional power plants, they can be considered as mostly relieved and thus not necessary to be included in the structural integrity/safety considerations.

Even though the LWRs are moderated and cooled by highly purified water, the water still contains chemicals, like boric acid, and impurities, like sulphate, chloride and peroxides that can cause corrosion. Suspended particulate material can also accelerate erosion processes, which can lead to wall thinning. In addition to this the reactor pressure vessels (RPVs) are exposed to degrading effect of the products from the fission reactions [23, 24].

The typical pressure boundary materials in the BWRs and the PWRs are carbon steels and stainless steels. For instance, the material of the steam tubes is typically austenitic stainless steel [24].

3.3 Fatigue

Fatigue is caused by periodic application of stresses by mechanical or thermal loading. The metal subjected to fluctuating stress will fail at stresses much lower

than those required to cause fracture in a single application of load [11]. The key parameters are the range of stress variation and the number of its occurrences [6]. The fatigue process can be roughly divided into four stages: cyclic hardening/softening, crack nucleation, crack propagation, and fracture [7].

Low-cycle fatigue, usually induced by mechanical and thermal loads is distinguished from high-cycle fatigue, mainly associated with vibration or high number of small thermal fluctuations. Although, there is no distinctive limit between these two types of fatigue, the traditional approach is to classify failures occurring above 10 000 cycles as high-cycle fatigue and those occurring below that value as low-cycle fatigue. An important distinction between low-cycle fatigue and high-cycle fatigue is that in high-cycle fatigue most of the fatigue life is spent in crack initiation, whereas in low-cycle fatigue most of the life is spent in crack propagation, because cracks are found to initiate within 3 to 10 % of the fatigue life [11]. An example of fatigue fracture of a structural component is presented in Figure 3.3-1. The cyclic nature of the fatigue crack growth through the component section can be recognised in the patterned fracture surface shown in the figure.

Figure 3.3-1. Fatigue damage of a shaft component, from ref. [3].

Fatigue failures occur in many different forms. Mere fluctuations in externally applied stresses or strains result in mechanical fatigue. Cyclic loads acting in association with high temperatures cause creep-fatigue. When the temperature of the cyclically loaded component also fluctuates, thermo-mechanical fatigue is induced. Recurring loads imposed in the presence of a chemically aggressive or embrittling environment give rise to corrosion-fatigue. The repeated application of loads in conjunction with rolling contact between materials produces rolling contact fatigue, while fretting fatigue occurs as a result of pulsating stresses along with oscillatory relative motion and frictional sliding between surfaces [25]. In NPP environments fatigue due to temperature fluctuation only, i.e. thermal fatigue, can also in certain cases be identified. All in all, the majority of damage/failures in power plant components can be attributed to one of the above fatigue processes. Such failures take place under the influence of cyclic loads with peak values being considerably lower than the allowed loads according to static fracture analyses.

One characteristic of fatigue in metals is work hardening under reversed loading conditions. With continued cyclic loading, the rate of hardening progressively diminishes and a quasi-steady state of deformation, known as saturation, is reached. Once saturation occurs, the variation of the resolved shear stress with the resolved shear strain is not altered by further load cycles and the stress-strain hysteresis loop develops a stable configuration. Obviously work hardening behaviour is a metal specific phenomenon [25].

The lowering of the yield strength upon reloading that follows unloading, even if the reloading is in the same direction as the original loading, is called the Bauschinger effect. This phenomenon decreases with continued cycling. Unsymmetric cycles of stress between prescribed limits will cause progressive increase in the strain response or “ratchetting” in the direction of the mean stress. Typically, transient ratchetting is followed by stabilisation (zero ratchet strain) for low mean stresses, while a constant increase in the accumulated ratchet strain is observed at high mean stresses [25].

The damage process leading to the formation of fatigue cracks is initiated by locally limited plastic deformation in the micro scale range of individiual crystallites at low nominant net stresses. Depending on the lattice orientation and on the dislocation configuration, slip bands can be activated causing irriversible slip processes, see Figure 3.3-2. The repeated loading leads to micro-scale damage accumulation. After a saturation of energy accumulation has occurred, at which state no further slip processes can take place in the crystallite, small micro-

cracks form. With an increasing number of load cycles these micro-cracks start to grow and additional regions undergo the process of micro-scale damage. As the crack grows to macroscopic size the stress intensity at the crack tip usually increases so that the crack growth is accelerated until the remaining ligament can no longer bear the stress and complete failure occurs [4].

Three fundamental aspects related to the fatigue crack initiation are: the significance of the free material surface, the irreversibility of cyclic slip, and environmental effects on micro-crack initiation. The micro-cracks usually initiate at the free surface of the material. The restraint on cyclic slip is lower than at inside the material because of the free surface at one side of the surface material. Furthermore, micro-cracks initiate more easily in slip bands with slip displacements perpendicular to the material surface [26], which seems to be logical when looking at Figure 3.3-2. There are two reasons for irreversibility. One argument is that (cyclic) strain hardening occurs which implies that all dislocations do not return to their original position. Another important aspect is the interaction with the environment [27].

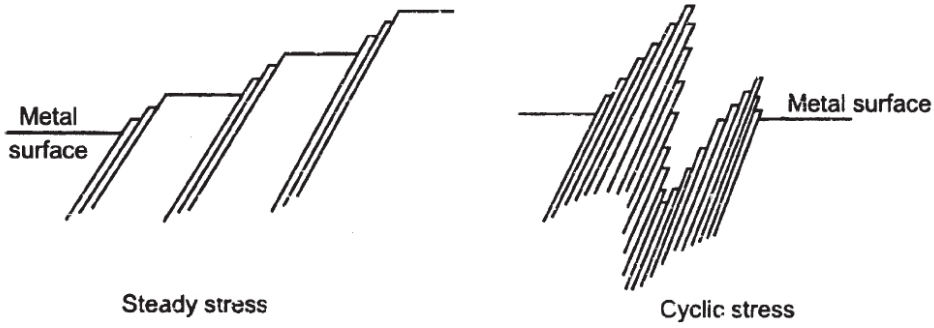

Figure 3.3-2. Geometry of slip at the material surface, from ref. [28].

The cyclic growth of a fatigue crack can be seen in the formation of striations, with one striation forming per load cycle, see Figure 3.3-3. The striations are supposed to be remainders of microplastic deformations at the crack tip, but the mechanism can be different for different materials. Because of micro-plasticity at the crack tip and the crack extension mechanism in a cycle, it should be expected that the profile of striations depends on the material type. Striations have not been observed in all materials, at least not equally clearly. Moreover, the visibility of striations also depends on the severity of load cycles. Striations have also shown that the crack front is a curved line and the crack tip is rounded [27].

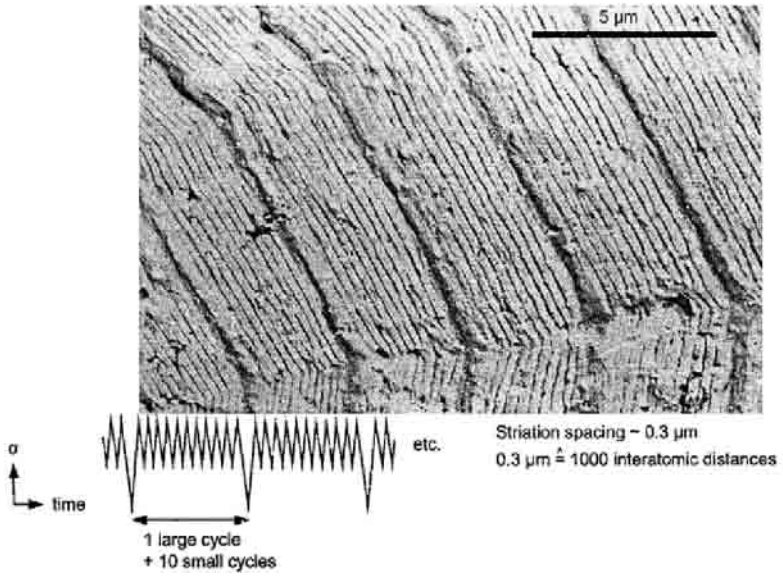

Figure 3.3-3. Correspondence between striations and load cycles during fatigue crack growth in an Al-alloy specimen, from ref. [27].

The fatigue life of a structural component under cyclic loading can be considered to consist of two phases, which are the crack initiation life followed by a crack growth period until failure. This can be represented in a block diagram, see Figure 3.3-4. Work hardening and other continuum type fatigue phenomena affect the component throughout the fatigue life.

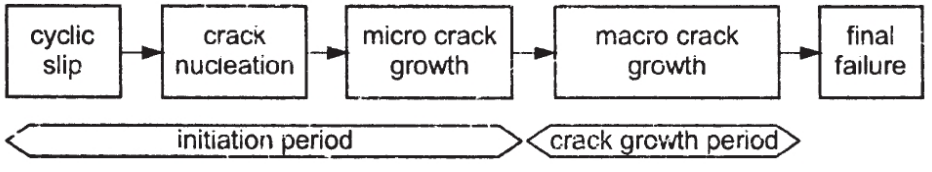

Figure 3.3-4. The different phases of the formation and growth of a fatigue crack, from ref. [27].

The fatigue limit is an important material property from an engineering point of view. It can be formally defined as a stress amplitude for which the fatigue life becomes infinite in view of the asymptotic character of the stress versus the number of load cycles (*S*-*N*) curve, see Figure 3.3-5. As fatigue tests must be terminated after a long testing time, it appears to be more logical to define a fatigue limit as the highest stress amplitude for which failure does not occur after

high numbers of load cycles. A more physically based definition of the fatigue limit could be defined as the threshold stress amplitude to take care of micro-crack nucleation and subsequent growth to a macro-crack [27].

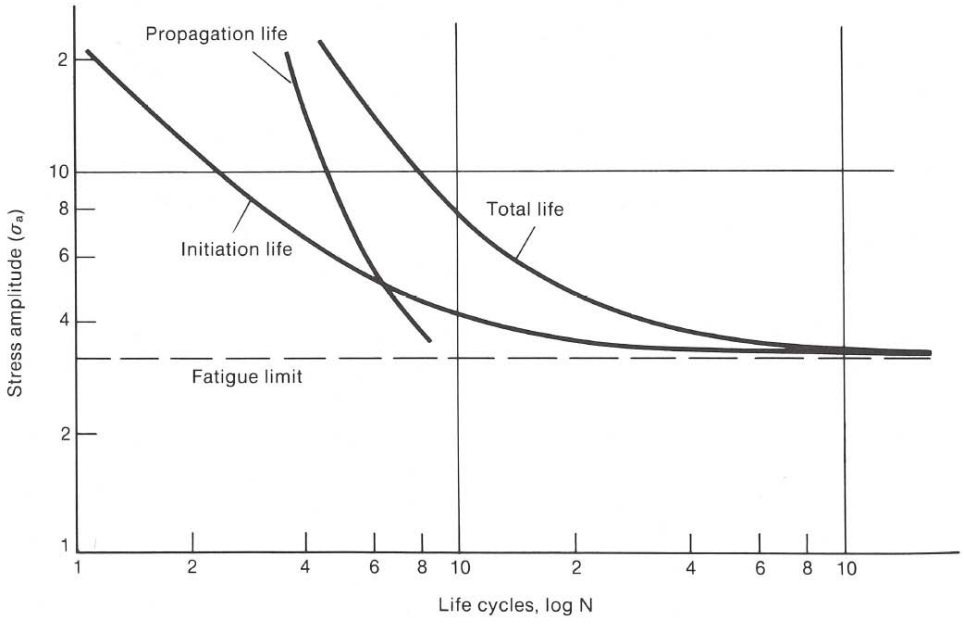

Figure 3.3-5. Outlook of a typical stress versus the number of load cycles (S-N) fatigue testing curve, from ref. [25].

Components/locations in conventional power plants which have experienced fatigue degradation include [29]: headers, downcomers, main steam piping, hot reheater piping, tubing, ductwork, precipitator, drums and geometry discontinuities, such as nozzles, reducers, transitions and small fillet radii.

Components/locations in NPPs which have experienced fatigue degradation include [1, 4]:

- BWRs; RPV, feed water piping, main steam piping and recirculation pump,
- PWRs; safe-ends, reactor coolant piping, feedwater piping and nozzles,
- LWRs in general; RPV internals,
- HWR RPVs; calandria vessel, pressure tubes and calandria tubes,
- steam generator; vessel shell, tubes and grid,

- steam and water piping vessels valves,
- main coolant pump; casing and shaft impeller,
- turbine; casing, blades and shaft,
- condensor tubes,
- geometry discontinuities in general; nozzles, reducers, transitions and small fillet radii.

3.4 Corrosion

Corrosion is the degradation of a material by chemical or electrochemical reaction with its environment. Most of the technical corrosion processes, however, are electrochemical in nature and are accompanied with hydrogen production. Corrosion reduces the component wall thickness, either uniformly or locally. The corrosion phenomenon is governed by the so called corrosion system which consists of the metallic material and the corrosive medium (the environment) with all the participating matter that can influence the chemical and physical behaviour and the corrosion parameters. The variety of chemical and physical variables of environments and materials leads to a large number of types and appearance of corrosion [4, 15].

In the case of electrochemical processes, corrosion occurs in several steps. Metal ions dissolve in liquid electrolyte (anodic dissolution) and hydrogen is produced in the process. This is the process of material loss from the corroded component and of the creation of the corrosion products. The free hydrogen can metallurgically interact with the metal (by adsorption, absorption or interstitial bonding) and can produce secondary damage, e.g. hydrogen embrittlement [15, 16].

When mechanical stresses or strains are acting in addition to the corrosion impact, the anodic dissolution of the metal can be stimulated, protective oxide layers can rupture or hydrogen absorption can be promoted. The combined action of a corrosive environment and mechanical loading can cause cracking even when no material degradation would occur under either the chemical or mechanical conditions alone [4, 15].

Corrosion can manifest itself in a number of forms, and there are generally accepted categories of corrosion based on the appearance and electrochemical processes. The types of corrosion include (but are not limited to) [30]:

- uniform attack,
- galvanic (two-metal) corrosion,
- crevice corrosion,
- pitting,
- intergranular corrosion,
- erosion corrosion, and
- environmental cracking.

Corrosion without mechanical loading

Corrosion without mechanical loading can be divided to uniform corrosion, local corrosion and selective corrosion.

Uniform corrosion refers to a uniform attack over surfaces of the material and results in thinning of the material. Uniform corrosion rates vary with fluid oxygen content, temperature and flow rate. When a protective Magnetite layer forms to the metal surface under uniform corrosion, which occurs e.g. for all hot water and steam pipes of unalloyed or low alloyed ferritic steel, the corrosion rate decreases considerably or may even stop. This process is not considered as an ageing mechanism, since the related material loss is very small [4, 15].

In case of inhomogeneities at the metal surface and/or local differences in the electrochemical reactivity of the environment, the creation of local cells is possible which results mostly in local corrosion attack. Localised corrosion includes pitting, crevice corrosion, etc. Pitting is commonly caused by the breakdown of the passive film on a metal in local areas, by species such as chlorides. Crevice corrosion results from local environment conditions in the restricted region of a crevice being different and more aggressive than the bulk environment [15, 16].

In selective corrosion, the attack is concentrated on distinct material phases, regions adjacent to the grain boundaries or specific alloying elements. The corrosion proceeds into the depth of the material without changing the overall geometry of the component. Since the corrosion attack propagates along the grain boundaries, the material damage proceeds from the surface into the bulk according to a grain disintegration process. An example of selective corrosion is the intergranular corrosion of sensitised austenitic stainless steels and nickel alloys. Environments with liquid that can cause intergranular corrosion in practice can include, among others, oxygen, chlorides, sulphates and hydroxides [4, 15].

Stress corrosion cracking (SCC)

SCC is a localised non-ductile failure which occurs only under the combination of three factors: tensile stress, aggressive environment and susceptible material. The SCC failure mode can be intergranular, IGSCC, or transgranular, TGSCC. In NPP, primary water stress corrosion cracking, PWSCC, and irradiation assisted stress corrosion cracking, IASCC, are also identified [4, 17]. An example of SCC is presented in Figure 3.4-1. For some combinations of metals and corrosive environments even very low stresses are sufficient to cause SCC. The phase of first macroscopic cracking is often preceded by a long incubation phase [4].

Actual SCC mechanisms are not clearly known yet [31]. However, many different mechanisms have been proposed to explain the synergistic interactions of stress and corrosion that occur at the crack tip, and there may be more than one process that causes SCC [32]. Generally, the mechanisms can be divided to anodic dissolution mechanisms and cathodic hydrogen induced cracking mechanisms. In case of hydrogen induced SCC, the additional effect beyond typical SCC exists in an interaction of hydrogen with the metal lattice. In this case, the level of mechanical stresses is of minor importance compared with the reaction of hydrogen. A prerequisite for hydrogen induced SCC is a small uniform or local corrosion attack of the material or a reaction between reaction layers and the electrolyte with subsequent hydrogen production [4].

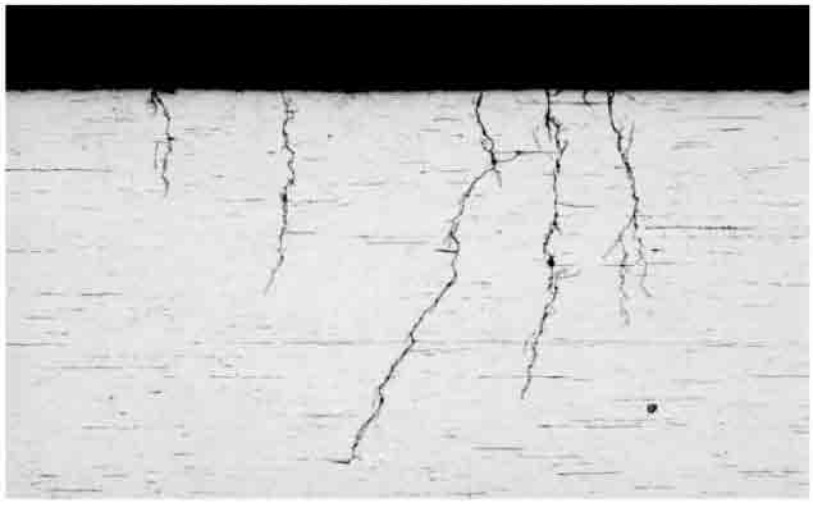

Figure 3.4-1. Microscopic detail of SCC in a steel component, from ref. [3].

SCC is a delayed failure process. That is, cracks initiate and propagate at a slow rate (for instance, 10E-9 to 10E-6 m/s) until the stresses in the remaining ligament of metal exceed the fracture strength. The sequence of events involved in the SCC process is usually divided into three stages [33]:

1. crack initiation,
2. steady state crack propagation, and
3. final failure.

IGSCC is associated with a sensitised material, e.g. sensitised austenitic stainless steels are susceptible to IGSCC in an oxidising environment. Sensitisation of unstabilised austenitic stainless steels is characterised by a precipitation of a network of chromium carbides with depletion of chromium at the grain boundaries, making these boundaries vulnerable to corrosive attack. TGSCC is caused by aggressive chemical species, especially if coupled with oxygen and combined with high stresses. PWSCC is a form of IGSCC and is defined as intergranular cracking in primary water within specification limits. So PWSCC can occur without the presence of additional aggressive species. An example of PWSCC is IGSCC of Inconel 600 alloy in primary water. IASCC refers to intergranular cracking of materials exposed to ionising radiation. As with SCC, IASCC requires stress, aggressive environment and a susceptible material. However, in the case of IASCC, a normally non-susceptible material is rendered susceptible by exposure to neutron irradiation [4, 15].

Flow accelerated corrosion (FAC)

FAC, also called corrosion/erosion mechanism, refers to the combined action of corrosion and erosion (i.e. the mechanical action of a fluid on a metal surface) [1, 6]. The corrosion resistance of unalloyed or low alloyed ferritic steels in water and steam depends on the formation of protective oxide layers. When these layers are removed, the corrosion attack on the metal surface can occur in the form of metal dissolution. The flow conditions shift the equilibrium between protection layer removal and formation which determines the material consumption. The severity of erosion varies with the material type, the fluid temperature, the fluid velocity, the oxygen content in the fluid and the component geometry. The result of FAC is an increased rate of attack on metal because of the relative movement between a corrosive environment and the metal surface. Carbon and low-alloy steels are susceptible to FAC [4, 15].

The FAC process is an extension of the generalised carbon steel corrosion process in stagnant water. In stagnant water, the carbon steel corrosion rate is low and decreases parabolically with time due to the formation of a protective oxide film at the surface. FAC takes place at low flow velocities and the corrosion rate is constant. The difference between generalised corrosion and FAC is the effect of water flow at the oxide-feedwater interface [1].

Consequences of the corrosion/erosion mechanism are thinning of component walls until leakage or rupture occurs, depending on the total stress as well as the deposition of the eroded particles at locations where there is a low flow velocity (wastage) [4].

Microbiologically influenced corrosion (MIC)

MIC is the accelerated corrosion of materials resulting from surface microbiological activity. MIC is characterised by the formation of microbial colonies and associated scale and debris on the surface of the metal. MIC affects carbon steels and, to a lesser extent, stainless steels and nickel alloys. Any buried system or system using untreated water is susceptible to MIC. The major factors increasing the growth of MIC are temperature, pressure, pH, water content and oxygen [15].

Components in conventional power plants which have experienced corrosion degradation in one or more of its various forms include [29]: headers, downcomers, tubing, ductwork, precipitator and drums.

Components in NPPs which have experienced corrosion degradation in one or more of its various forms include [1, 4]:

- BWRs; main steam pipe, safe ends, recirculation pipe and recirculation pumps,
- PWRs; pressurizer, feedwater piping, nozzles and reactor coolant pump,
- LWRs; RPV, RPV internals, control rod drive mechanisms, feedwater pipe and emergency diesel generators,
- HWR RPVs; calandria vessel,
- steam generator; vessel shell, tubes and grid,
- steam and water piping vessels valves,
- turbine; casing and blades,
- condensor tubes.

3.5 Creep

Creep is the deformation that occurs over a period of time in a material subjected to a stress, even below the elastic limit. Creep reaches a significant level above 0.4 times the melting point of the material [4, 6]. Due to thermal activation, materials can slowly and continuously deform even under constant stress and eventually fail. Depending on the component, the final failure may be limited either by deformation or by fracture [11]. An example of creep crack in a piping component is presented in Figure 3.5-1.

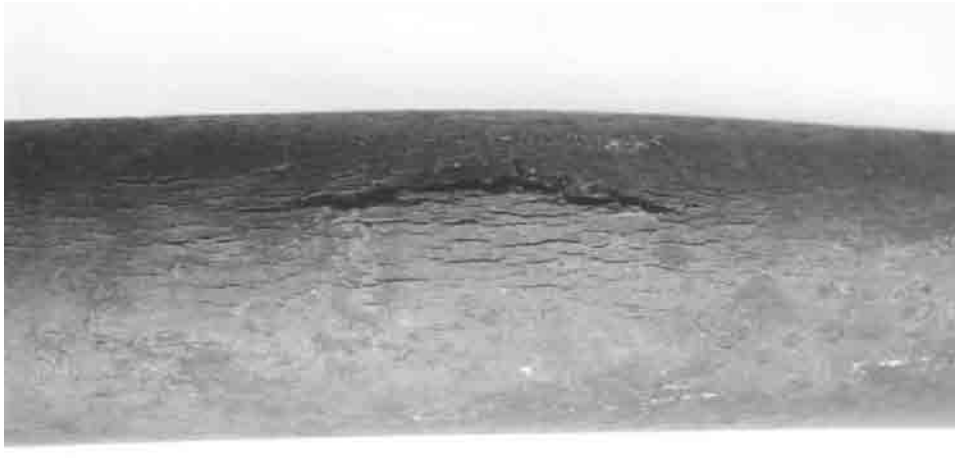

Figure 3.5-1. Creep induced crack that has propagated through a pipe wall, from ref. [3].

The propagation of creep is determined by several competing reactions, including [11]:

- strain hardening,
- softening processes; recovery, recrystallisation, strain softening and precipitate overageing,
- damage processes; cavitation and cracking.

Of the above mentioned reactions, strain hardening tends to decrease the creep rate, whereas the other reactions tend to increase the creep rate [11]. Basically, two processes occur in the micro-structure that affect the material properties [11, 4]: plastic deformation processes and changes in the microstructure.

Both of these processes are time dependent and they show certain interactions. The changes in the micro-structure can be caused by high temperatures alone, since they are the consequence of thermally activated mechanisms [4].

Deformation due to creep is usually divided into three regimes; primary, secondary and tertiary, see Figure 3.5-2. These regimes are controlled by different mechanisms. Components are usually designed to be operated only in the primary and secondary regimes. The time dependent creep damage processes occur according to the following steps [11, 4]:

- Creep damage in the primary and secondary regimes, in which the occurred damage is not irreversible.
- Nucleation of creep pores near the end of the second regime.
- Coagulation of the creep pores to form micro-cracks.
- Crack growth due to creep. In this regime spontaneous failure can occur when large sections of the material have already suffered from this process.
- Creep rupture. With increasing exposure time and accumulation of micro-structural damage the ability for creep deformation decreases and thus ruptures occur in the part that very low ductility.

An aggressive environment can have an influence on the creep behaviour and the degree of damage resulting from it. In metallic materials, an internal oxidation process can occur and accelerate the creep process [4]. The initial creep strength depends on the initial strength of the material at the considered temperature. If the thermally induced process (thermal ageing) leads to a decrease in strength, then more unfavourable conditions have to be expected concerning the long range creep behaviour [4, 11].

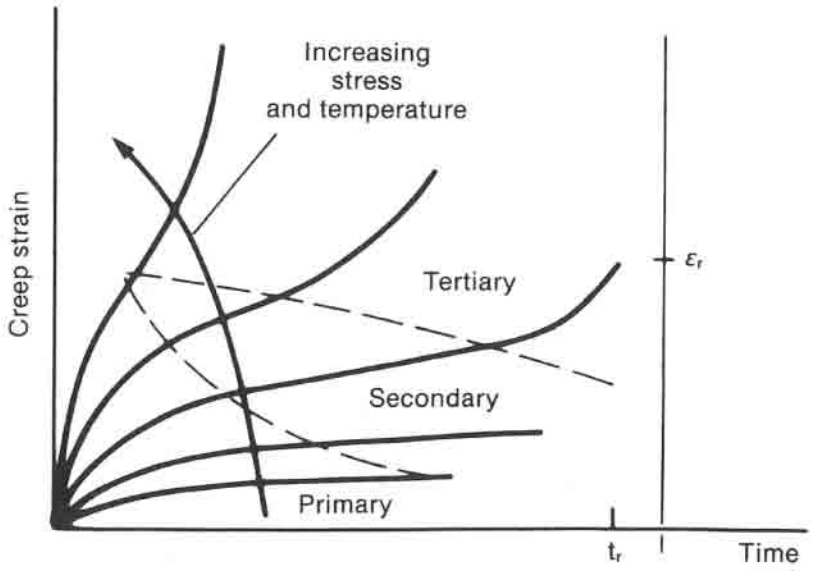

Figure 3.5-2. Schematic illustration of creep damage curve showing the three different creep regimes; primary, secondary and tertiary, from ref. [11]. Here ε_r is rupture strain and t_r is rupture time, respectively.

Components in conventional power plants which have experienced creep degradation include [29]: superheater and reheater headers, piping as well as superheater and reheater tubing.

Components in NPPs in which creep degradation has occurred include [1, 4]: RPV internals of PWRs and in HWR RPVs calandria vessel, pressure tubes and calandria tubes.

3.6 Irradiation embrittlement

Materials exposed to neutron irradiation undergo changes in microstructure and properties. The extent of the changes depends on the material, neutron flux, flux spectrum, fluence and irradiation temperature. In addition to the lattice defects caused by the interaction of fast neutrons with the material atoms, helium can be produced as a result of nuclear reactions. This damage mechanism occurs at neutron fluences above 10E+22 1/cm^2 and temperatures usually above 400 °C. Helium diffuses easily under elevated temperatures and forms voids [4, 6].

The effect of neutron irradiation on metals is mainly to increase the yield and ultimate strength and to reduce the fracture toughness. Helium production does

not only lead to changes in material properties but is also combined with an increase in volume (swelling) [4]. Fracture toughness is the property that governs the material resistance to fast fracture, which for ferritic steels is small at low temperature where the material behaves in a brittle manner, and increases with the temperature until the material becomes ductile. It is generally accepted that the effect of irradiation is to shift this fracture toughness curve to higher temperatures, the shape of the curve being only slightly affected with a small decrease of the upper shelf toughness in the ductile regime [4, 6].

The irradiation degradation sensitivity of the materials depends among other things on [4]: material type, chemical composition, heat treatment and initial mechanical properties. For steels the neutron irradiation is considered to cause significant ageing degradation only for neutron fluences above 10E+17 1/cm^2. Irradiation embrittlement is the major degradation mechanism associated with the ageing of RPVs of PWRs. It is less important for BWR RPVs because of the lower fluence experienced in the BWR vessel environment [32].

Components in NPPs that have experienced irradiation degradation include [1, 4]:

- BWRs; RPV internals, control rod drive mechanisms and emergency diesel generators,
- PWRs; RPV supports,
- LWRs; RPV, RPV internals,
- HWR RPVs; calandria vessel, pressure tubes and calandria tubes.

3.7 Thermal ageing

Thermal ageing refers to gradual and progressive changes in the micro-structure and properties of a material exposed to an elevated temperature for an extended period of time [6]. The dominating parameters responsible for thermal ageing processes are [4]: level of temperature, material state (micro-structure) and exposure time.

In addition to these phenomena, the environment can have an effect to the material state as well. In general, thermal ageing is a damage process typically causing decrease in the material strength properties, hardness, ductility and toughness. Under certain conditions, however, an increase in ductility can be observed, too. One of the dominating factors is the chemical composition of the material and its thermo-mechanical pre-service treatment [4].

The mechanisms occurring in the micro-structure during thermal ageing are of the following types [4]:

- precipitation of particles,
- transformation of phases,
- growth of precipitated phases and the grains of the matrix,
- dissolution of precipitates.

The rate of the above mentioned reactions is strongly dependent on the level of temperature. Such threshold temperatures can exist below which some of the processes are not being activated. The local chemical composition and the diffusion coefficient of the different phases and atoms play an important role [4].

Cast austenitic-ferritic stainless steels (duplex structures) and martensitic stainless steels are susceptible to thermal ageing in the normal operating temperature range of PWRs [34].

3.8 Other degradation mechanisms

Other mechanisms or loading phenomena degrading power plant components include erosion-cavitation, wear, loss of prestressing, water hammer, environment effects, concrete degradation and differential settlement. Here environment effects concern processes or phenomena like wetting-drying and freeze-thaw cycling and chemical attack [6, 17].

Examples of NPP components that have experienced these degrading mechanisms or loading phenomena are presented in the following. Wear has occurred in the steam generator tubes due to contact with anti-vibration bars. Typical components subject to a loss of prestressing are the prestressed cables in the primary containment. Concrete components may be affected by several degradation mechanisms, e.g. aggressive environment can increase porosity, and permeability as well as reduce concrete strength. Atmospheric carbon dioxide can cause concrete carbonation reducing the structural properties of the concrete. Flowing water over concrete surfaces can remove significant amount of concrete. Severe differential settlement can cause concrete cracking and/or misalignment of equipment and can lead to high stresses within the structure [6].

3.9 Interaction of degradation mechanisms

It has been noticed that some degradation mechanisms can provide a joint effect so that it is more severe than the arithmetically added result of their separate

effects. In these cases, the resulting degradation phenomenon is often quite complex. Due to this and also to the fact that the interaction of various degradation mechanisms is still a quite recent research topic, the physical mechanisms of most interaction phenomena are not clear. However, two cases of interacting degradation mechanisms are covered here, those being corrosion fatigue and creep fatigue, as good results concerning their assessment have already been achieved.

Corrosion fatigue

In case of fatigue, in corrosive environments the number of load cycles needed to crack initiation is considerably smaller than that needed in inert environment. In addition to crack initiation, the corrosive environment also influences the ensuing cyclic crack growth rate. The interaction of mechanical alternating stresses and corrosion attack usually leads to transgranular cracking with a low associated deformation. Since the corrosion mechanism is mainly time dependent and the fatigue mechanism is controlled by the number of cycles, a complex interaction between these mechanisms occurs. No threshold conditions exist for corrosion fatigue with respect to the corrosion system and stress amplitude [4].

In corrosion fatigue, the crack growth rate may be influenced by the following features and conditions [4]:

- characteristics of the corrosive environment, such as pH value, temperature, electrochemical potential or oxyen content in water,
- loading frequency and wave form,
- mean load and load amplitude,
- sulphur content of steel.

Several corrosion fatigue mechanisms have been proposed to explain the enhanced crack growth rates with varying degrees of success. The generalised corrosion fatigue cracking mechanism involves the single or mutual occurrence of hydrogen induced cracking and/or anodic dissolution at the crack tip. According to current understanding there appears to be at least four possible mechanisms of anodic dissolution [7]:

- slip dissolution,
- brittle film rupture,
- corrosion tunnelling,
- selective dissolution (dealloying).

Hydrogen embrittlement appears to be divided into the following five types of mechanisms [7]: decohesion, pressure, adsorption, deformation and brittle hydride.

The balance between various phenomena is difficult to sort out. A common approach is to assume that dissolution and hydrogen induced cracking processes are competitive, so that only one of them makes the major contribution to cracking and the others can be ignored. However, both processes (dissolution and hydrogen evolution) can occur simultaneously at the crack tips over ranges of potential that have been measured or that are suspected to occur [7].

Components in conventional power plants in which corrosion fatigue degradation can occur are those mentioned earlier experiencing fatigue, but which are also exposed to corrosive environment [29].

Components in NPPs having experienced corrosion fatigue degradation include [1, 4]:

- BWRs; RPV internals,
- HWR RPVs; calandria vessel, pressure tubes and calandria tubes,
- steam generator; tubes,
- steam and water piping vessels valves,
- main coolant pump; casing and shaft impeller,
- turbine; casing, blades and shaft,
- condensor tubes.

Creep fatigue

In power plant components which operate at relatively high temperatures, changes in prevailing conditions during operation cause transient temperature gradients. If these transients are repeated, the differential thermal expansion during each transient results in a thermally induced cyclic stress. The extent of the resulting fatigue damage depends on the nature and frequency of the transient, on thermal gradient in the component and on material properties. In case of such components, the damage caused by both fatigue and creep has to be taken into account [11].

The principal method of studying creep fatigue interactions has been to conduct strain controlled fatigue tests with and without a holding period (hold time) during some part/phase of the test. With higher frequencies and shorter hold times, fatigue dominates the degradation process, and the flaws initiate near the specimen surface and propagate transgranularly. With lower frequencies and longer hold times, creep begins to play a significant role in the degradation pro-

cess, and the initiating flaws are of a mixed mode involving both fatigue cracking and creep cavitation. With prolonged hold times and only seldom occurring load cycles, creep dominates the degradation process [11].

There is ample evidence to show that rupture ductility has a major influence on creep fatigue interaction. In case of ferritic steels and austenitic stainless steels, the lower the ductility, the lower is the creep fatigue endurance. In addition, long hold times, small strain ranges and low ductility favour creep dominated failures, whereas short hold times, intermediate stress ranges and high ductility favour creep fatigue interaction failures [11]. As an example, the effect of tensile hold time on fatigue endurance of type 316 stainless steel is shown in Figure 3.9-1 in the following.

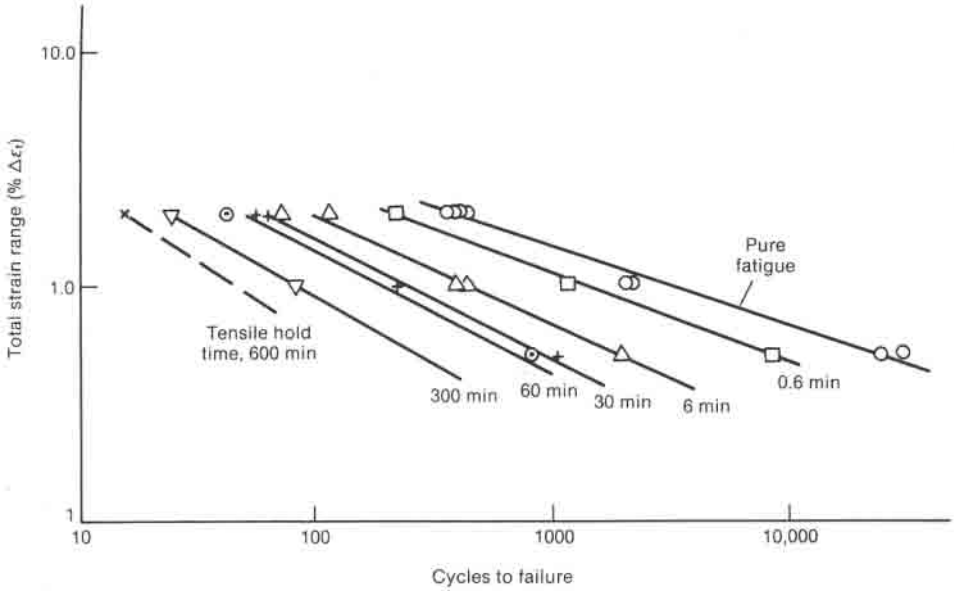

Figure 3.9-1. Effect of tensile hold time on fatigue endurance of type 316 stainless steel, from ref. [43].

Due to operational temperature range in NPPs being in general below the creep range of the metallic pressure boundary components, creep fatigue mainly relates to conventional power plants, where it can degrade those components mentioned earlier which have experienced fatigue, but which are also operated at temperatures that are near or exceed 0.4 times the melting point of the involved materials.

4. Deterministic analysis methods

4.1 Introduction

A brief overview of deterministic analysis methods is presented in the following. This is divided to structural mechanics based analysis methods, including fracture mechanics, and to some considerations concerning analysis methods based on other fields of science.

A description concerning the structural mechanics based analysis methods is provided with emphasis and an example on power plant components and conditions. In this connection, no actual computation equations/procedures are presented, but instead some relevant approaches and analysis tools are considered. Whereas in case of the fracture mechanics based analysis methods, which issue is also dealt with further in this thesis, some relevant computational parameters and procedures are briefly presented as well. Often, the connection between structural mechanics and fracture mechanics is such that the results obtained with the former procedures provide input data for computations carried out with those of the latter. Analysis methods based on other fields of science are mainly beyond the scope of this thesis, however some relevant connecting topics are pointed out.

4.2 Analysis methods based on structural mechanics

Structural mechanics mainly deals with mathematical modelling of structures, together with associated loading and supports, to compute stresses/forces and deformations they experience.

The basic function of any structure is to carry loads and transmit forces. In case of power plants, typical considered structures include straight pipe components, pipe bends, pipe T-joints and pressure vessels, as well as reinforced concrete structures, such as slabs and walls, which often support the aforementioned components.

The structural models describe the geometry and material properties of the considered structure. Depending on the strived accuracy, as well as shape and supports of the considered structure, the model can have one, two or three dimensional geometry. There are also several possible material models, for instance linear-elastic, elastic ideally-plastic, and elastic non-linear plastic. Also, the stress/strain hardening behaviour can be history dependent, with typical modelling options being then to use isotropically or kinematically evolving yield surface, or their combination. Further, more advanced material models exist, such as ORNL model [35] that covers both elastic-plastic material behaviour and thermal creep.

Generally, loads on structures fall into several categories, with some notable examples of these being dead loads, live loads and accident loads. In power plant environments the dead loads typically cover self-weights of the load bearing concrete and steel structures. Also, the self-weights of process components, such as those mentioned above, should be considered as dead loads as they are not movable, even though at time intervals component replacements may have to be carried out. Live or imposed loads are movable or actually moving loads. In power plant environments, these mainly include temperature, pressure and flow rate, all caused by the process fluid, being either water or steam. At operational conditions these load parameters have most of the time constant values, however during anticipated/budgeted controlled load transients, such as start-up and shut-down, they vary as well. The structures carrying these loads form in power plants the pressure boundary. When including loads to a structural model, some idealisations are performed. As power plant components are mainly exposed to mechanical and thermal loads, only they are considered in the following. Depending on the capability and scope of the structural model, mechanical loads can be included as pressures against surfaces, line loads distributed along a surface line, and as point specific forces. Also translations and rotations can be used as loads. Thermal loads are typically set to act on component surfaces. Depending on the approach, loads can be given as time dependent or independent.

There is a large variety of possibilities how a structure can be supported. The stiffness of support conditions can vary from rigid to very flexible. For instance, the support conditions of power plant piping systems are often relatively flexible, so as to allow thermal deformations to occur during load transients without causing excessive restrained thermal stresses. Whereas the NPP RPVs often have a support skirt, a steel structure that is welded around them at some height in the upper half, with the aid of which the RPVs firmly rest on a reinforced concrete structure. When including supports to a structural model, some idealisa-

tions are performed. Depending on the scope of the structural model, support conditions can be set on surfaces, lines, and points. Typical support modelling options include limiting at one or several locations translations and/or rotations in/around one, two or three directions to zero. Support conditions can be time dependent or independent.

When carrying out a structural mechanics based analysis, a model for the considered structure must be prepared first. Then convenient mathematical methods are sought for solving the unknown model parameters. In the simple case, the model can be a set of analytical equations. In case of power plant components, numerical structural models are often used. These are typically prepared using finite element method (FEM) based analysis codes. The basic principle concerning this methodology is to provide approximate solutions for the governing set of partial differential equations in a finite number of nodes using suitable interpolation functions. In the modelling process, the considered geometry is divided to a finite number of sub-regions, called elements, within and on the edges of which are nodes, to which in turn the solution values are interpolated from the integration points. There are numerous advanced commonly used general purpose FEM codes. Such FEM codes also allow using elements of differing types in the same model, as well as provide tools for sub-modelling, with which locally more dense element meshes can be realised. Other numerical techniques exist as well, such as finite difference method. To achieve sufficient accuracy using numerical methods, dense enough computation grids are to be used, and in time dependent analyses small enough time increments. In addition, case specifically combined methods can be used, i.e. FEM solutions supplemented with those computed using analytical equations.

In the following are structural mechanics modelling approaches used for analysing power plant components/systems, and some application examples:

- analytical equations; dimensioning of single components, computing stresses caused by inner pressure for straight pipe components,
- truss models; to describe behaviour of simple auxiliary support structures,
- beam models; dimensioning and stress distribution analyses of piping systems,
- shell models; pipe bends, some pressure vessels,
- solid three dimensional models; RPV, piping T-joints.

The types of analyses often performed for power plant components/systems include:

- linear or non-linear time dependent or independent static stress/strain analyses,
- heat transfer analyses,
- combined sequential or coupled heat transfer and stress/strain analyses,
- dynamic eigenvalue and/or eigenfrequency analyses.

As for the obtained results, typically they are time dependent or independent stress/strain fields and temperature fields. From the stress/strain analysis results, local/global maximum/minimum values are often sought, and such can take place e.g. in inner corner with relatively small radius or where wall thickness changes abruptly. The maximum stress values are compared to corresponding material strength, e.g. to see whether the component in question meets the associated structural strength requirements. Whereas in case of thermal results, in addition to maximum and minimum values often also temporary temperature gradients through wall are sought, because they in turn cause thermal stresses. Of particular interest of the time dependent stress/strain results are the local stress/strain fluctuations, because they form the corresponding stress/strain cycles needed in fatigue analyses often performed for power plant components. As for the dynamic analyses, their results are needed e.g. to assess the structural response to assumed earthquake loads.

Such results as nominal stresses, local stresses and stress fluctuations, from structural mechanics analyses, are often needed as input data in fracture mechanics based analyses.

Most analyses of mechanics are deterministic. In this approach, single or fully pre-determined values are used for all input data parameters, such as yield strength or frequency of load cycle occurrence. The input data parameters often having markedly distributed characteristics in reality, such as yield strength, are also considered as distributed in the probabilistic analyses applying structural reliability methods. Such distributions are formed by fitting a suitable distribution function to applicable experimental or simulated data. The results from deterministic analyses provide no data concerning their uncertainty/reliability, whereas those from structural reliability analyses are probabilities or probability distributions.

As an example concerning structural mechanics analyses, in the following is presented a numerical lifetime analysis for an outlet header in a conventional power plant. The analysis data are from the article [38]. The outer diameter of the outlet header is 711 mm, whereas its wall thickness and total length are 36 mm and 18 272 mm, respectively. The material of this component is ferritic-martensitic steel X20CrMoV121. As for loads, mainly load transient start-up and pressure variation during operation are considered. During the former of these load events both temperature and pressure rise in a controlled process within approximately three hours from room temperature and one bar to operational values of 535 °C and 2.6 MPa.

The overall element mesh of an Abaqus FEM model of a section of the outlet header and the tubes connecting to it is shown in Figure 4.2-1. For more details concerning the Abaqus code, see refs. [36, 37]. The outlet header is supported by the tubes, which are cut on certain length in the model, and appropriate deformation boundary conditions are given to the cut surfaces, as well as to those of the header region. For both the heat transfer and static analyses of the outlet header region of the model, isoparametric four node linear tetrahedron elements are used, whereas those used for the connecting tubes are isoparametric eight node linear hexahedron “brick” elements. The former element type contains one integration point, whereas the latter contains four. An example of the stress result distributions for the most stressed header/tube joint, namely that concerning Row5 tube, is shown in Figure 4.2-2 below for a selected time instant from the duration of load transient start-up [38].

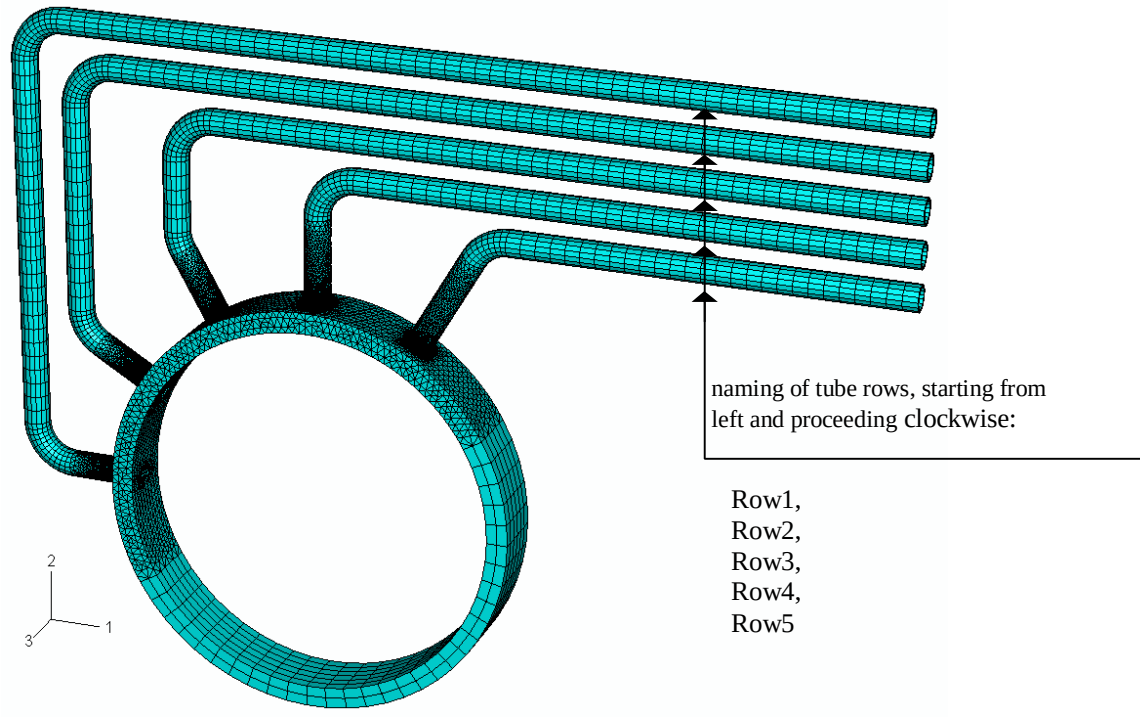

Figure 4.2-1. The overall element mesh of the FEM model of the outlet header section and tubes connecting to it. The number of elements/nodes is approximately 150 000/46 000, from ref. [38].

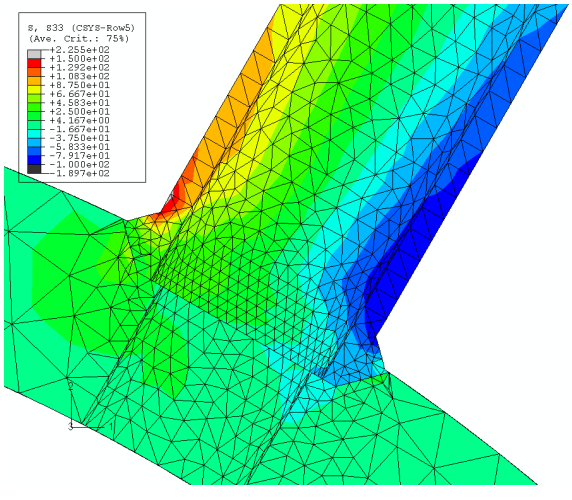

Figure 4.2-2. Distribution of axial stresses [MPa] in the Row 5 joint middle section of the FEM model of the outlet header and the tubes in the middle of load case start-up, from ref. [38].

4.3 Fracture mechanics based analysis methods

Fracture mechanics concerns the design and analysis of structures which contain cracks or flaws. On some size scale, all materials contain flaws, which are either microscopic, due to cracked inclusions, debonded fibers etc., or macroscopic, due to corrosion, fatigue, welding flaws, etc. Thus fracture mechanics is involved in any detailed design or safety assessment of a load bearing structure. As cracks can grow during service due to e.g. fatigue, fracture mechanics assessments are required throughout the lifetime of a structure or component, not just in the beginning of the lifetime.

Some theoretical background of fracture mechanics is presented in the following. At the top level, fracture mechanics is divided into linear-elastic fracture mechanics (LEFM) and elastic-plastic fracture mechanics (EPFM). Materials with relatively low fracture resistance that fall below their so called plastic collapse strength can be analysed on the basis of elastic concept through the use of LEFM. For other materials, the use of EPFM is often necessary.

For certain cracked component geometries subjected to external forces, it is possible to derive closed form expressions for stresses, assuming linear-elastic material behaviour. Westergaard [39] and Irwin [40] were among the first to publish such solutions.

There are three types of loading that a crack can experience, as Figure 4.3-1 illustrates. Mode I, where the principal load is applied normal to the crack plane, tends to open the crack. Mode II corresponds to in-plane shear and tends to slide the crack faces with respect to each other. Mode III refers to out-of-plane shear. A cracked component can be loaded with any of these modes, or with a combination of two or three modes.

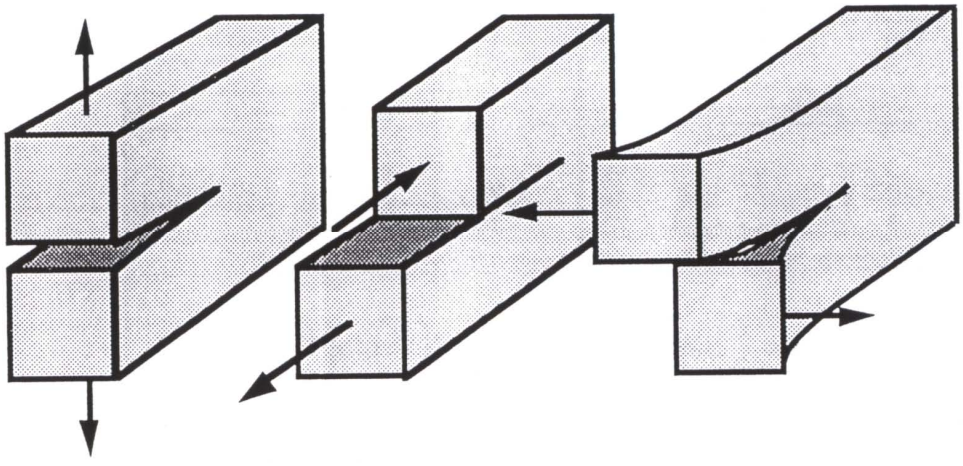

Figure 4.3-1. The three modes of loading that can be applied to a crack, from ref. [30].

Of the fracture mechanics parameters, the stress intensity factor, K, completely characterises the crack tip conditions in a linear-elastic material. Usually K is provided with a subscript to denote the mode of loading, i.e. K_I, K_{II} or K_{III}. The stress fields ahead of a crack tip in an isotropic linear-elastic material can be written with polar coordinates as:

$$\lim_{r\to 0}\sigma_{ij}^{(I)} = \frac{K_I}{\sqrt{2\pi r}} f_{ij}^{(I)}(\theta) \tag{4.3-1a}$$

$$\lim_{r\to 0}\sigma_{ij}^{(II)} = \frac{K_{II}}{\sqrt{2\pi r}} f_{ij}^{(II)}(\theta) \tag{4.3-1b}$$

$$\lim_{r\to 0}\sigma_{ij}^{(III)} = \frac{K_{III}}{\sqrt{2\pi r}} f_{ij}^{(III)}(\theta) \tag{4.3-1c}$$

where σ_{ij} is stress tensor, r and θ are the radial and angular coordinates of the polar system, and f_{ij} is a dimensionless function of θ, respectively. In a mixed mode problem, i.e. when more than one loading mode is present, the individual contributions to a stress component are additive [30]:

$$\sigma_{ij}^{(total)} = \sigma_{ij}^{(I)} + \sigma_{ij}^{(II)} + \sigma_{ij}^{(III)} \tag{4.3-2}$$

If one assumes that the material fails locally at some critical combination of stress and strain, then it follows that fracture must occur at critical stress intensity, K_{IC}. Thus K_{IC} is a measure of material fracture toughness. Failure occurs when $K_I = K_{IC}$. In general, the stress intensity factor (SIF) has the following form [30]:

$$K = BS\sqrt{\pi a} \tag{4.3-3}$$

where a [mm] is the crack depth (dimension of the crack in the principal direction of the crack growth), S [N/mm^2] is the remote stress resulting from the applied load, and $B = B(a)$ [-] is a factor that accounts for the geometry. For any crack in any practical problem, only the factor B needs to be derived. For many geometries B can be found in handbooks. Typically, rapidly occurring brittle fracture is associated with fracture toughness parameter, K_{IC}.

When fracture is accompanied with considerable plastic deformation, EPFM is applied. An often used fracture parameter in EPFM is called J-integral. J is simply the strain energy rate, and it can be derived from a conservation of energy criterion. In EPFM fracture occurs when [30]:

$$J = J_R \tag{4.3-4}$$

where J_R [J/mm^2] is the fracture energy, which represents the material fracture resistance. Consider an arbitrary counter-clockwise path Γ around the tip of the crack, as is shown in Figure 4.3-3. The J-integral is defined as [30]:

$$J = \int_{\Gamma} \left(w dy - T_i \frac{\partial u_i}{\partial x} ds \right) \tag{4.3-5}$$

where w [N/mm^2] is the strain density, T_i [N/mm^2] are the components of the traction vector, u_i [mm] are the displacement vector components, ds is a length increment along the contour Γ, whereas x and y are coordinate variables as shown in Figure 4.3-2. The strain energy density w in equation (4.3-5) is defined as [30]:

$$w = \int_0^{\varepsilon_{ij}} \sigma_{ij} d\varepsilon_{ij} \tag{4.3-6}$$

where σ_{ij} [N/mm^2] and ε_{ij} [mm/mm] are the stress and strain tensors, respectively. Typically, stabily and more slowly occurring ductile fracture is associated with fracture toughness parameter J_R.

Another applicable parameter used in EPFM is crack tip opening displacement (CTOD). Unlike in the case of linear-elastic materials, the crack tip may experience plastic deformation by blunting in strain hardening materials. The opening at the crack tip, i.e. CTOD, is a measure of fracture toughness. Crack tip blunting and CTOD, denoted here by δ, are illustrated in Figure 4.3-3.

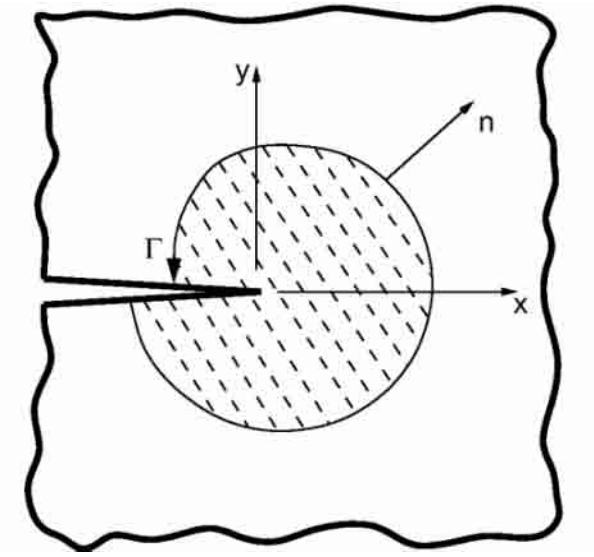

Figure 4.3-2. Arbitrary contour around the crack tip.

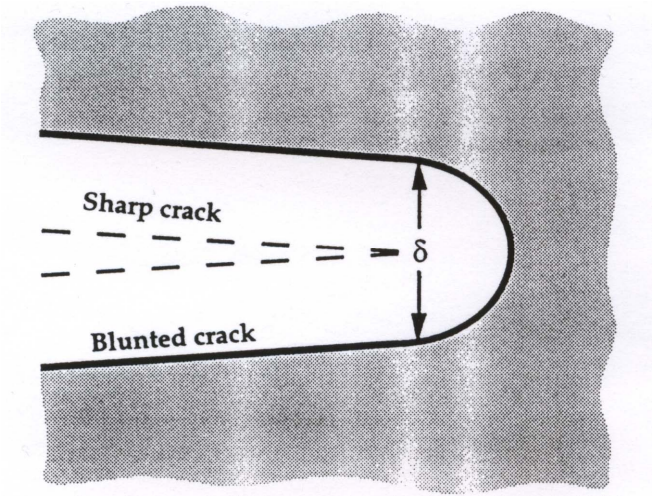

Figure 4.3-3. Blunting of the crack tip and CTOD, from ref. [30].

A general form for CTOD can be expressed as [30]:

$$\text{CTOD} = \delta = \frac{K_I^2}{m\sigma_y E} \tag{4.3-7}$$

where σ_y [N/mm^2] is the yield strength, E [N/mm^2] is the Young's modulus and m is a dimensionless constant that is approximately 1.0 for plane stress and 2.0 for plane strain. There exist a number of alternative geometric definitions for CTOD.

Hutchinson [41] as well as Rice and Rosengren [42] independently showed that J-integral characterises crack tip conditions in a non-linear-elastic material. They each assumed a power law relationship between plastic strain and stress. The result of their work is called the HRR singularity, which is one of most commonly used EPFM models. According to this model, the actual stress and strain distributions are obtained by applying the appropriate boundary conditions as follows:

$$\sigma_{ij} = \sigma_0 \left(\frac{EJ}{\alpha \sigma_0^2 I_n r} \right)^{\frac{1}{n+1}} \tilde{\sigma}_{ij}(n,\theta) \tag{4.3-8}$$

$$\varepsilon_{ij} = \frac{\alpha\sigma_0}{E}\left(\frac{EJ}{\alpha\sigma_0^2 I_n r}\right)^{\frac{n}{n+1}} \tilde{\varepsilon}_{ij}(n,\theta) \tag{4.3-9}$$

where σ_0 is reference stress (most often yield strength), r is polar coordinate with origin at the crack tip, α is dimensionless constant, n is strain hardening exponent and I_n is an integration constant that depends on n, whereas $\tilde{\sigma}_{ij}$ and $\tilde{\varepsilon}_{ij}$ are dimensionless functions of n and θ. These parameters depend also on the stress state, i.e. plane stress or plane strain. The J-integral defines the amplitude of the HRR singularity, just as SIF characterises the amplitude of the linear elasticity. Thus, J-integral completely describes the conditions within the plastic zone. A structure in small scale yielding has two singularity dominated zones: one in the elastic region, where the stress varies as $1/\sqrt{r}$, and one in the plastic zone, where stress varies as $r^{-1/(n+1)}$. The latter zone often persists long after the linear-elastic singularity zone has been taken over by crack tip plasticity.

In the following are analysis approaches used for fracture mechanics assessments of power plant components/systems, and some application examples:

- analytical equations; K, J-integral and CTOD values for static crack postulates in single material components with regular geometry and load distribution shape,
- weight/influence function based analysis codes; K and J-integral values for static and growing crack postulates in single material components with regular geometry and arbitrary load distribution shape,
- general purpose FEM codes; K, J-integral and CTOD values for static and growing crack postulates in single and multi-material components with arbitrary geometry and load distribution shape.

Fracture mechanics based structural integrity assessment procedures are covered in more detail further in this thesis, including both deterministic and probabilistic approaches, see Chapters 7, 8 and 12.

Most fracture mechanics analyses are deterministic, e.g. a single value of fracture toughness is used to estimate failure stress or critical crack size. Much of what happens in the real world, however, is not predictable. For instance, fracture toughness data in the ductile to brittle transition region are widely scattered. With structural reliability analyses, these distributed characteristics can be taken into account. The results from deterministic analyses provide no data concerning

their uncertainty/reliability, whereas those from structural reliability analyses are probabilities or probability distributions.

4.4 Analysis methods based on other fields of science

A field of science necessary for any kind of structural analyses concerning power plant systems/components is that associated with material properties/behaviour. Namely power plant environments not only include a relatively large number of different materials, for instance ferritic and austenitic steels of several types in the pressure boundary, but also provide a range of challenging mechanical loading, thermal and chemical conditions. Thus it is necessary to clarify how the material properties vary as a function of e.g. operational temperature range as well as how the inner surfaces of components respond to various kinds of chemical attacks. For instance, both the yield strength and ultimate strength decrease as a function of temperature, the extent of which is a material specific issue. Typically, relatively thin protective oxide layers form on the inner surface of power plant components. However, the layers can locally rupture as depending on changes in local chemical conditions, which in turn increases corrosion rate as fresh metal becomes exposed to corrosive conditions. The assessment of thermal ageing, which was mentioned earlier in Section 3.7, requires material science associated data as well. The clarification of these material behaviour/property issues requires experimental research.

Fluid mechanics is needed when simulating the flow patterns in more complex flow conditions, such as turbulent mixing of water flows of differing temperatures in piping T-joints. Results from these analyses include fluid temperature and pressure distributions as well as distributions for the heat transfer coefficient between the fluid and component inner surface. A more recent development is numerical fluid-structure interaction analyses. When an abrupt increase in flow rate occurs, e.g. caused by sudden closing of a valve, the pressure impulse can be of such magnitude that it may cause temporarily notable deformations to the component containing fluid. In such cases, these phenomena need to be taken into account in the structural integrity analyses. The results from the fluid mechanics analyses produce input data to structural mechanics based computations, including fracture mechanics.

Particle physics is needed when assessing the characteristics of the neutron irradiation that causes changes in microstructure and properties of the materials exposed to it. The extent of these changes depends on the material, neutron flux,

flux spectrum, fluence and irradiation temperature. The effect of neutron irradiation on metals mainly increases the yield and ultimate strength and reduces the fracture toughness. Thus, it is obvious that these effects need to be taken into account in structural integrity analyses. In practise, irradiation effects concern only NPP RPVs, as was explained in Section 3.6.

5. Probabilistic analysis methods

5.1 Introduction

There exists a number of methods to determine the probabilities of the variable(s) of interest of a system. Monte Carlo simulation is a simple and most accurate procedure to analyse probability distributions. This procedure has one major drawback, though, which is the often remarkable amount of computation work required in order to achieve sufficient accuracy for the results. This limiting or even prohibiting feature is emphasised especially in the situations where a very low probability is to be determined. Refined Monte Carlo methods provide rather sophisticated procedures, such as stratified sampling and importance sampling, which can help to overcome these difficulties [76]. As the efficiency, capacity and affordability of available computers keeps improving swiftly, Monte Carlo simulations become easier and more economical to perform.

Due to Monte Carlo calculations being often rather costly and laborious to perform, approximation methods for the calculation of variable probabilities are of great interest. Examples of these are first-order second-moment methods (FORMs) and second-order reliability methods (SORMs).

Determining probabilities from scarce and incomplete input data is another problem. The first question that arises is how to handle the data basis in order to end up with input distributions reflecting all the information available. This problem is dealt with in the statistical estimation theory. Once an appropriate statistical model has been set up and the parameters of this model have been determined from the input data, the probability of interest can be computed in a straightforward manner [76].

There are two basic philosophical schools in modern probability theory, one based on a frequency interpretation, and one based on a Bayesian interpretation or degree of belief. These are also known as the objective and the subjective interpretation, respectively. According to frequency interpretation, a probability

is an objective property of some event. In terms of failure probability, it is the expected probability of failure that is reflected. In Bayesian philosophy, a probability is considered as a subjective degree of belief, for example, in the chances of a particular event occurring. This probability, or degree of belief, depends on the amount of information available. Bayesian probabilities are also called subjective [45].

Before going on to describe in more detail the characteristics of various probabilistic methods, some basic definitions are presented first.

5.2 Failure probability and reliability

Failure probability, P_f, is often defined as the mean frequency with which the specified failure event would be expected to occur in a given period of operation, typically one year. When assessing the probability of failure, it is important to consider the future deterioration rate from all potential mechanisms. The rate of degradation may increase in time due to interaction between mechanisms (e.g. corrosion and fatigue). Factors, such as overload, misuse, or accidental damage that cannot be easily predicted should be assumed to occur at a constant average rate [3].

Reliability, R, is closely related to the failure probability, and expresses the probability of a component not failing [46]. The relation between reliability R and probability of failure P_f is expressed as [47]:

$$R = 1 - P_f \tag{5.2-1}$$

A rigorous structural reliability assessment involves taking into account all sources of uncertainty that may affect the failure of the component or system. This clearly involves taking into account all fundamental quantities entering the problem, and also the uncertainties that arise from lack of knowledge and idealised modelling. These terms are referred to as basic variables. The common engineering quantities they represent include: component diameter, wall thickness, material and contents density, yield strength, maximum operating pressure, maximum operating temperature, corrosion rate, etc. [45].

The structural reliability analysis procedure is outlined by the following steps [45]:

1) Identify all significant modes of failure of the structure or operation under consideration, and define failure events.
2) Formulate a failure criterion or failure function for each failure event.
3) Identify the sources of uncertainty influencing the failure of the events, model the basic variables and parameters in the failure functions and specify their probability distributions.
4) Calculate the probability of failure or reliability for each failure event, and combine these probabilities where necessary to evaluate the failure probability or reliability of the structural system.
5) Consider the sensitivity of the reliability results to the input, i.e. basic variables and parameters.
6) Assess whether the evaluated reliability is sufficient by comparison with a target.

5.3 Uncertainty and sensitivity

The sources of uncertainty that are relevant to structural reliability analysis can be primarily classified into two categories: 1) aleatoric uncertainties; being associated with physical uncertainty or randomness and, 2) epistemic uncertainties; being associated with understanding or knowledge [45].

Aleatoric uncertainty refers to the natural randomness associated with an uncertain quantity, and is often termed Type I uncertainty in reliability analysis. It can be further divided into subcategories as shown in Figure 5.3-1. Aleatoric uncertainty is quantified through the collection and analysis of data. The observed data may be fitted by theoretical distributions, and the probabilistic modelling may be interpreted in the relative frequency sense.

Epistemic uncertainty reflects the lack of knowledge or information about a quantity, and is often termed Type II uncertainty in reliability analysis. Epistemic uncertainty can further be divided into subcategories as shown in Figure 5.3-1.

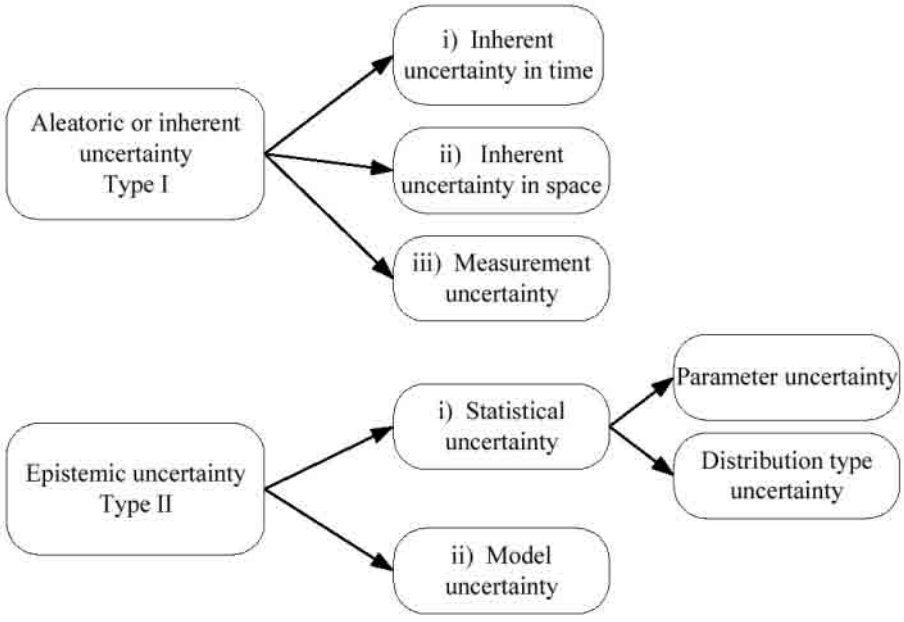

Figure 5.3-1. Two primary types of uncertainty and associated subcategories, from ref. [45].

Model uncertainty arises because many of the engineering models used to describe natural phenomena, to analyse stresses and to predict failure of components are imperfect. Models are often based on idealised assumptions, they may be based on empirical fits to test results or observed behaviour, and variables of lesser importance may be omitted for reasons of efficiency (or ignorance) [45].

There are difficulties in quantifying model uncertainty adequately. The errors in the model may be known in relation to more advanced models, but at any level of modelling there are errors relative to the unknown reality. Model uncertainty is often assessed on the basis of experimental results, but this too has a number of limitations. Tests themselves are idealisations or simplifications of reality, and are affected by scale, boundary effects, load rates, measurement errors, etc. Tests are often expensive, and the data need to be carefully screened to ensure that they are consistent. Ideally, the test data should cover uniformly the full range of the applicability of the model.

Statistical uncertainty can be considered to arise from [45]:

- Parameter uncertainty. This occurs when the parameters of a distribution are determined from a limited set of data. The smaller the data set the larger the parameter uncertainty.

- Distribution type uncertainty. This uncertainty arises from the choice of a theoretical distribution fitted to empirical data. It is a particular problem when deriving extreme value distributions.

It may not be possible to distinguish from each other the two types of statistical uncertainty in practice, since with limited data both the parameters and distribution type may be uncertain.

Development of mathematical models for structural analysis purposes consists of several logical steps, one of which should be the determination of parameters which are most influential on model output. A sensitivity analysis (SA) of the input parameters can serve as a guide to any further use of the model [48]. In general, SA is conducted by defining the model and its output parameters, together with their probability density functions and output variable(s), and then assessing the influences or relative importance of each input parameter on the output variable [48].

There is a number of reasons for conducting a SA, including the needs to determine which input parameters contribute most to output variability, which parameters are insignificant and can be eliminated from the final model, and which (group of) parameters interact with each other [48].

5.4 Response function and performance function

A random function can often be described by a number of parameters. In the ideal situation, the parameters are determined from an infinitely large sample. In practise, however, available data are usually limited or non-existent, so a combination of judgement and experience must often be used. Statistical tools can be used to measure the quality of the estimated parameters, i.e. to quantify the uncertainty in the estimates [52].

A common way to define a random variable in the literature is to denote it with a capital letter, X, and a certain value of it with a small letter, x. The distribution of a continuous random variable is controlled by probability density function, $f_x(x)$. Whereas the cumulative distribution function, $F_x(x)$, corresponds to a definite integral of the probability density function over some selected region.

The parameter used in the description of a physical problem is called a response function, Z [47]. This function describes a structural or mechanical response, such as stress, strain or crack growth in a structure. Response function can be a complete FEM model as well. The response function, Z, is expressed as a function of the random variable, X_i, as follows:

$$Z = Z\left(X_1, X_2, X_3, ..., X_n\right) \tag{5.4-1}$$

The performance or limit state function, *g*, gives the failure boundary or critical conditions of a physical problem. It is defined by:

$$g = Z_0 - Z = Z_0 - Z\left(X_1, X_2, X_3, ..., X_n\right) = 0 \tag{5.4-2}$$

where Z_0 is the limiting value of *Z*. The region $g \leq 0$ corresponds to failure, whereas $g > 0$ is the safe domain [51].

The probability of failure can now be defined mathematically as:

$$P_f = P\left[g \leq 0\right] = \int_{g \leq 0} f_x(x)dx \tag{5.4-3}$$

In some cases, equation (5.4-3) can be integrated analytically. In principle, the probability of failure or reliability can be evaluated using numerical integration, e.g. trapezoidal rule or Simpson's rule, etc. In practice, this is not generally feasible in probabilistic analysis because of the number of dimensions of the problem, being one dimension for each basic variable, and because the area of interest is usually in the tails of the distributions. Nevertheless, this equation is occasionally used in numerical form, and with dense enough computation grid it can potentially give accurate enough results [45]. There are procedures to overcome the difficulties encountered in calculating the failure probability, which issue is covered in more detail further in this chapter.

5.5 Commonly applied distribution functions

The number of continuous reliability distributions in available handbooks which empirically describe the scatter of material test data is considerable. The most commonly applied distribution functions include [46]: exponential distribution, normal or Gaussian distribution, log-normal distribution, Weibull distribution, gamma distribution and Gumbel distribution. Some of these functions are symmetric, such as normal distribution, whereas others are asymmetric, such as exponential distribution. Using these functions, probabilistic distributions have been developed e.g. for fracture toughness, initial flaw size and frequency of occurrence of load cycles.

5.6 Review of probabilistic analysis procedures

5.6.1 First-order second moment method (FORM)

To overcome the invariance problem with the failure function, it is necessary to transform the basic variables into independent standard normal variables. A space defined by independent standard normal variables is termed *U*-space, and basic variable space is termed *X*-space.

The transformation of independent variables can be undertaken from the cumulative distribution function, $F_x(x)$, i.e. from the identity [45]:

$$\Phi(u) = F_x(x) \tag{5.6-1}$$

$$x = F_x^{-1}[\Phi(u)] \tag{5.6-2}$$

where $\Phi(u)$ is the standard normal distribution function. Various techniques and software tools for the transformation of the non-independent variables are available.

FORM methods involve estimating the failure probability by linearising the failure surface at the closest point to the origin in standard normal space, or *U*-space, using e.g. Taylor series of the normalised random variables. Iteration is usually necessary to determine the closest point to the origin, and a number of iterative and optimisation techniques are available. The space outside the tangent hyperplane to the failure surface at the closest point to the origin corresponds approximately to the probability of failure.

Even though the failure surface in standard normal space is rarely planar the curvature at the point closest to the origin is usually so small that the first-order linearisation is valid for most purposes. The basic variable transformation and the first-order reliability estimate are illustrated in Figure 5.6-1 with two basic variables.

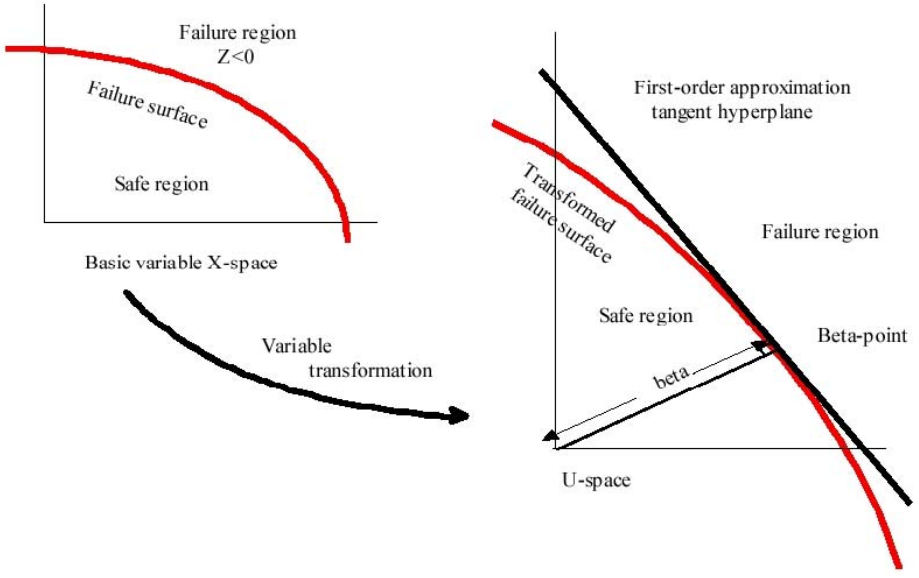

Figure 5.6-1. Illustration of transformation from basic variable space (left) to U-space (right) and first-order reliability estimate, from ref. [45].

The closest point from the failure surface to the origin in *U*-space is the most probable point (MPP) or design point. The distance between these two points is equal to the first-order reliability index, β, denoted as beta in Figure 5.6-1 [45]. This is also referred to as the geometrical reliability index or Hasofer-Lind reliability index [53].

After the first-order transformation, the level curves of the joint density functions become origin centered circles. The limit state surface is a hyperplane in the space of the transferred random variables, meaning the *U*-space. An approximation of the probability of failure is then given by:

$$P_f \approx \Phi(-\beta) \tag{5.6-3}$$

5.6.2 Second-order reliability method (SORM)

Second-order methods improve the accuracy of the first-order probability estimates by including curvature information at the point β, and by approximating the failure surface with a quadratic surface. First is necessary to iteratively identify the point β. The difference between the first- and second-order estimates

gives an indication of the curvature of the failure surface. If there is a significant difference it suggests that perhaps Monte Carlo methods should be used to confirm the probability of failure estimate. For most practical reliability applications, there is usually a small difference between FORM and SORM estimates [45], only.

In many engineering structural problems, the SORM method has satisfactory accuracy, but in some cases, it may lead to erroneous results. A reason for this is that the quadratic approximations may appear to be insufficient when the failure surface is oscillatory in nature or too irregular in the vicinity of the point of maximum likelihood. Moreover, a significant disadvantage of the FORM/SORM methods is that no estimation of the error made is available, and so it is very difficult to validate results [54]. Various methods have been developed to overcome these problems, see e.g. ref. [55].

A general but complicated expression for the failure probability of quadratic forms is derived in ref. [56]. A more convenient but approximate expression has been derived by Breitung as [57]:

$$P_f = \Phi(-\beta)\prod_{i=1}^{n}(1+\beta\kappa_i)^{-0.5} \tag{5.6-4}$$

where κ_i denotes the principal curvatures of the limit state at the minimum distance point.

5.6.3 Fast probability integration (FPI)

In FORM and SORM, the basic random variables are transformed into independent standard normal variables by exact mapping. In some cases, this is not easy to apply and in addition, the original limit state function may become distorted by this transformation. The FPI approach has been developed to overcome these drawbacks. With the FPI, the original distributions are approximated by standard normal variables, instead of transforming them into standard normal. Thus the FPI methods used for linearisation and normalisation are numerical procedures for solving multidimensional integral equations concerning general failure probability or reliability analyses [52].

For instance, the FPI method published by Wu and Wirsching [58] is a SORM, employing a three-parameter normal tail approximation. In this method, the equivalent normals are constructed using a least squares approach. A second

order approximation of the failure surface is used and then transformed into linear one in order to reduce the computational effort. It has been demonstrated, see ref. [59], that the FPI method in the ref. [58] is efficient and provides accurate failure probability estimates.

5.6.4 Mean value methods

Mean value method (MV)

When the response function is implicitly defined by a computer code, the general failure probability or reliability methods are difficult to apply. The MV method [60] is a first-order method that is suitable to be used under these circumstances. This method is based on the assumption that a first-order Taylor expansion of the response function exists. By omitting the higher order terms, the response function is expressed at the mean values as:

$$Z(X) = Z(\mu) + \sum_{i=1}^{n} \frac{\partial Z}{\partial X_i}(X_i - \mu_i) = a_0 + \sum_{i=1}^{n} a_i X_i \qquad (5.6\text{-}5)$$

where parameters a_0 and a_i are coefficients, and the derivatives are evaluated at the mean value points μ_i. The coefficients can in general be computed by numerical differentiation and the minimum number of performance function evaluations (computer runs) is (n+1), where n is the number of random variables [52]. Based on this linear approximation the cumulative distribution function for response function can be obtained directly, since the distributions for the random variables X_i are fully defined and the response function is explicit [61].

Advanced mean value method (AMV)

For non-linear performance functions, the MV solution is often not accurate enough. The AMV method [60, 62] takes the MV solution one step further and is capable of establishing full probability distributions even when the response function is not monotonic, which can result in truncated distributions. In the general failure probability or reliability methods, an iterative optimisation algorithm locates the MPP and then the response function is approximated by a Taylor expansion in the vicinity of this point. In the AMV method, the mean value approximation is used to locate the MPP and then, the corresponding failure

probability is calculated. Then, the analysis is performed again at this point in order to obtain the correct response value.

Advanced mean value method with iteration

In the AMV with iteration, the accuracy of the MPP location, as obtained with the mean value approximation, is improved with an iteration procedure. A new Taylor series expansion is then performed at the MPP obtained from the mean value solution. Another MPP may then be obtained by using the first-order failure probability or reliability method, after which the analysis is performed again at this point. The analysis process is continued in this iterative manner until sufficient accuracy is achieved [52].

5.6.5 Monte Carlo simulation (MCS)

Often when a mathematical formulation for probabilistic structural/fracture mechanics analysis can be defined, it is not possible to solve analytically. In these cases, a probabilistic solution may be obtained through Monte Carlo simulation (MCS). This simulation method is simply a repeated process of generating deterministic solutions to a given problem. Each solution corresponds to a set of deterministic values of the underlying random variables. The main element of a MCS procedure is the generation of random numbers from a specified distribution. There exist systematic and efficient methods for generating such random numbers from several common probability distributions [63].

Because a MCS solution generally requires a large number of repetitions, in particular for problems involving very rare events, its application to complex problems can be computationally costly. Hence, the MCS should be used with some caution. Often, MCS solutions may be the only means for checking or validating an approximate probability computation method [63].

Plain MCS offers a direct method for estimating failure probability. In essence, the technique involves sampling a set of values of the basic variables at random from the probability density function, and evaluating the failure function for the values to see if failure occurs. By generating a large number of samples, or trials, the probability density function is simulated, and the ratio of the number of trials leading to failure to the total number of trials tends to the exact probability of failure [45].

In order to evaluate the failure probability corresponding to a known performance function, $g(X_i)$, the MCS would consist of the following steps [64]:

1. Given the predefined probabilistic density functions (PDFs) of the random variables in the performance function, generate a single value of each variable.
2. Assess the performance function: if $g(X_i) < 0$, a system or component failure takes place.
3. Repeat steps 1 and 2 for N times.
4. Estimate the probability of failure by $P_f = N_f / N$, where N_f is the number of failures.

In order to evaluate the failure probability corresponding to an unknown performance function, the MCS method would consist of the following steps [64]:

1. Given the predefined PDFs of the random variables involved in the deterministic structural analysis (e.g., FEM), generate a single value of each random variable.
2. Perform the deterministic analysis, and record if failure is predicted.
3. Repeat steps 1 and 2 for N times.
4. Estimate the probability of failure by $P_f = N_f / N$, where N_f is the number of failures.

MCS offers a number of advantages [65]:

- The distributions of the model variables do not have to be approximated.
- Correlations and other inter-dependencies can be modelled.
- The level of mathematics required to perform a MCS is quite basic.
- Commercial software is available to automate the tasks involved in the simulation.
- Greater levels of accuracy can be achieved by simply increasing the number of calculated iterations.
- MCS is widely recognised as a valid technique so its results are likely to be accepted.
- The behaviour of the model can be investigated with great ease.

The main drawback with the plain MCS is the computational effort involved. To produce a reasonably accurate estimate of the failure probability, at least $100/P_f$

trials are required. For instance, for failure probabilities around 10E-04, this requires that at least 10E+06 simulations are performed [45].

MCS methods rely on the use of random numbers, which are most conveniently generated numerically with conventional computers. A number of random number generator types are available. However, it is important to realise that all generator types produce pseudo-random numbers that form a long sequence of numbers which, although may be expected to pass all standard tests for randomness, will eventually repeat. For most applications, standard random number generators, often available as functions in software libraries, are acceptable. However, there may be problems if a poor generator is used to generate many millions of samples in a problem involving a large number of basic (random) variables [45].

A variety of techniques have been developed to reduce the number of needed simulations. Generally speaking, these are called variance reduction techniques, and in favourable circumstances, they can be very efficient. These techniques include:

- Importance sampling; modifying the sampling density function to 'important regions' of the failure space,
- Stratified sampling; the sampling space is divided into subspaces from which the sampling is performed,
- Directional sampling; involves sampling along random vectors,
- Adaptive sampling; successive updating of the sampling density function,
- Axis orthogonal simulation; a semi-analytic technique.

These techniques can also be combined together. Knowledge of the failure region can be utilised to significantly improve the efficiency of MCS by tailoring the sampling scheme to the particular conditions.

5.6.6 Response surface methods

When the performance function g of a system is not explicitly known, FORM or SORM are not directly applicable. Therefore, MCS seems to be a suitable approach. The advantages of MCS are obvious, but an innate disadvantage of it is the formidable computational effort for problems involving low probability of failure or the problems that require a considerable amount of computation in each sampling cycle. To overcome this disadvantage, numerous variance reduc-

tion techniques have been proposed, such as those mentioned in the previous section. For certain problems, FORM or SORM can be effectively combined with MCS [66].

However, there are many practical problems that cannot be dealt with the above mentioned methods. Recourse must, therefore, be made to other methodologies which may not be as accurate as the above methods but are nevertheless feasible for a wider spectrum of problems. The response surface method (RSM) is such a method [66].

The basic idea of the RSM is to approximate the performance function g, which may be implicit and/or very time consuming to evaluate, with a response surface function (RSF) that is easier to deal with. The RSF typically takes the form of a set of polynomials. Regression is usually performed to determine the RSF by the least squares method. After the response surface has been fitted at a sequence of sampling points, the reliability analysis can then be carried out. The crux of the RSM is to fit the RSF to g at the sampling points, in particular in the neighbourhood of the design point [66].

5.6.7 Importance sampling (IS)

The main idea of IS is to restrict the sampling domain to the tail parts of the joint distribution of the basic random variables. For instance, the sampling domain can be restricted so that they remain inside a sphere the radius of which is β, which is the distance from the origin to the MPP. No failures occur inside this sphere, as MPP is the point in the failure space that is closest to the origin. This method has to be combined with an optimisation algorithm or analytical reliability method to find the MPP. The purpose of the IS is often to verify or to improve the accuracy of a solution that is obtained by employing an analytical method [52].

The IS is a particularly useful tool when the failure surface has a disadvantageous shape, i.e. a convex shape that produces a considerably higher failure probability than the corresponding hyperplane. Also, when there exist singularities at the failure surface or when there are several MPPs, e.g. if the failure surface is a circle the number of MPPs is infinite, IS is a very suitable analysis approach [52].

The achieved advantage with the IS as compared to plain MC is the considerably reduced amount of computational work required. Various IS methods in-

clude sphere-based importance sampling, adaptive importance sampling, Latin hypercube simulation (LHS) and stratified sampling.

Sphere-based importance sampling

The principal in this method is to formulate a spherical surface, inside which no sampling is performed. The radius of this spherical surface is defined in relation to the MPP. The smaller the searched probability, the more efficient is the solution, when compared to the MCS. The efficiency correspondingly decreases when the number of random variables increases, as the radius of the spherical surface becomes very small and hence the difference to the MCS remains very small. An example of the application of the sphere-based importance sampling is presented in Figure 5.6-2 [67].

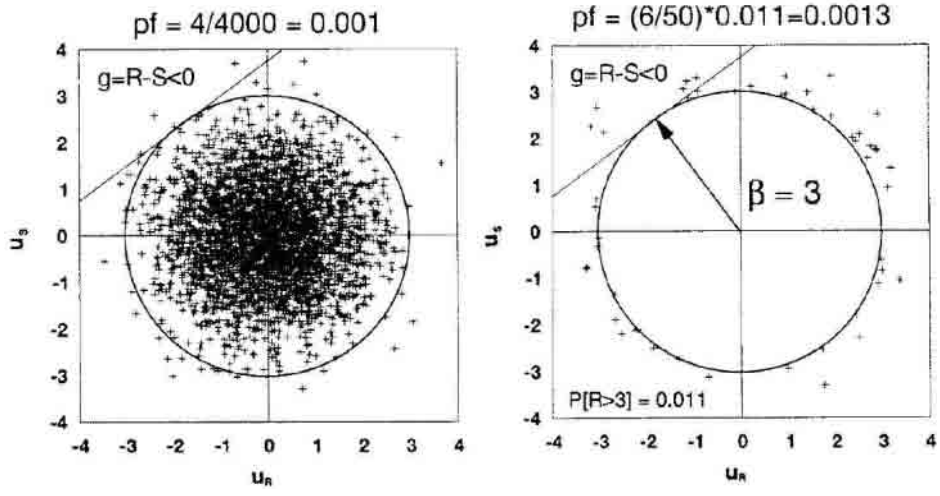

Figure 5.6-2. Sampling techniques employed in the MCS (left) compared to the sampling technique employed in the sphere-based importance sampling (right), from ref. [67].

Adaptive importance sampling (AIS)

AIS method is in principle similar to sphere-based importance sampling. The difference between these two methods is that in the AIS the region that limits sampling is modified in such a way that it stays in the so called safe side during the computational analysis. This is done because the first analysis result of the MPP is always approximate and thus one cannot entirely trust to the correctness of the limiting region that is based on it [67].

5.6.8 Latin hypercube simulation (LHS)

Models that contain a large number of parameters can be difficult to analyse using Monte Carlo methods. The difficulty arises in trying to obtain a representative sample of parameter values from their distributions. Having a large number of parameters requires a large number of Monte Carlo simulations to produce defensible results. One approach to obtaining a representative set of model output data is to use LHS to obtain a representative set of input samples to evaluate using the model.

LHS is based on stratified sampling of probability distributions. The approach is to divide each distribution into *n* intervals of equal probability. In the simulations, one point from each interval is sampled, so that the interval specific location is chosen randomly. Thus if each distribution is divided into two parts and there are *p* parameters, there will be 2 to the power of *p* sampling intervals. When a random approach is used for selection, then the order of intervals from which the points are sampled is also selected randomly [68]. An alternative is to use the median of each interval in the analysis [69].

LHS generally gives better results in calculating the tails of the distribution of risk and requires fewer simulations relative to ordinary Monte Carlo analysis. This may be of considerable importance when the number of parameters is large [69].

6. Risk analysis methods

6.1 Introduction

Risk analysis is a technique for identifying, characterising, quantifying and evaluating hazards. It is widely used to support regulatory and resource allocation decisions. The main goals of risk management are to minimise the occurrence of accidents by reducing the likelihood of their occurrence, reduce the impacts of uncontrollable accidents and transfer risk (e.g. via insurance coverage). The estimation of probability or frequency of hazard occurrence depends greatly on the reliability of the system components, the system as a whole and human-system interactions [49].

There are two major parts in risk analysis [49]:

- Determination of the probability of an undesirable event.
- Evaluation of the consequence of this hazardous event.

In general, there is a wide range of risk analysis methods and related theories. Here, the scope is to present a brief overview of this extensive topic.

6.2 Determination of risk values

In most risk assessments, the likelihood of an event is expressed in terms of probability, P_i, of that event. Alternatively, a frequency per year or per event (in units of time) may be used. Consequence, C_i, is a measure of the impacts of an event. This can be in the form of mission loss, payload damage, damage to property, number of injuries, number of fatalities, etc. [49].

The results of risk estimation are then used to interpret the various contributors to risk, which are compared, ranked and placed in perspective. The engineering definition of risk is now accepted as being the product of the likelihood and the consequence of the event [2]. Thus the risk assessment for an individual

risk, R_i, and the total risk, R, can be carried out by applying the following two equations [49]:

$$R_i = P_i C_i , \quad \text{for a possible event } i \text{ in the examined system} \tag{6.2-1}$$

$$R = \sum_{i=1}^{n} P_i C_i , \quad \text{for all possible events in the examined system} \tag{6.2-2}$$

6.3 Qualitative, quantitative and semi-quantitative risk analysis approaches

The risk analysis approaches can be divided to the following three categories [3]:

- qualitative,
- quantitative,
- semi-quantitative.

Qualitative risk analysis is based primarily on engineering judgements. The likelihood and consequences of failure are expressed descriptively and in relative terms. In a qualitative approach risks are usually presented in a risk matrix as combinations of the likelihood and consequences. Semi-quantitative risk analysis determines single numerical values for the probability of failure and the consequences from every cause and effect. The analysis of accident scenarios should generally be more numerically based and detailed than the qualitative approach, but may still contain a large element of engineering judgement. In a fully quantitative risk analysis, the likelihood and consequences of equipment failure are determined for each accident scenario from the underlying distributions of the variables using reliability analysis methods [3].

Both qualitative and quantitative risk assessment techniques are valuable for analysing the safety of nuclear and non-nuclear facilities. Their aim is to help to identify the important safety aspects of the design, operation, and maintenance of a facility by estimating the sources and magnitude of risk. Then, priorities for resource allocation can be established on the basis of risk [70].

Qualitative risk analysis approach

Qualitative risk approaches are based on assigning subjective scores to the different factors that are thought to influence the probabilities and consequences of

failure. The scores are then combined using simple formulae to give an index representing the level of risk. The resulting indices for different components (e.g. pipe regions, failure modes, or hazards) can then be ranked to determine components with the highest risk [45]. Examples of the relative terms used in qualitative risk analysis are very unlikely, possible, reasonably probable and probable for likelihood of failure, and high, medium and low for consequences of failure. For qualitative analysis to be used consistently, criteria for the descriptive categories of likelihood and consequence of failure should be defined [3].

Quantitative risk analysis approach

Quantitative risk analysis (QRA) systems are based on estimating the level of risk by direct assessment of the probability and consequences of failure. Most of the quantitative risk systems are based on Bayesian decision theory [45].

6.4 Review of risk analysis procedures

6.4.1 Failure mode and effect analysis (FMEA)

With the FMEA procedure, it is attempted to predict possible sequences of events that lead to a system failure, determine their consequences and device methods to minimise their occurrence or reoccurrence. FMEA is inductive in nature and, in practise, is used in all aspects of system failure analysis throughout the design process [49].

In general, FMEA procedure consists of a sequence of steps starting with the analysis at one level or a combination of levels of abstraction, such as system functions, subsystems or components. In FMEA analysis it is assumed that a failure mode is present and that it causes a failure. The effect of failure is then determined as well as the causative agent for the failure, i.e. the failure mechanism. The effect of the failure can be determined at various levels of abstraction starting at the component level. A criticality rating can also be determined for each failure mode and its resulting effect. The rating is normally based on the probability of the failure mode occurrence, the severity of its effect(s) and its detectability. Failures that score high in this rating can potentially be the source of system unreliability, and the corresponding failure modes should be removed [49].

One drawback of FMEA is that it provides very limited insight into probabilistic representation of system reliability. Another limitation is that FMEA is performed for only one failure at a time. This might not be adequate for systems

in which multiple failure modes can occur, with reasonable likelihood, at the same time. However, FMEA provides a lot of valuable qualitative information about the system design and operation [49]. The product of FMEA is a table of information that summarises the analysis of all relevant failure modes.

6.4.2 Fault tree Analysis

Fault trees represent relationships between a fault in a system and the associated events. There are two ways in which fault trees are used in the life cycle of a safety or mission critical system. In the first case, fault trees describe the faults that can happen in a system and relate them to their causes. In the second case, fault trees are taken as specifications of a part of the system requirements. Fault trees are applied in diverse industries, such as nuclear energy, process control, aerospace and aviation [73].

The fault tree analysis is a deductive process whereby an undesirable event, called the top event, is postulated, and the possible means for this event to occur are systematically deduced. For example, a typical top event looks like “failure of control circuit A to send a signal when it should”. The deduction process is performed so that the fault tree embodies all component failures that contribute to the occurrence of the top event. It is also possible to include individual failure modes of each component as well as human errors during the system operation. The fault tree itself is a graphical representation of various parallel and sequential combinations of faults that lead to the occurrence of the top event [49].

In general, there are three types of symbols in fault trees [49]: events, gates and transfers. The listing and meaning of these symbols can be found from textbooks and handbooks [49, 71, 72], and are not presented here. When postulating events in the fault tree, it is important to include not only the undesired component states (e.g. applicable failure modes), but also the time they occur. A cut set consists of those basic events the occurrence of which leads to the failure of the system [32]. Determining the fault tree cut sets involves some straightforward Boolean manipulation of events. The quantitative evaluation of fault trees involves the determination of the probability of the occurrence of the top event. Accordingly, unreliability or reliability associated with the top event can also be determined.

An example of a fault tree is shown in Figure 6.4-1. It shows an automotive brake system that consists of master cylinder, brake lining, wheel cylinder and brake fluid. The top event of this system is labeled as brake system failure. The

system will fail in case of the occurrence of any one of the following events [72]: master cylinder fails to produce required pressure, insufficient amount of brake fluid to transmit the pressure to the wheel cylinder, wheel cylinders fail to provide adequate braking, and brake lining fails to provide adequate braking.

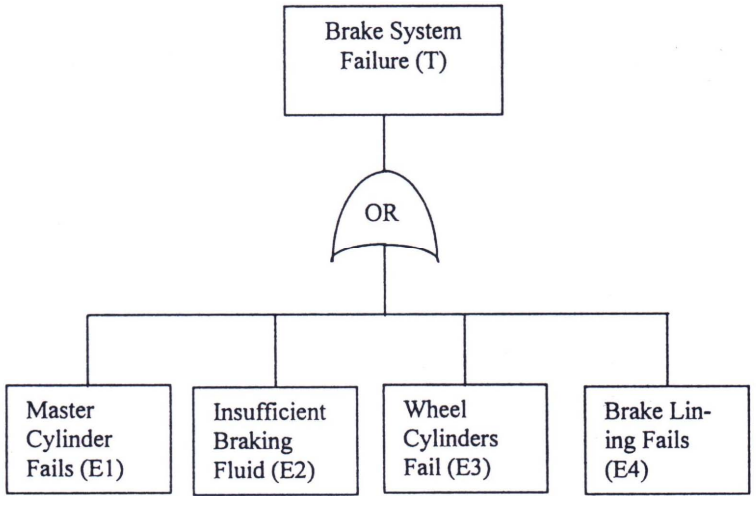

Figure 6.4-1. An example of a fault tree for an automotive break system, from ref. [72].

6.4.3 Event tree analysis

The event tree analysis is a convenient tool for analysing systems the successful operation of which depends on an approximately chronological but discrete operation of its components or units. For a simple system, the use of this method may not be necessary, but for complex systems, such as NPPs, event trees are particularly useful [49]. The range of applicability of event tree analyses is as wide as that of fault tree analyses.

The event trees are horizontally built structures that start from the left end, where the initiating event is modelled. This event describes a situation where a demand for the operation of a system occurs. Development of the tree proceeds chronologically, with the demand on each component or subsystem being postulated. The first component demanded appears first. At a branch point, the upper branch of an event shows the success of the event heading and the lower branch shows its failure. Event headings in event trees represent discrete states of the systems. These states can be represented by fault trees. This way the event tree sequences and the logical combinations of events can be considered. Evaluation

of event trees is straightforward. Each branch in an event tree is evaluated to determine its probability. The probability of each overall outcome is given by multiplying together the individual probabilities of the branches leading to that outcome [49].

When the initiating events in a system have been identified, event trees and required fault trees are constructed for each group of initiating events. An event tree connects an initiating event with damage states. Systems and components used to model the accident sequence progression are placed along the top of the event tree. The assumed success or failure of these systems leads to multiple event tree branches that result in specified damage states. The event tree branches occur at branch points that specify whether or not the system or component along the top of the event tree is functioning [32].

A simple event tree example of a failure of the corrosion protection (CP) system in a pipeline possibly leading to pipeline rupture is illustrated in Figure 6.4-2 [45].

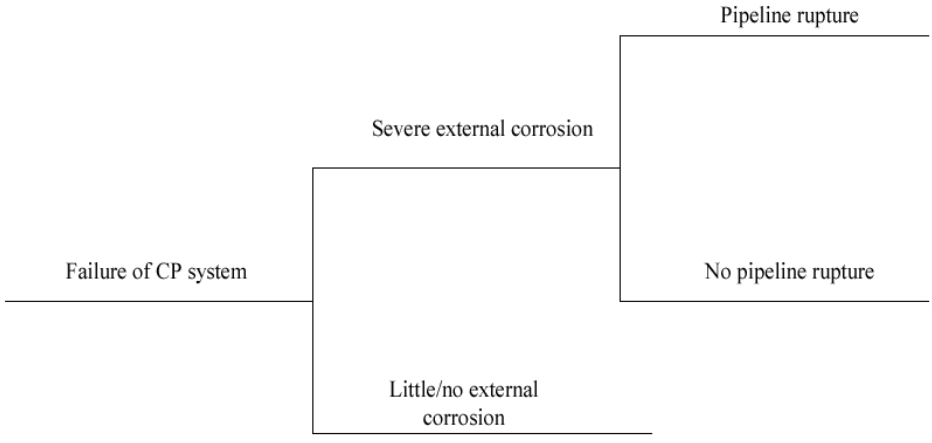

Figure 6.4-2. An example of a simple event tree, from ref. [45].

6.4.4 Expert opinion

The role of experts is important because their judgements can provide valuable information, particularly in view of the limited availability of technical data regarding many important uncertainties in risk analyses. Because uncertainties are often represented in terms of probability distributions, the information provided by expert opinion is often treated as probabilistic distributions. The motivation

for the use of multiple experts is simply the desire to obtain as much information as possible. The combination of probability distributions based on expert opinion summarises the accumulated information for risk analysts and decision makers. Procedures for combining probability distributions are often divided as mathematical aggregation methods or behavioural approaches [74]. These probabilities may be difficult to estimate even though reasonable engineering judgement is applied. This occurs because expert opinion under incomplete knowledge and limited data is inherently imprecise. In this case, the concept of uncertainty about a probability value is both intuitively appealing and potentially useful [75].

Application areas of expert opinion, also called expert judgement, are diverse, including nuclear engineering, aerospace, military intelligence, seismic risk and environmental risk from toxic chemicals [74]. Current PRA/PSA methodology uses expert opinion in the assessment of rare event probabilities [75].

The Delphi method [77, 78] is by far the most known method for eliciting and synthesizing expert opinions. The purpose and steps of the Delphi method depend on the nature of use. Primarily, the targets of application can be categorized into (1) technological forecasting, and (2) policy analysis. The technological forecasting relies on a group of experts on a subject matter of interest. The experts should be those having most knowledge on the issues or questions of concern. The issues and/or questions need to be stated by the study facilitators or analysts or monitoring team and high degree of consensus is sought from the experts [76].

A more recent useful guideline concerning the use of expert judgement/panel for NPP applications is “ENIQ Recommended Practice 11: Guidance on Expert Panels in RI-ISI” [80]. According to this guideline the role of an expert panel is to synthesise the views of various experts and identify and characterise the uncertainties in their analyses. A structured approach is needed in order to find a balance between the (often contrasting) arguments of experts representing different disciplines. Furthermore, an expert panel is important as it compels the different experts to openly discuss the technical bases of their arguments both among each other and with the decision maker. The guideline describes a complete approach for using an expert panel. This includes defining the role and responsibilities of the expert panel in RI-ISI as well as its composition. The described process covers planning, preparation and realisation of the expert panel, as well as the necessary associated documentation to be prepared.

Concerning applications for Finnish NPPs, the expert panel approach has been used to combine the deterministic information on degradation mechanisms and

probabilistic information on pipe break consequences. Then, the expert panel served both as a critical review of the preliminary results and as a decision support for the final definition of risk categories of piping [79].

6.4.5 Hazard and operability studies (HAZOP)

HAZOP is a structured brainstorming exercise by a group discussion designed to identify potential variations and deviations from the technical design or operating intent and their consequences. A list of guidewords is sometimes used to stimulate the discussions. Typically, these focus initially on credible variations of process parameters (flow, level, temperature) before branching out to consider human factors and less likely scenarios [3].

HAZOP is a procedural tool designed to highlight and identify hazards and operability problems in industrial plants that could reduce the ability of the plant to achieve productivity in a safe manner. Studies tend to be wide-ranging and threats to the integrity of pressure systems may only be considered briefly. This procedure is a tool for hazard analysis and it aims to ensure that weaknesses in the design intent are detected and acted upon [3].

6.5 Risk based regulations, guidelines and standards

There is a general trend towards the use of risk based regulations in areas where complex technological systems are in use. The use of quantitative risk analysis as a foundation for rational decision making is increasing in a number of engineering areas, e.g. aviation industry, space industry, nuclear industry, civil and marine engineering [81].

Some risk based regulations, guidelines and standards for risk analyses are listed below. The main emphasis is on nuclear industry, otherwise the selection is based on applicability of the documents in a wide range of areas.

Regulations and guidelines:

- U.S. Environmental Protection Agency: Policy for use of Probabilistic Analysis in Risk Assessment and Guiding Principles for Monte Carlo Analysis, EPA/630/R-97/001, EPA 1997.
- CPR, Committee for the Prevention of Disasters, Methods for the calculation of damage, “Green book”. Voorburg: Ministry of social affairs and employment, 1990.

- CPR, Committee for the Prevention of Disasters, Methods for determining and processing probabilities, “Red book”. The Hague: SDU, 1997a.
- CPR, Committee for the Prevention of Disasters, Methods for the calculation of physical effects, “Yellow book”. The Hague: SDU, 1997b.
- USNRC: An Approach for Using Probabilistic Risk Assessment in Risk-Informed Decisions on Plant-Specific Changes to the Licensing Basis, Regulatory Guide 1.174, U.S. Nuclear Regulatory Commission, 1998.
- USNRC: Use of Probabilistic Risk Assessment Methods in Nuclear Activities: Final Policy Statement, Federal Register, Vol. 60, p. 42622 (60 FR 42622), August 16, 1995.
- Probabilistic Safety Analyses. YVL Guide 2.8. Radiation and Nuclear Safety Authority (STUK), 2003.
- Management of Health and Safety at Work Regulations 1999. Approved Code of Practice and Guidance L21 (Second edition). Health and Safety Executive (HSE), 2000.
- Guide to Risk Assessment Requirements. Health and Safety Executive (HSE), 1996.
- CEOC – Risk Assessment: A Qualitative and Quantitative Approach. Confédération Européenne d'Organismes de Contrôle. R 35/CEOC/CR1 87 Def.
- Risk Based Inspection (RBI): A Risk Based Approach to Planned Plant Inspection. Health and Safety Executive (HSE) - Hazardous Installations Division, 1999.

Standards:

- International Standard ISO 2394: General Principles on Reliability for Structures, Second Edition, 1998-06-01.
- DS-Information DS/INF 85: Risk Analyses, requirements and terminology, Danish Standards Association, 1993.

- European Standard EN 1050:1996: Safety of machinery – Principles for risk assessment, European Committee for Standardisation, 1996.
- IEC International standard nr 60300-3-9: Dependability management-Part 3: Application guide- Section 9: Risk analysis of technological systems, International Electrotechnical Commission, 1995.
- British Standard BS 8444: Risk management, Part 3 Guide to analysis of technological systems – application guide, British Standards Institution, 1996.
- Australian/New Zealand Standard AS/NZS 3931: Risk analysis of technological systems – application guide, Standards Australia, Standards New Zealand, 1998.
- Canadian Standard CAN/CSA-Q850-97: Risk management: Guideline for Decision-Makers, Canadian Standards Association, 1997.

6.6 Concerns with risk assessment

In the following are briefly described some of the concerns that have been raised in the literature with risk assessment. It is important to be aware of the limitations of the used methodologies and the uncertainty or lack of confidence in the results.

Inclusion of model uncertainty

Model uncertainty is caused by the use of simplified or idealised mathematical models that are needed as operational tools in the risk analysis. By its very nature, model uncertainty is very difficult to assess and model, and it is often omitted. However, in many cases, when model uncertainty is allowed for it is an important influence on the evaluated probability [45].

If model uncertainty is for some reason omitted from a risk analysis, the results should be interpreted with some caution.

The tails of failure probability distributions

The sensitivity problem of the tails of the failure probability distributions is a common concern within structural reliability analyses. In a risk analysis, it is the probability content defined by the shape of the distribution tails that most influ-

ences the evaluated failure probability. By definition, data points located in the tail of the distribution are very unlikely to occur in a population of data.

Thus, even in the fortunate situation where a large data sample is available to define the distribution for a basic variable, very few data points at the tail of the distribution influence the modelling of the variable. It is often pointed out that statistics based on data at the centre of a distribution carry no information about the extremes, and so extrapolation is inherently untrustworthy. This is clearly an important concern when physical mechanisms governing the shape of the extreme tails are different from those governing the central part of the distribution [45].

In a well constituted problem with well defined basic variable models, tail sensitivity is rarely a concern. However, in a particularly sensitive situation, or where the modelling for the most sensitive variables is limited, the sensitivity of the reliability can be examined by using different, valid probability distributions. Clearly, a valid distribution should fit the data well, and should comply with any physical constraints or limitations.

Small failure probabilities and lack of data

It has been pointed out that typical probabilities of failure often evaluated from structural reliability analyses have no conceivable physical meaning if interpreted in a frequency manner. By their very nature, failures of structural components and components of pressure systems, and corresponding failure data are rare. Often, to obtain sufficient data to assess a failure rate for a specific application, it is necessary to consider very broad categories [45]. The problem with too little data can be managed by deriving confidence limits that can be determined from statistical analyses. By carrying out this type of analyses on the various data sources, an estimation of the variability of such data can be established [3]. The lack of statistically sufficient amount of empirical data necessary to estimate new parameters is one important reason to apply expert opinion [49].

Validation

The small failure probabilities for some components mean that evaluated failure probabilities cannot be properly and completely validated. To do so, it would either be necessary to observe a small number of similar components for a very long period, or to observe a very large population of structures for a shorter more practical period. Unfortunately, whilst this is to some extent possible for manufactured items, it is not possible for most pressure systems which are typically

more unique items, thus there is no population of nominally identical structures under nominally identical conditions that might be observed. However, for most component types there is a large enough population of components of similar type for at least allowing to obtain some crude comparative values. It may also be possible to calibrate the failure models from test data [45].

Completeness

There can never be a guarantee that all accident situations, causes, and effects have been considered. Indeed, a number of failures have occurred because the scenario was not and could not have realistically been envisaged. Therefore it is important to undertake rigorous hazard identification studies.

7. Deterministic degradation modelling methods for power plant components

7.1 Introduction

Modelling methods of the major degradation mechanisms concerning power plant components are considered in the following. Of these mechanisms, the three most often encountered ones in NPP environments are fatigue, SCC and irradiation embrittlement [32]. However, of the NPP types and components, only the PWR RPVs and LWR internals are susceptible to the last one of these. In conventional power plants, irradiation embrittelement is obviously not an issue. However, due to relatively high operational temperatures, in conventional power plants also creep has to be often taken into account in addition to fatigue and corrosion.

A brief overview is also presented of the various commonly applied component structural integrity assessment methods. These include methods that are defined in fitness-for-service procedures, codes, standards and research articles/reports, and which have been developed by both research institutes and private companies.

7.2 Fatigue

Fatigue is the progressive, locally confined, and permanent structural change that occurs in a material subjected to repeated or fluctuating strains at nominal stresses that have maximum values less than the static yield strength of the material. Fatigue may lead to emergence of cracks and cause fracture after a sufficient number of fluctuations. Fatigue damage is caused by the simultaneous action of cyclic stress, tensile stress, and plastic strain. If any one of these three is not present, a fatigue crack will not initiate and propagate. The plastic strain

caused by cyclic stresses initiates the crack, and tensile stresses promote crack growth. In the process of fatigue failure in an originally intact metal, micro-cracks arise, coalesce or grow to macro-cracks that propagate until the fracture toughness of the material is exceeded and final fracture will occur [7].

One of the most successful applications of the theory of fracture mechanics is in the characterisation of fatigue crack propagation. For an overview of the fracture mechanics based analysis methods, see Section 4.3. A fracture mechanics based analysis of fatigue flaw growth inevitably requires a thorough understanding of the assumptions, significance and limitations underlying the development of various crack tip parameters. In mechanical components, like boiler tubes, the principal sites of fatigue crack nucleation include voids, inclusions, dents, scratches, forging laps and folds, macroscopic stress concentrations, as well as regions of micro-structural and chemical non-uniformity [97].

All in all, there are several computational approaches for the cumulative fatigue damage analysis. Since the introduction of damage accumulation concept by Palmgren [98] and linear damage rule by Miner [99], both published several decades ago, a multitude of cumulative fatigue damage models have been developed. These models can be divided into six categories [100]:

- linear damage rules,
- non-linear damage curves and two-stage linearisation approaches,
- life curve modification methods,
- approaches based on crack growth concepts,
- continuum damage mechanics models, and
- energy based theories.

Approaches based on crack growth concepts and fracture mechanics are covered in more detail here. That is because most of the other cumulative fatigue models consider fatigue crack initiation or it reaching a macroscopic but still relatively small size as the limiting criteria, rather than the crack propagating to some limiting depth, through wall or to a size leading to plastic collapse. In case of cumulative continuum fatigue models it is also important to note that the order of loading events in load cycle sequences formed and assembled with commonly used procedures deviate from the actual chronological load history. A typical example of this approach is the often used rainflow load cycle counting procedure in its different modifications. As for fracture mechanics based crack growth computations, they strictly require the realistic chronological order of the load

history to be preserved, as the magnitude of each crack growth increment is dependent both on load amplitude and the current crack size.

The procedures for analysing constant amplitude fatigue under small scale yielding conditions are fairly well established, although a number of uncertainties remain. Variable amplitude loading, multi-axial loading, large scale plasticity, crack closure, overloads, weld residual stresses and short cracks introduce additional complications that are not yet fully understood.

Of the numerous developed cumulative fatigue damage models only some most notable and/or commonly used ones are considered here.

The method relating the stress level and number of load cycles, *S-N* curves, is used to predict the number of cycles to failure at a single stress level. The *S-N* curves conveniently display basic fatigue data on a plot of cyclic stress level versus the number of cycles to failure. Analytical representation of *S-N* curves is given in the form [32]:

$$NS^b = k \tag{7.2-1}$$

where b and k are material parameters estimated from test data obtained using identical specimens.

Linear damage rules

The Palmgren-Miner rule (or Miner's rule) is a linear damage accumulation rule used to predict the cycles to failure under variable amplitude loading. The Palmgren-Miner rule asserts that the damage fraction Δ_i at any stress level S_i is linearly proportional to the ratio of n_i, the number of cycles of operation under this stress amplitude to N_i, the total number of cycles that would produce a failure at that stress level. The damage fraction is computed as follows [99]:

$$\Delta_i = \frac{n_i}{N_i} \tag{7.2-2}$$

where $n_i \leq N_i$. If the stress amplitude is changed, a new partial damage is calculated for this new amplitude level, where the appropriate N_i is found form the *S-N* curve. The total accumulated damage D is then given by [99]:

$$D = \sum_i \Delta_i = \sum_i \frac{n_i}{N_i} \tag{7.2-3}$$

and failure is assumed to occur when $D \geq 1$. The main deficiencies with linear damage rule used are its load level independence, load sequence independence and lack of load interaction accountability.

Non-linear damage curves and two-stage linearisation approaches

Attempting to overcome the inaccuracies of linear damage rules, non-linear damage rule procedures have been developed. A representative and early example of non-linear damage rules is as follows [101]:

$$D = \sum_i \Delta_i^{x_i} = \sum_i \left(\frac{n_i}{N_i} \right)^{x_i} \tag{7.2-4}$$

where x_i is an exponent parameter related to the ith loading level.

As for two-stage linearisation approaches, they provide improvement to the shortcomings of the linear damage rule, while still retaining its simplicity. In the two-stage linearisation approaches, the fatigue damage is divided to two phases, those being crack initiation and crack propagation. A representative example of a double linear damage rule is as follows [102]:

$$D_I = \sum_i \left(\frac{n_I}{N_I} \right)_i \quad \text{crack initiation phase,} \tag{7.2-5a}$$

$$D_{II} = \sum_i \left(\frac{n_{II}}{N_{II}} \right)_i \quad \text{crack propagation phase,} \tag{7.2-5b}$$

where $N_I = N - N_{II}$, $N_{II} = B \cdot N \cdot \left(N_r / N \right)^{\alpha}$, N_r is a reference level for N, $B = 0.65$, and $\alpha = 0.25$. Here, the two constants B and α are determined from regression analysis of the experimental data. The presented values for them mainly correspond to high strength steels.

Life curve modification methods

In the life curve modification methods, the conventional *S-N* curve is modified to better follow the fatigue test data. An example of this approach accounting for load interaction effect is [103, 104]:

$$N_{\Sigma} = 1 \Big/ \sum \left(\beta_i / N_i' \right) \tag{7.2-6}$$

where N_{Σ} is the total accumulated life, whereas β_i and N_i' are the frequency of load cycles (n_i/N_{Σ}) and the modified life associated with loading level σ_i, respectively. The experimental verification results show that this model can provide accurate predictions of fatigue lives under repeated block loading. This predictive theory is also expanded to stochastic loading histories.

Continuum damage mechanics models

Continuum damage mechanics deals with the mechanical behaviour of a deteriorating medium at the continuum scale. The success of continuum damage mechanics application in modelling the creep damage process has led to extend this approach to ductile plastic damage, creep-fatigue interaction, brittle fracture and fatigue damage. For the one-dimensional case, the cyclic fatigue damage evolution can be generalized by a function of the load condition and damage state. The following non-linear damage evolution equation has been developed as based on measured changes in tensile load carrying capacity and using the effective stress concept [110, 111]:

$$D = 1 - \left[1 - \left(n / N_f \right)^{1/(1-\alpha)} \right]^{1/(1+\beta)} = 1 - \left[1 - r^{1/(1-\alpha)} \right]^{1/(1+\beta)} \tag{7.2-7}$$

where n is number of load cycles, N_f is number of load cycles to failure, β is a material constant and α is a function dependent on the stress state. This damage model is highly non-linear in damage evolution and is able to account for the mean stress effect. This model allows for the growth of damage below the initial fatigue limit, when the material is subjected to prior cycling above the fatigue limit. The model is able to take into account the influence of initial hardening effect by introducing a new internal variable which keeps track of the largest plastic strain range in the prior loading history. In addition, the mean stress effect is directly incorporated in the model. However, since a scalar damage varia-

ble is employed and the model is written in its uniaxial form involving the maximum and mean stresses, difficulties will inevitably occur when the model is extended to multiaxial loading conditions.

It has been noted that there is a connection between stress-strain cycling loop hysteresis energy and fatigue, which in turn led to the development of energy based cumulative damage theories, mainly considering strain energy [105]. It has been realised that an energy based damage parameter can unify the damage caused by different types of loading such as thermal cycling, creep, and fatigue. Energy based damage models also allow to include mean stress and multiaxial loads since multiaxial fatigue parameters based on strain energy have been developed [106, 107].

Energy based damage theories

By examining constant strain amplitude test data, it was found according to refs. [108, 109] that while the values of the cyclic strain hardening coefficient changed during the cycling process, the corresponding change for cyclic strain hardening exponent was negligible. This led to the development of the following cyclic stress-strain relation [109]:

$$\frac{\Delta\sigma}{2} = K^* \left(\frac{\Delta\varepsilon_p}{2} \right)^{n^*} r^{\beta} \tag{7.2-8}$$

where $\Delta\sigma$ is stress range, $\Delta\varepsilon_p$ is plastic strain, K^* and n^* are cyclic strain hardening coefficient and exponent determined near failure ($r = n/N_f = 1$), and β is the cyclic hardening rate. The expression for β is given as:

$$\beta = a \left(\frac{\Delta\sigma}{2} \frac{\Delta\varepsilon_p}{2} \right)^{b} \tag{7.2-9}$$

where a and b are constants, the values for which are obtained as based on experimental data. The exponent b is dimensionless, whereas the dimension of the parameter a is such that its product with $\Delta\sigma$ [MPa] and $\Delta\varepsilon_p$ [%] is dimensionless. The incremental rate of plastic strain energy, dW/dN, is then derived as:

$$\frac{dW}{dN} = 4\left(\frac{1-n^*}{1+n^*}\right) r^{\beta} K^* \left(\frac{\Delta\varepsilon_p}{2}\right)^{1+n^*} \tag{7.2-10}$$

where again $r = n/N_f$ and the energy accumulation is defined by introducing a parameter called the fraction of plastic strain energy, $\Phi = W/W_r = r^{1+\beta}$. Finally, the fatigue damage function is expressed as:

$$D = \Phi^{1/[(n'+\alpha)(1+\beta)]} = r^{1/(n'+\alpha)} \tag{7.2-11}$$

where $\alpha = \left(\Delta\sigma\Delta\varepsilon_p / 4\right)^{2\cdot b}\sqrt{a}$ and n' is the cyclic strain hardening exponent. This model represented by equation (7.2-11) is a non-linear, load dependent damage accumulation model. It accounts for the load interaction effect and the change in strain hardening through the stress response. This damage model is particularly suitable for materials which exhibit cyclic hardening.

Fracture mechanics based crack growth computation procedures

Fracture mechanics can be used to model fatigue of components. An overview concerning fracture mechanics is presented in Section 4.3. Materials with relatively low fracture resistance that fall below their so called plastic collapse strength can be analysed on the basis of elastic concept through the use of LEFM. For other materials, the use of EPFM is often necessary.

Fracture will occur when the stresses at the crack tip become too high for the material to bear. Under linear-elastic circumstances, the stress intensity factor K determines the entire crack tip stress field, whereas in case of ductile material accompanied with considerable plastic deformation J-integral applies. The corresponding fracture toughness/resistance, J_R, tends to increase during the fracture process, so that fracture will be slow and stable initially, until at some point instability occurs causing the fracture to become fast and uncontrollable. Thus, stable fracture may slow down and stop unless the stress level is further increased [32].

The growth of the crack that eventually leads to fracture occurs by mechanisms entirely different from the fracture itself. During most part of the cracking process, the crack is much smaller than the one that would cause fracture at the prevailing stress. Therefore, the crack tip stress field is less severe, and the size of the plastic zone smaller than at the time of fracture. Due to this small plastic zone, LEFM can often be applied. If the crack size is close to critical (fracture),

this may no longer be true, but because by far the longest time is spent in the growth of much smaller cracks, it is justifiable to use LEFM to obtain the time for crack growth with good accuracy [7].

For fatigue, the crack propagation equations are models that relate the crack growth rate to the level of cyclic stress. These fracture mechanics based computation procedures can be further divided to those intended for constant and variable amplitude loading, respectively. Apparently the models of the latter type can also be applied with sufficient accuracy to those of the former. However, this should be case specifically checked.

One of the earliest and also most often used fatigue crack propagation models is the Paris-Erdogan equation. It is an empirical formula that relates the cyclic crack growth rate to stress intensity factor range, as follows [112]:

$$\frac{da}{dN} = C(\Delta K)^m \tag{7.2-12}$$

where a [mm] is crack depth, N [-] is the number of load cycles, ΔK [MPa√m] is the stress intensity factor range, i.e. K_{max} - K_{min}, whereas C and m are material and environment specific constants. The exponent m is dimensionless, whereas the dimension of the parameter C is such that its product with $(\Delta K)^m$ is mm. The Paris-Erdogan equation assumes that the crack growth depends only on the stress intensity factor range. It also assumes that the stress amplitude is constant and that it is small enough so that LEFM is applicable and that the crack growth rate is independent of the previous load history. Failure occurs when the stress intensity factor exceeds the fracture toughness. In addition, the Paris-Erdogan equation describes crack growth only at intermediate values of fatigue crack growth curve, see Region II in Figure 7.2-1 below. Region II represents the intermediate crack propagation zone where the length of the plastic zone ahead of the crack tip is long compared with the mean grain size, but much smaller than the crack length, whereas Region I contains the stress intensity factor range threshold below which fatigue cracks do not propagate and Region III is characterised by rapid and unstable crack growth just prior to final failure [114].

A fatigue damage propagation model proposed by Forman [113], which covers both the intermediate and high ΔK regions, is:

$$\frac{da}{dN} = \frac{C_F(\Delta K)^{m_y}}{(1-R)K_C - \Delta K} = \frac{C_F(\Delta K)^{m_y}}{(1-R)(K_C - K_{\max})} \tag{7.2-13}$$

where C_F and m_y are material and environment specific constants, K_C [MPa√m] is fracture toughness and $R = K_{\min}/K_{\max}$ is stress ratio. Equation (7.2-13) indicates that as $K_{\max}$ approaches K_C, crack growth rate da/dN in turn tends to infinity. With equation (7.2-13), it is possible to predict both stable intermediate crack growth and accelerated crack growth rates for various stress ratios.

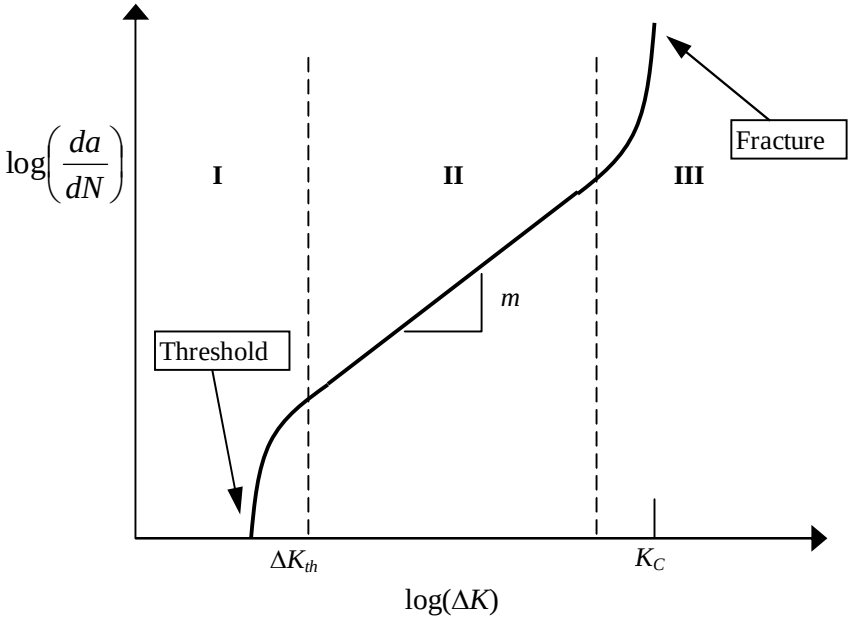

Figure 7.2-1. Typical fatigue crack growth behaviour in metals.

McEvily [115] developed another equation that can be fit to the entire fatigue crack growth curve, as follows:

$$\frac{da}{dN} = C(\Delta K - \Delta K_{th})^2\left(1 + \frac{\Delta K}{K_C - K_{\max}}\right) \tag{7.2-14}$$

where K_{th} [MPa√m] is crack propagation threshold. Equation (7.2-14) is based on a simple physical model rather than a purely empirical fit. The expression

distinguishes between two crack advancement modes; ductile striation and static mode. It is noted that for tests in non-aggressive environments the number of adjustable parameters becomes zero when ΔK values are large with respect to ΔK_{th} [114].

In general, it is considered that fatigue cracks do not grow when being closed, which can be the case when the surrounding stress field has turned to compression. As there is no unique definition of crack closure or crack opening, due to the gradual nature of the crack behaviour between the points of complete opening and closure, usually an average closure/opening stress intensity factor, K, is employed. As inconsistencies in assessing the K values for the first contact between the crack flanks could occur due to the fracture surface asperities, the use of an average value is recommended. The difference between the K values concerning opening, K_{op}, and closure, K_{cl}, is quite insignificant, thus using a single value K_{cl} has proven to be an adequate approximation.

According to Elber [116], a crack only propagates while its flanks are separated, and is then driven by the effective stress intensity factor range, ΔK_{eff}, as follows:

$$\Delta K_{eff} = K_{\max} - K_{cl} = U\Delta K \tag{7.2-15a}$$

where U is a factor depending primarily on the stress ratio R. By replacing the stress intensity factor range with the effective stress intensity factor range of equation (7.2-15a) in the Paris-Erdogan equation (7.2-12) yields [116]:

$$\frac{da}{dN} = C\left(\Delta K_{eff}\right)^m = C\left(U\Delta K\right)^m \tag{7.2-15b}$$

Concerning the factor U above, Shih and Wei [117] have reported a definite dependence on K_{max}, whereas Hudak and Davidson [118] attributed the confusion and controversy over the effect of loading variables on closure to experimental factors. McClung [119] has reported of three distinct K dependent regimes of crack closure and concluded that no single equation could describe the closure in all three regimes. Other attempts have included linking U to the specimen geometry, stress state and environment.

Wheeler [120] developed a fatigue damage propagation model based on yield zone concept for tensile overloads. To account for crack growth retardation, a retardation parameter, C_p, is introduced. This retardation parameter is dependent

on the current plastic zone, overload plastic zone and a shaping exponent. The Wheeler model equation together with definitions for its parameters can be expressed as [120]:

$$\frac{da}{dN} = C_p C(\Delta K)^m \tag{7.2-16}$$

where: C_p is retardation parameter,

$$C_p = \left(\frac{R_y}{a_p - a} \right)^{m1} \quad \text{for } (a + R_y) < a_p, \text{ and } C_p = 1 \text{ for } (a + R_y) > a_p,$$

R_y is extent of current yield zone,

a_p is the sum of a and largest prior yield zone,

$(a_p - a)$ is distance from a crack tip to the boundary of the yield zone caused by the last tensile overload in a sequence,

$m1$ is shaping exponent,

C, m are defined in connection of Paris-Erdogan model, see equation (7.2-12).

This model allows to use other crack propagation formulations as well, thus the right side of equation (7.2-16) can be written as: $C_p f(\Delta K)$, where $f(\Delta K)$ is a function describing the crack growth. When using the model, among the needed input data is initial crack length, a_0, and the computation process follows the load cycles, i.e. crack grows increment by increment. The limitation of this model [120] is that the values for the shaping exponent must generally be obtained experimentally. The model considers mainly variable amplitude loading conditions. Further, this model does not predict acceleration caused by compressive overloads (underloads).

Johnson [121] has developed a systematic technique for modeling fatigue crack growth under variable amplitude loading to account for interaction effects. The procedure includes a multi-parameter yield zone model, which accounts for crack growth retardation, acceleration and underload effects by decreasing or increasing the stress ratio. Modified Forman type crack growth equation was used in developing the model, as follows:

$$\frac{da}{dN} = \frac{C(\Delta K)^m}{(1-R_{eff})K_C - \Delta K} \tag{7.2-17}$$

where: $m = 1$ at $R \geq 0$, and $n = 2$ at $R < 0$,

threshold K range for variable amplitude loading;
$\Delta K_{th}^* = (1-R_{eff})\Delta K_{th}$,

$$R_{eff} = \frac{K_{\min} - K_{red}}{K_{\max} - K_{red}} = \frac{K_{\min,eff}}{K_{\max,eff}},$$

maximum allowable stress ratio; $R_{\max} = \left(\frac{0.2Z_{OL}}{t}\right) + 0.6$,

Z_{OL} = plastic zone diameter for the applied $K_{\max}$,

t = material wall thickness.

This model [121] includes the assumption that the load interactions are a result of the residual stress intensity due to plastic deformation at the crack tip. Further, constant amplitude loading data was used for computation of threshold ΔK under variable amplitude loading.

Wang et al. [122] proposed a simple model for the fatigue crack growth rate which considers the plastic component of the J-integral as a damage factor. The proposed damage accumulation theory assumes that: the total plastic strain energy density absorbed by the material is prior to reaching its ultimate state constant to be determined experimentally, the elastic strain energy density stored by the material does not cause damage and is released upon unloading. This model is expressed as:

$$\frac{da}{dN} = \alpha\left(\frac{K_{\max}^4}{\overline{\sigma}_y^2}\right)\left[\frac{1}{1-\xi^2} - \frac{1}{1-(R\xi)^2}\right]\left[\frac{1}{\sqrt{1-\xi^2}} - \frac{1}{\sqrt{1-(R\xi)^2}}\right]^2 \tag{7.2-18}$$

where: $\xi^2 = K_{\max}^2 / (2K_{eff})$,

$K_{eff} = \sigma_y \sqrt{\pi a}$,

α = constant determined according to the material and loading conditions,

$\overline{\sigma}_y$ = local yield strength,

σ_y = average local yield strength.

According to this fatigue damage model [122] the accumulated plastic strain energy will cause the material damaging and lead to failure. This plastic damage only occurs after the maximum elastic component has been reached. Based on the research to obtain the procedure equation (7.2-18), it was concluded that the crack growth rate is not only a function of ΔK, but also of average local yield strength, fracture toughness and amplitude of the applied effective stress intensity factor in Regions II and III. The mode1 was verified using the test results published in ASTM STP 789 [123]. The test data and equation predictions were then found to be in reasonably good agreement.

A more advanced development is the fatigue crack growth rate model by Forman and Mettu [124], which follows a cycle-by-cycle integration method as using the sigmoidal crack growth rate relationship, and which model is now also included in the quite recently published European Fitness For Service Network (FITNET) structural integrity assessment procedure/guideline [125]. The model equation is given as:

$$\frac{da}{dN} = C\left[\left(\frac{1-f}{1-R}\right)\Delta K\right]^n \frac{\left(1-\Delta K_{th}/\Delta K\right)^p}{\left(1-K_{\max}/K_C\right)^q} \tag{7.2-19}$$

where C, n, p and q are parameters for which material specific values are given in the procedure documentation. The values for parameters f, ΔK_{th}, $K_{\max}$ and K_C are obtained from associated functions which are dependent e.g. on stress ratio R, constraint conditions and thickness. The FITNET procedure covers a wide range of materials and takes into account the crack closure effect on the crack growth behaviour in more detail. On the other hand, the procedure contains many parameters the values for which need to be obtained experimentally in order to assure reliable computations.

Discussion on damage caused by multiaxial fatigue loading

Power plant components can be subjected to multiaxial fatigue loading, in which the cyclic loads in various directions may be applied at different frequencies and/or with a phase difference. In these circumstances of non-proportional multiaxial loading, the corresponding principal directions and/or principal stress ratios vary during a loading cycle or loading block. During recent decades, fatigue damage evaluation of components/structures under non-proportional multiaxial loading has become a growing research interest as conventional multiaxial fatigue criteria are based on proportional fatigue data, and hence, they are not applicable for non-proportional loading due to changing directions and/or ratios of the principal stresses [126].

The multiaxial fatigue degradation models proposed in the literature may be categorised into three groups: stress based, strain based and energy based methods [127, 128, 129]. In their comprehensive more recent review on the subject, Marquis and Socie [130] consider methods based on cyclic *J*-integral as a separate group from the energy based methods. For long life fatigue problems, most of the multiaxial fatigue criteria are stress based. In order to handle non-proportional loading effects on fatigue resistance, many new methodologies have been developed. They are based on various concepts, such as the critical plane approach, integral approach, mesoscopic scale approach, etc. [126].

An example of multiaxial fatigue degradation models based on equivalent stress intensity is presented in the following. For mixed mode loading, the fatigue crack growth rate may also be expressed by a simple Paris-Erdogan type model, see equation (7.2-12) earlier, where the stress intensity factor range is replaced by equivalent stress intensity factor range, ΔK_{eq}, so that the model equation becomes:

$$\frac{da}{dN} = C\left(\Delta K_{eq}\right)^m \tag{7.2-20}$$

The basis for the model by Tanaka [131] is that displacements behind the crack tip reach a critical value. This leads to the following formulation for the equivalent stress intensity factor range:

$$\Delta K_{eq} = \left[\Delta K_I^4 + 8\Delta K_{II}^4 + 8\Delta K_{III}^4 / (1-\nu)\right]^{0.25} \tag{7.2-21}$$

where ΔK_{II} and ΔK_{III} are the ranges for mode II and III stress intensity factors, see Section 4.3, and ν is Poisson's coefficient. The material constants in equation (7.2-20) are taken from standard mode I crack growth experiments. Crack growth under other loading conditions can be obtained with the use of the appropriate equivalent stress intensity factor range given by equation (7.2-21). Other forms of the equivalent stress intensity factor range have also been used.
As for strain energy density fatigue degradation models, Sih [132] proposed a criterion for mixed mode loading known as the strain energy density factor, *S*. It is based on the strain energy density around the crack tip and is expressed as:

$$S = a_{11}K_I^2 + 2a_{12}K_I K_{II} + a_{22}K_{II}^2 + a_{33}K_{III}^2 \tag{7.2-22}$$

where the coefficients a_{11}, a_{12}, a_{22} and a_{33} under plane strain are dependent on elastic modulus, Poisson's coefficient and the inclination angle of the crack, θ. Crack extension occurs when the strain energy density factor reaches a critical value in a direction defined by θ_0. This will be the direction of minimum strain energy density. For cyclic loading a cyclic strain energy density factor range is defined as:

$$\begin{aligned}\Delta S = 2\ \Big[& a_{11}(\theta_0)K_I^{\text{mean}}\Delta K_I + a_{12}(\theta_0)\left(K_{II}^{\text{mean}}\Delta K_I + K_I^{\text{mean}}\Delta K_{II}\right) + \\ & + a_{22}(\theta_0)K_{II}^{\text{mean}}\Delta K_{II} + a_{33}(\theta_0)K_{III}^{\text{mean}}\Delta K_{III}\Big]\end{aligned} \tag{7.2-23}$$

This equation includes both stress range and mean stress. Before computing the strain energy density factor, the direction of crack growth θ_0 must be determined from the necessary and sufficient conditions for crack growth, as follows:

$$\begin{aligned}&\partial S/\partial\theta = 0 \quad \text{at } \theta = \theta_0 \\ &\partial^2 S/\partial\theta^2 > 0 \quad \text{at } \theta = \theta_0\end{aligned} \tag{7.2-24}$$

Then the crack growth rate can be computed as:

$$\frac{da}{dN} = C_S(\Delta S)^{m/2} \tag{7.2-25}$$

where the values of the constants can be determined from the standard crack growth constants in equation (7.2-20) as follows:

$$C_S = C\left[\frac{2\pi E}{(1-2\nu)(1+\nu)}\right]^{m/2} \tag{7.2-26}$$

where ν is Poisson's coefficient. Concerning equivalent strain intensity models, any of the equivalent stress intensity models could be used with the appropriate substitution of $E\Delta\varepsilon$ or $G\Delta\gamma$ for the stress, where $\Delta\varepsilon$ is strain range, G is shear modulus and $\Delta\gamma$ is shear strain range. The strain intensity factor range, $\Delta K_I(\varepsilon)$ is often used for elastic-plastic loading conditions. Further, an effective strain intensity factor range, $\Delta K_{eq}(\varepsilon)$, can be written in terms of the strain ranges and crack geometry factors for modes I and II, the latter two being denoted as F_I and F_{II}. Equation (7.2-27) gives the effective strain intensity factor range based on the strain energy release rate as [130]:

$$\Delta K_{eq}(\varepsilon) = \left[\left(F_{II}\frac{E}{2(1+\nu)}\Delta\gamma\right)^2 + \left(F_I E\Delta\varepsilon\right)^2\right]^{0.5}\sqrt{\pi a} \tag{7.2-27}$$

In cyclic J-integral approach, crack growth is analysed by assuming that the cyclic J-integral range, ΔJ, controls the crack growth as [130]:

$$\frac{da}{dN} = C_J\left(\Delta J\right)^{m/2} \tag{7.2-28}$$

For elastic loading, ΔK and ΔJ are related and the constant C_J can be evaluated as:

$$C_J = CE^{m/2} \tag{7.2-29}$$

Alternatively, crack growth data could be fitted in terms of ΔJ to obtain the constants directly.

7.3 Corrosion

Of the various identified forms of corrosion, see Section 3.4, modelling of those which mainly concern power plant components are considered here. These corrosion mechanisms are general corrosion, pitting and stress corrosion cracking (SCC). Of the numerous models that have been developed for these corrosion mechanisms, only some notable ones are presented here.

7.3.1 General and pitting corrosion

General corrosion is the result of a chemical or electro-chemical reaction between a material and its environment. It is typically characterised by uniform attack resulting in material dissolution and sometimes corrosion product build-up. At ordinary temperatures and in neutral or near neutral media, both oxygen and moisture must be present to corrode steel. Generally, when humidity exceeds 70 %, a moisture film forms on the steel surface providing an electrolyte [133]. The ratio between humidity and temperature determines the thickness of the film. The thinner the film, the easier the diffusion of oxygen through the film that drives the corrosion reaction. Corrosion rates of carbon and low-alloy steels increase with rising surface temperatures until the electrolyte is evaporated [134]. For instance, in LWRs the steam generator tubes are susceptible to general corrosion [4].

Pitting corrosion is a localised corrosion attack in aqueous environments containing dissolved oxygen and chlorides. This corrosion degradation is more common in austenitic stainless steels than in carbon steels. When passivity breaks down at a spot on a surface, an electrolytic cell is formed with the anode at the minute area of active metal, and the cathode at the larger area of passive metal. The large electric potential difference between the two areas accounts for considerable flow of current with rapid corrosion at the anode. The anode does not spread because it is surrounded by passive metal, and as the mechanism continues it propagates deeper into the metal forming a pit [134]. For instance, in LWRs piping components of stainless steel are susceptible to pitting corrosion [4]

A number of computation procedures for general corrosion rates using electro-chemical and thermo-dynamic models exist both for carbon steels and austenitic stainless steels, see e.g. refs. [135, 137]. However, such models are not suitable for mechanical analyses of e.g. wall thinning due to corrosion, as the computed results mainly concern corrosion potential parameters, such as current density at

the corrosion site. A straightforward equation for assessment of general corrosion propagation depth, $d(t)$, is [138]:

$$d(t) = Ct^n \tag{7.3-1}$$

where t is time since the start of corrosion process, C is effective corrosion rate in absence of coating, and n is power law exponent for non-linear behaviour (where applicable), with C and n being empirical material and environment specific parameters.

A number of electro-chemical and thermo-dynamic models exist for pitting corrosion. The model for assessment of pitting propagation rate, V, by Engelhardt and Macdonald [139] is:

$$V(t) = V_0(1 + t/t_0)^n \tag{7.3-2}$$

where V_0 is initial pitting propagation rate, t is time since the start of corrosion process, t_0 is constant, and n is empirical material and environment specific constant. It is important to note that in many cases the period of time over which the approximation; $V(t) \approx V_0$ = constant, is valid can be comparable with the observation time (or even with the service life of the component/system).

7.3.2 Stress corrosion cracking (SCC)

Crack propagation is the favoured action once the stress intensity factor exceeds a critical value, which is mainly determined by the surface energy on the plane of crack propagation, and by the energy dissipated in the plastic zone ahead of the crack. In SCC, the high chemical corrosion rate at the crack tip is driven by the fast diffusion rate of embrittling impurities towards the crack tip. The surface energy is thereby reduced and the critical stress intensity factor decreases. This is an unstable process, which is possibly limited by the corrosion and/or the diffusion rate of impurities [32].

The computation models describing SCC and fatigue induced crack growth for intermediate region are often similar. The data resulting from SCC tests have been presented in both *S-N* curves and fracture mechanics formats [32]. However, often the scatter of SCC data plotted as crack propagation rate against K_I is remarkable, see e.g. ref. [140], thus leaving more accurate assessment of the dependence between these two parameters unclarified.

In simple fracture mechanics based treatments, SCC and fatigue crack growth computation procedures it is assumed that a stress field created at the crack tip causes the crack propagation. Note, that for fatigue, the time variable of interest is measured in number of load cycles, whereas for SCC it is measured in time units. The stress intensity factor K for SCC computations is based on a single tensile stress, whereas the stress intensity range ΔK is based on an alternating stress for fatigue crack propagation [32]. An illustration of SCC propagation rate as a function of K for metallic materials is shown in Figure 7.3-1.

The mathematical expression for intermediate (Stage 2) SCC rate equation is [136]:

$$\frac{da}{dt} = CK_I^n \tag{7.3-3}$$

where a is crack depth, t is time and K_I is the crack tip value of type I stress intensity factor, whereas C and n are material and environment specific constants. The popularity of this SCC equation is based on its simplicity and availability of values for constants C and n, which in turn are assessed based on experimental data.

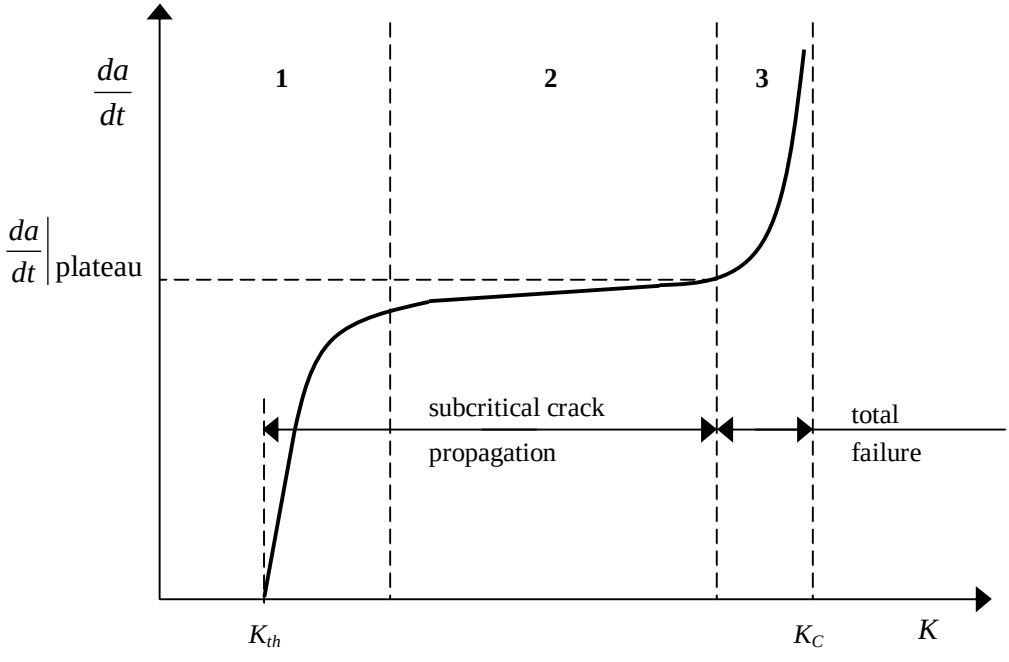

Figure 7.3-1. An illustration of SCC propagation rate as a function of K for metallic materials, showing the stages 1, 2 and 3 as well as the plateau velocity.

When considering smaller scale structure of metallic materials, two SCC modes are identified, namely intergranular SCC (IGSCC) and transgranular SCC (TGSCC), as mentioned earlier in Section 3.4. Values for material and environment specific constants *C* and *n* are presently available only for IGSCC. However, this SCC mode is encountered much more often in power plant environments than TGSCC.

A comprehensive explanation for Stage 1 behaviour has this far not been developed. According to one approach the crack tip strain rate increases rapidly with *K*. According to another approach the crack tip corrosion rate and transport of species within the crack increase rapidly with increasing crack volume and hence with *K* [33].

A further developed and in some applications useful modification of the Stage 2 SCC rate equation that also takes into account *K* threshold is [141, 142]:

$$\frac{da}{dt} = \exp\left[-\frac{Q_g}{R}\left(\frac{1}{T}-\frac{1}{T_{ref}}\right)\right]\alpha\left(K-K_{th}\right)^{\beta} \tag{7.3-4}$$

where: Q_g is thermal activation energy for crack growth = 130 kJ/mol,

R is universal gas constant = 8.314E-03 kJ/mol·K,

T is absolute operating temperature at crack location [K],

T_{ref} is absolute reference temperature used to normalise data = 598.15 K (325 °C),

α is crack growth rate coefficient = 2.67E-12 at 325 °C for da/dt in units of m/s and K in units of MPa√m,

K is crack tip stress intensity factor [MPa√m],

K_{th} is crack tip stress intensity factor threshold = 9 MPa√m,

β is exponent = 1.16.

Equation (7.3-4) is mainly applicable to alloy Inconel 600, which is a commonly used material for NPP pressure boundary components [141, 142].

A similar approach as equation (7.3-4) has been developed for Alloys 182 and 82 which are also commonly used NPP component materials. This equation is [143, 144]:

$$\frac{da}{dt} = \exp\left[-\frac{Q_g}{R}\left(\frac{1}{T} - \frac{1}{T_{ref}} \right) \right] \alpha f_{\text{alloy}}\, f_{\text{orientation}} \left(K\right)^{\beta} \tag{7.3-5}$$

where: f_{alloy} = 1.0 for Alloy 182 and 0.385 for Alloy 82,

$f_{\text{orientation}}$ = 1.0, except for crack propagation that is clearly perpendicular to the dendrite solidification direction, where $f_{\text{orientation}}$ = 0.5,

and otherwise the parameter explanations/values are the same as for equation (7.3-4).

Such more advanced SCC propagation models have been developed that take also into account electro-chemical characteristics and consequent behaviour of protective oxide layer. An example of these models is the SCC propagation equation by Shoji et al. [145]:

$$\frac{da}{dt} = \frac{Mi_0}{z\rho F\left(1-m\right)} \left(\frac{t_0}{\varepsilon_f} \right)^m \left[\beta \left(\frac{\sigma_y}{E} \right) \left(\frac{n}{n-1} \right) \right]^m \left(\frac{2dK/dt}{K} + \frac{da/dt}{r} \right) \times \times \left[\ln\left(\frac{\lambda K^2}{r\sigma_y^2} \right) \right]^{m/(n-1)} \tag{7.3-6}$$

where: M is atomic mass [kg/mol],

i_0 is initial value of decay curve of electric current on newly exposed surface [A/mm^2],

z is charge change at electrolysis (dimensionless),

ρ is density [kg/m^3],

F is Faraday constant [Coulomb/mol],

m is decay constant of current at newly exposed material surface (dimensionless),

ε_f is strain caused by break of protective film at crack tip (dimensionless),

t_0 is starting time of current decay at newly exposed material surface [s],

β, λ are constants (dimensionless),

σ_y is yield stength [MPa],

E is Young's modulus [MPa],

n is work hardening exponent in Ramberg-Osgood equation (dimensionless),

r is radial distance from crack tip [mm].

The SCC model expressed by equation (7.3-6) contains the assumption that the SCC propagation is regarded as a cyclic corrosive process assisted by strain relaxation. When protective oxide film on the surface of steel is broken by operational load, newly exposed surface corrodes following the Faraday's law for electrolysis to form a new film. This process is depicted in Figure 7.3-2 below.

However, equation (7.3-6) contains the uncertain variables r and m. As for m, it is possible to approximately estimate an adequate value by considering the solution conductivity, corrosion potential and the degree of chromium depletion on the grain boundaries. A similar derivation of crack growth rate can be made based upon the slip-oxidation mechanism [146].

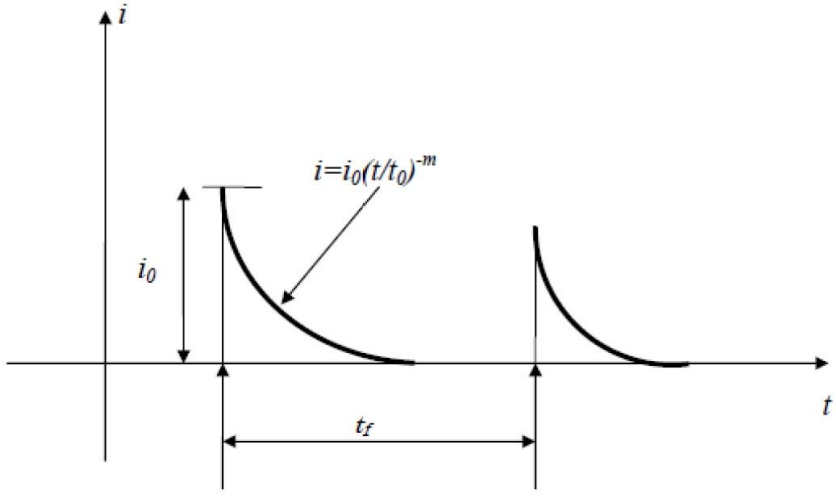

Figure 7.3-2. Current decay after break of protective film followed with formation and break of new film, from ref. [145].

A quite recent predictive methodology for SCC propagation using a mechano-chemical model based on a slip formation/dissolution was presented by Saito and Kuniya [147]. This model consists of combined kinetics of the plastic de-

formation process as a mechanical factor and the slip dissolution-repassivation process as an environmental factor at the crack tip. The model equations are:

$$\frac{da}{dt} = A_0 \left(\frac{\dot{\varepsilon}_{ct}}{C_m} \right)^n \tag{7.3-7a}$$

$$A_0 = \frac{M}{zF\rho_m} \frac{i_0 t_0^n}{(1-n)} \tag{7.3-7b}$$

$$C_m = 2\rho_d (\cos\theta) N_{\text{slip}} n_d b^2 \tag{7.3-7c}$$

where: $\dot{\varepsilon}_{ct}$ is crack tip strain rate,

n is numerical constant correlated with the degree of sensitisation, water conductivity and corrosion potential,

M is atomic weight of the metal,

z is number of electrons involved in the reaction rate,

F is Faraday's constant,

ρ_m is density of the metal,

i_0 is initial dissolution current density at the bare metal surface,

t_0 is short time constant,

ρ_d is dislocation density,

θ is angle between the direction of the slip plane and tensile stress,

N_{slip} is the number of active slip bands,

n_d is the number of dislocations contributing to formation of a slip band, and

b is Burgers vector.

Crack tip strain rate $\dot{\varepsilon}_{ct}$ is calculated from a separate equation, which is a function of for example K and K_{ISCC}, which is the threshold stress intensity factor for SCC. According to the ref. [147] the SCC propagation model enables to predict quantitatively the crack growth for a wide combination of materials, environments and stress conditions.

For instance, for austenitic stainless steel of type 304, which is a commonly used NPP piping component material, in water with temperature of 288 °C equation (7.3-7) is written after incorporation of associated parameter data as [147]:

$$\frac{da}{dt} = 1.1\times10^{-07} \times \left[2.5\times10^{10} \times \exp\left(-\frac{3\times10^{-19} - 1.5\times10^{-20} \times \left(K_I - 2\right)^{1/3}}{7.74\times10^{-21}} \right) \right] \quad (7.3\text{-}8)$$

The results presented in ref. [147] are in good agreement with the experimental SCC measurements performed for the same conditions.

Some remarks concerning the application of SCC propagation computation models are presented in the following. Firstly, all these models contain from a few to several material and environment dependent parameters, the values for which have to be assessed based on experimental data. Often, such parameter data are at least partly missing in the available technical literature. On the other hand, due to SCC tests being relatively expensive to carry out, most/all experimental SCC data are proprietary and thus not available. As for the published parameter data, the available values have mostly/invariably been conservatively developed as upper bound solutions based on the experimental data. As the scatter of SCC data sets is typically wide, the upper bound approach can in this connection lead to excessively conservative SCC equation parameter values. Mostly/invariably SCC model equations are limited to concern only sensitised materials, whereas in the operating NPPs, there are numerous components of SCC susceptible materials that have not experienced sensitising treatments/conditions. Such components are at most weakly susceptible to SCC. However, due to welding process the weld regions and adjacent heat affected zones (HAZs) are often sensitised. Consequently, in structural integrity assessments concerning SCC the crack postulates are often located to these regions. On the other hand, in weld and HAZ regions locally confined weld residual stresses have to be taken mostly/fully into account as well. In commonly used fitness-for-service handbooks, these stresses have also been developed as upper bound solutions based on the underlying experimental data, in this case conservatively on the tensile side. Furthermore, of the *K* values over the crack front, typically only that from the crack tip is used in the incremental SCC propagation computations, as in most cases it is also the maximum value. However, the variation of the *K* values along the crack front is typically relatively large, and consequently the crack tip value, being a conservative choice, describes quite poorly the overall/average growth

potential of the crack front. Thus the SCC propagation computations are often burdened with conservative assumptions coming from several sources at the same time. When performing computational SCC analyses, it is quite difficult to avoid ending up with excessively conservative results, and thus it appears that further procedure and test/input data treatment development would be necessary. Obviously, this calls for contributions from several fields/sources of science.

7.4 Creep

Creep degradation occurs in power plant components that operate at high temperatures relative to the material melting point. See Section 3.5 for a more detailed description of the issue. From a continuum point of view, the most relevant parameters with regard to creep degradation are the strain rate, $\dot{\varepsilon}$, and time to rupture, t_r. To obtain these, constitutive equations relating these parameters to stress and temperature have been developed.

One of the earliest and still commonly used constitutive equations for modelling creep is that by Norton [148], which expresses the relation between strain rate, $\dot{\varepsilon}$, and prevailing stress, σ, as follows:

$$\dot{\varepsilon} = A\sigma^n \tag{7.4-1}$$

where A is the rate coefficient (considered temperature dependent) and n the creep exponent, both being material specific independent constants for which values are obtained experimentally. This equation describes creep behaviour mainly in the secondary regime. Later on, more advanced and also more complex constitutive equations for modelling creep have been developed, e.g. those by Graham and Walles [149], Garofalo [150], Dyson and McClean [151] as well as Merckling [152].

Larson and Miller developed a time temperature parameter approach [154] that relates the stress state to the time of rupture. The approach combines the Arrhenius law for the thermally activated process rate with the constitutive equation by Norton (7.4-1), resulting with the following equation:

$$P_{LM}(\sigma) = T\left[\log(t_r) + C\right] = M - N\log(\sigma) \tag{7.4-2}$$

where P_{LM} is Larson-Miller parameter, T is temperature, t_r is time of rupture, M and N are material dependent parameters and $C = \log(nA)$. Other time tempera-

ture parameter equations have been developed as well, such as that by Manson and Haferd [153]. Equation (7.4-2) indicates that the Larson-Miller parameter is linear against logarithmic time. However, most often all time temperature parameters are fitted as polynomial stress functions.

Cumulative damage equations for creep exist as well. The most common approach to calculation of cumulative creep damage is to compute the amount of life expended by using time or strain fractions as measures of damage. When the fractional damages add up to unity, then failure is postulated to occur.

One commonly used cumulative creep damage equation, called life fraction rule, is expressed as [155]:

$$\sum \frac{t_i}{t_{ri}} = 1 \tag{7.4-3}$$

where t_i is time spent at condition i and t_{ri} is life to rupture at the same conditions, as obtained from associated standard/normative documents. As according to commonly used notation, the number of all considered conditions, n, is not shown in the equation. A similar creep damage model as that expressed by equation (7.4-3) but based on strains, called strain fracture rule, is expressed as [156]:

$$\sum \frac{\varepsilon_i}{\varepsilon_{ri}} = 1 \tag{7.4-4}$$

where ε_i is strain cumulated at condition i and ε_{ri} is rupture strain at the same conditions. Then, a creep damage approach combining time and strain, called mixed rule, is expressed as [157]:

$$\sum \left(\frac{t_i}{t_{ri}} \right)^{1/2} \left(\frac{\varepsilon_i}{\varepsilon_{ri}} \right)^{1/2} = 1 \tag{7.4-5}$$

Finally, a further developed combining model as compared to that expressed by equation (7.4-5), is [158]:

$$k \sum \left(\frac{t_i}{t_{ri}} \right) + (1-k) \sum \left(\frac{\varepsilon_i}{\varepsilon_{ri}} \right) = 1 \tag{7.4-6}$$

where k is constant. For the equations (7.4-3) to (7.4-6), creep failure is postulated to occur when the fractional damages add up to unity.

Numerous constitutive equations for modelling creep exist, and for application they all require a sufficient amount of experimental creep data for the material, time scale and temperature range in question. Typically at least partly/mostly such data are available on the technical literature. Here, however, local creep degradation modelling procedures are more on focus than those considered this far, being based on continuum approach corresponding to more globally occurring creep degradation.

Fracture mechanics based methods can also be applied for modelling creep degradation. Components that operate at high temperatures relative to the melting point of the material may fail by slow and stable extension of a macroscopic crack. Traditional approaches to design in the creep regime apply only when creep and material damage are uniformly distributed. Time dependent fracture mechanics approaches are required when creep failure is controlled by a dominant crack in the structure.

Deformation at high temperatures can be divided into four regimes: instantaneous (elastic) strain, and the earlier mentioned creep regimes primary, secondary and tertiary creep. The elastic strain occurs immediately upon application of the load. Whereas microscopic failure mechanisms, such as grain boundary cavitation, nucleate during tertiary creep. During the growth of a macroscopic crack at high temperatures, all four types of creep response can occur simultaneously in the most general case, see Figure 7.4-1. The material at the tip of a growing crack is in the tertiary stage of creep, since the material is obviously failing locally. The material may be elastic remote from the crack tip, and in the primary and secondary stages of creep at moderate distances from the tip.

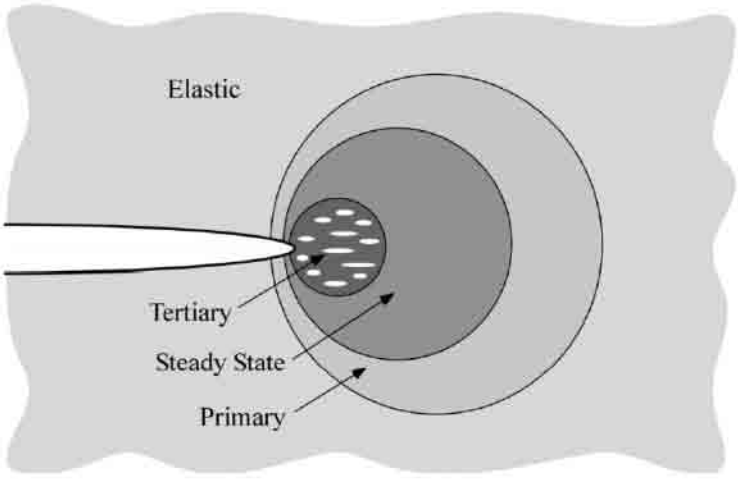

Figure 7.4-1. Creep zones at the vicinity of the crack tip, from ref. [30].

A formal fracture mechanics approach to creep crack growth was developed soon after the *J*-integral was established as an elastic-plastic fracture parameter. Landes and Begley [159], Ohji et al. [160] and Nikbin et al. [161] independently proposed what became known as the C^*-integral to characterize crack growth in a material undergoing steady-state creep.

The C^* integral is defined by replacing strains with strain rates, and displacements with displacement rates in the *J*-integral, see equation (4.3-5) in Section 4.3, as follows:

$$C^* = \int_\Gamma \left(\dot{w}dy - \sigma_{ij} n_{ij} \frac{\partial \dot{u}_i}{\partial x} ds \right) \tag{7.4-7}$$

where $\dot{u}_i$ are displacement rate components and $\dot{w}$ is the stress work rate (power) density, defined as:

$$\dot{w} = \int_0^{\dot{\varepsilon}_{kl}} \sigma_{ij} d\dot{\varepsilon}_{ij} \tag{7.4-8}$$

The analogy by Hoff [162] implies that the C^* integral is path independent, because *J*-integral is path independent. When strain rate in secondary creep follows a power law:

$$\dot{\varepsilon}_{ij} = A\sigma_{ij}^{n} \tag{7.4-9}$$

where A and n are material constants from the Norton equation (7.4-1), then it is possible to define a HRR type singularity for stresses and strain rates near the crack tip as:

$$\sigma_{ij} = \left(\frac{C^*}{AI_n r} \right)^{1/(n+1)} \tilde{\sigma}_{ij}(n,\theta) \tag{7.4-10a}$$

and:

$$\dot{\varepsilon}_{ij} = \left(\frac{C^*}{AI_n r} \right)^{1/(n+1)} \tilde{\varepsilon}_{ij}(n,\theta) \tag{7.4-10b}$$

where the constants I_n, $\tilde{\sigma}_{ij}$, and $\tilde{\varepsilon}_{ij}$ are identical to the corresponding parameters in the HRR model, see equations (4.3-8) and (4.3-9) in Section 4.3. Note that in the present case, n is a creep exponent rather than a strain hardening exponent. Just as the J-integral characterizes the crack tip fields in an elastic or elastic-plastic material, the C^*-integral defines crack tip conditions in a viscous material. Thus, the time dependent crack growth rate in a viscous material should depend only on the value of C^*. Experimental studies [159–162] have shown that creep crack growth rates correlate well with C^*, provided steady state creep, i.e. secondary regime creep, is the dominant deformation mechanism in the specimen.

The C^* parameter applies only to crack growth in the presence of global steady state creep. Explained in another way, C^* applies to long time behavior. When the crack grows with time, the behavior of the structure depends on the crack growth rate relative to the creep rate. In brittle materials, the crack growth rate is as fast that it overtakes the creep zone, and then crack growth can be characterized by K_I because the creep zone at the tip of the growing crack remains small. At the other extreme, if the crack growth is sufficiently slow for the creep zone to spread throughout the structure, C^* is the appropriate characterizing parameter. Riedel and Rice [163] defined a characteristic time for the transition from short time to long time behaviour, t_1, as:

$$t_1 = \frac{K_I^2 \left(1-\nu^2\right)}{(n+1)EC^*}, \quad \text{or;} \tag{7.4-11a}$$

$$t_1 = \frac{J}{(n+1)C^*} \tag{7.4-11b}$$

When significant crack growth takes place over time scales much less than t_1, the behavior can be characterized by K_I, while C^* is the appropriate parameter when significant crack growth requires times >> t_1. Based on a finite element analysis, Ehlers and Riedel [164] suggested the following simple equation to interpolate between small scale creep and extensive creep (short and long time behaviour, respectively):

$$C(t) \approx C^*(t_1/t+1) \tag{7.4-12}$$

where t is time. Unlike K_I and C^*, a direct experimental measurement of $C(t)$ under transient conditions is usually not possible. Saxena [165] defined an alternate parameter C_t which deviates to some extent from $C(t)$. The advantage of C_t is that it can be measured relatively easily. Saxena proposed the following interpolation between small scale creep and extensive creep:

$$C_t = (C_t)_{SSC}(1-\dot{\Delta}/\dot{\Delta}_t)+C^* \tag{7.4-13}$$

where $(C_t)_{SSC}$ is separately computed small scale creep limit for C_t, $\dot{\Delta}$ is total displacement rate and $\dot{\Delta}_t$ is creep displacement. In the limit of long time behavior, C^*/C_t = 1.0, but this ratio is less than unity for small scale creep and transient behaviour. The $C(t)$ parameter characterizes the stresses ahead of a stationary crack, while C_t is related to the rate of expansion of the creep zone. The latter quantity appears to be better suited to materials that experience relatively rapid creep crack growth. Both parameters approach C^* in the limit of steady state creep.

The primary creep may have an appreciable effect on the crack growth behaviour as well if the size of the primary zone is significant. Riedel [166] introduced a new parameter C_h^*, which is the primary creep analog to C^*. The characteristic time that defines the transition from primary to secondary creep, t_2, is defined by:

$$t_2 = \left[\frac{C_h^*}{(1+p)C^*}\right]^{(p+1)/p} \tag{7.4-14}$$

where p is material specific constant for primary creep. When primary creep strains are present also the interpolation scheme for $C(t)$ is modified [166]:

$$C(t) \approx \left[\frac{t_1}{t} + \left(\frac{t_2}{t} \right)^{(p+1)/p} + 1 \right] C^* \tag{7.4-15}$$

The creep damage models presented here contain from a few to several material and environment specific parameters, the values for which have to be assessed based on experimental data. At least partly, this parameter data may be missing in the available technical literature.

As for crack growth rates during creep, Nikbin, Webster et al. [167, 168, 169] have presented a model which is based on fracture mechanics to determine the time taken for the creep damage to accumulate at the crack tip starting from first initial elastic loading. Essentially, the steady state creep crack growth rate, da/dt, can be correlated with sufficient accuracy to the C^* as follows:

$$\frac{da}{dt} = D_0 C^{*\phi} \tag{7.4-16}$$

where D_0 and ϕ are material constants which can be measured experimentally using the NSW model, see ref. [167]. For most engineering metals equation (7.4-16) can be approximated as:

$$\frac{da_s}{dt} = \frac{3C^{*0.85}}{\varepsilon_f^*} \tag{7.4-17}$$

where da_s/dt is the steady state crack growth rate and ε_f^* is taken as the uniaxial failure strain. For plane stress conditions this failure strain is $\varepsilon_f^* = \varepsilon_f$, whereas for plain strain conditions it is $\varepsilon_f^* = \varepsilon_f / 30$. This range describes the effects of constraint on crack growth due to both material properties and size/geometric factors. Then, the initial crack growth rate, da_0/dt, can be approximated in relation to that in the steady state as:

$$\frac{da_0}{dt} = \frac{da_s/dt}{n+1} \tag{7.4-18}$$

For most engineering materials the values of n usually fall within the range of 5 to 10, which suggests that da_0/dt is approximately 10 % of the corresponding steady state value.

In design and for predicting remaining life in operation of components in elevated temperatures, extensive use is made of test data obtained with specimens subjected to uniaxial loading [11]. However, components in service generally experience multi-axial loading conditions. It is therefore necessary to establish effective stress criteria governing creep and rupture under multi-axial stress conditions and to be able to interpret them in terms of uniaxial test data. In addition, the redistributions of stresses occurring with creep must be taken into account. For a brief review of the former of these two aspects, see the paper by Roberts et al. [170].

7.5 Irradiation embrittlement

The material changes caused by neutron irradiation that may affect the use of the NPP reactor pressure vessels (RPVs) are connected to the fracture resistance of materials. As a rule, irradiation reduces the fracture toughness of the materials and therefore it is important to know the rate of reduction as a function of irradiation dose. Here, the description concerning computation of irradiation embrittlement of NPP RPVs corresponds mainly to that in the U.S. ASME code Section XI [173, 174] together with the U.S. Regulatory Guide 1.99, Revision 2 [171]. Most European approaches for evaluating irradiation effects in reactor pressure vessels are based on the ASME code [173, 174] procedure. In some countries, like U.K., no accepted standard approach exists, but a case by case best estimate analysis is carried out [177]. Many countries apply the ASME code directly, but in some countries like France [175, 176] the approaches have, however, experienced a national variation.

The reduction in the fracture toughness is evaluated with the aid of material specific reference nil-ductility temperature, RT_{NDT}. This temperature is determined from the nil-ductility temperature (NDT) and the Charpy-V impact test. The NDT temperature is determined in accordance with the ASTM Standard E 208 [172]. If the minimum impact energy and lateral expansion in the Charpy-V test (3 specimens) are at least 68 J and 0.9 mm, respectively, at a temperature equal to NDT + 33 °C, the NDT temperature is taken to represent RT_{NDT}. If the Charpy-V properties do not meet the above criterion, RT_{NDT} is taken as the tem-

perature at which the requirements are reached, minus 33 °C. Normally, for modern steels RT_{NDT} is equal to NDT.

The ASME code is based upon linear-elastic fracture mechanics. The French approach originates from the ASME methodology, but it is more flexible, e.g. to account for possible plasticity effects. Both approaches assume that the temperature dependence of fracture toughness is not affected by irradiation, enabling the fracture toughness temperature dependence to be described by a single curve. The shift is either determined based upon Charpy-V impact tests or from the chemical composition of the material, applying a chemistry factor.

The ASME code Section XI [173] includes both a static fracture initiation reference curve and a crack arrest reference curve. It is additionally assumed that the difference between static initiation and crack arrest is constant. Both curves are given as a function of effective temperature (T-RT_{NDT}), where RT_{NDT} is as explained above. For the fracture mechanical assessment of normal operation conditions, the crack arrest curve also describes crack initiation. Reference [173] provides also equations for both of these curves. The crack arrest reference curve is intended to describe normal operation conditions, and the static fracture initiation reference curve emergency and faulted conditions. In addition to the different reference curves, also safety factors are applied. The French approach applies essentially the ASME fracture toughness reference curves, but the safety factors are different and also the definition of upper limiting plateau, i.e. “upper shelf”, differs from that in ASME.

In the ASME code approach, the irradiation induced shift of the RT_{NDT} is defined as the shift in the 41 J impact energy transition temperature, TK_{41J}. It is assumed that the true static fracture toughness shift and crack arrest shift is equal to or less than ΔTK_{41J} (ΔRT_{NDT}). Reference [171], requires the use of an additional margin in the determination of RT_{NDT}. For welds, the margin is 31 °C and for base metal, 19 °C. In both cases, the margin is not, however, more than ΔRT_{NDT} /2. This margin is put on top of the experimental ΔRT_{NDT}.

Based upon ΔRT_{NDT} the fluence dependence can be calculated as [171]:

$$\Delta RT_{NDT} = (CF) f^{(028-0.10\cdot\log(f))} \tag{7.5-1}$$

where CF is the radiation embrittlement coefficient and f is the neutron fluence (×10E-19 n/cm^2) with E > 1 MeV. When two or more credible surveillance data

sets are available, the radiation embrittlement coefficient is determined from the experimental data by least square fitting.

Definitions of critical fracture toughness for the lower bound crack initiation value K_{IC} and the lower bound crack arrest value K_{Ia} are presented in Appendix A of ASME Section XI [173]. The effects of irradiation on the crack initiation and arrest fracture toughness can be estimated by applying the shift in the RT_{NDT} to shift the ASME lower bound curves by moving the curves by the same shift amount, but leaving the shapes unaltered. These relationships are expressed as [32, 178]:

$$K_{IC} = \min\begin{cases} 33.2 + 2.806 \times \exp\left[0.02 \cdot \left(T - RT_{NDT_0} - \Delta RT_{NDT} + 100\right)\right] \\ 200 \end{cases} \quad (7.5\text{-}2)$$

$$K_{Ia} = \min\begin{cases} 26.78 + 1.233 \times \exp\left[0.0145 \times \left(T - RT_{NDT_0} - \Delta RT_{NDT} + 160\right)\right] \\ 200 \end{cases} \quad (7.5\text{-}3)$$

where RT_{NDT_0} is the initial NDT temperature for unirradiated material, while K_{IC} and K_{Ia} are expressed in units of ksi$\sqrt{\text{in}}$, and T, RT_{NDT_0} and ΔRT_{NDT} in units of °F.

The French approach differs from the ASME methodology. The irradiation induced shift of the RT_{NDT} is defined as the shift in the 56 J impact energy transition temperature, $TK_{56\text{J}}$, or the shift in the 0.9 mm lateral expansion transition temperature, $TK_{0.9\text{mm}}$, whichever is greater. The lateral expansion corresponding to a certain energy level is affected by the material yield strength. Increasing the yield strength makes plastic deformation of the specimen more difficult. Therefore, ΔRT_{NDT} is generally controlled by $\Delta TK_{0.9\text{mm}}$. The French approach does not apply additional safety margins. The French codes [175, 176] allow the fluence dependence of ΔRT_{NDT} to be determined experimentally, but do not give any recommendations for the type of expression to be used.

As for the chemistry factor, the European approaches also apply that concept in an effort to determine the irradiation shift directly from the steel chemistry. For the ASME methodology type steels, ref. [171] gives different chemistry factors for welds and base metal in a tabulated form. Even when ΔRT_{NDT} is calculated with the chemistry factor, one is required to use the additional safety margin prescribed in ref. [171]. The French codes contain chemistry factor equations which are dependent on phosporus, copper and nickel.

7.6 Modelling of interaction of degradation mechanisms

Modelling of interaction of degradation mechanisms is considered in the following. Theoretically and in several cases in practise, the number of possible combinations for interacting degradation mechanisms is relatively high. More than two degradation mechanisms can participate in the interaction. However, the scope is here limited to cover the major degradation mechanism interaction phenomena encountered/experienced in the power plant environments. These cases of interacting degradation mechanisms are corrosion fatigue and creep fatigue. In the first case, joint damage by crack growth is considered, whereas in the second case, more general cumulative damage is covered as well. Concerning corrosion fatigue, environmental fatigue correction factor approach for incorporating effects of environment into fatigue evaluations is briefly described as well.

Corrosion fatigue

Corrosion fatigue is fatigue enhanced by corrosion reactions. Since fatigue failures usually occur at stress levels below the yield strength after a number of cycles, the presence of a corrosive environment reduces the number of cycles to failure as well as the stress level at which failure occurs. The nominal fatigue limit, if any, is eliminated. Thus, corrosion fatigue is the reduction of the fatigue resistance of a material due to the presence of a corrosive environment. Although corrosion fatigue is characterized by cracking like SCC, corrosion fatigue is not environment specific, i.e., all environments will reduce the fatigue life of a component. In almost all corrosion fatigue cases, cracking is transgranular [138].

Many models which combine fatigue and stress corrosion effects have been suggested for use in predicting the corrosion fatigue crack growth rate as a function of fatigue loading frequency. These models can be divided into three categories:

- superposition models [179],
- competition models, and
- models for environmentally modified material deformation and fatigue properties [180–183].

The superposition models and the competition models are developed based on the following assumptions: (1) an environmental fracture process is independent from the mechanical fatigue fracture process, and (2) the mechanical fatigue fracture process in a corrosive environment is identical with the process in an inert environment.

Corrosion fatigue can be load cycle dependent, time dependent, or dependent on both of these. Of these the load cycle dependent corrosion fatigue corresponds to a simple acceleration of the fatigue crack growth that is insensitive to the loading frequency. The crack growth rate can be represented by an acceleration factor, Φ, multiplied by the inert growth rate [30]:

$$\left(\frac{da}{dN}\right)_{\text{aggressive}} = \Phi\left(\frac{da}{dN}\right)_{\text{inert}} \tag{7.6-1}$$

This expression can be applied for ΔK values above the fatigue threshold ΔK_{th} for the inert environment. The acceleration factor Φ may be a constant or it may vary with ΔK. Load cycle dependent corrosion fatigue normally occurs in environments that do not result in significant environmentally assisted cracking (EAC) under static loading and where mass transport and electrochemical reactions that contribute to fatigue acceleration are very rapid. Time dependent corrosion fatigue can be modelled by a simple superposition of the inert fatigue crack growth rate with the environmental cracking rate, as follows [30]:

$$\left(\frac{da}{dN}\right)_{\text{aggressive}} = \left(\frac{da}{dN}\right)_{\text{inert}} + \frac{1}{f}\left(\frac{d\bar{a}}{dt}\right)_{\text{EAC}} \tag{7.6-2}$$

where $\left(d\bar{a}/dt\right)_{\text{EAC}}$ is the average environmental crack growth rate over a loading cycle, and f is the loading frequency. Most material/environment combinations display both cycle dependent and time dependent behaviour. Combining equation (7.6-1) and equation (7.6-2) gives the following more general expression for corrosion fatigue [30]:

$$\left(\frac{da}{dN}\right)_{\text{aggressive}} = \Phi\left(\frac{da}{dN}\right)_{\text{inert}} + \frac{1}{f}\left(\frac{d\bar{a}}{dt}\right)_{\text{EAC}} \tag{7.6-3}$$

Concerning the equations (7.6-1) to (7.6-3), the inert terms are computed with a suitable fatigue crack growth procedure in Section 7.2 and the EAC terms with a suitable procedure in Section 7.3.2, respectively. By definition, the growth rate is independent of frequency for cycle dependent corrosion fatigue. The time dependent corrosion fatigue is sensitive to the frequency, as equation (7.6-2) indicates. At high frequencies, the crack growth rate approaches the inert rate

because the EAC growth per cycle is negligible. At low frequencies, the environmental crack growth per cycle dominates over fatigue, and the rate is proportional to 1/*f*. When there is a combination of time dependent and cycle dependent acceleration of crack growth rate, the former dominates at low frequencies and the latter dominates at high frequencies.

Another variable that can affect the corrosion fatigue crack growth rate is the wave form of the cyclic loading. If, for example, the cyclic loading followed a square wave form instead of a sine wave, one might expect the average EAC growth rate to be greater because the maximum load is held for a sustained period with a square wave form. A saw-tooth waveform might be expected to produce less environmental cracking per cycle, all else being equal. A mitigating factor is that environmental cracking is often faster during periods when *K* is increasing. In those instances, a square wave form might actually result in less environmental cracking per cycle because a sustained load is less damaging than a continually rising load.

Environmental fatigue correction factor approach

The report NUREG/CR-6909 [184] by USNRC provides an environmental fatigue correction factor (F_{en}) methodology that is considered acceptable for incorporating the effects of reactor coolant environments on fatigue usage factor evaluations of metal components for new reactor construction. The methodology reflects the earlier development on the subject carried out in Japan, presently it is included in the JSME codes for nuclear power generation facilities, see refs. [185, 186]. In the ref. [184] the environmental fatigue correction factor methodology for performing fatigue evaluations is described for the four major categories of structural materials, those being carbon steel, low-alloy steels, wrought and cast austenitic stainless steels, and Ni-Cr-Fe alloys, respectively.

The effects of reactor coolant environments on the fatigue life of structural materials are expressed in terms of a nominal environmental fatigue correction factor, $F_{en,nom}$, which is defined as the ratio of fatigue life in air at room temperature, $N_{air,RT}$, to that in water at the service temperature, N_{water}, as follows [184]:

$$F_{en,nom} = N_{air,RT} / N_{water} \tag{7.6-4}$$

For the above mentioned four major categories of structural steels the nominal environmental fatigue correction factor has the following form:

$$F_{en,nom} = \exp\left(C1 - C2 \times S^* \times T^* \times O^* \times \dot{\varepsilon}^*\right) \tag{7.6-5}$$

where S^*, T^*, O^* and $\dot{\varepsilon}^*$ are transformed sulphur content, temperature, level of dissolved oxygen and strain rate, whereas C1 and C2 are constants, respectively. For these four transformed input data parameters, the definitions are given steel category specifically. The values of the two constants C1 and C2 vary case specifically between 0 and 1. For carbon and low-alloy steels, all transformed input data parameters are defined as a function of their nominal values, whereas for wrought and cast austenitic stainless steels and Ni-Cr-Fe alloys, the same applies otherwise but $S^* = 1$. For the two latter steel categories also O^* is constant, though with steel category and in some cases water chemistry specifically differing values. The minimum value of $F_{en,nom}$ is one, corresponding to conditions below the strain amplitude threshold.

The necessary input data for this fatigue evaluation procedure includes partial fatigue usage factors U1, U2, U3, …, Un, as determined in ASME Section III [174] for Class 1 fatigue evaluations. To incorporate environmental effects into the Section III fatigue evaluation, the partial fatigue usage factors for a specific stress cycle or load set pair is multiplied by the environmental fatigue correction factor:

$$U_{en,1} = U_1 F_{en,1} \tag{7.6-6}$$

where the fatigue usage factor values are determined according to the current code fatigue design curves, as given e.g. in Appendix I of ASME Section III [174]. The cumulative fatigue usage factor, U_{en}, considering the effects of reactor coolant environments is then calculated as:

$$U_{en} = U_1 F_{en,1} + U_2 F_{en,2} + U_3 F_{en,3} + \ldots + U_i F_{en,i} + \ldots + U_n F_{en,n} \tag{7.6-7}$$

where $F_{en,i}$ is the nominal environmental fatigue correction factor for the “i”th stress cycle, see Paragraph NB-3200 [174], or load set pair, see Paragraph NB-3600 [174]. Because environmental effects on fatigue life occur primarily during the tensile loading cycle (i.e. rising ramp with increasing strain or stress), this calculation is performed only for the tensile stress producing portion of the stress cycle constituting a load pair. The values for parameters such as strain rate, temperature, dissolved oxygen in water, and for carbon and low–alloy steels sulphur content, are also needed to calculate F_{en} for each stress cycle or load set pair.

Nearly all of the existing fatigue *ε-N* data concerning ref. [184] are obtained under uniaxial loading histories with constant strain rate, temperature, and strain amplitude. However, the actual loading histories encountered during service of NPPs are far more complex, and the stress/strain responses are in general three dimensional. The modified rate approach has been proposed to predict fatigue life under changing test conditions. It allows calculating F_{en} under conditions where temperature and strain rate are changing. The correction factor, $F_{en}(\dot{\varepsilon}, T)$, is assumed to increase linearly from 1 with increments of strain from a minimum value ε_{min} [%] to a maximum value ε_{max} [%]. Then, F_{en} for the total strain transient is computed as:

$$F_{en} = \sum_{k=1}^{n} F_{en,k}(\dot{\varepsilon}_k, T_k)\left(\frac{\Delta\varepsilon_k}{\varepsilon_{max} - \varepsilon_{min}}\right) \tag{7.6-8}$$

where n is the total number of strain increments, and k is the subscript for the "k"th incremental segment. An illustration of the application of the modified rate approach is presented in Figure 7.6-1 below.

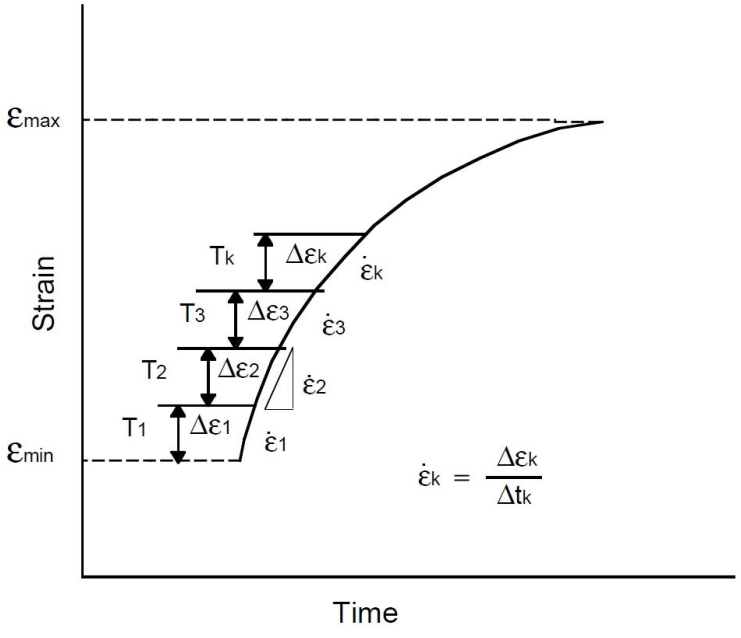

Figure 7.6-1. Application of the modified rate approach to determine the environmental fatigue correction factor F_{en} during a transient, from ref. [184].

However, the description of the modified rate approach appears insufficient for computing the strain values and consequent F_{en} values for actual NPP piping components concerning typical load transients with varying load parameter values. Namely, the partial usage factors U_i are computed according to the Paragraphs NB-3200 and NB-3600 of ref. [174] for load cycles as defined therein, and the correspondence of these cycle definitions and the rising ramps with increasing strain or stress considered by the modified rate approach is unclear for the various possible kinds of load cycles encountered in the actual NPP environments. Moreover, the choice of sign for the cycle specific stress intensities computed according to the Paragraph NB-3200 of ref. [174] is not unambiguous, and neither is the choice of the associated strain component. Other gaps concerning the conduct of application of the F_{en} approach in practise exist as well. The main shortcoming of the NUREG/CR-6909 [184] F_{en} approach appears to be its uniaxial nature, which remarkably limits its feasibility to actual plant conditions where the stresses/strains experienced by components are in general three dimensional.

More recently, ASME has provided Code Case N-792, Fatigue Evaluations Including Environmental Effects [187], to supplement fatigue assessment procedures in ref. [174]. This document [187] contains Fen based methodology for incorporating the effects of reactor coolant environments on fatigue usage factor evaluations of metal components, which is mostly the same as that presented in the report NUREG/CR-6909 [184]. The new developments include general guidance on combining plant load transients to load cycles for fatigue analysis purposes, also presented are slightly updated versions of the ANL S-N fatigue design curves in air given in ref. [184] for carbon steel, low-alloy steels, wrought and cast austenitic stainless steels and Ni-Cr-Fe alloys. It is also mentioned in ref. [187], that for the four mentioned material types it can be used for evaluation of thermal and mechanical fatigue, as caused by the LWR environment during service. On the other hand, the provided approach for assessment of strain rate is more limited than e.g. the modified rate approach described in the NUREG/CR-6909 [184], see equation (7.6-8) above. Namely, it is simply given as the stress intensity divided by Young's modulus multiplied by the time from the start of load transient for the stress difference corresponding to the stress intensity to reach the maximum value, i.e. a strictly linear approach. However, it is also mentioned in ref. [187], that the presented strain rate computation approach has interim status, and that the rules for determination of strain rate for NPP piping components are in the course of preparation.

Creep fatigue interaction

Changes in loading conditions during operation cause transient temperature gradients to power plant components operating mostly at relatively high temperatures. Due to restrained thermal expansion these transients cause thermally induced stress cycles. The extent of ensuing fatigue damage depends on the severity and frequency of occurrence of these transients as well as of the material properties. Components which are subject to thermally induced stresses generally operate within creep range so that damage caused by both fatigue and creep has to be taken into account [11].

The most common approach to take into account the simultaneous effect of creep and fatigue is based on linear superposition. This procedure, combining the damage summation of Robinson for creep [155] and that of Miner for fatigue [99], is expressed as [188]:

$$\sum \frac{N}{N_f} + \sum \frac{t}{t_f} = D' \tag{7.6-9}$$

where N/N_f is the cyclic portion of the life fraction, in which N is the number of cycles at a given strain range and N_f is the pure fatigue life at that strain range. The time dependent creep life fraction is t/t_r, where t is the time at a given stress and t_r is the time to rupture at that stress. The stress relaxation period is divided into time blocks during which an average, constant value of stress prevails, and for each time block t/t_r is computed and summed up. D' is the cumulative damage index. When $D' = 1$, failure is assumed to occur.

A strain based damage rate approach which takes into account the rate of damage accumulation has been proposed by Majumdar and Maiya [189-192]. They view the total damage as consisting of fatigue induced crack growth, da_{FA}/dt, and creep induced cavity growth, da_{CA}/dt. If the two damage mechanisms are additive, the damage rate is given by the sum of the following two equations:

$$\left(\frac{1}{a_{FA}}\right)\frac{da_{FA}}{dt} = \begin{cases} T\left|\varepsilon_p\right|^s \left|\dot{\varepsilon}_p\right|^{k2} & \text{for tension,} \\ C\left|\varepsilon_p\right|^s \left|\dot{\varepsilon}_p\right|^{k2} & \text{for compression.} \end{cases} \tag{7.6-10}$$

and:

$$\left(\frac{1}{a_{CA}}\right)\frac{da_{CA}}{dt} = \begin{cases} G\left|\varepsilon_p\right|^s\left|\dot{\varepsilon}_p\right|^{k3} & \text{for tension,} \\ -G\left|\varepsilon_p\right|^s\left|\dot{\varepsilon}_p\right|^{k3} & \text{for compression.} \end{cases} \tag{7.6-11}$$

where T, C, G, $k2$, $k3$ and s are material parameters dependent on temperature, environment and the metallurgical state of the material, ε_p and $\dot{\varepsilon}_p$ are the current and absolute values of plastic strain and plastic strain rate, respectively, whereas a_{FA} and a_{CA} are the crack and cavity size at time t. The parameters T and C are included to account for differences in growth rates in tension and compression. Equation (7.6-10) describes the crack growth induced damage due to fatigue, whereas equation (7.6-11) describes the crack growth induced damage due to creep, respectively. The parameters T and C are included to account for differences in growth rates occurring in tension and compression. The parameter G is given the appropriate sign for the tensile or the compressive stress regime. Final failure is computed as the reciprocal of the sum of the crack and cavity damage.

For cases where the fatigue and creep damages are interactive (not additive), Majumdar and Maiya have proposed the following slightly modified equation [193]:

$$\left(\frac{1}{a_{FA}}\right)\frac{da_{FA}}{dt} = \left(T \vee C\right)\left[1+\alpha\ln\left(\frac{a_{CA}}{a_{CA,0}}\right)\right]\left|\varepsilon_p\right|^s\left|\dot{\varepsilon}_p\right|^{k2} \tag{7.6-12}$$

Here it is assumed that cavities of size larger than $a_{CA,0}$ interact with fatigue induced crack and increase the crack growth rate. As for parameter α, when it equals zero the fatigue crack growth is unaffected by the cavities and reverts to continuous cycling as according to equation (7.6-10). The equation for the creep induced cavity growth does not alter, i.e. equation (7.6-11) is applied as such. The damage rate approach allows taking into account the effects of various wave shapes on fatigue life. This model has been successfully applied e.g. to 1Cr-Mo-V steels [194] and austenitic stainless steels [189-192].

The crack growth rate computation equations proposed Majumdar and Maiya contain several parameters the values for which have to be determined experimentally. Nikbin, Webster et al. [169, 195] concluded that a more straightforward model containing less parameters to be assessed experimentally can be

derived for computation of crack growth rate due to joint effect of fatigue and creep. This model equation for computing the total/combined crack growth rate, $(da/dN)_{TOTAL}$, is:

$$\left(\frac{da}{dN}\right)_{TOTAL} = C(\Delta K)^m + \frac{da/dt}{f} \tag{7.6-13}$$

where the first term on the right side is the Paris-Erdogan equation for fatigue induced crack growth, see equation (7.2-12), f is frequency and da/dt is computed according to equation (7.4-16), respectively.

The creep fatigue interaction damage models presented here contain from a few to several material and environment specific parameters, the values for which are obtained as based on experimental data. At least partly this parameter data may be missing in the available technical literature.

7.7 Commonly applied component degradation assessment procedures

One convenient way to categorise various structural integrity/degradation assessment procedures is to divide them into low and high temperature procedures [196]. Low temperature procedures can be further divided into assessment procedures based on failure assessment diagram (FAD) calculation procedures and fitness-for-service guides, assessment procedures based on crack driving force (CDF) techniques and other procedures. More recently, also procedures that apply for both high and low temperatures have been developed.

Low temperature procedures

Low temperature structural integrity/degradation assessment procedures can be further divided to the following subgroups [196]:

- assessment procedures based on FAD approach;
  - calculation procedures,
  - fitness-for-service guides,
- assessment procedures based on CDF techniques,
- others.

The FAD methodology is based on the use of an integrated graphical representation where fracture failure and plastic collapse are simultaneously evaluated by

means of two non-dimensional variables (L_r and K_r). These two variables represent the ratio between the applied value of either stress or stress intensity factor and the resistance parameter of the corresponding magnitude (yield strength or fracture toughness). Once the plotting plane is determined by the variables L_r and K_r, each procedure defines a critical failure line which establishes the safe or acceptable zone. This zone is the area bounded by the mentioned line and the axes. The procedures which apply FADs have been divided into two different groups according to differences in structural applications and objectives [196].
The following documents contain a FAD calculation procedure:

- R6 Method, Revision 4 [200],
- BSI PD6493 [202],
- SSM; A Combined Deterministic and Probabilistic Procedure for Safety Assessment of Components with Cracks [203].

The following documents, in addition to containing a FAD procedure, contain a fitness-for-service Guide:

- EXXON, Fitness-for-service Guide [204],
- MPC, Fitness-for-Service Evaluation Procedures for Operating pressure vessels, tanks and piping in refinery and chemical service [205],
- API 579, Recommended Practice for Fitness-in-Service [206].

The assessment methodology of the procedures based on the use of CDF diagrams is different from the philosophy of FAD based documents. The evaluation of fracture failure and plastic collapse are not computed simultaneously. Therefore, two independent steps are needed. On the one hand, a direct comparison between applied stress or load and flow stress or limit load, and on the other hand, a diagram should be plotted where the applied stress intensity factor, *J*-integral or crack tip opening displacement (CTOD) is compared with the corresponding toughness values. The CDF diagrams are easier to interpret in a physical sense than the FADs. Moreover, if the CDF technique is used together with the *J-R* curve, the full crack propagation history is described [196].

The following documents present a CDF technique:

- GE-EPRI Approach [207, 208],
- ETM, The Engineering Treatment Model for Assessing the significance of crack-like defects in engineering structures [209] and The En-

gineering Treatment Model for assessing the significance of crack-like defects in joints with mechanical heterogeneity (strength mismatch) [210].

Documents that present other procedures than FAD or CDF:

- ASME Section XI [173] code, which contains figures and tables to which the real situations can be compared to,
- RSE-M Code [211], which is very similar to ASME code,
- KTA Code [212], which is very similar to ASME code.

High temperature procedures

The early approaches to high temperature life assessment show methodologies which are based on defect free assessment codes. The fracture mechanics based procedures basically followed the low temperature assessment procedures that have been developed within Europe and elsewhere [196].

The high temperature procedures include:

- ASME Code Case N-47 [213],
- RCC-MR Code [214],
- R5 Method [215],
- BS PD 6539 [216].

The early approaches to high temperature life assessment methodologies include ASME Code Case N-47 [213] and the French RCC-MR [214]. These procedures have many similarities, and both of them are based on lifetime assessment of uncracked structures. ASME Code Case N-47 [213] is the first design code to formally include linear damage summation as a method of predicting material failure at high temperature, consisting of a fatigue (Miner cycle summation) component and a creep (Robinson time summation) component. The French Code RCC-MR [214] incorporates many of the concepts behind ASME Code Case N-47 [213] but with modified stress analysis procedures. One advantage of the more recent R5 Method [215] approach is that a defect may be postulated and the subsequent behaviour may be predicted for likely service cycles. Whereas a step-by-step high temperature creep crack growth computation procedure is given in the British Standard document PD 6539 [216].

Combined high and low temperature procedures

During recent years, four European structural integrity/degradation assessment procedures that apply for both high and low temperatures have been published. These are SINTAP (Structural Integrity Assessment Procedures for European Industry) [197], FITNET (European Fitness For Service Network) [125], HIDA procedure [198] and FKM guideline [199]. These structural integrity/degradation assessment procedures cover all types of power plants as well as most of other types of industry plants. They also include compendia of analytical structural and fracture mechanics parameter solutions for most common industry plant component types, such as plates, straight pipes, pipe bends, T-joints and pressure vessels.

8. Probabilistic degradation modelling methods for power plant components

Time dependent probabilistic models can be used to identify possible trends and to predict the future behaviour of components. Different probabilistic approaches to model ageing phenomena are used depending on the degradation mechanism in question.

In straightforward reliability calculations, the components are often assumed to have a constant failure rate, i.e. the component failures occur according to a homogeneous Poisson process. In the Poisson process, it is assumed that the occurrences of successive events are exponentially distributed with the same parameter. The component failure rates generated from large amount of data in reliability databases are usually based on the assumption of constant failure rate [217].

The ageing of components which have a mean time to failure that is significantly shorter than the assumed plant lifetime is called short-term ageing. Typically, there is a lot of failure data available concerning such components and thus statistical analyses can be performed. This mainly concerns active components, such as pumps and valves. In the case of long-term ageing, the amount of failure data is very limited. This mainly concerns passive components, such as pipes. Then, information of the degree of component degradation is obtained by surveillance and condition monitoring. The evaluation of the expected remaining lifetime is based on monitored parameters. The behaviour of degradation mechanisms is often stochastic and thus probabilistic techniques should be applied in the modelling.

A brief description concerning some probabilistic approaches to model ageing of power plant component is presented in the following.

8.1 Probabilistic structural mechanics based modelling methods

Here, the scope of described probabilistic modelling methods mainly concerns initiation and growth of cracks in passive power plant components. Because the critical crack size depends on the magnitude of the applied load, a fracture criterion that relates the stress amplitude and the crack length to failure must be applied if the stresses are varying. Thus, to estimate the fatigue reliability of a component, four factors must be explicitly considered. These are load history, initial crack distribution, crack growth history as a function of the load history and a failure criterion. Because there is much scatter in empirical crack propagation data, the crack growth rate should be modelled probabilistically [32].

There are three basic classes of probabilistic models for crack propagation. The most commonly used type involves randomisation of an appropriate crack growth equation, e.g. the Paris-Erdogan model, see equation (7.2-12). Other types of models include evolutionary probabilistic models (Markov or diffusion models) and cumulative jump models [32].

The randomisation is carried out by introducing appropriate quantities characterising random effects into the empirical crack growth law. For instance, one approach to modelling random fatigue is to treat the parameters of the Paris-Erdogan equation, C and m, as random variables. By doing so, the variability in the stress range, material properties and environmental factors can be characterised [32].

8.2 Probabilistic fracture mechanics based methods

8.2.1 Introduction

Of the many possible degradation mechanisms, failure due to crack growth is the dominant degradation mechanism for most power plant components that are made of metal(s). Crack initiation and growth in these components can be caused by various phenomena, such as fatigue and corrosion, or their combination. Many of the shortcomings of traditional deterministic analysis methods can be alleviated or overcome by applying probabilistic analysis methods.

The main disadvantages of all deterministic analysis methods are that [45]:

a) Properties and partial safety factors (where used) are often not given as best estimates or most likely values, with the result that it is not possible to estimate the most likely strength of the structure.

b) The risk of failure or collapse, or the overload necessary to cause failure or collapse, may vary widely for different structural members and components, and different types of structure.

c) The assumption that most design parameters are known constants rather than statistical variables is in most cases a gross simplification.

d) The safety factor approach is not so easy to apply in assessment of existing structures and for making maintenance decisions.

Most fracture mechanics analyses are deterministic, e.g. a single value of fracture toughness is used to estimate failure stress or critical crack size. Much of what happens in the real world, however, is not predictable. For instance, since fracture toughness data in the ductile to brittle transition region are widely scattered, it is not appropriate to view fracture toughness as a material constant having a single value. Other factors also introduce uncertainty into fracture analyses. A structure may contain a number of flaws of various sizes, orientations and locations. Extraordinary events, such as earthquakes and accidents can result in stresses significantly higher than the intended design level. Because of these complexities, crack growth should be viewed probabilistically rather than deterministically [30].

Probabilistic fracture mechanics (PFM) provides an approach for probabilistic modelling of initiation and growth of cracks in components. The advantages of PFM include also the possibility of modelling clearly the uncertainties related to the material degradation process, and thus being able to perform sensitivity analyses of the factors affecting this process. For ageing management purposes it is of interest, for example, to evaluate how changes in operating conditions can affect the failure probability of the structure [87].

The earliest PFM developments include aircraft applications. However, the emphasis in the first efforts was more on crack initiation than fracture mechanics aspects. Recently, the most common object of application has been pressurised components, primarily RPVs and piping in NPPs. Weld joints have received a particular interest, as fabrication defects and cracks tend to concentrate in those regions [90].

PFM is based on deterministic fracture mechanics (DFM) procedures, but considers one or more of the input variables to be random instead of having a single deterministic value. For example, initial crack size is typically one of the rarely well known variables. Rather than assuming a fixed given initial size, this parameter can be projected over a range of sizes with probabilities of occurrence

and detection estimated for each size. In the simplest case, a DFM analysis would then be performed after inspection for each size to provide the crack size distribution as a function of time (or stress load cycles) in service. The failure probability at any time is then equal to the probability of having a crack larger than the critical size (which can also be a random variable) [90].

Often one or more of the fracture mechanics variables is not known with sufficient certainty, and many of the input variables should be considered random. Fracture mechanics input parameters typically considered to be random include [90]:

- Initial crack size;
  - depth,
  - length,
  - location,
- Crack detection probability;
  - detection probability as a function of size,
  - uncertainty in crack size for a given level of indication,
- Material properties;
  - subcritical crack growth characteristics,
  - fracture toughness,
  - tensile properties,
- Service conditions;
  - stress levels,
  - load cycle rate,
  - temperature,
  - environment.

Not all of these parameters are considered random in every application. Only those variables with uncertainty or scatter producing the greatest effects on life or reliability calculations need to be recognised as such. The failure probability at any given time may be determined by combining conventional fracture mechanics calculations with an appropriate statistical approach. The results can then be used to ascertain the suitability of the component for service.

8.2.2 PFM analysis procedure

A typical PFM analysis is described in the following. First, one or more parameters or variables are randomised, depending on the characteristics of the em-

ployed analysis model. Parameters or variables that can be considered as random were presented in Section 8.2.1. Then crack growth simulations are performed. Fracture mechanics models employed are based on LEFM, e.g. Newman-Raju solutions, weight and/or influence functions, or on EPFM or on a combination of LEFM and EPFM. During the crack growth simulation, pre- and in-service inspections are considered and failure judgements of failure states, e.g. leak or rupture, are performed. Cumulative failure probabilities are calculated as a function of time in operation [44]. A flow chart example of a PFM analysis is shown in Figure 8.2-1 below.

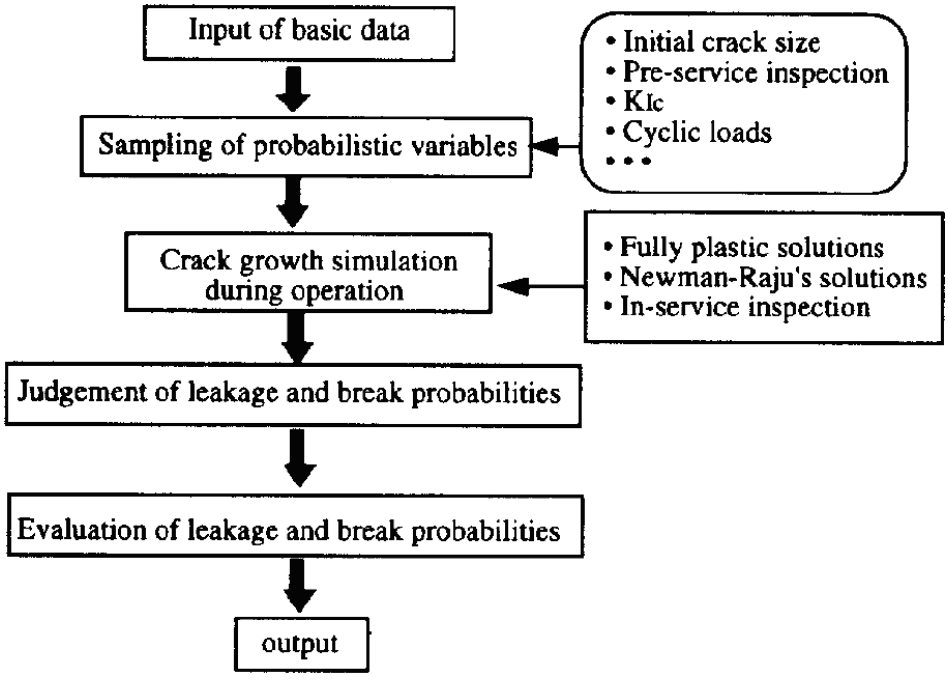

Figure 8.2-1. A flow chart of a PFM analysis, from ref. [44].

Most of the applications of PFM for power plant components lead to very low failure probabilities which have to be determined by sophisticated numerical procedures from rather scarce and incomplete input data.

8.2.3 Engineering models and PFM

Many components, which could be otherwise rejected, can be saved by removing such arbitrary and unrealistic worst case assumptions as simultaneous occur-

rence of improbable events, and allowing the model to account probabilistically for actual variation in critical parameters which are based in test results and/or experience. PFM is applied to remove such unrealistic conservatism in component reliability analyses, though in their pure form they have limitations similar to, but not as pronounced as those concerning deterministic analyses.

Two methods are available to alleviate these shortcomings in pure PFM. The first is to use conservative bounds for input variable probability distributions where accurate distributions are unavailable. The resulting conservative pure PFM analysis represents a notable improvement compared to deterministic model on which it is based. The primary reason for this consequence is that PFM in any form terminates the assumption that all conceivable deleterious events will occur simultaneously. The second method consists of calibrating the PFM model against all available relevant experience. Here calibrated PFM essentially represents a combination of the database and pure PFM approaches [90].

When considered individually, probabilistic engineering models contain a number of inherent limitations with respect to reliability prediction. These same limitations are present when models are constructed as a component of a pure PFM analysis [90].

PFM models are based on conventional DFM principles. Hence uncalibrated tools cannot treat problems for which fracture mechanics tools are not available. Any of the components of a DFM analysis, e.g. crack size and stress history, can be treated as a random variable, in which case the model becomes a probabilistic one.

The basic assumptions inherent for DFM are naturally included in the respective PFM models. Additional assumptions are usually made when a PFM model is constructed for a particular application. It may also be assumed, for example, that only one crack will exist and that the crack will be situated in a weld [90].

Currently, there are many methods and applications for PFM in various manufacturing industries, nearly all of which are based on LEFM models. In contrast, probabilistic analyses based on EPFM models are not widespread and are only currently gaining notice, particularly for applications in pressure boundary components. It is well established that EPFM models provide more realistic measures of fracture behaviour of cracked structures with high toughness and low strength materials compared to LEFM models. Cracked components composed of these materials, when used in power plants, pose a serious threat to structural integrity. In addition, the operational temperature region of power plants is above the brittle-to-ductile transition temperature of the component materials. Then, the fracture response is essentially ductile, and the material is

capable of considerable inelastic deformation. As such, EPFM should be applied in fracture analyses of these components [91].

The probabilistic aspects of crack repair are drawing attention nowadays as well. It is often assumed that all detected cracks are repaired and that no new cracks or adverse conditions are introduced during the repair process, even though this assumption may not be realistic. Still, assumptions have to be made in the development of a probabilistic treatment. Typical assumptions might include consideration of crack depth, aspect ratio, fracture toughness and subcritical crack growth characteristics to be independent [90].

8.2.4 Numerical PFM methods

Numerical techniques for generation of failure probabilities from PFM models are generally required for more complex problems. Application of these techniques does not necessarily lead to a large amount of computations or complicating factors, as workable techniques are readily available. Numerical results from the construction of PFM models are produced in a variety of ways. The numerical techniques include: stress/strength overlap, variance/covariance, convolution and MCS.

The stress/strength overlap can be calculated once the statistical distributions of both parameters are known or estimated. However, estimating these distributions can be difficult. In the case of fatigue crack growth, the time dependent strength distribution would at least depend on the following input parameters and their interactions: initial crack size, fracture toughness, material properties and environment. In all but the simplest cases, a separate numerical generation technique would have to be employed to calculate the individual stress and strength distributions.

Variance/covariance analysis by perturbation techniques is based on the assumption that some variables will deviate by relatively small amounts from their respective means. This technique is also known as the method of system moments [92]. It provides estimates of the moments (mean, variance, skewness, etc.) of the dependent variable from the moments of the independent variables and the partial derivatives of the functional relationship between the independent and dependent variables. However, this technique is only approximate. It increases in accuracy as the variances of the independent variables decrease. Only the moments of the distribution of the dependent variables are provided [90].

The convolution method, which is sometimes referred to as “direct synthesis”, derives the probability density function of the dependent output random variable from the functional relationship between the dependent and independent variables and the probability density functions of the independent variables. In principle, this method is capable of providing analytical results. However, the derivation of the multidimensional integrals is often a complicated task. Difficult numerical integrations are usually required and care must be taken to obtain accurate results. The incorporation of relatively simple statistical and physical dependencies among the input variables is also very difficult [90].

MCS, being a general numerical technique for determining the distribution of the dependent variables, is broadly applicable to the generation of numerical results from PFM models [93, 94]. The inclusion of dependencies between input variables is a straightforward procedure with MCS.

As described earlier in Section 5.6.5, MCS consists of selecting a value for each input variable at random from its assumed statistical distribution for substitution into the underlying deterministic model. In the context of a typical PFM problem, initial crack size, a_0, crack growth rate and nominal stress values are randomly sampled, and the effective crack size, a, is computed after a number of load cycles, N. Similarly, a value for K_{IC} is sampled and used along with the sampled values of stress to provide the critical crack size value, a_c. The proportion of times that a exceeds a_c is equal to the probability of failure with N cycles. A single simulation computation is therefore precisely equivalent to a single application of the corresponding DFM analysis, with the exception that some of the input values have been selected randomly [90].

In many instances, the probability of failure will be small. Hence, many simulations would be required for accurate enough results. This can be alleviated by selective sampling from the distributions of the input variables, thus drawing from the tails of the distributions controlling the failure probabilities. Selectivity is then compensated for during the analysis of the numerically generated results. Sampling procedures are discussed in Section 5.6.

In the following is described an example concerning importance sampling. If it is known that large initial crack sizes associated with small probability are required for the failure to occur, it is not necessary to randomly sample from the initial crack size distribution. This is because the vast majority of sampled cracks would be from the much more likely portion of small cracks. Then, importance sampling would involve sampling only from the large crack end of the initial

crack size distribution. The results would then be compensated by the probability of having an initial crack in the portion of the sampled distribution.

Stratified sampling is another sampling method that can be used to reduce the large amount of computational work related to assessment of small probabilities. Figure 8.2-2 illustrates a typical stratification of an initial crack sampling space composed of normalised crack depth, a/t, and aspect ratio, a/c, of a semi-elliptical surface crack, where t is wall thickness and c is half of the crack length. The sampling space is divided into a number of mutually exclusive small subspaces, called cells. A predetermined number of samples are then taken from each of those cells. Within each cell, an individual sampling is carried out according to a postulated initial crack distribution [44]. The cumulative failure probability up to time t is computed as:

$$P_f(T \le t) = \sum_j^m \frac{N_f(t)}{N_j} P_j \tag{8.2-1}$$

where m is the total number of cells, N_j is the number of samples taken from the j:th cell, $N_f(t)$ is the number of failed samples in the j:th cell up to time t, and P_j is the probability that an initial crack exists in the j:th cell.

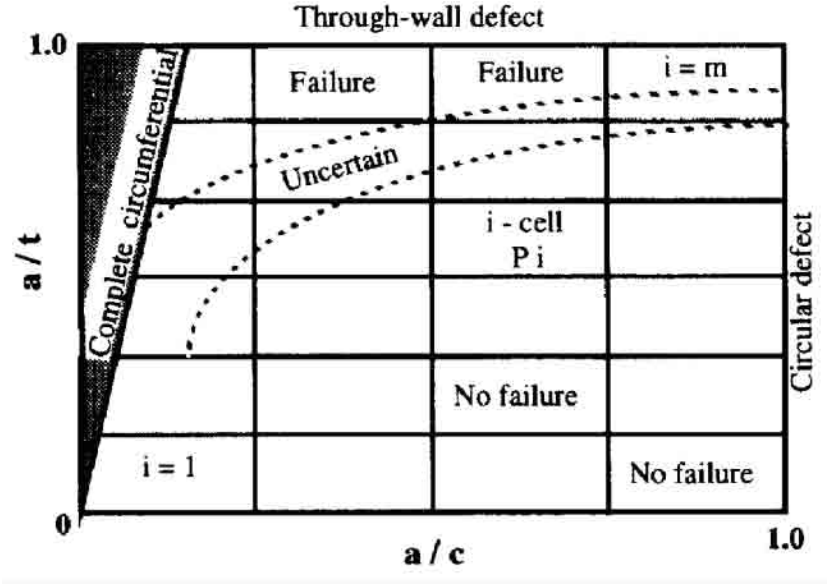

Figure 8.2-2. The stratification of sampling space, from ref. [44].

As shown in Figure 8.2-2, the crack samples located in the upper part of the sampling space seem more likely to fail than those in the lower parts. A region of uncertainty may exist between “Failure” and “No failure” regions. Since the samples taken from the “No failure” region would never lead to failure, considerable reduction in the amount of computational work can be expected by ignoring these cells in a sampling plan. Since the assessment of the region of uncertainty cannot be known before calculation, many cells and samples would be selected from the whole sampling space to ensure computational accuracy. Computation time would increase as a function of the number of cells and samples employed. To overcome this problem, a parallel processing algorithm combined with the stratified MC method is very useful [95, 96].

8.3 Statistical modelling methods

8.3.1 Short-term ageing models

The models discussed in the following are applicable to estimate component ageing from failure data.

Modelling of ageing with probability distribution functions

The time dependence in failure occurrence can be expressed with the failure rate, $\lambda(t)$, defined as the probability of failure given the component has been in operation for a certain time [32, 217]:

$$\lambda(t) = \frac{f(t)}{R(t)} \tag{8.3-1}$$

where t is time, $f(t)$ is the probability density function of component failure and $R(t)$ is reliability function. The failure rate is also called the hazard rate. The reliability of the component at time t can be defined as [32, 217]:

$$R(t) = \exp\left[-\int_0^t \lambda(\tau) d\tau \right] \tag{8.3-2}$$

If the probability of a failure within a short time interval (t, $t + \Delta t$) is independent of the age of the component, t, the failure times are exponentially distributed and

the failure occurrence is independent of time. In this case, the failure rate is constant. A distribution is an increasing failure rate distribution if [218]:

$$R(t|x) = \exp\left[-\int_{x}^{x+t} \lambda(\tau) d\tau \right] \tag{8.3-3}$$

is increasing when $x \geq 0$ for each $t \geq 0$. When the failure rate is increasing, it is said that component is ageing. Several distributions commonly used in reliability engineering are suitable to describe events with an increasing failure rate. These include Weibull, gamma and log-normal distributions.

In reliability engineering, Bayesian methods are of special interest since the amount of failure data of power plant components is often very sparse. These methods are used to include all relevant information to the estimation of model parameters. In the Bayesian approach, the probabilities are always conditioned to the background information. Thus, the Bayesian approach requires the definition of the prior distributions. The choice of the form of the prior distribution is generally based on computational reasons. The parameter values of prior distributions may be based on the existing data and/or expert opinions. The basic principles of Bayesian approach are described for example in ref. [219].

Modelling approaches to short-term ageing

In general, the failure rate of components changes over time as is shown in Figure 8.3-1, which depicts the so called bathtub curve. The first interval, from time t_0 to t_1, represents early failures due to material and/or manufacturing defects, and is usually referred to as the burn-in or infant mortality period. The second interval, from time t_1 to t_2, is the period of random failures and is usually approximated by a constant hazard rate. It is often referred to as the useful life of the component or system. The part of the curve after t_2 represents the so called wear-out failures, where the failure rate increases as the component deteriorates. With respect to ageing, this is the period of the component lifetime that is of concern [32].

The probabilistic short-term ageing models of power plant components presented here are divided to three groups [217]:

- component replacement models,
- ageing models of repairable components,
- ageing models of tested stand-by components.

The repair or replacement time of components is assumed to be very short as compared to the failure time and is thus neglected. The uncertainty of the times between failures is described with a distribution which is called the intensity of the process [217].

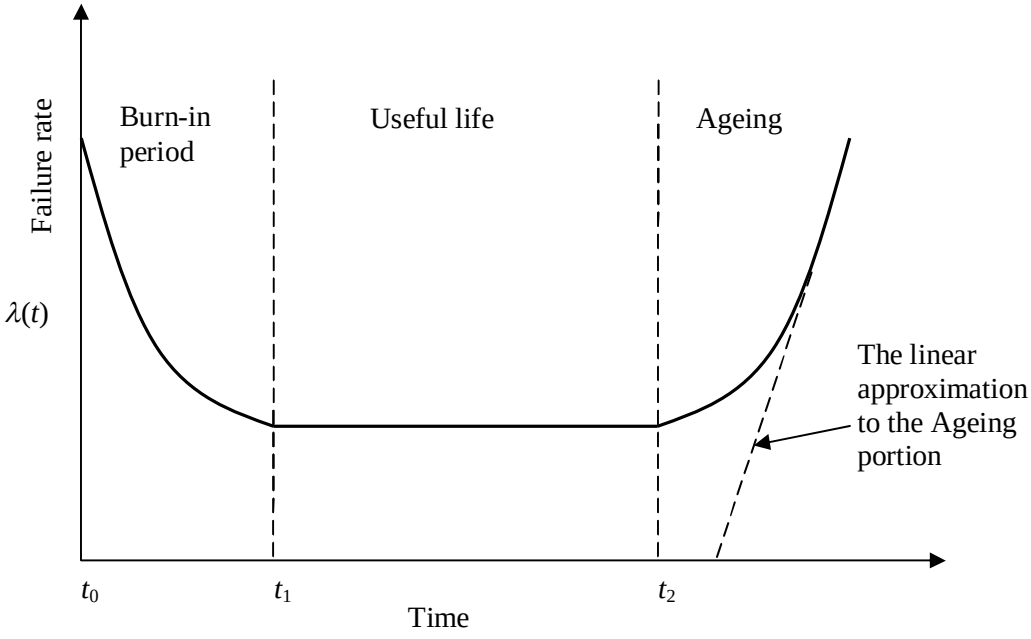

Figure 8.3-1. Component failure rate as a function of time.

If the failed components are replaced with new ones, which can be considered as identical to the failed components in the beginning of their lifetime, the failure histories can be described with renewal processes [220]. A renewal process, *F*, is a sequence of independent, identically distributed non-negative random variables, of which all do not disappear. If the time for the replacement of a component is negligible and the time to failure of each component is distributed identically, the successive intervals between failures can be treated as random variables of a renewal process. The expected number of renewals (i.e. failures) during the time interval (0, *t*) is called the renewal function, $M(t)$. It can be expressed in terms of the underlying distribution as [220]:

$$M(t) = \sum_{k=1}^{\infty} F^{(k)}(t) \tag{8.3-4}$$

where $F^{(k)}(t)$ is the *k*-fold convolution of *F*.

As the successive failure times are distributed according to the same distribution in a renewal process, the mean times between component failures remain also constant. The statistical estimation of renewal processes reduces to the estimation of the parameters of the underlying life length distribution, if the subsequent life lenghts have been observed.

The renewal models cannot be applied in the case of repaired or maintained damaged components. This is because the times between events cannot be straightforwardly considered as independent and identically distributed random variables. If the development of the hazard function is assumed to be influenced by component repairs, it becomes dependent on the history. In ageing analyses, it is assumed that a baseline failure rate is increasing due to the environmental conditions during the component service [217].

Some hypothetical examples of the behaviour of the failure function are shown in Figure 8.3-2. Case (a) of Figure 8.3-2 illustrates a situation where the failure rate is increasing in time and is not affected by the failures, i.e. after repair the condition of the components is assumed to be the same as just before the failure. A more realistic model is illustrated in Case (b), where a basic failure rate is assumed to be increasing but after the failure a decrease in the failure rate describes the effect of maintenance. In Case (c) the maintenance is assumed to have a fractional effect on the failure rate [217]. It may also be assumed that the increase in failure rate begins in the "Ageing" region of the bathtube curve.

The failure rate mode presented at Case (a) of Figure 8.3-2 can be modelled as a non-homogeneous Poisson process. The probability $p_n(t)$ that failures have occurred during time interval (0, t) is [217]:

$$p_n(t) = \frac{\Lambda(t)^n}{n!} \exp\left[-\Lambda(t)\right] \tag{8.3-5}$$

where $\Lambda(t)$ is the integral of the intensity, called the cumulative failure function, which in turn is defined as:

$$\Lambda(t) = \int_0^t \lambda(t) d\tau \tag{8.3-6}$$

When $\lambda(t)$ is constant the model reduces to the homogeneous Poisson process. For ageing components, $\lambda(t)$ is increasing with time. The most commonly used non-homogeneous Poisson process is the Weibull process.

In a linear ageing model, the effects of the ageing process on the component failure probability are expressed as a simple linear equation that relates the component failure rate to exposure time of the component to the ageing mechanism(s). The failure function is defined in this case as [221]:

$$\lambda(t) = \lambda_0 + \alpha t \tag{8.3-7}$$

where λ_0 is the constant random failure rate and α is called the ageing acceleration rate. The second term of equation (8.3-7) describes the "Ageing" region of the total failure rate, see Figure 8.3-1. Other frequently used ageing models are the exponential failure rate model and the Weibull failure rate model. They are defined, in this order, by [222]:

$$\lambda(t) = \lambda_0 \exp(\alpha t) \tag{8.3-8}$$

$$\lambda(t) = \lambda_0 \left(\frac{t}{t_0} \right)^{\alpha} \tag{8.3-9}$$

where t_0 is time for start of operational lifetime, as shown in Figure 8.3-1.

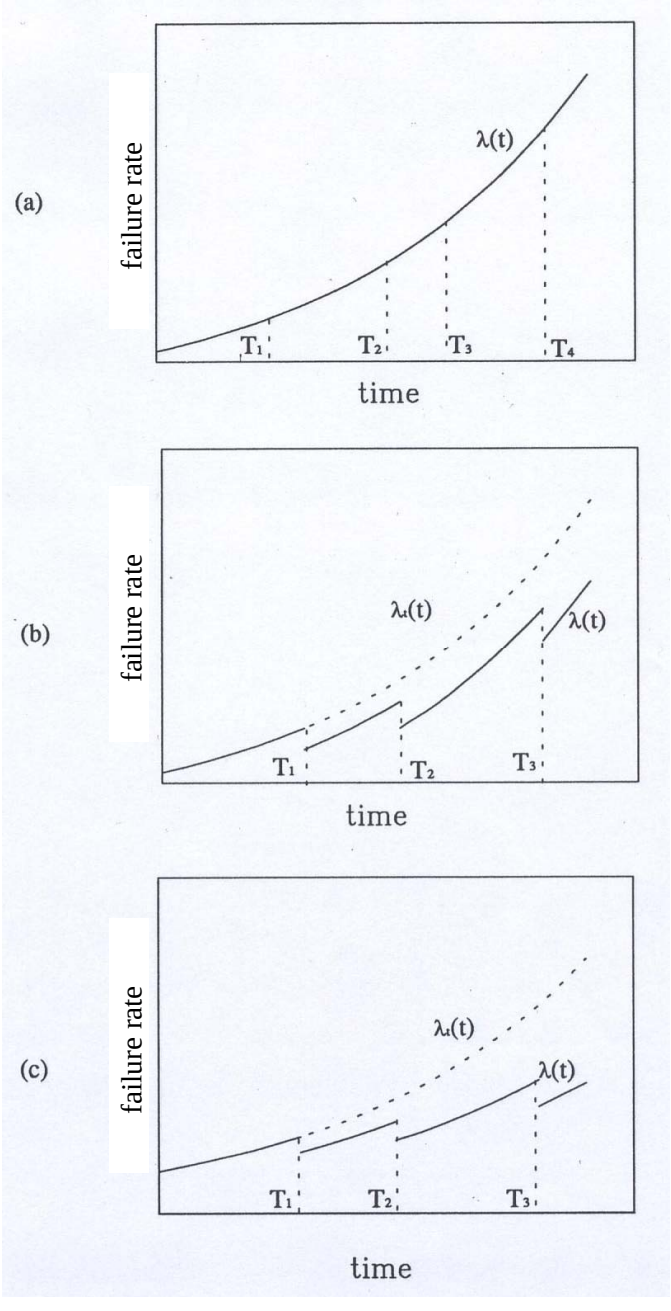

Figure 8.3-2. Realisations of failure rates of some ageing models with imperfect repair, from ref. [217].

Each of the three models presented in equations the (8.3-7) to (8.3-9) has its historical roots in machine and material lifetime analyses, the Weibull failure rate being the most commonly used of the three. The linear failure rate, which is the simplest of these models, has been used in determining age dependent risk [221, 223]. Wolford et al. [224] observed that the linear failure rate performed poorly in more instances than the other two models and due to its non-exponential form was most difficult to work with analytically.

If there is a sample of recorded component lifetimes that is large enough and the parametric constraints do not greatly contradict the true underlying lifetime distribution, the data will most likely fit these three models adequately. However, as mentioned earlier, failure data pertaining to component ageing is scarce and justification for parametric models is sometimes doubtful. It is not certain how much data are exactly needed for accurate definition of model parameters. In ref. [225], it is suggested that the size of a data sample should be at least 100 in the case of Weibull rate model. In ref. [32], it is suggested that good approximate tests and confidence intervals can be obtained with somewhat smaller samples.

When it is assumed that maintenances cause a decrease in the otherwise increasing failure rate, as is in Case (b) of the Figure 8.11, the failure rate is defined as a function of time and number of failures/maintenances by [217]:

$$\lambda(t) = \lambda_t(t) - \sum_{j=1}^{k} a_i \ , \quad t \in [T_k, T_{k+1}) \tag{8.3-10}$$

where $\lambda_t(t)$ is increasing failure rate, T_k are maintenance times and a_i is the maintenance specifically constant effect of i:th maintenance. The maintenance effect a_i must be defined so that $\lambda(t)$ remains positive. It may also be assumed that the maintenance affects the failure rate in a multiplicative way, as is illustrated in Case (c) of the Figure 8.11. Now the failure rate can be defined as [217]:

$$\lambda(t) = a(i)\lambda_t(t), \quad t \in [T_k, T_{k+1}) \tag{8.3-11}$$

The decrease may be expressed for instance with the fractional learning model, where the failure rate is a function of events, as [217]:

$$\lambda(t) = Ac^i \ , \quad t \in [T_i, T_{i+1}) \tag{8.3-12}$$

where c is the reduction factor and A is the event rate parameter before the first event. More generally, the repair may be assumed to have an effect on some parameter θ of the failure rate as [217]:

$$\lambda(t) = \lambda_t(t, \theta_i) \tag{8.3-13}$$

where θ_i is the maintenance specifically constant value of θ at i:th maintenance. The models above present only some specific cases of repairable component ageing models, several other corresponding models may be developed.

Besides the models of repairable components, the ageing of tested stand-by components may be modelled in terms of failure probability in the test situation. In such models, the time may be discretised to describe for instance i:th test interval which may facilitate the computations. The probability of failure is assumed to be constant during the test interval. The increase of the number of failures in a test may be due to the fact that components wear between the tests, and degraded but not yet failed items are not identified in the test. Furthermore, the repaired component may not correspond to a new one after the repair. An example of an ageing model for tested stand-by components is the modified binomial model. In this model, the successful cases in tests are binomially distributed but the distribution parameter is allowed to evolve in time. This kind of model can be used to detect a trend in the results [217].

Unless the ageing model suits perfectly the underlying failure rate for the examined components, the model results may not be directly applicable. To overcome this drawback, it is suggested [32] to use a non-parametric inference based procedure. This includes a test for increased failure rate, a test for increased failure rate average, and test for “new better than used”.

8.3.2 Long-term ageing models

Information about long-term ageing of components is obtained via condition monitoring. This data can be used e.g. to assess the remaining lifetime of the components. Examples of long-term ageing mechanisms include crack growth in metals, which issue is discussed in Chapter 7, and the combined thermal and radiation ageing of polymeric insulating materials in cables. The evaluation of long-term ageing is often based on the expected physical phenomena causing the component degradation.

The use of probabilistic models instead of deterministic ones is needed, when the experiments show a significant scatter in the results. Examples of such uncertainties are variations in material properties and changes in environmental conditions.

Modelling approaches to long-term ageing

The probabilistic long-term ageing models of NPP components presented here are divided into three groups [217]:

- randomised deterministic models,
- stress-strength-time models,
- cumulative damage models that apply Markov chains.

In the randomisation of deterministic models, parameters describing uncertain phenomena are treated as random variables, or a random noise term is added in the model to account for variations. The scatter in the results of experiments is used to estimate the distribution parameters. One approach to randomisation of deterministic models is PFM, see Section 8.2. The advantage of PFM is the possibility of modelling clearly the uncertainties related to the ageing mechanism, and thus being able to perform sensitivity analyses for the factors affecting it.
The time evolution of structural reliability can be described with a time dependent model, where the applied stress or load and the strength of the structure are stochastic processes. Stresses and strengths may vary during long operation intervals as a function of time or the number and/or severity of stress applications. Ageing denotes the decrease in strength as a function of time, cyclic damage denotes the decrease in strength as a function of the number of stress cycles and cumulative damage denotes the case in which the decrease in strength is by both the number and severity of stress applications. Component failure occurs when strength has decreased below a stress dependent level. Failure can also occur when the cyclic or cumulative damage has exceeded a certain limit corresponding to the strength.

The reliability of the component can be defined as [32]:

$$R(t) = P\left(Y(\tau) > X(\tau)\right), \quad \tau \in [0, t] \tag{8.3-14}$$

where $Y(t)$ denotes the strength of the component and $X(t)$ denotes the applied stress.

The stress-strength-time models may be classified according to the uncertainty about stress and strength [226]. Both stress and strength can basically be classified as deterministic, random-fixed or random-independent. Illustrations of some stress-strength-time modelling cases are presented in Figure 8.3-3.

Case (a) of Figure 8.3-3 describes conditions where strength is assumed to be constant and stress is an increasing random function. If the degree of degradation corresponding to the accumulated stress can be described with a Wiener process [227], the failure time distribution has the form:

$$f(t) = \frac{y}{\sigma\sqrt{2\pi}} \frac{1}{t\sqrt{t}} \exp\left[-\frac{(y-\mu t)^2}{2\sigma^2} \right] \tag{8.3-15}$$

where y is the constant value for strength, μ denotes mean, σ denotes standard deviation and t is time.

Case (b) of Figure 8.3-3 illustrates a cumulative damage model, where load peaks occurring at random weaken the strength a discrete amount. If the times between the occurrences of loading events are exponentially distributed with the same parameter and the strength decrease is constant, this case can be modelled as a Poisson process. Additional uncertainty arises if the strength of the component is not necessarily reduced by the shock [217].

Case (c) of the Figure 8.3-3 illustrates a case where the occurrences and durations of loads are random, but the level of stresses is constant. It is assumed that the decrease in strength during each loading depends on the duration of the loading. If the occurrences of the loads are Poisson distributed and the duration of each load is exponentially distributed, the reliability of the structure can be computed [217].

Let us assume that the stress rate and the duration are exponentially distributed with parameters λ and μ. The failure occurs when the strength has decreased below a critical level, which is called d. The reliability of the structure is the probability that during the time interval (0, t) the accumulated time in the stress state ($T(t)$) is less than the critical value d [228]:

$$P(T(t) \le d) = e^{-\lambda\cdot(t-d)} \left\{ 1 + \sqrt{\lambda\mu(t-d)} \int_0^d \frac{e^{-\mu y}}{\sqrt{y}} I_1\left[2\sqrt{\lambda\mu(t-d)y} \right] dy \right\} \tag{8.3-16}$$

where $I_1(x)$ is the modified Bessel function of order 1 [229]:

$$I_1(x) = e^{-\frac{1}{2}\pi i} J_1\left(xe^{\frac{1}{2}\pi i} \right) \tag{8.3-17}$$

where J_1 is the Bessel function of the first kind of order 1.

Case (d) of the Figure 8.3-3 illustrates circumstances in which there are two sources for stress, one being constantly in effect (e.g. temperature or radiation) and the other consisting of a variety of discrete shock loads. The accumulated stress is then [217]:

$$X(t) = \int_0^t X_c(t)dt + aN(t) \tag{8.3-18}$$

where X_c is the continuous load and $N(t)$ is a point process describing the occurrence of shocks. The failure occurs when the accumulated stress $X(t)$ exceeds the strength. The strength may be assumed as random but independent of time.

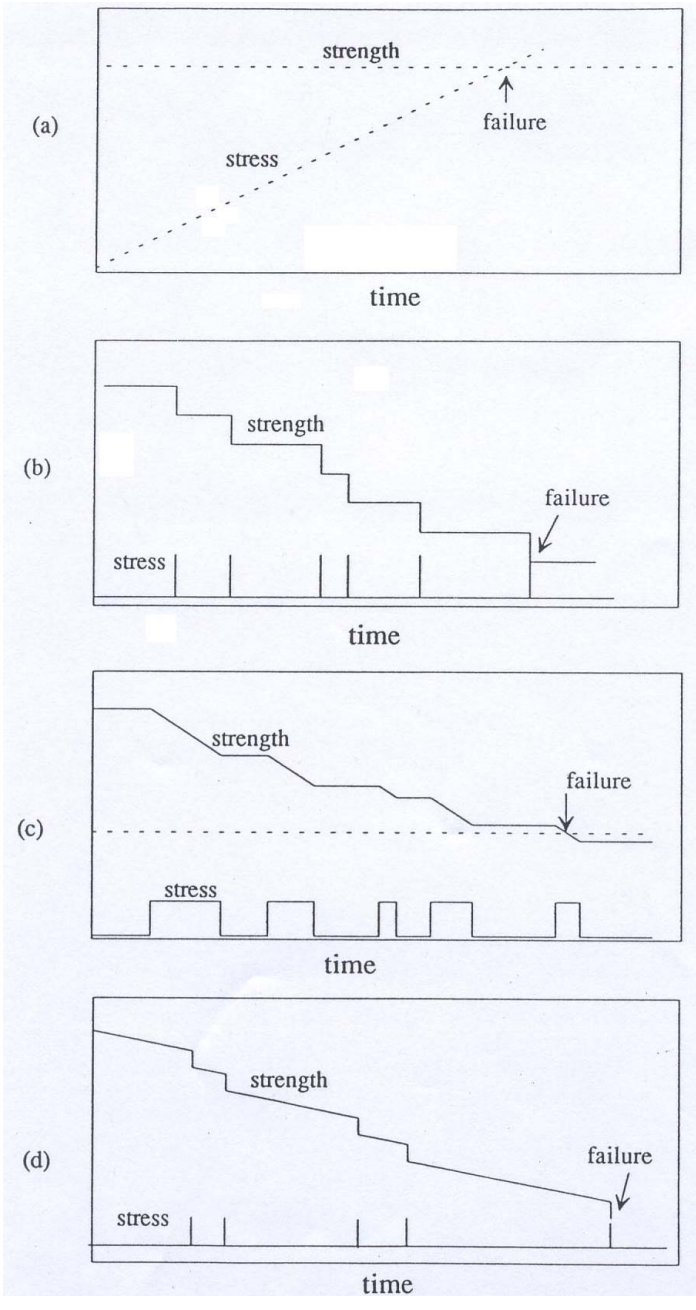

Figure 8.3-3. Some simplified stress-strength-time modelling situations, from ref. [217].

The simplified cases above are applicable only to very limited situations. In practise, the formulation of the functions $Y(t)$ and $X(t)$ causes problems. There

are almost invariably difficulties in obtaining stresses and especially in obtaining strength.

Discrete time Markov models are applicable to describe situations where the damage is caused by cyclic loadings. If, in addition, the amount of damage is discretised to specific damage states, the cumulative damage can be modelled with Markov chains [230].

An example of an ageing mechanism, which can be described with a stationary, discrete time and state Markov process, is fatigue crack growth. The crack growth can be modelled with a transition probability matrix, where the states represent the depth of the crack and the discrete time describes the fatigue cycles. The final state, here defined as n, corresponds to the situation where the crack has propagated through the component wall, e.g. that of a pipe. The initial size of the crack, π_0, is described with the following state vector:

$$\pi_0 = \begin{bmatrix} p_0 & p_1 & \cdots & p_i & \cdots & p_n \end{bmatrix} \tag{8.3-19}$$

where p_i are the initial probabilities of various damage states. After k cycles, the crack size distribution π_k is:

$$\pi_k = \pi_0 \cdot \mathbf{P}^k \tag{8.3-20}$$

where $\mathbf{P}$ is the transition probability matrix, which contains the transition probabilities from each damage state to all considered more severe damage states. If a detected crack is repaired and no new cracks initiate during the inspections, the inspection procedure can be described with matrix $\mathbf{D}$, which contains the detection probabilities of cracks.

The crack depth distribution after m cycles with one inspection between the cycles k and k+1, when $k < m$, can be computed as:

$$\pi_m = \pi_0 \cdot \mathbf{P}^k \cdot \mathbf{D} \cdot \mathbf{P}^{m-k} \tag{8.3-21}$$

This approach concerns the cyclic loading and the Markov property is assumed only between the crack tip at the end of the cycle. In this case, the crack propagation is not continuous in time. In this example, it was assumed that at the time instant t the number of loadings needed to determine the distribution of the crack depth is known. The model becomes continuous if the cycles are assumed to occur randomly according e.g. to a Poisson process.

9. Risk analysis applications for power plant systems

9.1 Introduction

Risk analysis applications presented here are used in several industries. Due to their complexity, wide scope and importance in power plant applications, they are presented here in this separate chapter. The considered risk analysis applications are PRA/PSA and RI-ISI. A detailed description of these approaches would be beyond the scope of this thesis, thus instead an overview is presented here.

9.2 Probabilistic risk/safety assessment

Introduction

PRA/PSA is a technique used to identify combinations of events that compose accident sequences and estimate their frequency of occurrence together with consequences. An accident sequence typically includes an initiating event followed by any number of failures or successes of control and mitigating functions, enabling conditions that retard or allow the accident sequence, and the responses of systems or equipment to developing conditions. The scope of applicability of PRA/PSA is wide, it can be used for analysing of almost any complex technical system. In addition to power plants the technique is also applicable e.g. for car manufacturing, aerospace, chemical and process industries. In most countries, the method is referred to as PSA. In the United States the method is referred to as PRA. Recently, The Finnish Radiation and Nuclear Safety Authority (STUK) has adviced/announced that also in Finland this method should be referred to as PRA. Despite having two names, the technique is practically the same.

Accident sequences are usually developed using event trees. Different paths through each event tree represent different accident sequences beginning with the same initiating event but having a different outcome because of system failures or conditions that occur during the course of the accident. Branches of an event tree that represent failures of complex systems or processes are often developed using fault trees. Fault trees are used to help the analyst systematically deduce the possible causes of a failure or fault.

To estimate the probability of an accident sequence, each event in the sequence is assigned a probability or frequency from operational data, calculations and/or expert judgements. The frequency for an accident sequence is estimated using probability mathematics to combine the probabilities of the events which in turn combine to create the sequence. Uncertainty in the probability or frequency estimates is included in the frequency estimates of the accident sequences using simulation and other mathematical techniques. Accident sequences for complex systems or processes can then be ranked according to the severity of their consequences and the estimated frequency of their occurrence [82].

PRA/PSA usually answers three basic questions [1, 49, 71]:

1. What can go wrong with the studied technological entity, or what are the initiators or initiating events that lead to adverse consequences?
2. What and how severe are the potential detriments, or the adverse consequences that the technological entity may be eventually subjected to as a result of the occurrence of the initiator?
3. How likely to occur are these undesirable consequences, or what are their probabilities or frequencies?

Motivations to perform PRA/PSA

In many modern technological applications (e.g., nuclear power, chemical processing industry, etc.), PRA/PSA has proven to be a systematic, logical, and comprehensive tool to assess risk (likelihood of unwanted consequences) for the purpose of [84]:

- increasing safety in design, operation and upgrade,
- saving money in design, manufacturing or assembly and operation.

In general, a PRA/PSA is needed when decisions need to be made that involve high stakes in a complex situation. Appropriate resource allocation depends on a

well formed risk model. Developing a comprehensive scenario set is a special challenge, and systematic methods are essential [85].

Scope of PRA/PSA

As for power plant environments, presently PRA/PSA is applied mainly for NPPs. Concerning NPPs, three PRA/PSA levels are usually defined. These are described as follows [83, 86]:

- Level 1 PRA/PSA: Conditional core damage (CDF) is usually estimated in this level. In general, in this level the events and event sequences that can lead to the exceeding of plant safety limits are identified and their probabilities of occurrence are quantified.
- Level 2 PRA/PSA: Containment failure and radionuclide release frequencies are usually estimated in this level, given that a core damage state occurs. Level 2 PRA/PSA builds on the results of level 1 PRA/PSA, identifying the ways in which releases of fission products can occur from the plant. In addition to quantifying the likelihoods of the releases, also the actual amounts of fission products released are estimated in this level.
- Level 3 PRA/PSA: The offsite consequences from a release, e.g. early and latent cancer fatalities, given a radionuclide release occurs, are estimated in this level. Level 3 PRA/PSA builds on the results of a level 2 PRA/PSA, estimating the public health risks and environmental consequences. This level provides insight into the accident mitigation and emergency response provisions.

Steps in conducting a PRA/PSA

The steps in conducting a PRA/PSA are listed in the following [49]:

- methodology definition; development of an inventory of possible techniques for the desired analysis,
- familiarisation and information assembly; collection of general data, the physical layout of the system or process (e.g. facility, plant, design), administrative controls, maintenance and test procedures as well as protective systems,

- identification of initiating events; identification of events (abnormal events) that could result in a hazard,
- sequence or scenario development; definition of a complete set of scenarios that include all the potential propagation paths that can lead to the loss of confinement of the hazard following the occurrence of an initiating event,
- system analysis; application of event tree and fault tree techniques to considered systems,
- internal events external to the process; correspond to events that originate within a system,
- external events; correspond to events that originate outside of the system,
- dependent failure considerations; identification of dependencies between event paths, such as those due to coupling between their failure mechanisms, and their inclusion to both event trees and fault trees,
- failure data analysis; predicting future availability of equipment based on past experiences and test data, quantification of initiating events, component failures and human errors,
- quantification; fault tree and event tree sequences are quantified to determine the frequencies of scenarios and associated uncertainties in the calculation.

Uncertainty and sensitivity in PRA/PSA

Randomness (variability) in the physical processes modelled in the PRA/PSA imposes the use of probabilistic models. The development of scenarios introduces model assumptions and model parameters which are based on what is currently known about the physics of the relevant processes and the behaviour of systems under given conditions. It is important that both natural variability of physical processes and the uncertainties in knowledge of them are properly accounted for [85].

The most widely used method for determining the uncertainty in the output risk assessment is to use a sampling process, in which values for each basic event probability are derived by sampling randomly from the probability distribution of each event. These probabilities are then combined through the risk expression to determine the value of the risk assessment for that sample. This

sampling process is repeated many times to obtain a distribution on the risk assessment [85].

Sensitivity analyses are also frequently performed in a PRA/PSA to indicate analysis inputs or elements whose value changes cause the greatest changes in partial or final risk results. They are also performed to identify components in the analysis to whose quality of data the analysis results are or are not sensitive [85].

Summary of PRA/PSA approach

PRA/PSA is generally used for low probability and high consequence events for which insufficient statistical data exist. If enough statistical data exist to quantify system or subsystem failure probabilities, use of some of the PRA/PSA tools may not be necessary [84]. An illustration of the main steps of a PRA/PSA analysis is shown in Figure 9.2-1. All in all, PRA/PSA analyses are carried out to support decisions.

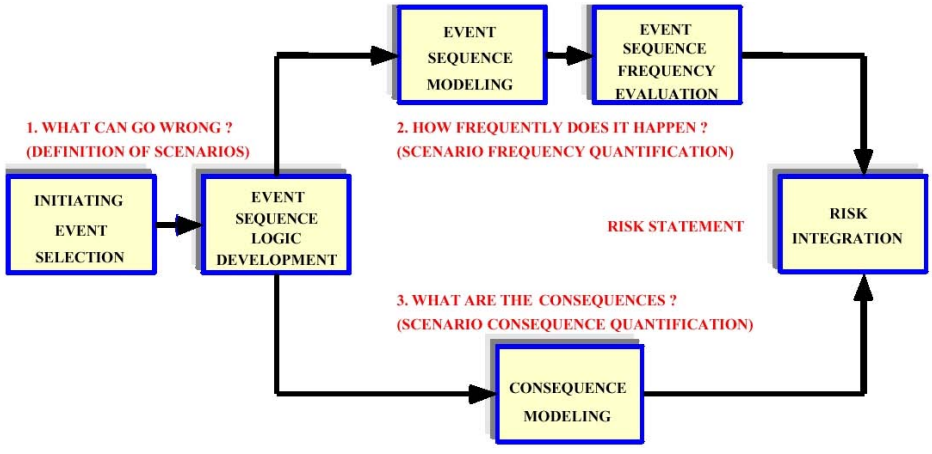

Figure 9.2-1. A diagram of the main steps of PRA/PSA analysis approach, from ref. [84].

Living PRA/PSA

Nuclear facilities, because of their complex nature, are subject to change with time. These changes can be physical (resulting from plant modifications, component ageing, etc.), operational (resulting from enhanced procedures, etc.) and organisational. In addition, there are also changes in our understanding of the plant, due to the analysis of operational experience, implementation of data collection systems, development of improved models, etc. Therefore, if the PRA/PSA is

to be of continuing use in the enhancement and understanding of plant safety, the PRA/PSA must be updated or modified when necessary to reflect the above changes. This has led to the concept of a “living PRA/PSA”, which can be defined as a PRA/PSA which is updated as necessary to reflect the current design and operational features with providing detailed documentation of the updating process [88].

Acceptable risk levels

The acceptability of risk by individuals depends on the degree of control over the risk producing activity that they perceive they have. Typically, people demand much lower risks from activities over which they have no control, e.g. commercial airliners [85]. Establishing the boundaries and guidelines for risk acceptability is a government responsibility. These levels may change as technology improves or emphasis changes with regard to environmental issues [50].

The Nuclear Regulatory Commission (NRC) of U.S.A. has established safety goals for NPPs as follows [236]:

- The individual early fatality risk in the region between the site boundary and one mile beyond this boundary will be less than 5E-07 per year (one thousandth of the risk due to all other causes).
- The individual latent cancer fatality risk in the region between the site boundary and 10 miles beyond this boundary will be less than 2E-06 per year (one thousandth of the risk due to all other causes).

These goals were established using as a criterion the requirement that risks from NPPs should be smaller than other risks by a factor of 1000. Thus, the individual latent cancer fatality risk due to all causes was taken to be 2E-03 per year. Because of the large uncertainties in the estimates of fatalities, the NRC is using subsidiary goals in its daily implementation of risk informed regulation. These are the reactor core damage frequency and the large early release frequency. The latter refers to the release of radioactivity to the environment.

The Finnish Radiation and Nuclear Safety Authority (STUK) has also defined a set of numerical design objectives for Finnish NPPs, which are given in Guide YVL 2.8, Probabilistic Safety Analyses [89]. According to STUK the following numerical design objectives cover the whole NPP:

- The mean value of the probability of core damage is less than 1E-05/year.

- The mean value of the probability of a release exceeding the target value defined in section 12 of the Council of State Decision (359/91) must be smaller than 5E-07 per year. However the containment has to be designed in such a way that its integrity is maintained with a high likelihood in case of both low and high pressure core damage.

According to STUK the risks associated with various accident sequences of the PRA/PSA are to be compared with each other to ensure that no dominant risk factors deviating from the common risk level remain at a plant [89].

Some benefits and drawbacks of PRA/PSA

After completing the compulsory PRA/PSA efforts, performing organisations have usually discovered benefits beyond mere compliance with regulation. These have included new insights into and an in-depth understanding of [1]:

- Design flaws and cost effective ways to eliminate them in design prior to construction and operation.
- Normal and abnormal operation of complex systems and facilities even for the most experienced design and operating personnel.
- Design flaws and hardware related, operator related and institutional reasons impacting safety and optimal performance at operating facilities and cost effective ways to implement upgrades.
- Approaches to reduce operation and maintenance costs while meeting or exceeding safety requirements.
- Technical bases to request and receive exemptions from unnecessarily conservative regulatory requirements.

The current PRA/PSA models usually include the following drawbacks [32]:

- As a general practise, event tree and fault tree analyses of current PRAs/PSAs do not include passive SSCs, such as RPV and reactor coolant piping. The argument for doing so is that the failure rates for the passive SSCs are negligibly small. Although this argument may be reasonable when SSCs are new, a critical evaluation of this assumption is needed when the subjects of the investigation are older.
- The traditional PRA/PSA approach assumes a constant rate for each component failure mode.

- Except for failure rates of identical components that have been covered by common cause failure analyses and by complete state-of-knowledge correlation, the current PRA/PSA methodology does not model other kind of dependencies.
- Failure probabilities of events other than hardware failure, such as human error rates and component unavailability because of testing and maintenance, could be different for older plants than for new plants. The current PRA/PSA methodology does not make such a distinction.

9.3 Risk informed in-service inspection (RI-ISI)

9.3.1 Introduction

Presently, the risk-informed in-service inspection (RI-ISI) analysis approaches are applied to NPP piping systems, whereas risk-based inspection (RBI) approach is applied for conventional power plants and other industry plants involving structural systems bearing relatively severe loads and involving periodic inspections. RI-ISI reflects recent developments in PRA/PSA methodology, the understanding of degradation mechanisms and the experience gained from the operating experience of NPPs. RI-ISI aims at rational plant safety management by taking into account the results of plant specific risk analyses. The fundamental idea is to identify high-risk locations where the inspection efforts should be concentrated. The objective is to provide an ongoing improvement in the overall plant safety, measured by risk, together with reduced irradiation doses for the inspection teams [237].

In-service inspection (ISI) is an essential element of the defence in depth concept. ISI consists of non-destructive examination (NDE) as well as pressure and leakage testing. ISI helps to confirm that basic nuclear safety functions are preserved and that the probability of radioactive materials breaching containment is reduced.

The development of a RI-ISI programme requires expertise from a number of different disciplines including inspection, maintenance, design, materials, chemistry, stress analysis, systems, PSA, operations and safety. It also requires a long-term co-ordinated management commitment through inspection qualification, inspection result analysis and final feedback to the risk analysis, in order to maintain a living ISI programme. Before resorting to a risk-informed pro-

gramme, it is essential, therefore, to obtain the backing and commitment of the utility and plant management [237].

An impending failure and its consequences are not prevented or changed by RI-ISI unless additional mitigating actions are taken. Inspection is an initiator for actions such as the repair or replacement of deteriorating equipment, or a change to the operating conditions. By identifying potential problems, RI-ISI increases the chances that mitigating actions will be taken, and thereby reduces the frequency of failure [3].

RBI requires a wide range of information in order to assess the probability and consequences of equipment failure and develop an inspection plan. A plant database containing an inventory of the equipment and associated information is a useful way of managing the relevant data [3].

In the top level, the RI-ISI analysis is divided into the following three parts:

- assessment of consequences,
- assessment of degradation potential,
- assessment of risks and the consequent forming of a risk informed inspection program.

The plant specific PRA/PSA tool is used for the quantification of piping failure consequences. The PSA allows the calculation of several risk importance measures, such as risk increase factor, RIF (known also as risk achievement worth, RAW), and risk reduction factor, RDF (known also as risk reduction worth, RRW). In connection to RI-ISI, conditional core damage probability, CCDP, and conditional large early release probability, CLERP, have become commonly used consequence measures.

There are basically the following three options/approaches for quantitative assessment of leak and rupture probabilities/frequencies of piping components:

- use of PFM and/or other structural reliability approaches,
- statistical estimation from experience data, e.g. large databases,
- use of formal expert judgement, e.g. based on deterministic structural models.

A best result is achieved with a combination of all these approaches. However, how much each of these approaches weighs as compared to others under various conditions depends on several aspects, the foremost of which typically being the amount and quality of available and applicable degradation data. When NPP

piping degradation data are available only scarcely, the role of structural reliability approaches is strongly emphasised, and to a considerable extent that of expert judgement as well.

9.3.2 On principles of RI-ISI

RI-ISI aims at a rational plant safety management strategy by taking into account the results of plant specific risk analyses. The fundamental principles of any risk informed inspection programme are [237]:

1) The ability to define the consequence, probability and risk associated with structural failures so that the ISI programme can focus on an integrated defence in depth strategy.
2) The identification of an inspection programme that will decrease the risk from selected sites as far as it is practical and with due consideration of the costs and accumulated radiation dose to plant workers.

The advantage of such an approach is the optimisation of the inspection efforts. The term optimise in this context is seen as a process that maintains defence in depth, whilst [237]:

a) improving or at least maintaining the overall plant safety,
b) minimising the radiation dose to personnel involved in the inspection activities,
c) providing improved plant reliability.

9.3.3 Process of risk-informed inspection planning

The main elements constituting the process of risk informed inspection planning are as follows [237]:

1) Assurance of the long term commitment of senior management to the risk informed methodology.
2) Formation of the RI-ISI assessment team.
3) Definition of the scope of the equipment/structures to be considered in the application.
4) Collection and analysis of the information required to carry out the risk assessment.

5) Definition of the level of the evaluation.
6) Assessment of the probability of failure for all the components included in the scope of the application.
7) Assessment of the consequences of failure for all the components included in the scope of the application.
8) Ranking of the risks associated with all the components.
9) Performing sensitivity studies to determine the impact of changes in key assumptions or data.
10) Choice of the components to be inspected according to chosen criteria.
11) Assessment of the implication on inspection qualification.
12) Feed back of the obtained information (after completing the inspection).

9.3.4 Qualitative, quantitative and semi-quantitative methods for RI-ISI

In principle, three different approaches to the use of risk concepts in developing ISI programs can be considered: the purely quantitative, the semi-quantitative and the purely qualitative approach. In the quantitative approach, both failure probabilities and consequences are assessed with physical models and expressed in physical units. In the qualitative approach, the failure probabilities are assessed qualitatively, taking into account only the involved degradation mechanism(s) and some factors affecting their severity, with simply dividing these mechanisms to classes having such descriptive names as high, medium, low and none, corresponding to the assumed levels of severity/threat. Both in quantitative and qualitative approaches, the consequences are considered and expressed with the same quantitative measures. Of the commonly applied RI-ISI methods, a notable example of a qualitative approach is the EPRI RI-ISI procedure [17, 240, 241], whereas a representative example of a quantitative one is the PWROG Methodology [242, 238, 239]. The semi-quantitative approach combines features from both quantitative and qualitative approaches.

In the nuclear industry, the risks are assessed with PRA/PSA, which is a quantitative approach. The use of PSA is the foundation of risk informed approaches in the nuclear industry, and thus a purely qualitative approach to RI-ISI that does not make use of PRA/PSA insights would be difficult to justify.

Ideally, a purely quantitative approach should be chosen whenever feasible, as only in such framework, it is possible to quantify the risk change achieved when implementing the RI-ISI program. However, it is recognised that the current state of knowledge and understanding of some of the degradation mechanisms and the availability of the required plant data can be insufficient to accurately quantify the probability of failure. Likewise, many current PRA/PSA analyses may not be detailed enough for the level required in an ISI application, and thus the consequence analysis must be complemented by some degree of qualitative assessment.

Thus, the most feasible approach to the development of any RI-ISI program today would arguably be the semi-quantitative one, based on a plant specific PSA and with due recognition of the current mechanistic understanding of any degradation mechanisms.

9.3.5 Brief overview and comparison of two main RI-ISI methodologies

The two main RI-ISI methodologies that are also widely applied in Europe are: PWROG methodology [242, 238, 239] and EPRI methodology [17, 240, 241]. Recently has been published a notable IAEA report [243] on current status, issues and development of RI-ISI methodologies. Some European countries have adapted these methodologies to their particular context, but have not added developments that differ from the original methods. Flow charts presenting the methodologies of these two RI-ISI methodologies are presented in Figures 9.3-1 and 9.3-2 in the following.

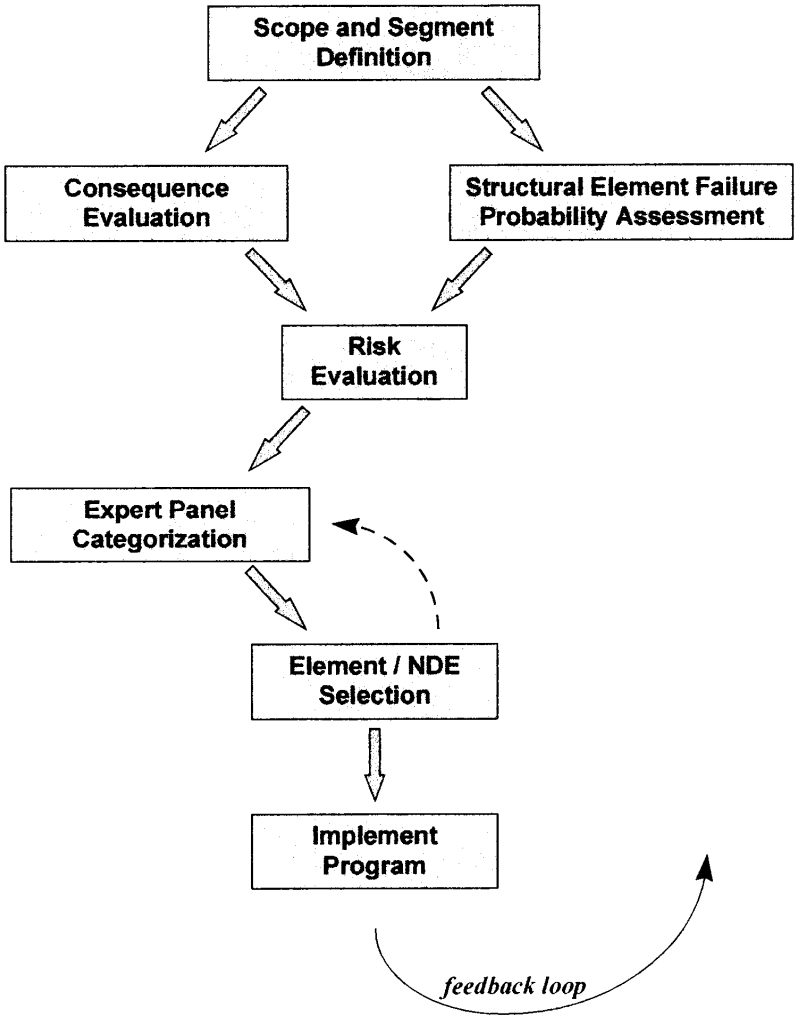

Figure 9.3-1. Flow chart of PWROG RI-ISI methodology, from refs. [242, 238, 239].

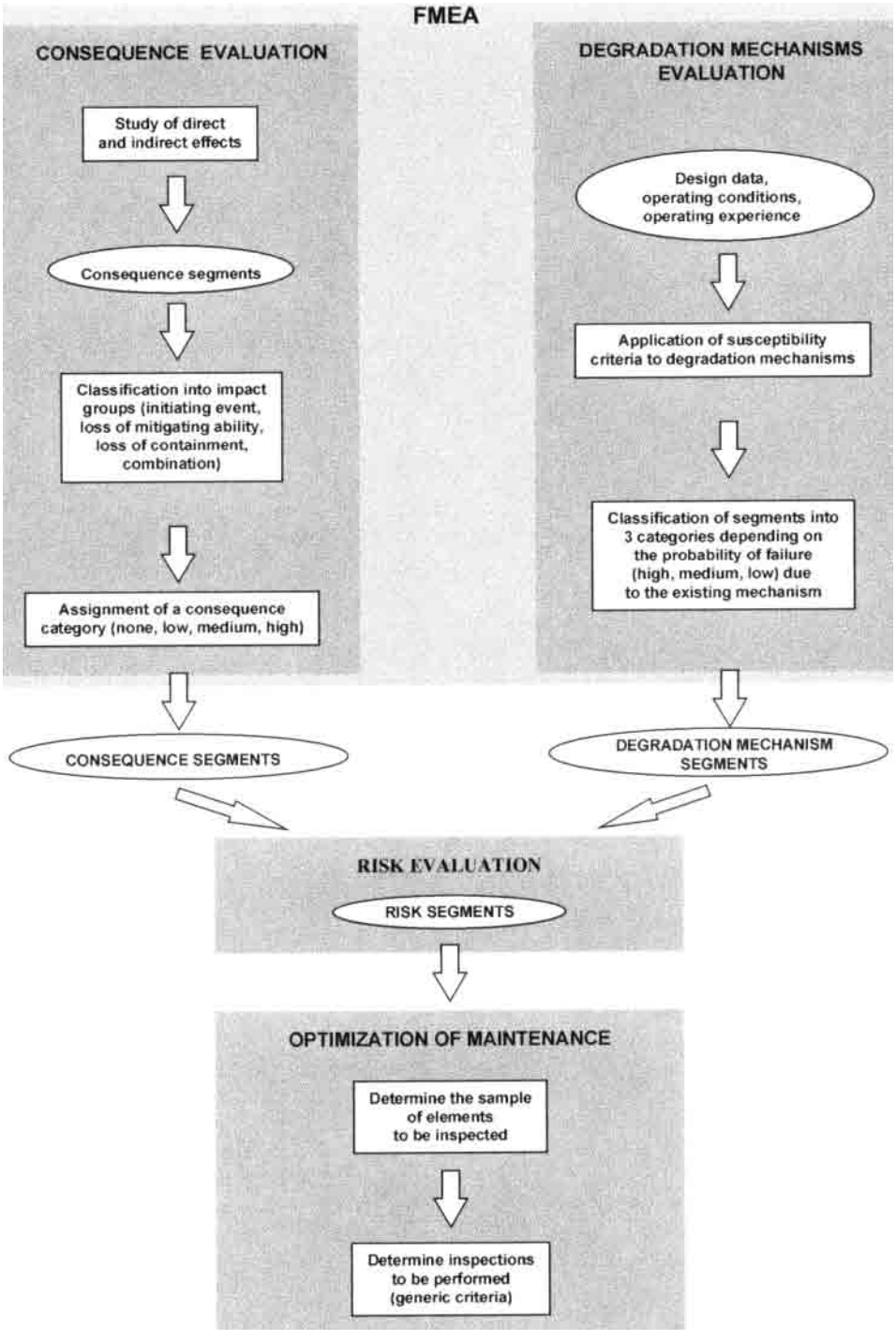

Figure 9.3-2. Flow chart of EPRI RI-ISI methodology, from refs. [17, 240, 241].

The main steps or structure in both the EPRI and PWROG methodologies are rather similar: scope definition, segmentation, probability of failure analysis and failure consequence analyses, risk ranking and finally selection of inspection sites.

The main differences arise from the way of performing the failure probability analyses. In the EPRI methodology, the approach is basically qualitative, and quantification is basically done by using bounding values. In the PWROG methodology, a specific structural reliability analysis tool is used to quantify the failure probabilities. The use of risk importance measures is somewhat different. In the PWROG methodology, the risk ranking is based on RRW, while EPRI methodology uses CCDP (and CLERP).

There are also other minor differences related e.g. to the segmentation, and the final selection of inspection sites follows different rules. The impact of these differences has been studied in an OECD-JRC co-ordinated RI-ISI benchmarking project RISMET [251].

9.3.6 Probability of detection of cracks

The effectiveness of inspection is an important input parameter in RI-ISI analyses. A quantitative measure of inspection effectiveness is needed in order to calculate the reduction in risk associated with inspection. Quantitative estimates of the inspection capability enable a better optimisation of ISI.

The reliability of NDT techniques is usually quantified using flaw detection reliability in terms of the probability of detection (POD). The detection probability is typically presented in the form of POD functions, which describe the detection probability as a function of the flaw size, e.g. flaw depth or length. However, the construction of a POD function requires a considerable amount of data before statistical confidence is achieved. In case of NDT methods, it is often expensive and time consuming to produce such a large amount of data. For a recent notable document on POD issues, see ref. [254]. It contains a literature review of some important papers and reports, a review of the statistical models that have been proposed for quantification of inspection reliability as well as descriptions and recommendations on statistical best practices for producing POD curves.

The quantification of the POD is not a straightforward task. The output from the European Network for Inspection Qualification (ENIQ) qualification process [252] is generally a statement concluding whether or not there is high confidence

that the required inspection capability will be achieved in practice, for the specified inspection system, component and defect range. However, the ENIQ methodology is not designed to provide a quantitative measure of inspection capability of the type which can be used by quantitative RI-ISI. It also means it is difficult to "benchmark" the confidence associated with any given inspection qualification. The POD curves used in U.S. applications, e.g. in the SRRA code of the PWROG RI-ISI methodology [239], have been subject to criticism due to sometimes unrealistically high detection capability assumptions.

The development of full POD curves seems both impossible, and for RI-ISI applications also impractical. Simplified estimates would be of sufficient accuracy in RI-ISI applications. Studies on the sensitivity of the risk reduction to POD have been documented e.g. in ref. [252]. The simplified POD step functions can then be implemented in the analysis process and used for calculating the effect of inspections, as is shown e.g. in recent VTT reports [244, 253].

If the failure probability is not evaluated using a PFM approach, but an estimate is given based on expert judgement or a statistical approach from experience data, a simplified approach can be used for the evaluation of the impact of inspections. Then only a single POD value is used, without accounting for the detection limit.

9.3.7 RI-ISI approach developments by VTT

VTT has aimed at developing a RI-ISI approach which uses quantitative classification for both failure potential and consequence assessment, but recognising the above mentioned limitations in failure probability quantification [244].

In RI-ISI approaches, NPP piping systems are for risk analysis purposes typically divided into regions/parts called segments. In the VTT approach, the segmentation follows the basic principle, that within a segment, the degradation mechanism(s) and the consequence(s) of a piping failure remain unaltered. This is similar to the segmentation in the EPRI methodology. The VTT approach also includes an expert panel to review the initial risk ranking. This is in line with the ENIQ Framework Document [237] and the Finnish regulations.
As a result, a more accurate and refined modification of the qualitative EPRI RI-ISI risk matrix procedure was suggested at VTT. The modifications include [245]:

- changing the degradation category in the risk matrix from qualitative to quantitative,

- assessing the piping segment failure probabilities with a PFM based analysis tool developed at VTT, instead of evaluating them roughly based just on operational/process conditions as is done in the EPRI procedure, and
- assessing and optimising the piping segment risks with a Markov system based analysis tool developed at VTT.

The overall method of the applied discrete time Markov procedure for piping risk analyses can be summarised in six steps as follows [245, 246]:

1. crack growth simulations based on PFM,
2. construction of degradation matrix transition probabilities from PFM simulations and database analysis of crack initiation frequencies,
3. model for inspection quality, which is used to construct inspection matrix transition probabilities,
4. Markov model to calculate pipe rupture probabilities for chosen inspection schemes,
5. obtaining pipe rupture consequences from plant specific PSA, and
6. comparison of results for different inspection strategies, where measures of interest include yearly rupture probability, yearly core damage probability and average values for both of these over plant lifetime.

The PFM part of the VTT RI-ISI approach has also been benchmarked against some of other PFM analysis tools in a recent international project called PODRIS, see ref. [247]. These other PFM/RI-ISI analysis tools were NURBIT by Det Norske Veritas (DNV) [248, 249, 250] and JRC approach (which is based on a probabilistic implementation of the R6 Method, Rev. 4 [200], and a discrete time Markov process analysis). In PODRIS, the main interest was to investigate whether it is justifiable to use a simplified POD curve. The PFM analysis tools were applied to a small but representative set of NPP pipe components, from both BWR and PWR units, whereas the considered degradation mechanism was SCC. A good correspondence between the PFM results computed with these three tools was achieved. As for other significant results, they indicate that the use of a simplified POD could be justifiable in RI-ISI applications.

9.3.8 RISMET project – benchmarking of RI-ISI methodologies

The RISMET project was launched in 2005 by the Joint Research Centre of the European Commission (JRC) together with the Nuclear Energy Agency of the OECD (NEA), with the aim of benchmarking several RI-ISI methodologies. It featured more than twenty participating organisations from Europe, U.S.A., Canada and Japan, representing utilities, regulators and research organisations. Also VTT participated in RISMET [251].

In RISMET, various RI-ISI methodologies were applied to the same case, consisting of four selected piping systems at the Swedish Ringhals 4 PWR unit [251]. The applied RI-ISI methodologies were: SKIFS [255], PWROG [242, 238, 239], PWROG-SE (an adaptation of the original PWROG methodology to the Swedish regulatory environment), EPRI [17] and ASME Code Case N-716 [256]. The RI-ISI applications were compared among each other and to the deterministic ASME XI ISI selection procedure.

The scope of the benchmark was limited to four systems, but the variety regarding safety class, potential degradation mechanisms and pipe break consequences ensured a good coverage of issues for a comparative study. The risk-informed methodologies showed some significant differences and resulted in slightly different risk ranking and selection of inspection sites. However, the results of the benchmark indicated that the risk impact of these differences is small, and the RI-ISI approaches identify safety important piping segments that are ignored by approaches not using the PSA. The results of the benchmark exercise RISMET improve the knowledge on differences in approaches and their impact on plant safety, and promote the use of RI-ISI [257].

10. Power plant component ageing analyses

Ageing of various SSCs affects the safety of power plants. The objective of component ageing analyses is to identify the degradation mechanisms of components and the increase in failure occurrences, to assess the remaining lifetime of components and to find suitable means to prevent or mitigate the effects of ageing. This chapter deals mainly with ageing analyses concerning NPP components.

The ageing analyses should be focused on those components that are the most significant from the safety point of view. Other significant selection criteria, especially for components which are not safety critical, are availability and costs. For most PWRs, the most safety significant components are [231]: RPV, vessel internals, pressuriser, steam generators, main primary pipes, main primary pump, containment, cables and concrete structures. For most BWRs, the most safety significant components are [231]: RPV, vessel internals, pressuriser, steam generators, main primary pipes, recirculation pump, containment, cables and concrete structures.

After the components are selected, the analysis methods for ageing detection and prediction are chosen. The suitability of a procedure depends on the selected component and on the available data. When the ageing is detected, suitable techniques are applied to prevent or mitigate the effects of ageing. Ageing research programmes have been conducted in several countries, e.g. in the U.S., Japan and France [32, 232, 233, 234].

10.1 Selection of components for analyses

The evaluation of safety significance and ageing sensitivity of components can be based on the analysis of operating experience, expert opinions and probabilistic techniques for prioritising and determining risk significance of ageing. The

results from PRA/PSA can (and usually are) be used in association with the probabilistic techniques [4]. If the collected degradation and failure data is properly analysed and reported, the operating experience data can be effectively used to identify systems and components which are susceptible to ageing.

A NPP has a large variety of components, many of which are essential for overall plant safety. Some of the safety related components contribute more than others towards ensuring plant safety and the extent to which these components are susceptible to ageing also varies considerably [235]. It is neither practical nor necessary to evaluate and quantify the extent of the many thousands of individual power plant components. Therefore, a more rational and cost effective approach is required. The approach presented here is based on a systematic selection and prioritisation of safety important NPP components for more detailed ageing analyses.

IAEA has proposed a component selection process for NPPs [235], which is based on a systematic examination of all systems and structures from a safety perspective. This examination is based on the following precepts:

- Required safety margins for NPP components have to be maintained at all times.
- Safety important components in a NPP have already been classified.
- The failure of safety important components can result in different degrees of loss of system safety functions, with or without severe consequences.
- Current maintenance, testing and inspection programmes in NPPs include different strategies of varying effectiveness to deal with ageing effects.
- Safety important components may experience varying degrees of degradation due to ageing under different loading and environmental conditions.
- Methods used for monitoring ageing effects in specific components and structures may vary significantly.
- Existing databases pertaining to ageing effects in NPP components are not sufficiently comprehensive.

10.2 Identification of ageing mechanisms

The process used for identifying deterioration mechanisms for pressure systems and other systems containing hazardous materials should be conducted in a wide ranging and systematic manner. It is more effective if it involves experienced staff from different disciplines rather than being the work of a single person. Acceptable processes could include combinations of the following [3]:

- review of specific plant history and information from previous inspections,
- review of experience across similar industries or plants,
- expert elicitation of knowledge of structural integrity and materials,
- use of check-lists and mechanism descriptions,
- computer based expert systems.

10.3 Mitigation of ageing effects

In the last phase of ageing analyses, decisions on management of ageing should be made on the basis of identified degradation mechanisms and their severity. The primary goal in this phase is to find suitable methods to prevent, mitigate or restore the effects of ageing [6, 217]. Thus the basic management methods are controlling and slowing down ageing as well as replacement of components.

The application of these methods is component specific, depending on e.g. the expected ageing rate and mechanisms, the possibilities of replacement and early failure detection possibilities. In the case of repairable or replaceable components which will age relatively fast compared to the plant lifetime, the ageing management means following the efficiency of current maintenance procedures and reviewing the test programmes. In the case of components which are difficult to replace, the efforts may be focused on the reduction of environmental stressors, re-evaluation of surveillance and condition monitoring methods.

The effects of ageing on SSCs are detected through different mechanisms in plant operation, such as preventive/corrective maintenance, inspections, monitoring and performance monitoring of SSCs. The mechanism that has given rise to the degradation of the behaviour or characteristics of component material can be determined through the subsequent analysis of these effects. The selection of an efficient method for mitigating ageing in component material depends on an accurate determination and evaluation of the degradation mechanism that caused the ageing [6].

One principal concept in ageing and maintenance management is the concentration of effort on reduction of the failure probability of the most important components [87]. Reliability centered maintenance (RCM) is a method for establishing a scheduled preventive maintenance programme resulting in improved component reliability and minimised costs [258]. The RCM approach intends to optimise the use of maintenance resources by identifying the most critical components with respect to safety, availability or maintenance costs, and selecting for these components the most appropriate maintenance procedures with the aid of decision logic.

Commonly applied ageing management methods for SSCs in NPPs can be grouped into three main categories [6]:

- change of SSC design,
- change/recovery of material characteristics,
- change of operating parameters.

11. Probabilistic ageing and risk analysis tools

There are many software tools that can be used for system and component risk and ageing analyses. An overview of some of the noteworthy of these tools is presented in the following. The emphasis is on component analysis tools which are presented first, following with a more brief presentation of the system analysis tools. The emphasis of this presentation is on the component analysis tools. The overview ends with a summary of the presented analysis tools.

In the general analysis applications, any failure mode, fracture or other, can be addressed using the appropriate limit states. Validation of such software is usually carried out by benchmark exercises between different programs since often it is not feasible to compare results with real failure statistics, due to their scarcity. The probabilistic analysis approaches in the presented software vary from FORM and SORM to MCS. Some of the presented analysis tools are commercially available and some are so called in-house programs, the availability of which may be limited or non-existent.

11.1 Component ageing and risk analysis software

PRAISE

PRAISE is a PFM computer code for estimating probabilities of leaks and breaks in NPP cooling piping. The code was originally developed at Lawrence Livermore National Laboratory (LLNL) for the assessment of seismic events on the failure probability of PWR piping. PRAISE is an acronym for Piping Reliability Analysis Including Seismic Events [259]. Latest version of the code is named WinPRAISE, which is a Windows version of the original PRAISE code [260].

PRAISE considers the initiation and/or growth of crack-like defects in piping welds. This meaning that both fabrication cracks and those induced by service

are covered. The initiation analyses are based on the results of laboratory studies and field observations in austenitic piping material operating under BWR conditions. The considerable scatter in such results is quantified and incorporated into a probabilistic model. The crack growth analysis is based on deterministic fracture mechanics principles, in which some of the input parameters, such as initial crack size, are considered to be random variables. MCS, with stratified sampling on initial crack size, is used for probabilistic computations [261].

Presently PRAISE contains models for the analysis of both SCC and fatigue crack growth. In the case of SCC, the growth model is divided into two parts: the early growth of initiated crack and fracture mechanistic crack growth. The fracture mechanistic SCC growth rate model parameters are based on data on growth rates in fracture mechanics specimens. The code has features for fatigue crack growth analysis in both ferritic and austenitic steels. The probability of detection (POD) of cracks is based on a model where the POD is a function of the crack area [260].

PRO-LOCA

The PFM based PRO-LOCA analysis code has been developed for predicting break probabilities for loss-of-coolant-accidents (LOCAs) in NPP piping systems. In brief, the background of PRO-LOCA is that in 2003 the USNRC began its development [262] with the intension to adopt and apply advances in fracture mechanics models, and thereby to provide the successor to the PRAISE code. Like PRAISE, the PRO-LOCA code addresses the failure mechanisms associated with both pre-existing cracks and service induced cracks. Both fatigue and intergranular SCC (IGSCC) are addressed. In addition, PRO-LOCA can also predict failure probabilities for primary water SCC (PWSCC). Other improved capabilities are in the areas of leak rate predictions and the prediction of critical/unstable crack sizes. PRO-LOCA has also been incorporated an improved basis for simulating weld residual stress (WRS) distributions.
In the recent MERIT project, PRO-LOCA has been developed further, and in summary the code has now the following features [263]:

- crack initiation models for fatigue or stress corrosion cracking for previously unflawed material,
- sub-critical crack growth models for fatigue and SCC for both initiated and pre-existing circumferential defects,

- models for flaw detection by inspections and leak detection, and
- crack stability.

The PRO-LOCA code can thus predict the leak or break frequency for the whole sequence of initiation, subcritical crack growth until wall penetration and leakage, and instability of the through-wall crack (pipe rupture) [263]. The results obtained with the PRO-LOCA code are a sequence of failure frequencies which represents the probability of a surface crack developing, a through-wall crack developing, and six different sizes of crack opening areas corresponding to different leak flow rates or LOCA categories. Note that the level of quality assurance of the PRO-LOCA code is such that the code in its current state of development is considered to be more of a research code than a regulatory tool.

NURBIT

NURBIT developed by Brickstad and Zang [250] is a RI-ISI/PFM software. In order to perform the probabilistic evaluations, a computer code named PIFRAP (PIpe FRActure Probabilities) was developed. PIFRAP contains the analysis programs LBBPIPE and SQUIRT for the evaluation of crack growth and leak rates. PIFRAP calls upon these programs for different values of initial crack length and required quantities for the integration are obtained to give the leak and rupture frequency. Later, NURBIT was developed [250], which includes the features in PIFRAP for the failure frequency evaluation. In addition, NURBIT also performs a complete RI-ISI selection based on a risk ranking procedure including the selection of the most appropriate inspection interval. Here risk means the core damage frequency, commonly used in PSA studies. NURBIT version 2.0 also includes a cost-benefit analysis where the balance between inspection costs and failure costs are made.

The PIFRAP code is based on the model described by Nilsson et al. [266]. A more thorough description of the PIFRAP model with sensitivity analyses can be found from the SKI report describing the application to establish risk informed ISI priorities for Oskarshamn 1 piping [265].

The PIFRAP code is intended for calculation of the failure probability of a specific pipe cross section with a certain stress state and possibly containing a circumferential crack growing due to IGSCC. A number of assumptions were made for the probabilistic analysis [267]:

- stresses are deterministic,
- crack growth is deterministic,
- initial crack depth is fixed to 1.0 mm,
- initial length of the crack is random (based on Swedish distribution data),
- the probability of not detecting a crack at an ISI depends on crack length and crack depth (the actual function used was not dependent on the crack length, but a possible dependence on length is retained in the general equations),
- there is a detection limit for leakage flow, and above this limit there is a probability of not detecting a leakage flow.

Due to the assumptions made, the growth of the crack will be deterministic and will only depend on the initial crack length for a given geometry and given stresses. The probabilistic data to the PIFRAP code are [267]:

- the probability that a crack with an assumed depth is initiated during a certain time interval,
- initial length of the crack (initial crack length/depth is calculated from statistical data backwards, to a calculated length when the depth is 1.0 mm),
- the probability of not detecting a crack at an ISI,
- the probability of not detecting a leak rate for a given leak rate detection limit.

In addition, the code requires deterministic data on pipe geometry, loading conditions and material properties [267].

ProSACC

The analysis software ProSACC [268] developed by Det Norske Veritas (DNV) contains both deterministic and probabilistic analysis capabilities. The deterministic part of the software ProSACC may be used both for assessment of detected cracks or crack like defects and for defect tolerance analysis. The procedure, which is based on the R6 Method [201], could be used to calculate possible crack growth due to fatigue or stress corrosion and to calculate the reserve margin for failure due to fracture (if wanted, including a limited amount of stable crack growth) and plastic collapse. ProSACC also has an option, which enables

assessment of cracks according to the 1995 edition of the ASME Boiler and Pressure Vessel Code, Section XI [173], Appendices A, C and H for assessment of cracks in ferritic pressure vessels, austenitic piping and ferritic piping, respectively. ProSACC mainly considers surface crack postulates in plates, hollow cylinders and spheres.

The probabilistic part of the software ProSACC is based on a PFM procedure that calculates two different failure probabilities:

- probability of failure, defect size given by NDT/NDE,
- probability of failure, defect not detected by NDT/NDE.

Probabilistic VTTBESIT

The analysis software VTTBESIT developed by both VTT [244, 246, 247, 269] and Fraunhofer-Institut für Werkstoffmechanik (IWM, Germany) [270, 271, 272], contains both deterministic and probabilistic analysis capabilities. Mainly, the probabilistic features are considered here.

With VTTBESIT it is possible to quickly compute mode I stress intensity factor values along the crack front as well as crack growth. The covered component geometries are hollow cylinders and straight plates. The code was originally intended for deterministic fracture mechanics based crack growth analyses, but its scope has been extended by adding probabilistic capabilities to the code. Both cracks caused by fabrication and those induced by service are considered.

The probabilistically treated crack growth analysis input data parameters are as follows:

- depth of initial cracks,
- length of initial cracks,
- frequency of load cycle occurrence.

For the time being, other crack growth analysis input data parameters are considered to have single deterministic values.

In VTTBESIT analyses, the crack growth increment in each time step is computed from the respective crack growth equation. The covered crack growth mechanisms are fatigue and SCC. The simulation ends either when the crack depth reaches the outer pipe surface, or the time cycles reach the end of plant lifetime. For each analysed case, thousands of separate simulations are calculated, and for each of these, values of the above mentioned distributed input data parameters/variables are sampled at random from the respective probabilistic

distributions. Typically each simulation run spans several decades of assumed plant operation with the crack depth calculated yearly, conditional on the existence of an initial flaw. The annual crack depth information for each simulation is transferred to the second phase of the analyses.

In the second phase, the analyses are based on Markov process. This method is a stochastic process in which the probability distribution of the current state is conditionally independent of the path of past states, a characteristic called the Markov property, see Section 8.3.2 for a more detailed description concerning Markov models. In the VTT application, the states of the Markov process correspond to crack penetration depths through component wall, and the transition probabilities those from a lower state to higher states (deeper cracks). On the other hand, the effects of inspections are included in the model as transitions from a cracked state to the flawless state, as each time a crack is detected it is assumed that the component in question is repaired or replaced with a new i.e. intact one. The effect of inspections is taken into account with POD functions.

For the whole duration of the assumed operational plant lifetime the results obtained from a VTTBESIT analysis cover yearly piping component failure probabilities for different inspection strategies, including also the case of no inspections, for the considered degradation mechanism, being either fatigue or SCC. These results can then be used further e.g. in RI-ISI analyses.

STRUREL

STRUREL (STRUctural RELiability) is a general purpose reliability software series that has been developed by Reliability Consulting Programs GmbH [273] for performing different computational tasks. The program comprises several independent but interrelated programs:

- STATREL; statistical analysis of data, simulation, distribution fitting and analysis of time series,
- COMREL; time-invariant and time-variant analysis of component reliability,
- SYSREL; reliability analysis of systems,
- NASCOM; finite element code for structural analysis,
- NASREL; module combining COMREL with NASCOM.

STATREL enables appropriate distributions to be derived for datasets input from e.g. spreadsheets. Goodness of fit tests are also included to demonstrate the

best fitting method to be used. COMREL comprises 44 models and limit state equations can be input for failure modes not addressed. The program includes MC simulation, FORM and SORM methods, and for the case of the time-variant version it includes methods for incorporating random and point-in-time events. SYSREL enables multiple failure criteria for parallel and series systems to be evaluated, including conditional events. It links directly with COMREL, making it straightforward to check individual failure criteria before combining them in a system analysis.

STRUREL has applications in many fields, including nuclear industry, and there exists many examples of its use for fracture, fatigue, collapse, corrosion and general strength problems [274].

ProSINTAP

ProSINTAP (PRObabilistic Structural INTegrity Assessment Procedure) automates MCS and FORM analysis of the failure assessment diagram and is only applicable to fracture and collapse failure modes [275, 276]. It consists of five input data decks: Geometry, Loading, Material, NDE and Analysis.

The Geometry section comprises stress intensity factor solutions for a range of plate and hollow cylinder geometries with surface and through-thickness cracks. The load module enables through thickness distributions of applied and welding residual stress to be incorporated. In the material module, yield strength, rupture stress and fracture toughness and their associated statistical distributions are input. This requires the mean and standard deviation of each parameter as defined by the normal, log-normal or Weibull distribution. The NDE module enables defect sizing as input data, but also allowing for treatment as an exponential distribution. The Analysis module enables the user to select MCS or FORM methods and to apply partial safety factors if required in order to achieve a specified target reliability method.

CALREL

CALREL (CALibration of RELiability) is a general purpose structural reliability analysis program developed by the University of Berkeley, California [277]. The code is designed to work on its own or to operate as a shell program in conjunction with other structural analysis programs. Structural failure criteria are defined in terms of one or more limit state functions. The specification is by the user through user defined subroutines.

CALREL is capable of computing the reliability of structural components as well as systems. Specific macro commands are available for the following types of analyses:

- first-order component reliability analysis,
- second-order component reliability analysis by both curvature fitting and point fitting methods,
- first-order reliability bounds for series systems,
- first-order reliability sensitivity analysis for independent and dependent variables with respect to distribution and limit state function parameters,
- directional simulation for components and general systems, employing first or second-order fittings of the limit state surfaces,
- MCS for components and general systems.

CALREL has a large library of probability distributions for independent as well as dependent variables. Additional distributions may be included through a user defined subroutine. CALREL is available for purchase from UC Berkeley as both object and source code.

STAR 6

STAR 6 [278] is a reliability software developed by British Energy for automating reliability analyses of the fracture and collapse analysis procedures in R6 Method [200]. It is similar in approach to ProSINTAP and includes FORM and MCS, but a more extensive library of stress intensity factor solutions for different component geometries is included [200].

NESSUS

NESSUS is a general purpose tool for computing the probabilistic response or reliability of structures, developed by Southwest Research Institute (SwRI) [279].

The framework of NESSUS allows the user to link traditional and advanced probabilistic algorithms with analytical equations, external computer programs including commercial finite element codes and general combinations of the two. The finite element codes NESSUS has interface to include ABAQUS, NASTRAN and PRONTO. Also, NESSUS provides a built-in finite element structural modelling capability [280].

Eleven probabilistic algorithms are available in NESSUS. These include MCS, FORM, SORM, FPI, MV, AMV and LHS. In addition, NESSUS allows linking of different analysis packages or analytical functions to allow a general relationship of physical processes to predict the uncertainty in the performance of the system [280].

NESSUS can compute the cumulative distribution function of system performance (e.g. stress or strain) or include the strength of the system to compute the reliability. Traditional reliability analysis involves computing the probability of the stress, S, exceeding the strength, R, or $P[R < S]$ or $P[g < 0]$, where g is the limit state function. R and S may be complex models involving other random variables such that $R = R(X_i)$ and $S = S(Y_i)$. In NESSUS function g is formulated such that $g = g(X_i, Y_i)$, and thus it accounts for possible correlation between the stress and strength parts of the performance measure. NESSUS provides also a general formulation of function g that allows linking of different analysis codes and analytical functions. For example, a stress or strain from a finite element analysis can be used with a fatigue life equation or S-N curve to define the performance of a structure. The results for a component analysis in NESSUS are reliability or cumulative distribution function and importance factors. The importance factors indicate which variables contribute most to the unreliability and may be used for design changes or manufacturing process modifications [280]. NESSUS licences are available for purchase.

NASGRO

Deterministic analysis software NASGRO, developed by SwRI, is a suite of computer programs comprised of analysis modules linked together by graphical user interfaces (GUIs) [281]. The objective in developing NASGRO was to improve an earlier computer code to accommodate more recent advancements in fracture mechanics and crack propagation theory and to meet the needs for damage tolerance and durability analyses [282].
The capabilities of NASGRO include:

- fatigue crack growth and fracture analysis,
- structural life assessment,
- stress computation,
- fatigue crack growth properties processing and storing.

When using NASGRO, various types of analyses can be performed in an interactive mode using the GUIs for each module. Material properties for crack growth can be chosen from a large database by selection from a menu. The material property module can also be used to enter, edit and curve fit crack growth data. Analysis in complex two dimensional geometries with or without cracks to obtain stress intensity factors and stresses can be performed using the boundary element module of NASGRO. The software is commercially available.

BRT-CICERO

Electricité de France (EDF) has developed software BRT-CICERO [283] for both deterministic and probabilistic evaluation of pipe wall thinning due to flow accelerated corrosion (FAC). It has been in use in every French NPP unit since 1994.

In the modelling of FAC, the main parameters of influence that are taken into account are: effect of the water chemistry: pH, oxygen, steel composition (Cr, Cu, Mo), influence of mass transfer in single phase flow, influence of temperature and geometry.

BRT-CICERO provides e.g. the following results:

- wear and wear rate of the pipe wall,
- evolution of residual thickness determined from the nominal thickness and the tolerances of the nominal thickness.

The probabilistic computations allow to:

- follow the evolution of the fractiles of the residual thickness distribution as a function of time,
- follow the evolution of the probability that the residual component thickness is less than the critical thickness as a function of time,
- evaluate the residual lifetime of selected component.

The probabilistic module calculates the evolution of the 1E-03 fractile of the residual thickness distribution until it reaches the critical thickness. The probability for thickness being less than critical is evaluated after this. When the 1E-03 fractile estimate appears to be higher than the critical value, plane MCS is applied. If not, MC variance reduction technique is applied. Due to its proprietary nature, a detailed documentation of BRT-CICERO or the code itself are not available for purchase [1].

PROPSE

DNV has developed software PROPSE (PRObabilistic Program for Safety Evaluation) [284] for computation of probability of failure when the NDT/NDE have found/missed a defect in NPP piping system inspections. PROPSE contains two different algorithms to calculate the probability of failure: simple MCS with an error estimate on probability of failure, and application of FORM with sensitivity factors using the most probable point of failure in a standard normal space.

In PROPSE, the following assumptions are made:

- crack depth is assumed as log-normally distributed,
- constant crack aspect ratio is assumed, where a conservative assumption is to use a high value, e.g. 30,
- fracture toughness is assumed as normally distributed,
- material yield strength is assumed as normally distributed, and covariance for tensile strength is assumed to be the same as for the yield stress.

According to PROPSE, the resulting failure probabilities are usually very small for shallow defects in moderately stressed components. This illustrates the general observation that there is a distinct difference, in terms of failure probabilities and risk for core damage, between those components which have an active damage mechanism and those which have not. In PROPSE, failure is predicted when the surface crack reaches a critical condition. Through-wall cracks are not considered in the present program version.

SRRA

SRRA (The Structural Reliability & Risk-Assessment) [285, 242] is an analysis software for assessing pipe component failure probabilities. It is developed by Westinghouse to support piping RI-ISI analyses. Besides pipe components, SRRA is applicable for probabilistic integrity assessment of RPVs and RPV internals.

The SRRA applies PFM approach and MCS to simulate the effect of time dependent degradation mechanisms and infrequent loading events and to derive the probability of piping failure for a variety of failure modes. In SRRA, the user is required to provide best estimate (median) values for various input parameters related to pipe material, geometry, operating conditions, NDE, service stresses and cycles. Each parameter is associated with a statistical distribution and standard deviation which are based on industry data and detailed analyses are not

required to be entered by the user. Similarly, assumptions for initial flaw distributions are built-in to the program based on industry correlations with respect to weld geometry and pre-service inspection.

The SRRA code has the capability to simulate the effect of a variety of time dependant material degradation mechanisms for components of carbon steel and stainless steels. These mechanisms include:

- low-cycle fatigue crack growth of an existing (fabrication) flaw,
- crack growth of an existing flaw due to SCC,
- wall thinning due to material wastage.(e.g. by FAC),
- high-cycle fatigue induced stresses exceeding the fatigue crack threshold.

In each MC simulation trial, the code simulates the effect of the modelled degradation over time and at each time step the pipe stability against rupture is checked with respect to design limiting loading conditions. Design limiting stress input data may also be attributed with a frequency corresponding to the frequency of occurrence of the corresponding loading event, such as earthquake, waterhammer or a pipe break.

SRRA computes the lifetime failure probability for three different failure mode types concerning piping pressure boundary:

- small leak (i.e. through-wall flaw with minor leakage),
- large leak (i.e. a through-wall flaw that leads to leakage beyond a user-defined value),
- full break (i.e. complete severance of the pipe cross-section).

Based on user defined input data for ISI interval and POD model, for the applicable NDE technique SRRA also calculates the (reduced) failure probability, assuming that flaws detected by ISI will be mitigated before failure can occur. By entering best estimate leak detection capability, credit may also be given to the reactor coolant leak detection system in the calculation of large leak and break probabilities. Again, it is assumed that mitigating actions would be taken on a detected through-wall flaw, before such a flaw would develop into a large leak or break.

VISA-II

With VISA-II analysis software [286] developed by Oak Ridge National Laboratory (ORNL), it is possible to assess the failure probability of a PWR RPV under pressurised thermal shock (PTS) conditions.

The VISA II code is divided into two parts to define stress and strength models needed for the following MC analyses. The deterministic part defines the stress model and the probabilistic part defines the strength model. In the first part, a deterministic fracture mechanics analysis is performed for a temperature and pressure transient entered by the software user. This analysis estimates values of crack tip temperatures and applied stress intensity factors for several crack depths. These values are used by the probabilistic analysis performed in the second part. The second part treats flaw depth and fracture toughness of vessel materials as random variables. The sampled values of fracture toughness are compared with the stress intensity factors (estimated in the first part) at a sampled flaw depth to determine crack initiation and growth. The proportion of through wall cracks in a large number of passes through the simulation loop is an estimate of the conditional probability of through-wall cracking (vessel failure).

The VISA II code uses closed form solutions for heat transfer and stress calculations. It uses influence coefficients for calculating applied stress intensity factors. The necessary input data for the deterministic analysis include: (a) pressure and temperature of the reactor coolant as a function of time for a given PTS transient, (b) surface heat transfer coefficient, (c) material properties, and (d) wall thickness and radius of the vessel. Effects of cladding are included in the heat transfer and stress analysis. The software provides a selection of initial crack distributions.

For each pass through the simulation loop, simulated values of initial RT_{NDT}, fluence at the inner wall, flaw (crack) size, flaw location, and copper and nickel contents are selected from their respective distributions. These sampled values are eventually used to determine the fracture toughness. With these values fixed for a given pass, the software performs time history analysis for a given transient. At the end of each time step, the simulated value of the fracture toughness is compared with the applied stress intensity factor at the crack tip. If the fracture toughness is less than the applied stress intensity factor, crack initiation occurs, otherwise, the simulation moves to the next time step. If crack initiation occurs, the crack is extended 0.25 in. and the crack arrest toughness K_{Ia} is simulated. If crack arrest occurs, the simulation moves to the next time step, otherwise the

crack is extended another 0.25 in., and a new value of K_{Ia} is simulated. This process continues until either the crack grows through wall or the transient is completed. The conditional probability of through wall cracks is obtained by dividing the number of simulations (passes) that resulted in through wall cracking by the total number of simulations that were made.

For each time step, the sampled value of fluence at the crack tip is calculated. Then, the value of the shift in RT_{NDT} is calculated using sampled values of copper and nickel and the attenuated fluence. The calculated value of the shift is then added to the sampled initial RT_{NDT} to obtain the adjusted RT_{NDT}, which is used to estimate the simulated fracture toughness. This fracture toughness is compared with the applied stress intensity factor determined in the first part of the analysis.

RR-PRODIGAL

The structural reliability software RR-PRODIGAL [299] by Rolls-Royce consists of the following three program parts: DANCER, ISIBREAK and SNOWBREAK. DANCER and ISIBREAK evaluate the probability of failure of a welded joint, whilst SNOWBREAK evaluates the probability of failure for an area, such as an area of stress concentration, which includes a period of defect initiation prior to crack growth to failure.

The objective of the program DANCER is to simulate the number and size of defects generated during the welding process. Its output is a histogram or frequency plot of the defects that may formate during the normal build of a weld. The program is designed for multi-pass welds only and can handle ‘Single’ and ‘Double Vee’ weld constructions. In the software methodology, both the technical expertise of welding process engineers and mathematical modelling are used to build a model that will simulate the weld manufacture and the errors that lead to different types of defects. The defects that may initiate in weld beads include center cracks, lack of fusion, slag, pores with tails and cracks in heat affected zones. Various welding processes are addressed including submerged metal arc welding. The model simulates the effects of both radiographic and dye penetrant surface inspections. With this methodology, the model attempts to build up, rather than measure, a defect distribution and density for a given type or family of welds [287, 288]. DANCER does not use MCS to obtain the failure probability. Instead, since the failure criteria are deterministic, a conditional probability of failure follows directly from the distributions of Paris-Erdogan

crack growth rate equation parameters. Thus, a set of conditional failures can be determined and hence the distribution of the conditional failure probabilities over the range of initial defects is determined [299].

The first function of ISIBREAK is to utilise the stress input data to estimate the conditional probability of failure for defects of varying size and position within a weld. The conditional probability of failure of a defect is the probability that it will cause failure given that it exists. ISIBREAK then obtains the calculated weld defect distribution from a DANCER file and combines it, using a simple mathematical technique, with the conditional probability of failure to calculate an overall probability of failure for the weld. Of degradation mechanisms, only fatigue induced crack growth is considered, whereas the applied failure criteria are based on procedures in the R6 Method, Rev. 4 [200]. The effect on the probability of failure of one or several in-service inspections (ISI) during the life of a component can also be included to the analyses. It is the task of the software user to enter the PODs as ISIBREAK does not contain POD data.

The SNOWBREAK routine in RR-PRODIGAL is an attempt to estimate the probability of failure from non-weld areas. Its primary use is for areas of stress concentration where defects could initiate at the surface by fatigue and then grow on through the wall of the component. When a defect has initiated, the crack growth to failure follows basically the same procedure as that used in ISIBREAK except that only one conditional situation, that of a 2 mm surface breaking defect, requires analysis. However, one important assumption is that there is a positive correlation between the crack initiation and the crack growth.

PROST

PROST (PRObabilistic STructure Analysis) [300] is a PFM analysis software to evaluate leak and break probabilities of piping systems in nuclear power plants. A graphical user interface supports the necessary data input.

With PROST, leak and break probabilities from pre-existing semi elliptical shaped inner surface cracks driven by cyclic loading conditions (fatigue) can be estimated. The calculation of the subcritical crack growth and the final instability are based on deterministic fracture mechanics principles. The probabilistic nature is determined by the uncertainties of the input data entering the deterministic routines. The deterministic fatigue crack growth rate is calculated by slightly modified Paris-Erdogan equation.

Uncertainties in the data on geometry, material properties and crack size of a given fatigue problem can be considered via different distribution functions. For each parameter the selection possibilities includes the normal, log-normal, weibull and exponential distribution function. The functions can be truncated on request by input of a minimum and maximum value. Additionally, it is possible to consider the parameter to be deterministic with a fixed value.

Two different types of loading conditions are distinguished in PROST. The first are cyclic load sets recurring with user defined frequencies, which are dominant for fatigue problems. The second are stochastic load sets, like seismic events or transients, which occur with user defined probabilities. User defined weld residual stresses can be included as well.

The user can choose if he wants to consider ISI in the computation, which is realised by entering a POD curve. The user can determine the POD curve by specifying ten crack depth values and their corresponding detection probabilities in percent together with the time inspection interval. Internally, this data are used to identify if during an inspection a crack is detected or not.

Two probabilistic computation procedures are available in PROST. The first is the plain MCS. For this method, a combination of the distributed parameters will be selected randomly and the crack propagation for a given time period is computed. The second option is a stratification method based on a variance reduction technique. For this method, the user can select two out of all distributed parameters (usually the crack depth and the crack length to depth aspect ratio) to be integrated.

The regular output file contains the information about all given input parameters including the run time variables. Then for all combinations that fail are listed the actual parameters, failure time, failure mode, crack depth, crack length, stress intensity factors for the maximum and minimum load at deepest and surface point and the combination probability. In a second output file, the accumulated failure probability is given as a function of time. If the stratification method was selected, processed 5 %, 50 % and 95 % failure probability curves as a function of time are given too. The 50 % curve represents the expected failure probability that is equivalent with the results of a MCS run, depending strongly on the mean values of the distribution functions of the input parameters.

11.2 System ageing and risk analysis software

CAFTA

CAFTA is an integrated tool to perform PRA, incorporating linking event tree/fault tree methodology [292]. Using CAFTA one can build, quantify and analyse event tree/fault tree models of considerable size or complexity. CAFTA is developed by Data Systems & Solutions, a joint venture between Rolls-Royce and Science Applications International Corporation (SAIC). Since 1992, Data Systems & Solutions has worked with the Electric Power Research Institute (EPRI) to develop a suite of Windows based PRA/PSA software tools and applications. One result of this effort is CAFTA, which has over 1500 users worldwide [292].

CAFTA includes e.g. the following integrated modules: The Fault Tree Editor for building, analysing and maintaining fault trees, The three level Reliability Database Editor for controlling model data, The Cutset Generator for generating minimal cut sets from the Fault Tree Editor, and The Cutset Editor for viewing probability and structural changes.

SAPHIRE

SAPHIRE (Systems Analysis Programs for Hands-on Integrated Reliability Evaluations) is a software application developed for performing a complete PRA/PSA using a PC. SAPHIRE is developed by the Idaho National Engineering and Environmental Laboratory (INEEL), the funding for which is provided by USNRC [289].

The functions and modules in SAPHIRE include: functions for creating event trees and fault trees, Models And Results Database (MAR-D), System Analysis and Risk Assessment (SARA), Fault Tree, Event Tree and Piping Instrumentation Diagram (FEP) and Graphical Evaluation Module (GEM). Presently, SAPHIRE has been distributed to thousands of users in the U.S.A. and throughout the world. These users include USNRC staff, national laboratories, industry contractors, vendors, utilities, architectural engineering firms, consultants, universities, other government agencies and government contractors [72].

WinNUPRA

WinNUPRA is a self-contained, integrated, PSA/PRA software package for Level 1 PRA/PSA analyses [290]. The WinNUPRA software package is developed by Scientech Inc. and the NUPRA User's Group. WinNUPRA consists of six major analysis modules designed to generate and analyse minimal cut set solutions of various fault trees and cut set equations for accident sequences. Operations are provided for direct solution of fault trees, for their minimum cut sets, and for Boolean manipulation (merging) of cut set equations. WinNUPRA is used in several NPPs and chemical process facilities in the U.S.A. and other countries.

RiskSpectrum PSA

RiskSpectrum PSA [291] developed by Relcon Scandpower Inc. is a fault tree and event tree software tool licensed for use in many NPPs worldwide. The software provides a user interface for modelling from the basic fault tree with AND and OR gates to advanced fault tree and event tree integration of sequences in linked event trees with boundary conditions and common cause failure (CCF) events. The integrated analysis tool is specially designed for solving large PSA models and covers e.g. the following analysis options: minimal cut set, sensitivity, importance and time dependent analysis. The latest program version was released in 2010.

FaultTree+

FaultTree+ is an interactive graphics and analysis software for performing a PRA/PSA using integrated fault tree, event tree and Markov analyses. The software allows analysing large and complex fault and event trees producing the minimal cut representation for fault tree TOP events and event tree consequences. The code is developed by Isograph Inc. [293]. FaultTree+ has been used to perform systems reliability analysis by a wide range of different industries for nearly three decades.

FaultTree+ provides CCF analysis, importance analysis, uncertainty and sensitivity analysis facilities. The program allows constructing a single project database containing generic data and event tables, fault trees with multiple TOP events, event trees originating from different initiating events, CCF tables and consequence tables. Fault tree TOP events may be used to represent specific

columns in the event tree. Multiple branches are also handled to allow for partial failures. Users may feed the end branches of event trees into secondary event trees eliminating the need for the user to reproduce identical event tree structures leading to identical consequences.

AvSim+

AvSim+, also developed by Isograph Inc., provides a MC simulation package for analysing systems availability and reliability problems using fault trees or reliability block diagrams [294].

AvSim+ provides means to construct fault tree or network diagrams (reliability block diagrams) by using drag and drop facilities. When using fault trees, AvSim+ automatically organises the diagram after receiving logical connection data. When using networks, AvSim+ automatically deduces the failure logic of the system after receiving block structure and logical connection data. Once a logical fault tree or network structure is defined one can define failure and maintenance models to represent the performance of components within the system. These models could be simple failure and repair models or they could represent complex dependencies including ageing, spares requirements, labour availability, operational phases, standby arrangements, etc.

Historical data (times to failure and times to repair) are automatically analysed using the Weibull Analysis facility and connected directly through to component failure models. This allows the updating of their historical data records observing the effects on predicted system performance. By allocating safety, environmental and operational consequences to selected system failures one is able to determine the frequency and duration of each type of consequence. Severity values may be assigned to a given consequence allowing safety, environmental and operational criticality values to be determined over the lifetime of the system.

LOGAN Fault and Event Tree Analysis

The LOGAN Fault and Event Tree module is a program developed by Reliass Inc. for the construction, evaluation and printing of fault and event trees and is widely used for quantitative risk assessment [295]. Fault trees can be linked to event trees by specifying a fault tree which calculates a branch probability. If the fault trees contain common events, the effects of the resulting non-independence are accounted for. The system lays out the diagrams automatically.

The fault and event tree capabilities of LOGAN Fault and Event Tree module include: fault/event tree integration, integrated reliability database, print-out in conventional top-down format or LOGAN horizontal format, minimal cut set analysis, various forms of sensitivity analysis, and optimisation of proof test intervals to minimise testing while achieving safety/reliability targets.

Weibull++

Weibull++ 6 software [296] developed by ReliaSoft Corporation allows performing life data analyses utilising multiple lifetime distributions, including all forms of the Weibull distribution and generalised gamma distribution. According to ReliaSoft [296], their software products and services are currently used by hundreds of companies, including e.g. ABB, Siemens and TÜV, with an active reliability engineering program.

The capabilities of the code include analysis of data from various censoring schemes, degradation analysis, warranty analysis, non-parametric analysis and analysis of variance. The Degradation Analysis utility allows extrapolating the failure times of a component based on its performance over a period of time. One can analyse the extrapolated failure times as times-to-failure data. In addition, one can use the competing failure modes analysis option to assign a separate distribution to each failure mode identified in the data set.

CARA-FaultTree

CARA-FaultTree [297], developed presently by ExproSoft, is a tool for fault tree analysis and construction. Performance measures calculated by the code include: unavailability, average availability, survival probability, mean time to failure, frequency of TOP event and failure frequency distribution. Computed component importance measures include: Birnbaum's reliability, Birnbaum's structural, Vesely-Fussell, criticality importance, improvement potential and order of smallest cut-set. Other notable computed results include: importance measures at cut-set level, unavailability at cut-set level and uncertainty analysis.

ITEM ToolKit

ITEM ToolKit software [298] is a suite of prediction and analytical modules developed by Item Software Inc. It uses globally recognised standards and methodologies to analyse components, systems and projects. ITEM ToolKit

allows taking a total system approach in analysing individual systems and components. This allows the optimisation of design targets with respect to component selection, increased safety and reduced liability. One can analyse reliability and availability at the component or system level and view the entire project. The analysis capabilities of the software include: FMECA, computation of unreliability and unavailability, analysis of uncertainty and sensitivity, analysis of CCFs and creation of minimal cut sets. Each of the several modules of the software is designed to analyse and calculate the failure rates of components and systems in accordance with the appropriate standard. According to software developer [298], ITEM ToolKit is widely used throughout the world by companies in defence, aerospace, electronics and other industries.

FinPSA

STUK started to develop living PSA computer code SPSA in 1988. Level 1 part of this code was taken into use in 1991. Since then, the algorithm has been continuously developed, and its efficiency and robustness have been demonstrated in many benchmarks and in practical PSA use. FinPSA is a new version of SPSA for Microsoft Windows [301].

FinPSA is developed for teamwork. PSA models can be shared or private models. Shared models reside in a server, and can be accessed and edited simultaneously by several users. The PSA team can solve minimal cut sets together with several computers utilizing parallel computation.

FinPSA searches for cut sets for each event tree sequence. After the search, the cut sets of individual sequences are automatically combined and grouped according to userdefined hierarchy of consequences. On the top level, FinPSA produces cut set files classified by consequence only. Any number of intermediate levels can be defined.

FinPSA works together with common Windows programs for importing and exporting data base tables, fault trees, events trees, and almost every item in the model. Results are available in several formats to Windows clipboard, printer and files.

Preliminary version of FinPSA level 1 is available. The development of FinPSA will continue with new features like:

- task-oriented model for control systems (from RELVEC code),
- asymmetric common cause failures, additional CCF models,
- level 2 (dynamical containment event trees already implemented in SPSA).

11.3 Summary of ageing and risk analysis software

There exists a large number of software for ageing and risk analysis of systems and components. It would have been way beyond the scope of this thesis to go through all or even most of them. Thus, only some of the most noteworthy examples of these analysis tools are covered in this thesis.

It appears that most of the available ageing degradation analysis tools consider only one or two degradation mechanisms. This is a drawback, as the number of failure mechanisms encountered in NPPs is much greater. Thus, it appears that for the time being several analysis codes are needed if one wishes to cover the degradation of all safety significant NPP systems and components.

Many of the system analysis tools presented in this thesis, e.g. those with fault and event tree analysis capabilities, can be applied within many industries, e.g. nuclear, aerospace, chemical, process and transportation. There exists, however, a number of system analysis tools that are specifically developed for power plant industry purposes. These include e.g. SAPHIRE and PSA Professional.

Probabilistic models that predict rare events cannot be validated by comparing the results to observed failure and degradation data. One way to verify these models to some extent is to benchmark the independently developed models describing the same phenomena against each other. Thus, the main sources of difference can be identified, based on which the models can be developed further. Comparisons of this kind have been made e.g. for the following models [247, 264, 302, 303]:

- SRRA against PRAISE,
- PROPSE against STAR6,
- ProSINTAP against STAR 6,
- NURBIT against WinPRAISE,
- probabilistic VTTBESIT against NURBIT,
- RR-PRODIGAL, ProSACC, PROST and WinPRAISE against each other.

In several cases these comparisons have resulted in identification of errors and model improvements.

12. Probabilistic lifetime analysis application for piping components

12.1 Introduction

Two analysis codes are used in the lifetime analysis application for piping components. The first and obvious one of them is the probabilistic VTTBESIT, developed at VTT, and the second one is PIFRAP, both of which are described in more detail in Chapter 11. With these analysis tools, it is possible to calculate e.g. yearly failure probabilities for the considered piping cross-sections. To allow performing the present computational analyses, the probabilistic VTTBESIT was developed further to some extent. As for PIFRAP, the analysis code version 2.0 rev. 0 published in 1997 is used.

The analyses consist of a set of Monte Carlo simulations with probabilistic VTTBESIT, and of some PIFRAP computations for comparison purposes. The considered degradation mechanism is SCC. All examined pipe cross-sections are similar butt welds. As in the NPP piping components SCC typically occurs as a circumferentially oriented inner surface crack in the heat affected zone (HAZ) adjacent to weld, such postulates are also considered in the present analyses. The examined characteristics in the computations cover e.g. three different initial crack distribution assumptions, three pipe sizes and three considered time spans. The last issue means the service time in years from the start of operation.

12.2 Examined piping components and associated input data

The computational probabilistic analyses are performed for three pipe sizes. These sizes are assumed to correspond to representative small, medium and large pipes in Finnish BWR NPP reactor circuit piping systems, respectively,

and they were provided by expert personnel from TVO [307], which is gratefully acknowledged.

12.2.1 Geometry

The geometry input data concerning all computations are presented in the following. As the considered pipe cross-sections are assumed to be located in straight pipe components, the needed geometry input data are quite limited. The cross-section dimensions of the three pipe component sizes considered in the probabilistic lifetime analyses are presented in Table 12.2-1.

Table 12.2-1. Representative Small, Medium and Large BWR reactor circuit pipe sizes selected for probabilistic lifetime analyses.

Pipe	Outer diameter [mm]	Wall thickness [mm]	Outer radius/wall thickness [-]
Small	60	4.0	7.50
Medium	170	11.0	7.73
Large	510	26.0	9.81

12.2.2 Material properties

The base material of the considered pipe components is assumed to be austenitic stainless steel TP 304, which is a commonly used material type for NPP piping system components. As the material property data of welds are often more difficult to obtain, the commonly used option to assume the material properties of the adjacent base material for the weld material is also applied here. In most cases, this is a conservative assumption, as typically the strength properties of the weld materials are to some extent better than those of the base materials. Material property values for various metallic NPP component materials are taken from Section II of the ASME code [305]. The obtained data are in the form of tables, and presented here for a representative range of temperatures. On the other hand, for the operational temperature of 286 °C of Finnish BWRs the material property values were interpolated, as for that particular temperature the material property values were not given in the ref. [305]. The presented yield strength values correspond to 0.2 % of strain in uniaxial tension test.

Table 12.2-2. Strength properties of type 304 austenitic stainless steel as a function of temperature, see Tables 2a, U and Y1 in Section II of ASME code [305].

Temperature [°C]	Yield strength [MPa]	Design stress [MPa]	Tensile strength [MPa]
20	172	115	483
100	146	115	452
150	132	115	421
200	121	110	406
250	114	103	398
275	111		
286	109	102	397
300	108	98	393

Table 12.2-3. Some mechanical properties of type 304 steel as a function of temperature, see Tables TCD, TE-1 and TM-1 of Part D of Section II of ASME code [305].

Tempera-ture [°C]	Elastic modulus [GPa]	Thermal conductivity [W/m°C]	Specific heat [J/kg°C]	Coefficient of ther-mal expansion [(1/°C)*10 $^{-06}$]
21	195	14.9	484	15.2
38		15.1	486	15.4
66		15.6	496	15.6
93	190	16.1	506	15.8
121		16.6	516	16
149	186	17	520	16.2
177		17.5	529	16.4
204	183	18	535	16.5
232		18.3	539	16.7
260	178	18.9	544	16.9
286	176	19.2	548	17.0
316	174	19.6	551	17.2

The assumed welding type is shielded metal arc welding (SMAW), which is a commonly used method for fabricating NPP piping welds. According to ref. [203], when the base material of the pipe is austenitic stainless steel and temperature is 288 °C, the fracture toughness data for this welding type are: K_{IC} = 182 MPa·√m, J_{IC} = 168 kJ/m^2, and for the base material: K_{IC} > 350 MPa·√m, J_{IC} > 620 kJ/m^2. Table 12.2-4 presents the values of parameters C and n used in the SCC rate equation for the considered austenitic stainless steel (SS) TP 304.

Table 12.2-4. The values of parameters C and n used in the SCC equation for the considered material. The dimensions used in the crack growth equation are: [da/dt] = mm/s, [K_I] = MPa·√m. The dimension of C is [(mm/s)/((MPa·√m)^n)] whereas n is dimensionless.

Material	C	n	Environment	Refs.
SS TP 304	4.5E-12	3.00	water	[308]

12.2.3 Loads and failure mechanisms

The loads considered in the analyses are mechanical and thermal. The crack postulates are assumed to be located in the HAZ, as that region is more susceptible to SCC than the base or weld material. Due to the choice of examined location, the residual stress distribution caused by the welding process must be considered as well. Thus, the considered mechanical loads are operational process pressure, as caused by the water inside pipe components, and residual stress distribution in and near the weld. Thermal loading is also caused by the water inside the pipe components. The outer surfaces of NPP piping components are typically thermally insulated, and for most of the time the temperature outside the insulation is of the scale of room temperature.

Both applied analysis tools, VTTBESIT and PIFRAP, allow considering two degradation mechanisms, which are intergranular SCC (IGSCC) and fatigue (in case of PIFRAP limiting to high cycle vibration). Here, the only considered degradation mechanism is IGSCC. The considered crack growth type is mode I, with corresponding stress intensity factor K_I [MPa√m] as the governing load parameter. As all considered crack postulates are circumferentially oriented and located in the inner surface, only axial stresses are taken into account, i.e. stresses acting perpendicular to crack faces.

Under operational conditions, the values of inner pressure caused by and temperature of the fluid are 7.0 MPa and 286 °C, respectively. The axial membrane

stresses, σ_{AXIAL} [N/mm^2], caused by the inner pressure are computed with the following analytical equation [306]:

$$\sigma_{\mathrm{AXIAL}} = \frac{p(D/2 - t)}{2t} \tag{12.2-1}$$

where p [N/mm^2] is pressure, D [mm] is outer diameter and t [mm] is wall thickness.

The residual stress distributions present in a structure are the result of the manufacturing history and the elastic-plastic properties of the structure. The former referring to the mechanical and thermal processes executed during the whole production sequence and the latter to the elastic-plastic behaviour of the structure. Typically, in NPP piping component welds, the local maximum values of WRSs are of the scale of material yield stress in tension, and local minimum values of the same scale in compression, respectively. Thus, the locally confined WRSs often provide the dominant component to total stress distribution within and near the weld region.

The distributions of the axial WRSs in the weld centre-line and HAZ are assumed according to two commonly applied procedures, namely the ASME recommendations [309, 310] and the SINTAP procedure [311, 312]. These two procedures provide conservatively defined WRS distributions e.g. to NPP piping component welds. When actual WRS measurement data are not available, as is in the present case, handbook WRS distribution assumptions are often used. The WRS distributions could also be simulated more accurately by FEM, but again due to lack of data concerning the actual welding process, this option was not resorted to, as such simulations require input data for a relatively large number of parameters. For Medium and Large pipe sizes, the WRS distributions were assumed according to the SINTAP procedure [311, 312], but for Small pipe size according to the ASME recommendations [309, 310], as the former procedure is limited to cover wall thicknesses from 9 to 84 mm. Mainly, these limits concern ferritic steels, but to ensure that appropriate WRS distributions are applied to the Small pipe size of austenitic stainless steel and with wall thickness of 4.0 mm, the WRS equations in the ASME recommendations [309, 310] were used. The axial stress distributions applied in the probabilistic lifetime analyses of the Small, Medium and Large pipe components are presented in Figures 12.2-1 to 12.2-3. The horizontal axis in all these figures corresponds to radial coordinate through wall with the origin in the inner surface. The dominant role of the WRSs in the total axial stress distributions can clearly be seen in these figures.

In some piping components, thermal expansion can cause thermal stresses. This can happen, when the piping component supports resist thermal expansion. Totally rigid support conditions can cause very high thermal stresses to the piping component. However, mostly the NPP piping components are supported quite flexibly. One potential location for thermal stresses is pipe bends. Due to lack of specific data, no thermal stresses are included in the computations.

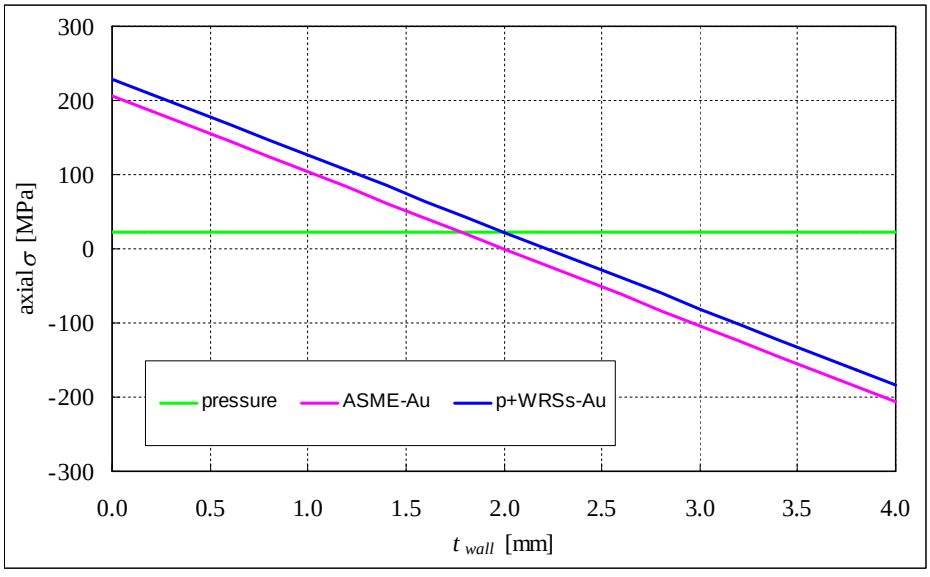

Figure 12.2-1. The axial stress distribution through wall used in the probabilistic lifetime analyses of the Small pipe component. The colours of the curves correspond to: green; stress caused by pressure, light red; WRSs acc. to ASME recommendations, blue; total stress.

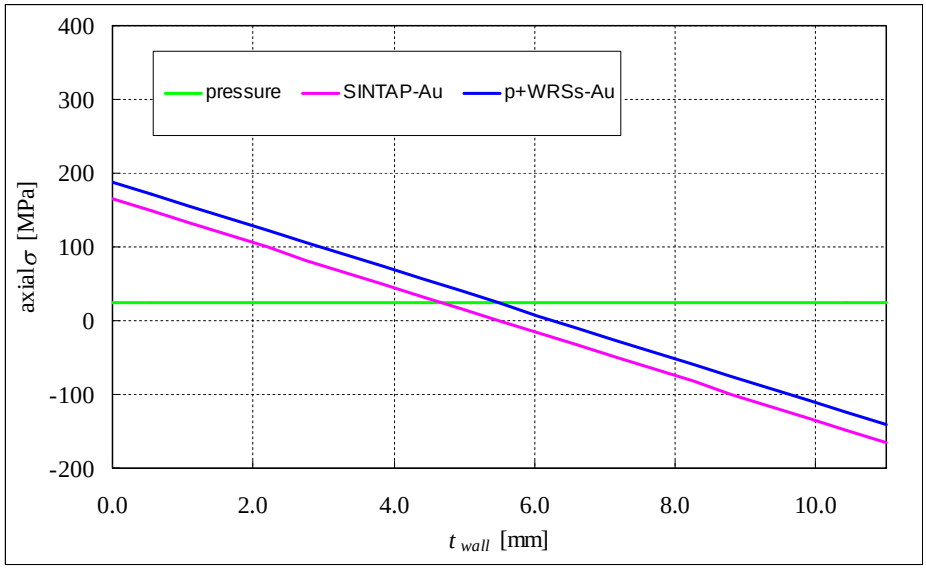

Figure 12.2-2. The axial stress distribution through wall used in the probabilistic lifetime analyses of the Medium pipe component. The colours of the curves correspond to: green; stress caused by pressure, light red; WRSs acc. to SINTAP procedure, blue; total stress.

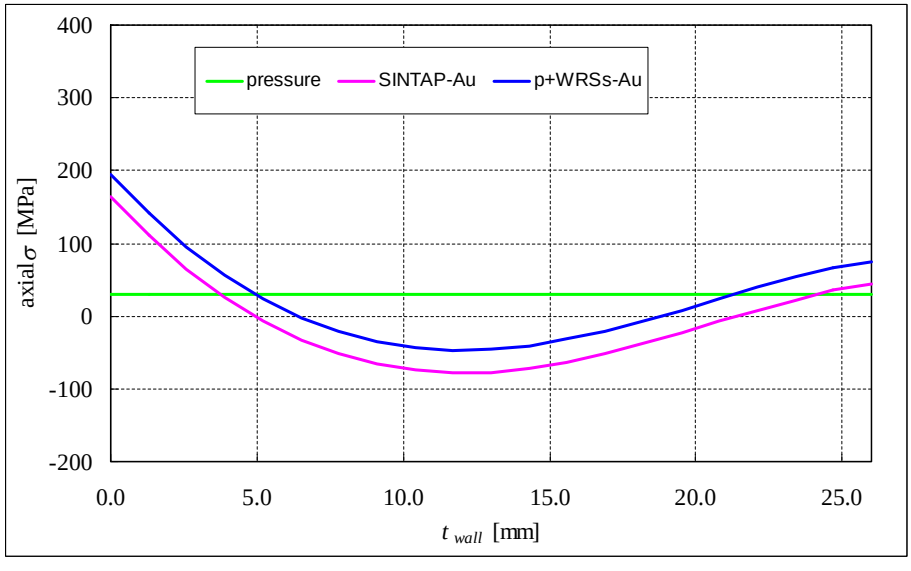

Figure 12.2-3. The axial stress distribution through wall used in the probabilistic lifetime analyses of the Large pipe component. The colours of the curves correspond to: green; stress caused by pressure, light red; WRSs acc. to SINTAP procedure, blue; total stress.

12.2.4 Initial crack size distributions

As mentioned earlier, three different initial crack distribution assumptions are used in the probabilistic analyses. These distributions are briefly described in the following.

Existing fabrication cracks

The assessment of probabilistic distributions for depth and length of the existing fabrication/manufacturing cracks in stainless steel piping used here are from ref. [313] by Khaleel and Simonen. In developing these to some extent conservative distributions, it was assumed that the welds for all pipe sizes used the manual metal arc process and that the welds (except for the 0.25 inch wall thickness) were inspected using radiographic inspection. The initial cracks were circumferential, and were conservatively placed at the inner pipe surface. The semi-elliptical surface cracks had depths between zero and (with a low probability) the full wall thickness. Surface lengths were between a semi-circular shape and (with a low probability) the full pipe circumference. Log-normal distributions were used to characterize the crack depths. The parameters of these log-normal distributions are listed in Table 12.2-5 in the following.

The log-normal distribution equation used in defining depth probabilities, $f_x(x)$, for existing manufacturing cracks in stainless steel piping is [313]:

$$f_x(x) = \frac{1}{\sqrt{2\pi}\sigma_y x} \exp\left[-\frac{\left(\ln x - \mu_y\right)^2}{2\sigma_y^2} \right], \text{ and} \qquad (12.2\text{-}2a)$$

$$\mu_y = \ln \tilde{X} \qquad (12.2\text{-}2b)$$

where x is the variable for which the probability is calculated, σ_y is the shape parameter, μ_y is the scale parameter and $\tilde{X}$ is the median of x.

Table 12.2-5. Parameters for log-normal crack depth probability distribution for existing manufacturing cracks in stainless steel piping, from ref. [313]. For wall thicknesses falling between the presented ones the corresponding parameter values are to be interpolated.

Pipe wall thickness	**Parameters**			
	Median flaw depth	**Shape parameter**	**Flaw density per inch of weld**	**Flaws per weld**
[inch]	[inch]	[-]	[1/inch]	[-]
0.250	0.1063	0.1784	0.0047	0.0440
0.562	0.0991	0.2669	0.0028	0.0480
1.000	0.0892	0.3672	0.0035	0.0960
2.500	0.0555	0.4993	0.0256	2.0508

The probability distribution for lengths of existing manufacturing cracks in stainless steel piping is defined using crack aspect ratio, which is given here as $\beta = b/a$, where b is the total length of the surface crack and a is the crack depth. The probability distribution for aspect ratio β is given by [313]:

$$f_0(\beta) = \begin{cases} 0, & \beta < 1 \\ \dfrac{C_\beta}{\lambda\beta(2\pi)^{1/2}} \exp\left[-\dfrac{1}{2\lambda^2}\left(\dfrac{\ln\beta}{\beta_m} \right)^2 \right], & \beta \geq 1 \end{cases} \qquad \text{(12.2-2c)}$$

where $\lambda = 0.5382$, $C_\beta = 1.419$, and $\beta_m = 1.136$. This aspect ratio distribution was assumed to be independent of the flaw depth.

SCC induced initial cracks in VTTBESIT

The assessment of probabilistic distributions for depth and length of SCC induced initial cracks in stainless steel piping used here are from ref. [245] by Cronvall et al. The development of these distributions was based on the flaw data from nine Swedish BWR units, see ref. [304]. This data consists of 98 detected SCC cases, all of which are circumferentially oriented cracks at the inner pipe surfaces. In the assessment of probabilistic distributions for initial crack sizes, not all of the above mentioned 98 crack cases were considered, which may affect the applicability of these distributions for the present analyses to some extent.

The fitted exponential probabilistic density functions for estimated depth and length distributions of SCC induced initial cracks are presented as probability density against relative crack dimension in Figure 12.2-4.

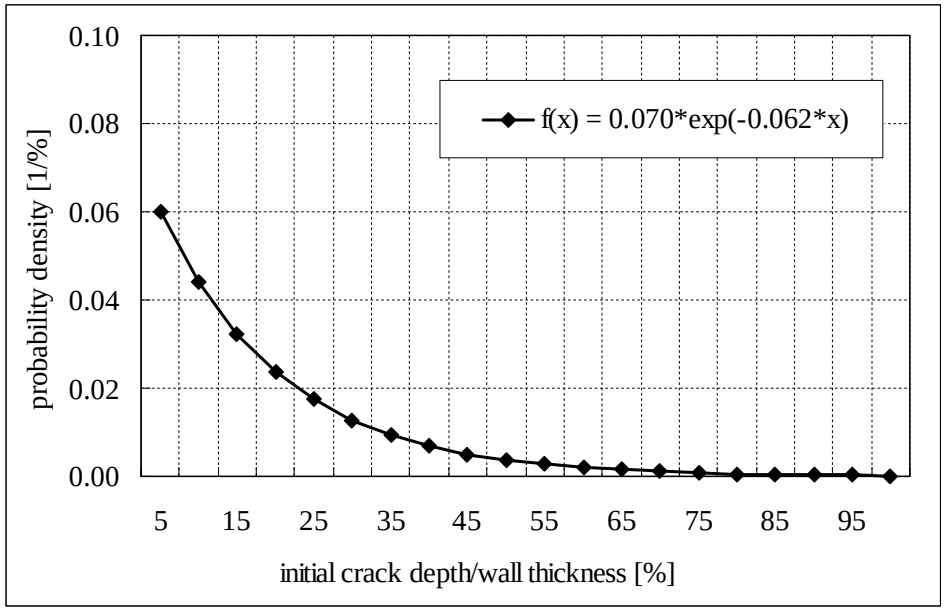

Figure 12.2-4a. The fitted exponential probabilistic density function for estimated depth distribution of SCC induced initial cracks, from ref. [245]. In the legend “f” stands for probability density and “x” for relative initial crack depth.

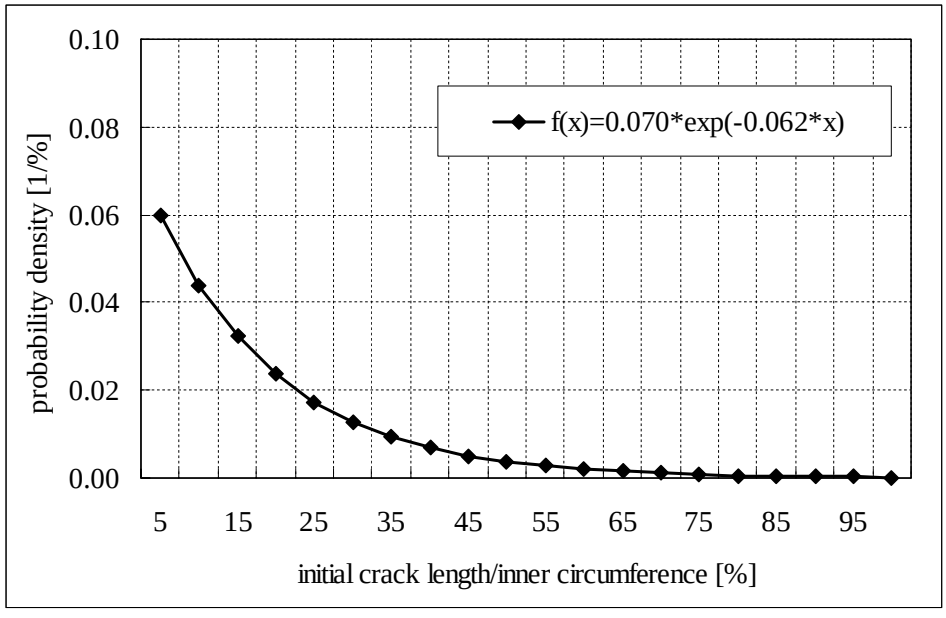

Figure 12.2-4b. The fitted exponential probabilistic density function for estimated length distribution of SCC induced initial cracks, from ref. [245]. In the legend "f" stands for probability density and "x" for relative initial crack length.

SCC induced initial cracks in PIFRAP

The assessment of probabilistic distributions for depth and length of SCC induced initial cracks in stainless steel piping used in PIFRAP is based on the same flaw data from the nine Swedish BWR units [304], as the above described distributions developed by Cronvall et al. [245].

In PIFRAP, the depth for SCC induced initial cracks in stainless steel piping is assumed to be fixed to 1.0 mm. For developing a distribution for initial crack lengths, the original data of detected cracks were first modified so as to better correspond to assumed initial sizes. This treatment was such that the measured length of each detected crack was reduced two times the distraction of the measured crack depth and 1.0 mm. A truncated exponential function was fitted to thus obtained modified set of crack lengths.

12.3 Analysis characteristics

The scope of the probabilistic analyses is described below. This is followed by some relevant details concerning the analysis flow of the two applied analysis codes, probabilistic VTTBESIT and PIFRAP.

12.3.1 Scope of probabilistic analyses

The scope of the probabilistic analyses with VTTBESIT:

- considered pipe sizes; the earlier described Small, Medium and Large pipe components,
- considered initial crack size distributions; fabrication cracks from ref. [313] and SCC induced cracks from ref. [245], i.e. altogether two different distributions for both initial crack depth and length,
- considered crack depths in relation to wall thickness; 25 %, 50 %, 75 % and 100 %, the last one corresponding to pipe failure,
- considered time spans from the start of operation; 20 years, 40 years and 60 years,
- thus the scope of analyses is all in all 72 computed probabilities.

The scope of the probabilistic analyses with PIFRAP:

- considered pipe sizes; the earlier described Small, Medium and Large pipe components,
- considered initial crack size distributions; SCC induced cracks from ref. [304],
- considered crack depths in relation to wall thickness; 100 %, as corresponding to pipe failure, note that with PIFRAP version 2.0 rev. 0 it is not possible to compute probabilities for cracks with depth less than 100 %,
- considered time spans from the start of operation; 20 years, 40 years and 60 years,
- thus the scope of analyses is all in all 9 computed probabilities.

The effect of periodic pipe component inspections is not considered here. However, both applied analysis codes do allow the inclusion of inspections, which are typically performed in NPPs yearly. The probability of detecting a crack in inspections is dependent of its size, so that the larger it is the more probable is its detection. Typically, crack detection probabilities are assessed with POD functions, as mentioned earlier. In all analysed cases the operational lifetime was assumed to be 60 years.

12.3.2 Details concerning the analysis flow of the two applied analysis codes

Details concerning the analysis flow of probabilistic VTTBESIT

The probabilistic VTTBESIT calculates the probability of failure for a loaded pipe with circumferential or axial cracks that may propagate due to SCC or low/high-cycle fatigue. Failure is taken to mean the event when the crack postulate has grown to just reach the opposite surface of the pipe component, most often the outer surface. Account is taken to the probability that the crack remains undetected during successive inspections. As mentioned above, inspections are not taken into account here. The theory and procedure behind the probabilistic VTTBESIT are given in refs. [246, 247].

The following assumptions are made for the probabilistic analyses [246, 247]:

- for SCC analyses the stresses are assumed to be deterministic, for fatigue induced crack growth analyses their cyclic frequency of occurrence is assumed as Poisson distributed,
- the crack growth equation and its parameters are assumed to be deterministic,
- both depth and length of initial crack postulates are assumed to be random with exponential probability density functions.

Due to these assumptions, the growth of the crack due to SCC will be deterministic and will only depend on the initial crack depth and length for a given geometry and given stresses.

As mentioned earlier, to allow performing the computational analyses the probabilistic VTTBESIT was developed further to some extent. More precisely, the possibility to compute the probabilities for growing crack postulate to reach the depths of 25 %, 50 % and 75 % of wall thickness were is to the analysis code.

The basic failure probability equation of VTTBESIT can be expressed as:

$$p_{FS,i,tj}(t) = \frac{N(a \geq a_{FS,i})}{N} f_{i0} \qquad (12.3\text{-}1)$$

where $p_{FS,i,tj}(t)$ [-] is failure probability corresponding to selected degradation/failure state, t [years] is time, $N(a \geq a_{FS,i})$ [-] is the number of times the Monte Carlo simulations have reached or exceeded the selected degradation/failure state in terms of crack depth a [mm], N [-] is the total number of Monte Carlo simulations, and f_{i0} [-] is the rate of crack initiation due to SCC.

The rate of crack initiation due to SCC, f_{i0}, was here based on the mentioned Swedish IGSCC data with the value of this parameter being 4.08E-04, see ref. [304].

In order to be on the safe side, the fracture toughness properties used in the analyses were those of the weld material. Other used material properties were those of the base material.

Details concerning the analysis flow of probabilistic PIFRAP

PIFRAP calculates the probability of failure for a loaded pipe with circumferential cracks that may propagate due to IGSCC or IGSCC in combination with high cycle fatigue, water hammer loads, seismic loads etc. Failure is taken to mean a complete break due to J –integral controlled fracture or plastic collapse. The value of the J-integral is calculated according to the R6 procedure. Account is taken to the probability that the crack remains undetected during successive inspections. As mentioned above, inspections are not taken into account. The theory and procedure behind PIFRAP are given in reference [315].

The following assumptions are made here for the probabilistic analyses [304]:

- the stresses are assumed to be deterministic,
- the crack growth law and its parameters are assumed to be deterministic,
- the initial crack depth is assumed to be fixed to 1.0 mm,
- the probability that a crack with the assumed depth is initiated during the time interval (t_i, $t_i + dt$) is given by the function $f_i(t_i)dt$.

Due to these assumptions, the growth of the crack will be deterministic and will only depend on the initial crack length for a given geometry and given stresses. The growth of the above mentioned crack postulate is calculated with the procedure presented in ref. [248].

The failure probability equation of PIFRAP can be expressed as [304]:

$$p_f(t,T) = \int_{l_c}^{2\pi R_i} p_{f0}(t,T,l_0) f_{al}(l_0) dl_0 \qquad (12.3\text{-}2)$$

where t [years] is time, T [years] is service life, p_{f0} [-] is conditional probability of rupture given the initial crack length l_0. The lower length limit l_c [mm] is the solution of the equation $t_F(l_c) = T$, where t_F [years] is time of rupture. Finally, p_f is divided by the time (T - t), i.e. p_f represents the probability for a rupture, measured per reactor year as a mean value for the remaining operating time of the plant.

In order to be on the safe side, the fracture toughness properties used in the analyses were those of the weld material, and the rest of the material properties used were those of the base material. The authors of the program use the same approach in ref. [304].

12.3.3 Sub-critical crack growth

In the sub-critical crack growth analyses, the propagation of an initial surface crack through the pipe wall is assessed.

In both the probabilistic and deterministic modules of VTTBESIT, the fracture mechanics based crack growth rate equation used in the simulations depicting the intermediate (stage 2) SCC, as obtained from refs. [136, 314], is:

$$\frac{da}{dt} = CK_I^{\,n} \qquad (12.3\text{-}3)$$

which was presented earlier in Section 7.3.2. Values for these constants are presented in Section 12.2.2.

In PIFRAP the crack growth calculations are performed by the PC program LBBPIPE, which is a program for leak-before-break analysis of circumferential cracks in pipes subjected to IGSCC or fatigue. LBBPIPE estimates the growth of an initial surface crack through the pipe wall to leakage, and from that point the growth of a through thickness crack to final failure of the pipe. Crack opening areas and mass leak rates are also calculated for the leaking crack.

The crack growth rate concerning IGSCC can be defined in two ways. The first way is by providing the crack growth rate equation coefficients. The crack growth rate equation used in PIFRAP is [304]:

$$\frac{da}{dt} = C_0\left(K_I - C_1\right)^n \tag{12.3-4}$$

where the input data parameters are otherwise the same as in equation (12.3-3), with the value of additional parameter C_1 being here zero, i.e. no threshold for propagation of SCC is considered. Thus here, equation (12.3-4) is upon application the same as equation (12.3-3).

The rate of crack initiation due to SCC, f_{i0}, is the earlier mentioned 4.08E-04 [304].

12.4 Results and discussion

The numerical results from the probabilistic VTTBESIT and PIFRAP analyses for to the considered three pipe sizes are presented in the following, see Tables 12.4-1 and 12.4-2 as well as Figures 12.4-1 and 12.4-2. As mentioned earlier, the assumed operational lifetime is 60 years.

Table 12.4-1. The results from the probabilistic SCC analyses with VTTBESIT for pipe sizes Small, Medium and Large with initial crack size distribution as fabrication cracks.

Time from start of operation [years]	**Reached crack depth through wall [%]**	**Probability; Small pipe [1/year/weld]**	**Probability; Medium pipe [1/year/weld]**	**Probability; Large pipe [1/year/weld]**
20	25	4.08E-04	3.36E-04	1.22E-06
20	50	4.05E-04	2.53E-05	0.00E+00
20	75	1.15E-04	1.02E-06	0.00E+00
20	100	0.00E+00	0.00E+00	0.00E+00
40	25	4.08E-04	3.86E-04	9.34E-06
40	50	4.07E-04	8.41E-05	0.00E+00
40	75	1.22E-04	5.67E-06	0.00E+00
40	100	0.00E+00	0.00E+00	0.00E+00
60	25	4.08E-04	4.01E-04	2.63E-05
60	50	4.07E-04	1.34E-04	0.00E+00
60	75	1.27E-04	1.18E-05	0.00E+00
60	100	0.00E+00	0.00E+00	0.00E+00

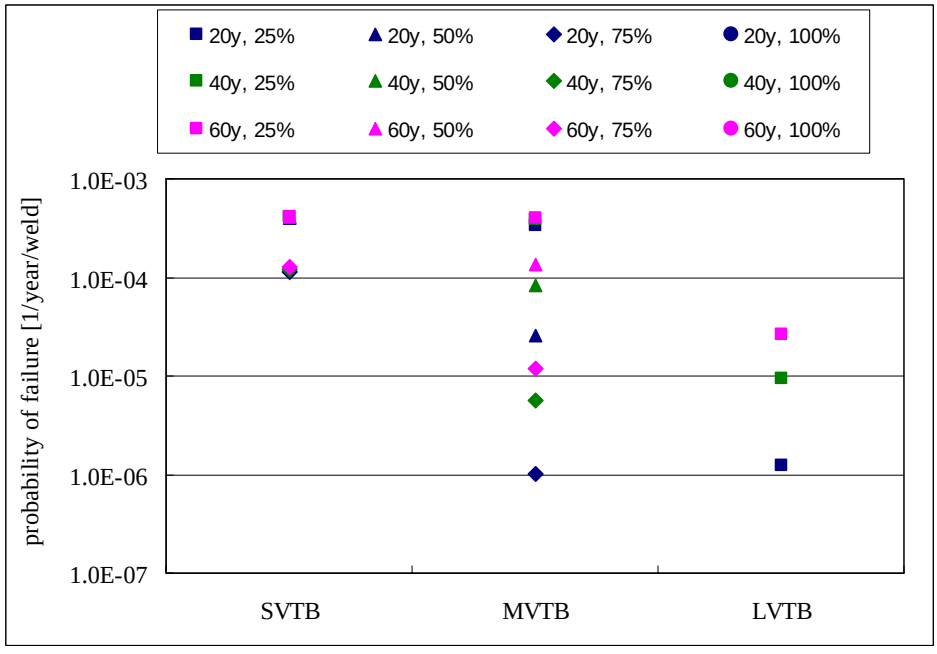

Figure 12.4-1. The results from the probabilistic SCC analyses with VTTBESIT for pipe sizes Small, Medium and Large with initial crack size distribution as fabrication cracks. Here SVTB, MVTB and LVTB correspond to Small, Medium and Large pipe sizes.

Table 12.4-2. The results from the probabilistic SCC analyses with VTTBESIT for pipe sizes Small, Medium and Large with initial crack size distribution as SCC induced initial cracks.

Time from start of operation [years]	Reached crack depth through wall [%]	Probability; Small pipe [1/year/weld]	Probability; Medium pipe [1/year/weld]	Probability; Large pipe [1/year/weld]
20	25	3.65E-04	3.61E-04	3.23E-04
20	50	3.41E-04	3.37E-04	1.95E-05
20	75	3.02E-04	3.02E-04	3.43E-06
20	100	2.19E-04	2.28E-04	6.53E-07
40	25	3.91E-04	3.90E-04	3.87E-04
40	50	3.80E-04	3.79E-04	2.56E-05
40	75	3.56E-04	3.58E-04	3.67E-06
40	100	2.82E-04	2.94E-04	1.18E-06
60	25	3.98E-04	3.97E-04	3.97E-04
60	50	3.89E-04	3.89E-04	1.75E-04
60	75	3.69E-04	3.71E-04	4.04E-06
60	100	2.82E-04	2.94E-04	1.22E-06

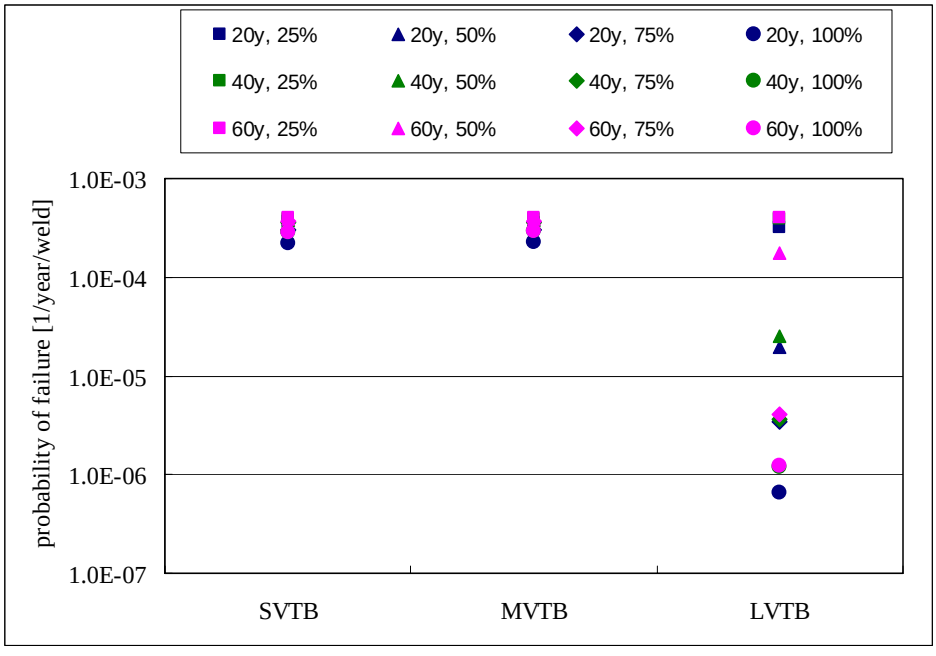

Figure 12.4-2. The results from the probabilistic SCC analyses with VTTBESIT for pipe sizes Small, Medium and Large with initial crack size distribution as SCC induced initial cracks. Here SVTB, MVTB and LVTB correspond to Small, Medium and Large pipe sizes.

The results from the probabilistic SCC analyses with PIFRAP for pipe sizes Small, Medium and Large with initial crack size distribution as SCC induced initial cracks [304] are presented in Table 12.4-3, as well as in Figure 12.4-3. As mentioned earlier, the assumed operational lifetime is 60 years.

Table 12.4-3. The results from the probabilistic SCC analyses with PIFRAP for pipe sizes Small, Medium and Large with initial crack size distribution as SCC induced initial cracks [304]. Note that with PIFRAP version 2.0 rev. 0 it is not possible to compute probabilities for cracks with depth less than 100 % of wall thickness.

Time from start of operation [years]	**Reached crack depth through wall [%]**	**Probability; Small pipe [1/year/weld]**	**Probability; Medium pipe [1/year/weld]**	**Probability; Large pipe [1/year/weld]**
20	100	1.84E-04	2.50E-04	3.01E-04
40	100	2.26E-05	3.19E-05	3.33E-05
60	100	0.00E+00	0.00E+00	0.00E+00

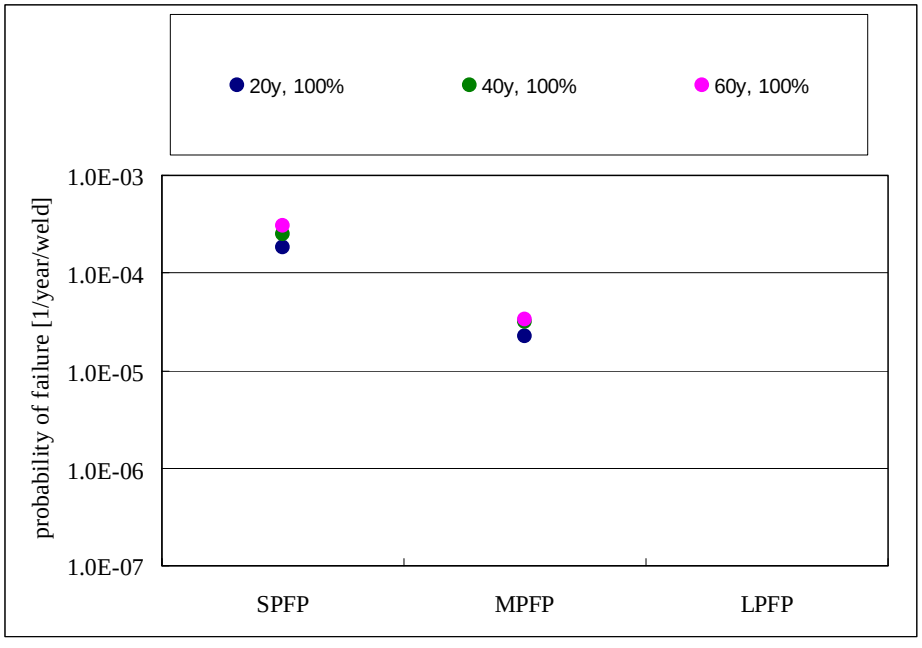

Figure 12.4-3. The results from the probabilistic SCC analyses with PIFRAP for pipe sizes Small, Medium and Large with initial crack size distribution as SCC induced initial cracks [304]. Here SPFP, MPFP and LPFP correspond to Small, Medium and Large pipe sizes.

As for the analysis result diagrams, the scaling of them has been selected so that most of the results could be included visibly enough together with the associated scatter. As the scaling of the vertical axis in the diagrams is logarithmic, the cases with result value of zero are not included in them, however these and all other result cases can be found in the corresponding result tables.

As for SCC analysis results obtained with probabilistic VTTBESIT, in some cases, there was notable variation in the results, whereas in others they were quite conformable. Within the considered time spans of 20, 40 and 60 years, the probability to reach 25 % of wall thickness was greater than zero in all cases, varying approximately between 10E-06 to 10E-04. Concerning fabrication cracks, in case of Small and Medium pipe sizes the probabilities for crack postulates to reach 50 and 75 % of wall thickness varied approximately between 10E-06 to 10E-04, whereas for Large pipe size these probabilities were zero. Concerning SCC induced initial cracks, for all pipe sizes the probabilities for crack postulates to reach 50 and 75 % of wall thickness was greater than zero, varying

again approximately between 10E-06 to 10E-04, however with the mean value being to some extent smaller than that corresponding to probability to reach 25 % of wall thickness. Concerning fabrication cracks, for all pipe sizes the probability for crack postulates to reach 100 % of wall thickness was zero, whereas concerning SCC induced initial cracks this probability varied for all pipe sizes approximately between 10E-07 to 10E-04. Concerning both fabrication cracks and SCC induced initial cracks, the maximum probability for crack postulates to reach 100 % of wall thickness within the considered time spans of 20, 40 and 60 years was 2.94E-04, whereas the corresponding minimum probability value was zero.

As for SCC analysis results obtained with PIFRAP, they were in all cases quite conformable as compared to VTTBESIT results. As mentioned earlier, with PIFRAP version 2.0 rev. 0 it is not possible to compute probabilities for cracks with depth less than 100 % of wall thickness. Within the time spans of 20 and 40 years, in all cases the probability for SCC induced initial cracks to reach 100 % of wall thickness was greater than zero, varying approximately between 10E-05 to 10E-04. However, for the time span of 60 years this probability was in all cases zero. The maximum probability for crack postulates to reach 100 % of wall thickness within the considered time spans of 20, 40 and 60 years was 3.01E-04, whereas the corresponding minimum probability value was zero.

When concerning the effect of pipe size to VTTBESIT results, the outer diameter plays no role in them, as only the wall thickness matters here. From the results it can be seen, that the higher the total tensile stress, the higher the failure probabilities. As in all cases here the tensile stresses are at maximum in the inner surface, and consequently the initial crack postulates that all open to that surface are prone to propagation. The most severe total stress distribution is associated with the Small pipe size, which consequently leads to the highest crack growth and failure probability results. Here the cases with fabrication cracks and SCC induced initial cracks lead to quite matching probability results, those remaining within the range from 10E-04 to 10E-03. However, for Medium and Large pipe sizes, there are notable differences between the probability result sets concerning fabrication cracks and SCC induced initial cracks. With fabrication cracks the scatter of probability results is of several decades for these pipe sizes, whereas with SCC induced initial cracks they are considerably more conformable. Further, with fabrication cracks the probability results are for these pipe sizes in general lower than with SCC induced initial cracks. This difference is explained by initial depth of fabrication cracks being limited on average to approximately

2.5 mm, whereas the SCC induced initial cracks can be deeper than that (with a small probability), and with larger wall thicknesses this limitation leads to comparably lower crack growth and failure probabilities.

Similar effects as those described for VTTBESIT results above can be recognized also in the corresponding PIFRAP results. Namely, again in case of the Small pipe size, being associated with the most severe total stress distribution, the resulting failure probabilities are highest. The Medium pipe size cases result with the second highest failure probabilities, and the Large pipe size cases with the lowest failure probabilities, respectively.

Not only the maximum total tensile stresses through wall affect the crack growth and failure probabilities, but the shapes of through wall stress distributions need to be considered as well. Namely, for the Small and Medium pipe sizes the shape of the total stress distribution is linear, whereas that for the Large pipe size is non-linear. In both stress distribution shape cases, there are regions both in tension and in compression. This is obviously realistic, as the dominant stress component, being WRSs, has to be self-balancing in the axial direction. The nearer to the inner surface the total stress distribution turns from tension to compression, the slower is the ensuing crack growth. For the Small and Medium pipe sizes, this turning point is approximately in the middle of the wall, whereas for the Large pipe size it is approximately 25 % from the inner surface. This partly explains why in case of this latter pipe size the resulting failure probabilities are also the lowest.

The analysis results obtained with probabilistic VTTBESIT are more scattered than those obtained with PIFRAP. This can be mainly attributed to the differences in the used initial crack assumptions, all being in the form of probabilistic density functions. Namely, concerning probability against size, the distribution of SCC induced initial cracks in PIFRAP falls mostly somewhere between the distributions of fabrication cracks and SCC induced initial cracks in VTTBESIT. This is reflected in the results so that the failure probabilities obtained with PIFRAP reside mainly between those obtained by VTTBESIT. It could be assumed that with exactly same initial crack distributions these two codes will provide quite accurately matching results for the same set of analysis cases.

All in all, the thicker the pipe wall, the generally less severe the WRSs are and consequently also the total stress distribution. In the light of the obtained probabilistic SCC analysis results, this leads to lower failure probabilities for pipe components with thicker walls.

The presented probabilistic results are supposed to be conservative, due to the assumptions made with input data. As the actual WRS distributions were not available, the to some extent conservative distributions given in refs. [309, 310, 311, 312] were used. As the material property data of the weld material were not available, those of the base material were used, and typically the strength properties of the materials of the latter type are lower than those of the former. Moreover, the material strength data of the base material were obtained from a normative ref. [305], where the given values are invariably lower than those obtained from the actual material test result data, which in this case were not available either.

As or more significant than looking at single pipe failure probability values, is to compare these values against each other. This viewpoint also serves the needs of RI-ISI analyses for NPP piping systems. The formation of component groups according to risk level in RI-ISI is preceded by formation of component groups according to failure probability and failure consequences.

Some characteristics of both probabilistic VTTBESIT and PIFRAP as modelling tools are discussed in the following. It is a drawback that quite few input data parameters are allowed to be random, those being for VTTBESIT the depth and length of initial cracks as well as frequency of occurrence of cyclic loads, and for PIFRAP only the length of the initial cracks. These are features which cannot be changed or modified by the program user. However, the values of many material properties are distributed and therefore a single value cannot correctly describe them. For instance, fracture toughness is a distributed parameter. The inclusion of realistic load histories consisting of typical NPP load transients of various types is possible with VTTBESIT but is not with PIFRAP. Neither VTTBESIT nor PIFRAP do allow considering a change in water chemistry during a single analysis run, as both codes accept only constant values for SCC equation parameters. As a single analysis typically covers several decades of plant operation, this limitation unrealistically does not allow taking into account the improvements of water chemistry carried out in many NPPs, e.g. when SCC has been detected after some number of years in operation. The advantages of both VTTBESIT and PIFRAP include relatively short analysis run times, due to which it is easy to perform sensitivity analyses. Further, the inclusion of physical models is another advantage of both VTTBESIT and PIFRAP. Compared to purely statistical modelling tools, which completely omit the modelling of physical degradation phenomena, the PFM approach of VTTBESIT and PIFRAP describes much more realistically component degradation.

In the light of the discussion above concerning the scope and characteristics of VTTBESIT and PIFRAP, the probabilistic analysis results presented in this section are at least to some extent suggestive. Arguably, the best use of the single result values can be achieved by comparing them against each other, which would give the quantified order of proneness to degradation/failure. More precisely, this would provide for considered single failure probabilities such interpretation as how many times more/less a particular pipe weld is prone to fail than the others. All in all, in order to achieve more accurate/realistic analysis results, the shortcomings concerning input data and analysis scope of these two analysis codes should be improved.

13. Summary and suggestions for future research

Lifetime analyses of structural systems and components are discussed in this thesis. These analyses necessitate a thorough knowledge of structural properties, loads, the relevant ageing mechanisms and prevailing environmental conditions. In general, the nature of ageing models of structural systems and components can be deterministic, probabilistic or a combination of these two types. Ageing models of all these kinds are presented. When the resulting failure probabilities from probabilistic analyses are combined with knowledge of system or component failure consequences, it is also possible to perform a risk analysis. In practise, the ageing analyses are usually performed with a suitable analysis tool, i.e. with analysis software. A selection of probabilistic system and component ageing and risk analysis tools together with an application example are also presented in this thesis.

The power plant components have generally substantial safety margins when properly designed and constructed. However, the available margins for degraded structures are not well known. In addition, age related degradation may affect the dynamic properties, structural response, structural resistance/capacity, failure mode and location of failure initiation. A better understanding of the effect of ageing degradation on structures and components, especially passive components, is needed to ensure that the current licensing basis is maintained under all loading conditions [10]. Ageing degradation can be observed in a variety of changes in physical properties of metals, concrete and other materials in a power plant. These materials may undergo changes in their dimensions, ductility, fatigue capacity, mechanical or dielectric strength. Ageing degradation presents itself as a variety of ageing mechanisms, physical or chemical processes such as fatigue, cracking, embrittlement, wear, erosion, corrosion and oxidation. These ageing mechanisms act on components due to a challenging environment with high heat and pressure, radiation, reactive chemicals and synergistic effects [5].

Both physical and probabilistic ageing models for power plant components are presented in the thesis. Component ageing analyses are discussed as well. In the top level they consist of selecting components for analyses, identification of ageing mechanisms and mitigation of ageing effects.

Concerning structural as well as risk analysis methods for power plant components, those presented and discussed in this thesis include:

- deterministic analysis methods,
- probabilistic analysis methods,
- risk analysis methods,
- deterministic degradation modelling methods,
- probabilistic degradation modelling methods,
- ageing and risk analysis applications,
- conduct and process of ageing degradation analyses.

As for structural and risk analysis applications, the emphasis here is on the component analysis tools. Some of the presented tools are capable for analyses of both individual components and systems comprising several components. In the general applications, any failure mode, fracture or other, can be addressed using the appropriate limit states. Validation of such software is usually carried out by benchmark exercises between different programs since it is not feasible to compare results with real failure statistics due to their scarcity. The probabilistic analysis approaches of the presented software vary from FORM and SORM to MCS. Some of the presented analysis tools are commercially available and others are proprietary.

Presently, RI-ISI is a very topical subject in Finland, because the Finnish Radiation and Nuclear Safety Authority (STUK) now requires RI-ISI analyses for all piping systems of both existing and planned/future NPPs [316]. Keeping this in mind, it has been attempted to cover RI-ISI here from a number of viewpoints to get a wider description of this subject. The RI-ISI associated issues considered in this thesis include:

- introduction and basics of RI-ISI,
- principles of RI-ISI,
- process of risk-informed inspection planning,
- qualitative, quantitative and semi-quantitative methods for RI-ISI,
- RI-ISI approach developments by VTT,
- brief overview and comparison of three main RI-ISI methodologies, and
- benchmarking of RI-ISI methodologies in the recent RISMET project.

The computational application part of this thesis concerns probabilistic failure and lifetime analyses to a relatively small but representative set of NPP piping components. In addition to data concerning structural properties, primary and secondary loads, supports and environment, also data concerning relevant degradation mechanisms and failure modes are needed. Essential sources for piping degradation and failure data are international and plant specific databases. In the probabilistic failure analysis computations, two analysis codes were used, those being probabilistic VTTBESIT developed by VTT and IWM, and PIFRAP developed by DNV. The matching of the obtained analysis results is at least good. The main source causing in some cases deviations in the results is the differences and limitations in the treatment of input data parameters, whereas the applied PFM analysis procedures are quite similar.

All in all, lifetime and risk analyses of power plant components and systems are disciplines that require combined knowledge from several fields of science. These include structural mechanics, fracture mechanics, probability mathematics, and material science. As lifetime and risk analysis procedures are in a developing stage, there are many aspects and features that call for further research.

Some drawbacks and concerns of risk assessment that would need further research/development are presented in the following:

- model uncertainty,
- the sensitivity of the tails of the failure probability distributions,
- the knowledge that is represented by data based on too few statistics,
- the small failure probabilities for some components mean that evaluated failure probabilities cannot be properly and completely validated,
- in risk analyses, quantities are omitted either intentionally, e.g. human errors, or unintentionally because of a lack of data, or full understanding of the system.

Incorporation of unavoidable ageing effects of SSCs into PRAs/PSAs is a subject that would benefit from further research/development. In a fairly recent and thorough study [1], it was attempted to apply linear ageing failure rate model to incorporate ageing effects into PRA/ PSA. The results showed that this task is cumbersome, and not all questions were answered. Living PRA/PSA is one way with which problems related to time dependent ageing can be approached. However, as a living modification PRA/PSA is simply just updated as necessary to

reflect the current design and operational features, it does not have the capability to predict how time dependent SSC ageing affects failure probabilities and risk.

The advantage of PFM is the possibility of modelling clearly the uncertainties related to the structural degradation process, and thus being able to perform sensitivity analyses for the factors affecting this process. However, there are still methodological problems and there is no standard format for how to perform PFM analyses. This is a problem that can be overcome through the development of computational procedures. Concerning this issue, ENIQ has quite recently published a notable report [317] on ensuring the applicability of PFM and other structural reliability approaches. This report summarises the verification and validation requirements that structural reliability models and associated analysis codes should satisfy in order to be suitable for such purposes. As for PRA/PSA approach, it has been used extensively to analyse entire complex systems in nuclear industry and elsewhere. PFM has had a more limited area of application and has been used for more specialised purposes concerning certain single components e.g. in primary systems of NPPs. Since both techniques have the same goal, a better utilisation of them could potentially be beneficial. A difference between PFM and PRA/PSA that causes difficulties is on which level the input data are based on actual observations. It is highly desirable to obtain standardised methods for PFM analyses like the one that has been developed for PRA/PSA. While PFM procedures lack standardisation, any comparison between components that have been analysed with different methods will be at least to some extent questionable.

Even though most degradation phenomena are quite well known, there are still degradation phenomena the physical mechanisms of which are not clear. An example of such degradation phenomena is SCC. These degradation phenomena need further research.

Through improved knowledge of various degradation phenomena, more accurate models of them can be formulated. In general, physical degradation models need development in many areas, which include scope, range of validity, accuracy and realistic consideration of the underlying physical phenomenon or phenomena.

For instance, the considerably high level of conservatism in the current SCC propagation computation approaches could be relieved. This could include further developing the computation procedures as well as providing more realistic estimates for certain model input parameters. Namely, the strictness in the upper bound approach used in the treatment of the underlying data concerning experimentally defined model parameters characterising environment and material as

well as WRS distributions could be to some extent relaxed. The aim would be to obtain a reasonably conservative SCC propagation computation approach.

Another topical example is the environmental fatigue correction factor approach, i.e. the Fen procedure [184]. The approaches to compute strain rates, combine load transients to cycles as well as to select and treat strain and stress components should be clarified. Presently, the scope and accuracy of this approach is not sufficient for application concerning NPP environments.

Often, modelling problems are caused by scarce and unreliable input data. One problem that would also benefit from further research is the modelling of several degradation phenomena acting simultaneously. Statistical ageing models of SSCs are not hampered by the above mentioned problems. On the other hand, since statistical ageing methods omit the modelling of the underlying physical phenomenon or phenomena, their applicability is limited.

Improved degradation models would also be beneficial from the viewpoint of RI-ISI. With more accurate and realistic degradation models, more reliable failure probabilities could be calculated. These results could in turn be used to perform a more accurate quantitative risk analysis. Based on the results from such risk analysis, a more realistic proposal of a new inspection program could be prepared. The number of locations included in the inspection program is often considerably smaller in new RI-ISI programs than in older and more conservative inspection programs developed with deterministic approach. Thus, remarkable benefits could be achieved in the forms of financial savings and shorter times which NDT personnel have to work under radiation exposure.

It appears that most of the available NPP SSC lifetime analysis codes consider only one or two degradation mechanisms, which is a drawback, as the number of failure mechanisms encountered in NPP environments is much greater. Thus, it appears that for the time being several codes are needed, if one wishes to cover the degradation of all safety significant NPP systems and components. This causes problems, as the failure probability results given by various analysis codes may not be comparable due to differences in analysis models and required input data. Thus, it would be necessary to develop either one analysis program that considers all relevant degradation phenomena or a family of analysis programs, each of which would cover one or two degradation phenomenon or phenomena and the failure probability results of all of which would be comparable. The analysis programs should also be able to consider the distributed nature of at least all those parameters the actual nature of which is markedly distributed. Another capability that is needed when considering power plant environments is

that the applied degradation modelling tools should be able to consider plant specific features and characteristics. Other capabilities that degradation modelling tools of components should be able to consider are small failure probabilities and quantification of the effectiveness of NDT. The effect of NDT techniques is usually quantified using flaw detection reliability in terms of POD curves, which describe the detection probability as a function of the flaw size, e.g. flaw depth or length. However, the construction of a POD curve requires a considerable amount of data before statistical confidence is achieved. In the case of NDT methods, it is often expensive and time consuming to produce such a large amount of data. One possibility for further research would be to collect all available good quality NDT data and develop simple POD functions environment, degradation mechanism and material type specifically for a representative set of power plant pipe sizes.

Databases are one possible solution to the problems related to the input data needed in the risk and ageing analyses. The amount of NPP piping component degradation data in the international databases has increased and quality improved, respectively, which consequently allows improving accuracy in the statistical piping degradation estimates. An example of such a database is OPDE (OECD Piping Failure Data Exchange), which is an advanced good quality piping failure database containing data from 12 countries using nuclear energy, see refs. [318, 319]. On the other hand, the inclusion of plant specific features and characteristics in the degradation analyses necessitates the availability of plant specific databases. The development and better availability of component degradation/failure databases will hopefully provide means for how the problems related to small failure probabilities, i.e. to very rare events, could be alleviated or even overcome.

References

1. Smith, C. L., Shah, V. N., Kao, T. Apostolakis, G. Incorporating aging effects into probabilistic risk assessment – A feasibility study utilizing reliability physics models. Report NUREG/CR-5632, U.S. Nuclear Regulatory Commission (USNRC), 2001. 131 p. + app. 112 p.

2. Chapman, O. J. V. Risk-informed approaches. In: Integrity of pressurised components of nuclear power plants. EUROCOURSE 2001. 17 to 21 September 2001, MPA-Stuttgart. 19 p.

3. HSE Health & Safety Executive. Best practice for risk based inspection as a part of plant integrity management. Prepared by TWI and Royal & SunAlliance Engineering for the Health and Safety Executive. Contract research report 363/2001. 122 p. + app. 57 p.

4. Safety aspects of nuclear power plant ageing. IAEA-TECDOC-540. International Atomic Energy Agency (IAEA), Vienna, Austria, 1990. 200 p.

5. Aging nuclear power plants: Managing plant life and decommissioning. Report OTA-E-575, U.S. Congress, Office of Technology Assessment, U.S. Government Printing Office, Washington DC, September 1993.

6. Safe management of NPP ageing in the European Union. Final report. European Commission, Nuclear Safety and Environment, 2001. 363 p.

7. ASM handbook. Vol. 19. Fatigue and fracture. ASM International, U.S.A., 1998. 2592 p.

8. Grandemange, J. M., Pichon, C. Les modes de dégradation des composants du circuit primaire des REP. Journée SFEN du 8 décembre 1998 “Sûreté des installations anciennes”, Paris.

9. Saint Raymond, P. Sûreté des installations anciennes. Journée SFEN du 8 décembre 1998, Paris, France.

10. Braverman, J. I. et al. Assessment of age-related degradation of structures and passive components for U.S. Nuclear Power Plants. Report NUREG/CR-6679, U.S. Nuclear Regulatory Commission (USNRC). Washington D.C., U.S.A., 2000.

11. Viswanathan, R. Damage mechanisms and life assessment of high-temperature components. ASM International, U.S.A., 1989. 497 p.

12. Tuurna, S., Cronvall, O., Heikinheimo, L., Hänninen, M., Talja, H., Tiihonen, O. State of the art report – Lifetime analysis of boiler tubes. Technical Research Centre

of Finland (VTT), Industrial Systems, research report TUO74-021828. Finland, 2003. 61 p. + app. 2 p.

13. Jaffee, R. Metallurgical problems and opportunities in coal fired steam power plants. Met. Trans., Vol. 10A, 1979, pp. 139–165.

14. Ehrlich, K., Konys, J., Heikinheimo, L., Leistikow, S., Steiner, H., Arnoux, P., Schirra, M. Final Report on In-core and Out-of-core Materials Selection for the HPLWR. VTT research report TUO74-021277. Technical Research Centre of Finland (VTT), Espoo Finland, 2003. 56 p.

15. Uhlig's corrosion handbook. 2nd Edition. Revie, R. W. (Ed.). John Wiley & Sons, Inc., Ottawa, Ontario, Canada, 2000. 1391 p.

16. Talbot, D., Talbot, J. Corrosion science and technology. CRC Press LLC, Boca Raton, Florida, 1998.

17. Mitman, J. (Project manager). Revised risk informed in-service inspection evaluation procedure. Electric Power Research Institute (EPRI). Interim Report EPRI TR-112657. California, U.S.A., April 1999.

18. Weston, K. Energy conversion. Electronic version. U.S.A., 2000. 527 p. + app. 65 p.

19. Assessment and management of ageing of major nuclear power plant components important to safety: BWR pressure vessels. IAEA-TECDOC-1470. International Atomic Energy Agency (IAEA), Vienna, Austria, October 2005. 117 p.

20. Miteva, R., Taylor, N. G. General review of dissimilar metal welds in piping systems of pressurised water reactors, including WWER designs. Report EUR 22469 EN. European Commission, Joint Research Centre (JRC), Petten, Netherlands, 2006. 62 p.

21. Main characteristics of nuclear power plants in the European Union and candidate countries. European Commission, report EUR 2056 EN, 2001. 163 p.

22. Cronvall, O. Welding residual stress relaxation in NPP components under operation – A literature study. Research report VTT-R-02200-10. Technical Research Centre of Finland (VTT), Espoo, Finland, 2010. 80 p. + app. 2 p.

23. Tipping, P. Lifetime and ageing management of nuclear power plants: A Brief overview of some light water reactor component ageing degradation problems and ways of mitigation. International Journal of Pressure Vessels and Piping, 66, 1995, pp. 17–25.

24. Morgan, W. C., Livingston, J. V. (Compilers). A review of information useful for managing aging in nuclear power plants. Division of Engineering Office of Nuclear

Regulatory Research, U.S. Nuclear Regulatory Commission (NRC), Contract DE-AC06-76RLO 1830 NRC FIN B2865. U.S.A., 1997. Copied 4.8.2004 from: http://www.pnl.gov/ etd/product/Riumahtm/3978B.html.

25. Suresh, S. Fatigue of materials. Cambridge University Press, England, 1991. 586 p.

26. Backofen, W. Formation of slip-band cracks in fatigue. In: Proc Int Conf on the Atomic Mechanisms of Fracture. Tech Press, MIT. John Wiley & Sons, 1959. Pp. 435–49.

27. Schijve, J. Fatigue of structures and materials in the 20th century and the state of the art. International Journal of Fatigue Vol. 25, 2003, pp. 679–702.

28. Forsyth, P. The application of 'fractography' to fatigue failure investigations. Roy Aircraft Est. Tech. Note Met. 1957; 257.

29. Lamping, G. Investigation and correction of boiler tube failures. In: Boiler Tube Failures in Fossil Power Plants. Dooley, B. & Broske, D. (Ed.). Electric Power Research Institute (EPRI), 1987. Pp. 4-1–4-16.

30. Anderson, T. L. Fracture mechanics, fundamentals and applications. 3rd Edition. CRC Press, June 2005.

31. Aaltonen, P. et al. Facts and views on the role of anionic impurities, crack tip chemistry and oxide films in environmentally assisted cracking. Espoo, Finland: VTT Industrial Systems, 2002. 68 p. + app. 21 p. (VTT Tiedotteita – Research notes: 2148). ISBN 951-38-6051-5. http://www.vtt.fi/inf/pdf/tiedotteet/2002/T2148.pdf.

32. Sanzo, D. et al. Survey and evaluation of aging risk assessment methods and applications. Report NUREG/CR-6157. U.S. Nuclear Regulatory Commission (USNRC), Washington D.C., U.S.A, 1994. 159 p.

33. Jones, R. H. (Ed.). Stress-corrosion cracking. ASM International, Ohio, 1992. 448 p.

34. Meyzaud, Y., Soulat, P. In-Service aging of pressurised water reactor steam supply system materials. RGN Int. Edition-Vol. A- July 1996.

35. Guidelines and procedures for design of class 1 elevated temperature nuclear system components. Nuclear standard NE F9-5T, U.S. Department of Energy, Nuclear Energy Programs, September 1986, U.S.A.

36. Abaqus/standard user's manual. Version 6.10. Dassault Systèmes Simulia Corp., Providence, Rhode Island, U.S.A., 2010.

37. Abaqus theory manual. Version 6.10. Dassault Systèmes Simulia Corp., Providence, Rhode Island, U.S.A., 2010.

38. Cronvall, O., Calonius, K., Junninen, P. Structural analysis and lifetime assessment of outlet headers. In: Proceedings of conference BALTICA VII – Life Management and Maintenance for Power Plants, Vol. 1. Technical Research Centre of Finland (VTT), VTT Symposium 246. Finland, Espoo, 2007. Pp. 83–105.

39. Westergaard, H. M. Bearing Pressures and Cracks. Journal of Applied Mechanics, Vol. 6, 1939, pp. 49–53.

40. Irwin, G. R. Analysis of stresses and strains near the end of a crack traversing a plate. Journal of Applied Mechanics, Vol. 24, 1957, pp. 361–364.

41. Hutchinson, J. W. Singular behavior at the end of a tensile crack tip in a hardening material. Journal of the Mechanics and Physics of Solids, Vol. 16, 1968, pp. 13–31.

42. Rice, J. R., Rosengren, G. F. Plane strain deformation near a crack tip in a power-law hardening material. Journal of the Mechanics and Physics of Solids, Vol. 16, 1968, pp. 1–12.

43. Brinkman, C., Korth, G., Hobbins, R. Estimates of creep-fatigue interaction in irradiated and unirradiated austenitic stainless steels. Nuclear Technology, Vol. 16, 1972, pp. 297–307.

44. Yagawa, G., Yoshimura, S. A study on probabilistic fracture mechanics for nuclear pressure vessels and piping. International Journal of Pressure Vessels & Piping, Vol. 73, 1997, pp. 97–107.

45. Probabilistic methods: Uses and abuses in structural integrity. Prepared By BOMEL Limited, Health and safety executive hazardous installations Directorate, England, 2001. 103 p. + app. 117 p.

46. Provan, J. W. Probabilistic approaches to the material-related reliability of fracture sensitive structures. In: Probabilistic Fracture Mechanics and Reliability. Provan, J. W. (Ed.). Martinus Hijhoff Publishers, 1987. Pp. 1–45.

47. Arnold, J. C., Milton, J. S. Introduction to probability and statistics, principles and applications for engineering and the computing sciences. McGraw-Hill, Inc., Third Edition. Singapore, 1995. 829 p.

48. Saltelli, A. et al. Sensitivity analysis of model output: Variance-based methods make the difference. In: Proceedings of the 1997 Winter Simulation Conference. Andradóttir, S., Healy, K., Withers, D., Nelson, B. (Eds.). 8 p.

49. Modarres, M. What every engineer should know about reliability and risk analysis. Marcel Dekker Inc. New York, 1993. 351 p.

50. Webster, S. E., Bannister, A. C. Methods, applications and software for structural reliability assessment. Report No. SL/WEM/R/M8663/5/01/C, Corus UK Limited, Rotherhamn, U.K, 2001. 52 p. + app. 29 p.

51. Brückner, A. Numerical methods in probabilistic fracture mechanics. In: Probabilistic Fracture Mechanics and Reliability. Provan, J., W. (Ed.). Martinus Hijhoff Publishers, 1987. Pp. 351–386.

52. Lodeby, K. Literature survey on methods of uncertainty management in life predictions for mechanical structures. Research report, Göteborg University, Sweden, 2000. 41 p.

53. Hasofer, A. M., Lind, N. C. Exact and invariant second-moment code format. J. Engr. Mech. Div. Proc. ASCE. 100(EMI), 1974, pp. 111–121.

54. Cambier, S., Guihot, P., Coffignal, G. Computational methods for accounting of structural uncertainties, applications to dynamic behavior prediction of piping systems. Structural safety, Vol. 24, 2002, pp. 29–50.

55. Hohenbichler, M., Rackwitz, R. Improvement of second-order reliability estimates by importance sampling. Journal of Engineering Mechanics Vol. 114, No. 12, 1988, pp. 2195–2199.

56. Fiessler, B., Neumann, H. J., Rackwitz, R. Quadratic limit states in structural reliability. Journal of the engineering mechanics division, Proceedings ASCE, Vol. 105, No EM4, 1979.

57. Tvedt, L. Distribution of quadratic forms in normal space – Application to structural reliability. Journal of Engineering Mechanics, ASCE, Vol. 116, No. 6, pp. 1183–1197.

58. Wu, Y. T., Wirsching, Ph. H. New algorithm for structural reliability estimation. Journal of the engineering mechanics division, ASCE, 1985.

59. Wu, Y. T. Demonstration of a new, fast probability integration method for reliability analysis. Journal of Engineering for Industry, Vol. 109, 1987.

60. Wu, Y. T., Millwater, H. R., Cruse, T. A. Advanced probabilistic structural analysis method for implicit performance function. AIAA Journal, Vol. 28, No. 9, pp. 1663–1669.

61. Mavris, N., Bandte, O. A Probabilistic approach to multivariate constrained robust design simulation. Research report, Georgia Institute of Technology, U.S.A, 1997.

62. Wu, Y. T., Burnside, O. H., Cruse, T. A. Probabilistic methods for structural response analysis. Computational Mechanics of Probabilistic and Reliability Analysis. Liu, W. K. & Belytschko, T. (Eds.). Elmpress International, 1989.

63. Ang, A. H.-S., Tang, W. H. Probability concepts in engineering planning and design. Volume II, Decision, risk, and reliability. John Wiley & Sons. U.S.A., 1984. 530 p. + app. 33 p.

64. Long, M. W., Narciso, J. D. Probabilistic design methodology for composite aircraft structures. Report No. DOT/FAA/AR-99/2. U.S. Department of Transportation, Federal Aviation Administration. U.S.A., 1999. 138 p.

65. Vose, D. Quantitative risk analysis: a guide to Monte Carlo simulation modelling. John Wiley & Sons. U.K., 1996. 328 p.

66. Zheng, Y., Das, P. K. Improved response surface method and its application to stiffened plate reliability analysis. Engineering Structures, Vol. 22, 2000, p. 544–551.

67. Riha, D. S. Importance sampling methods. In the course: 11th Annual Short Course on Probabilistic Analysis and Design, Computational Methods and Applications. September 11–15, 2000. Southwest Research Institute (SwRI), San Antonio, Texas.

68. Inman, R. L. 1999 Latin Hypercube sampling. In: Encyclopedia of statistical sciences, Update Vol. 3, Wiley, New York, U.S.A. Pp. 408–411.

69. Smith, E. Uncertainty analysis. In: Encyclopedia of environmetrics, Vol. 4, El-Shaarawi, A. H., Piegorsch, W. W. (Eds.). John Wiley & Sons, 2002, U.K. Pp. 2283–2297.

70. Mahn, J. A. et al. Qualitative methods for assessing risk. Sandia Report, SAND95-0320, Sandia National Laboratories. U.S.A, 1995. 78 p.

71. Vesely, W. E., Goldberg, F., Roberts, N., Haasl, D. Fault tree handbook. Report NUREG-0492, U.S. Nuclear Regulatory Commission (USNRC), Washington D.C., U.S.A, 1981. 209 p.

72. Wang, J. X., Roush, M. L. What every engineer should know about risk engineering and management. Marcel Dekker Incorporated. U.S.A., 2001. 252 p.

73. Palshikar, G. K. Temporal fault trees. Information and Software Technology, Vol. 44, 2002, pp. 137–150.

74. Clemen, R. T., Winkler, R. L. Combining probability distributions from experts in risk analysis. Research report, Duke University, U.S.A., 1997. 37 p.

75. Donghan, Y. Modeling and measuring the effects of imprecision in accident management. Annals of Nuclear Energy, Vol. 29, 2002, pp. 821–833.

76. Ayyub, B. M., Popescu, C. Verification and validation of probabilistic computational mechanics methods. Research report, University of Maryland, U.S.A. 10 p.

77. Dalkey, N. C., Helmer, O. An experimental application of the Delphi method to the use of experts. Journal of the Institute of Management Sciences, Vol. 9, 1963, pp. 458–467.

78. Helmer, O. “Analysis of the Future: The Delphi Method,” and “The Delphi Method – An Illustration”. Bright (Ed.), Techn. Forecasting for Industry and Government, Prentice Hall, NJ, 1968.

79. Pulkkinen, U., Simola, K. An expert panel approach to support risk-informed decision making. Report STUK-YTO-TR172. Radiation and Nuclear Safety Authority (STUK), Helsinki, Finland, November 2000. 18 p.

80. ENIQ Recommended practice 11: Guidance on expert panels in RI-ISI. ENIQ Report nr. 34. European Network for Inspection and Qualification (ENIQ), EUR 22234 EN, Petten Netherlands, June 2008. 22 p.

81. Abrahamsson, M. Treatment of uncertainty in risk based regulations and standards for risk analysis. Research Report 3116. Lund University, Sweden, 2000. 82 p.

82. Rao, D. V. Nuclear reactor safety & reliability analysis. Los Alamos National Laboratory, Division 11: Probabilistic Risk Analysis. 31.8.2002 from: http://www.lanl.gov/orgs/d/d11/research/nureactor.shtml.

83. Cameron, R. F., Willers, A. Use of risk assessment in the nuclear industry with specific reference to the Australian situation. Reliability Engineering & System Safety, Vol. 74, 2001, pp. 275–282.

84. Stamatelatos, M. G. Risk assessment and management, tools and applications. NASA Headquarters, Office of Safety and Mission Assurance. 1.9.2002 from: http://smo.gsfc.nasa.gov/crm/crm_publications/presentation_1.pdf.

85. Stamatelatos, M. G. (Project manager). Probabilistic risk assessment procedures guide for NASA managers and practitioners. Version 1.0. NASA Headquarters. Office of Safety and Mission Assurance. Washington, D.C., U.S.A., March 31, 2002.

86. Travers, D. Addressing PRA quality in risk-informed activities. Report SECY-00-0162. U.S. Nuclear Regulatory Commission (USNRC). Washington D.C., U.S.A., 2000.

87. Simola, K. Reliability methods in nuclear power plant ageing management. VTT Publications 379, VTT Technical Research Centre of Finland, Finland, 1999. 38 p. + app. 96 p. http://www.vtt.fi/inf/pdf/publications/1999/P379.pdf.

88. Living probabilistic safety assessment (LPSA). IAEA-TECDOC-1106, International Atomic Energy Agency (IAEA), Vienna, Austria, 1999. 60 p.

89. Probabilistic Safety Analyses. YVL Guide 2.8. Radiation and Nuclear Safety Authority (STUK), 28 May 2003. 9 p.

90. Besuner, P. M. Probabilistic fracture mechanics. In: Probabilistic fracture mechanics and reliability. Provan, J. W. (Ed.). Martinus Hijhoff Publishers, 1987. Pp. 387–436.

91. Rahman, S., Kim, J. S. Probabilistic fracture mechanics for nonlinear structures. International Journal of Pressure Vessels and Piping, Vol. 78, 2001, pp. 261–269.

92. Hahn, G. J., Shapiro, S. S. Statistical models in engineering. John Wiley and Sons, Inc. 1967.

93. Harris, D. O., Lim., E. Y., Delhia, D. D. Probability of pipe fracture in the primary coolant loop of a PWR plant. Vol. 5, Probabilistic fracture mechanics analysis. Report NUREG/CR-2189, U.S. Nuclear Regulatory Commission (USNRC). Washington D.C., U.S.A., 1981.

94. Lim., E. Y. Probability of failure in the primary coolant loop of a PWR plant. Vol. 9. PRAISE computer code user's manual. Report NUREG/CR-2189, U.S. Nuclear Regulatory Commission (USNRC). Washington D.C., U.S.A., 1981.

95. Yoshimura, S., Zhang, M.-Y., Yagawa, G. Life extension simulation of aged reactor pressure vessel material using probabilistic fracture mechanics analysis on a massively parallel computer. Nuclear Engineering and Design, Vol. 158, 1995, pp. 341–350.

96. Toshimura, S. et al. Proceedings of 1995 ASME/ ISME PVP Conference, Vol. PVP-304, 1995. P. 437.

97. Suresh, S. Fatigue of materials. Cambridge University Press, England, 1991. 586 p.

98. Palmgren, A. Die Lebensdauer von Kugellagern. VDI-Zeitschrift, Vol. 68, No. 14, 1924, pp. 339–341.

99. Miner, M. A. Cumulative damage in fatigue. Journal of Applied Mechanics, Vol. 67, 1945, pp. A159–A164.

100. Fatemi, A., Yangt, L. Cumulative fatigue damage and life prediction theories: a survey of the state of the art for homogeneous materials. International Journal of Fatigue, Vol. 20, No. 1, 1998, pp. 9–34.

101. Marco, S. M., Starkey, W. L. A concept of fatigue damage. Transactions of the ASME, Vol. 76, 1954. Pp. 627–632.

102. Manson, S. S., Halford, G. R. Practical implementation of the double linear damage rule and damage curve approach for treating cumulative fatigue damage. International Journal of Fracture, Vol. 17, No. 2, 1981, pp. 169–192.

103. Leipholz, H. H. E. Lifetime prediction for metallic specimens subjected to loading with varying intensity. Computers & Structures, Vol. 20, Nos. 1–3, 1985, pp. 239–246.

104. Leipholz, H. H. E. On the modified S-N curve for metal fatigue prediction and its experimental verification. Engineering Fracture Mechanics, Vol. 23, No. 3, 1986, pp. 495–505.

105. Inglis, N. P. Hysteresis and fatigue of Wohler rotating cantilever specimen. The Metallurgist, 1927, pp. 23–27.

106. Ellyin, F. Cyclic strain energy density as a criterion for multiaxial fatigue failure. In: Biaxial and Multiaxial Fatigue. EGF 3. Brown, M. W., Miller, K. J. (Eds.). Mechanical Engineering Publications, Suffolk, UK, 1989. Pp. 571–583.

107. Glinka, G., Shen, G., Plumtree, A. Multiaxial fatigue strain energy density parameter related to the critical fracture plain. Fatigue & Fracture of Engineering Materials and Structures, Vol. 18, No. 1, 1995, pp. 37–46.

108. Niu, X. D. Memory behavior of stress amplitude responses and fatigue damage model of a hot-rolled low carbon steel. In: Mechanical Behavior of Materials – V, Proceedings of the Fifth International Conference, Vol. I. Yan, M. G., Zhang, S. H., Zheng, Z. M. (Eds.). Pergamon Press, Oxford, 1987. Pp. 685–690.

109. Niu, X., Li, G. X., Lee, H. Hardening law and fatigue damage of a cyclic hardening metal. Engineering Fracture Mechanics, Vol. 26, No. 2, 1987, pp. 163–170.

110. Chaboche, J. L. A differential law for nonlinear cumulative fatigue damage. In: Materials and Building Research. Paris Institut Technique Du Batiment Et Des Travaus Publies. Annales de l'ITBTP, HS No. 39, 1974. Pp. 117–124.

111. Chaboche, J. L. Lifetime predictions and cumulative damage under high-temperature conditioned. In: Low-cycle Fatigue and Life Prediktion, ASTM STP 770. Amzallag, C., Leis, B. N., Rabbe, P. (Eds.). American Society for Testing and Materials, Philadelphia, PA, U.S.A., 1982. Pp. 81–103.

112. Paris, P. C., Erdogan, F. A Critical analysis of crack propagation laws. Journal of Basic Engineering, Vol. 85, 1960, pp. 528–534.

113. Forman, R. G. Study of fatigue crack initiation from flaws using fracture mechanics theory. Engineering Fracture Mechanics, Vol. 4, No. 2, 1972, pp. 333–345.

114. Beden, S. M. et al. Review of fatigue crack propagation models for metallic components. European Journal of Scientific Research, Vol. 28, No. 3, 2009, pp. 364–397.

115. McEvily, A. J. On closure in fatigue crack growth. In: ASTM STP 982, American Society for Testing and Materials. Philadelphia, 1988. Pp. 209–219.

116. Elber, W. The significance of fatigue crack closure. ASTM STP 486, 1971, pp. 230–242.

117. Shih, T. T., Wei, R. P. A study of crack closure in fatigue. Engineering Fracture Mechanics, 1974, Vol. 6, pp. 19–32.

118. Hudak, S. J., Davidson, D. L. The Dependence of crack closure on fatigue loading variables. ASTM STP 982, 1988, pp. 121–138.

119. McClung, R. C. The influence of applied stress, crack length, and stress intensity factor on crack closure. Metallurgical Transactions, Vol. 22A, 1991, pp. 1559–1571.

120. Wheeler, O. E. spectrum loading and crack growth. Transactions of the ASME Series D. Journal of Basic Engineering, Vol. 94, 1972, pp. 181–186.

121. Johnson, W. S. Multi-parameter yield zone model for predicting spectrum crack growth. ASTM STP 748, 1981, pp. 85–102.

122. Wang, W., Cheng, T. Fatigue crack growth rate of metal by plastic energy damage accumulation theory. Journal of Engineering Mechanics, Vol. 120, No. 4, 1994, pp. 776–795.

123. Miller, M. S., Gallagher, J. P. An analysis of several fatigue crack growth rate (FCGR) descriptions. In: Fatigue crack growth measurement and data analysis, ASTM STP 738. Hudak, S. J., Bucci, R. J. (Eds.). American Society for Testing and Materials, U.S.A., 1981. Pp. 205–251.

124. Forman, R. G., Mettu, S. R. Behaviour of surface and corner cracks subjected to tensile and bending loads in a Ti-6Al-4V alloy. In: Fracture Mechanics 22th Symposium, ASTM, ASTP STP 1131, Philadelphia. Ernst, H. A., Saxena, A., McDowell, D. L. (Eds.), 1992. Pp. 519–646.

125. FITNET – Final technical report. Version 27. European Fitness for Service Network (FITNET), November 2006. 127 p.

126. Li, B., Santos, J. L. T., Defreitas, M. A computerized procedure for long-life fatigue assessment under complex multiaxial loading. Fatigue & fracture of engineering materials & structures, Vol. 24, 2001, pp. 165–177.

127. McDowell, D. L. Basic issues in the mechanics of high cycle metal fatigue. International Journal of Fracture, Vol. 80, 1996, pp. 103–145.

128. Garud, Y. S. Multiaxial fatigue: a survey of the state of the art. J. of Test. Eval. Vol. 9, 1981, p. 165.

129. Papadopoulos, I. V. A review of multiaxial fatigue limit criteria. In: Advanced Course on High-Cycle Metal Fatigue. Dang Van, K., Papadopoulos, I. V. (Eds.). ICMS, Udine, Italy, 1997.

130. Marquis, G. B., Socie, D. F. Multiaxial Fatigue. In: Comprehensive Structural Integrity Volume 4. Cyclic loading and fatigue. Milne, I., Ritchie, R. O., Karihaloo, B. (Eds.), 2003, Elsevier Ltd.

131. Tanaka, K. Fatigue crack propagation from a crack inclined to the cyclic tensile axis. Engineering Fracture Mechanics, Vol. 6, 1974, pp. 493–507.

132. Sih, G. C. Mechanics of fracture, 1. In: Noordhoff International Publishing, Leyden, 1973. Pp. 23–44.

133. Metals handbook. Volumes 1 and 13. 9th Edition. American Society for Metals International, 1987.

134. Aging effects for structures and structural components (Structural tools). Report TR-114881, Electric Power Research Institute (EPRI), Palo Alto, U.S.A., April 2000. 137 p.

135. Anderko, A. et al. Computation of rates of general corrosion using electrochemical and thermodynamic models. Corrosion, Vol. 57, 2001, pp. 202–213.

136. Congleton, J., Craig, I. H. Corrosion fatigue. In: Corrosion Processes. Parkins, R. N. (Ed.). Applied Science Publishers, 1982.

137. Anderko, A., Young, R. D. A Model for calculating rates of general corrosion of carbon steel and 13%Cr stainless steel in CO_2/H_2S environments. Paper No. 1086. CORROSION/2001, Houston, U.S.A., March 11–16, 2001.

138. Guide for predicting long-term reliability of nuclear power plant systems, structures and components. Report 1002954. Electric Power Research Institute (EPRI), Palo Alto, U.S.A., December 2002. 208 p.

139. Engelhart, G., Macdonald, D. D. Unification of the deterministic and statistical approaches for predicting localized corrosion damage I: Theoretical foundation. Corrosion Science, Vol. 46, 2004, pp. 2755–2780.

140. Morin, U., Jansson, C., Bengtsson, B. Crack growth rates for Ni-base alloys with the application to an operating BWR. In: Sixth international symposium on environmental degradation of materials in nuclear power systems – Water reactor systems. August 1–5, 1993. San Diego, California, U.S.A. Pp. 373–378.

141. Materials Reliability Program (MRP) - Crack Growth Rates for Evaluating Primary Water Stress Corrosion Cracking (PWSCC) of Thick-Wall Alloy 600 Materials (MRP-55). Revision 1. EPRI Report 1006695, Electric Power Research Institute (EPRI), Palo Alto, 2002. 53 p.

142. White, G. A. , Hickling, J., Mathews, L. K. Crack growth rates for evaluating PWSCC of thick-wall alloy 600 material. Proceedings of the 11th International Conference on Environmental Degradation of Materials in Nuclear Power System – Water Reactors – Stevenson, 2003.

143. Materials Reliability Program (MRP) - Crack Growth Rates for Evaluating Primary Water Stress Corrosion Cracking (PWSCC) of Alloy 82, 182 and 132 Welds (MRP-115). EPRI Report 1006696, Electric Power Research Institute (EPRI), Palo Alto, 2004. 274 p.

144. White, G. A. et al. Development of crack growth rate disposition curves for primary water stress corrosion cracking (PWSCC) of alloy 82, 182, and 132 weldments. Proceedings of the 12th International Conference on Environmental Degradation of Materials in Nuclear Power System – Water Reactors. Allen, T. R., King, P. J., Nelson, L. (Eds.). TMS (The Minerals, Metals & Materials Society), 2005.

145. Shoji, T. Suzuki, S., Ballinger, R. G. Theoretical Prediction of SCC Growth Behavior. Proceedings of 7th Int. Symposium on Environmental Degradation of Materials in Nuclear Power Systems – Water Reactors, 1995, NACE. P. 881.

146. Reliability centered lifetime prediction of environmentally assisted cracking. Report 1007871, Electric Power Research Institute (EPRI), Palo Alto, 2003. 256 p.

147. Saito, K., Kuniya, J. Mechanochemical model to predict stress corrosion crack growth of stainless steel in high temperature water. Corrosion Science, Vol. 43, 2001, pp. 1751–1766.

148. Norton, F. N. The creep of steel at high temperature. McGraw-Hill, 1929.

149. Graham, A., Walles, K. Relations between long and short time properties of commercial alloys. JISI, Vol. 179, 1955, pp. 105–120.

150. Garofalo, F. Fundamentals of creep and creep rupture in metals. New York, Macmillan, 1965.

151. Dyson, B. F., McClean, M. Microstructural evolution and its effects on the creep performance of high temperature alloys. In: Microstructural Stability of Creep Resistant Alloys for High Temperature Applications. Strang, A., McClean, M. (Eds.). IOM, 1998. Pp. 371–393.

152. Merckling, G. Metodi di calcolo a confronto per la previsione dellulteriore esercibilità in regime di scorrimento viscoso. In: Proceedings Conference on Fitness for Service, Giornata di Studio CESI-CONCERT, Milan, 28 November 2002.

153. Manson, S. S., Haferd, A. M. A Linear time-temperature relation for extrapolation of creep and stress rupture data. NASA TN2890, 1952.

154. Larson, F. R., Miller, J. A Time-temperature relationship for rupture and creep stresses. Transactions of ASME, Vol. 74, 1952, p. 765–771.

155. Robinson, E. L. Effect of Temperature variation on the creep strength of steels. Transactions of ASME, Vol. 160, 1938, pp. 253–259.

156. Lieberman, Y. Relaxation, tensile strength and failure of E1 512 and Kh1 F-L steels. Metalloved Term Obrabodke Metal, Vol. 4, 1962, pp. 6–13.

157. Voorhees, H. R., Freeman, F. W. Notch sensitivity of aircraft structural and engine alloys. Wright Air Development Center Technical Report, Part II, January 1959. P. 23.

158. Abo El Ata, M. M., Finnie, I. A study of creep damage rules. ASME Paper No. 71-WA/Met-1, American Society of Mechanical Engineers, New York, U.S.A., December 1971.

159. Landes, J. D., Begley, J. A. A Fracture mechanics approach to creep crack growth. In: ASTM STP, 590. American Society for Testing and Materials, Philadelphia, PA, U.S.A, 1976. Pp. 128–148.

160. Ohji, K., Ogura, K., Kubo, S. Transactions of the Japan Society of Mechanical Engineers, Vol. 42, 1976, pp. 350–358.

161. Nikbin, K., M., Webster, G.A. Turner, C. E. In: Cracks and fracture, ASTM STP 601, American Society for Testing and Materials, Philadelphia, PA, 1976. Pp. 47–62.

162. Hoff, N. J. Approximate analysis of structures in the presence of moderately large creep deformations. Quarterly of Applied Mathematics, Vol. 12, 1954, pp. 49–55.

163. Riedel, H., Rice, J. R. Tensile cracks in creeping solids. In: ASTM STP 700, American Society for Testing and Materials, Philadelphia, PA, 1980. Pp. 112–130.

164. Ehlers, R., Riedel, H. A Finite element analysis of creep deformation in a specimen containing a macroscopic crack. In: Proceedings of 5th International Conference on Fracture, Pergamon Press, Oxford, 1981. Pp. 691–698.

165. Saxena, A. Creep crack growth under non-steady-state conditions. In: ASTM STP 905, American Society for Testing and Materials, Philadelphia, PA, 1986. Pp. 185–201.

166. Riedel, H. Creep Deformation at crack tips in elastic-viscoplastic solids. Journal of the Mechanics and Physics of Solids, Vol. 29, 1981, pp. 35–49.

167. Nikbin, K. M., Smith, D. J., Webster, G. A. An engineering approach to the prediction of creep crack growth. Journal of Engineering Materials and Technology, ASME, Vol. 108, 1986, pp. 186–191.

168. Kaguchi, H., Djavanroodi, F., Nikbin, K. M., Webster, G. A. Prediction of transient effects during the early stages of creep crack growth. In: Proceedings of the DVM Conference. Rie, K. T. (Ed.). Berlin, Germany, September 1994.

169. Webster, G. A., Nikbin, K. M., Chorlton, M. R., Celard, N. J. C., Ober, M. A comparison of high temperature defect assessment procedures. Journal of Materials at High Temperatures, Vol. 15, Nos. 3–4, 1998, pp. 337–347.

170. Roberts, B. W., Ellis, F. V., Bynum, J. E. Remaining creep or stress rupture life under non steady temperature and stress. Transactions of ASME, Journal of Engineering Material and Technology, Vol. 101, 1979, pp. 331–336.

171. Regulatory Guide 1.99. Radiation embrittlement of reactor vessel materials. Revision 2. U.S. Nuclear Regulatory Commission (USNRC), Washington, 1988.

172. ASTM E208 – 06. Standard test method for conducting drop-weight test to determine nil-ductility transition temperature of ferritic steels.

173. Section XI. ASME boiler and pressure vessel code. American Society of Mechanical Engineers (ASME), New York, U.S.A., 2010 Edition.

174. Section III. ASME boiler and pressure vessel code. American Society of Mechanical Engineers (ASME), New York, U.S.A., 2010 Edition.

175. RCC-M design and construction rules for mechanical components of PWR nuclear islands. Plus 2002 Addendum. AFCEN, Paris, France, 2000 Edition.

176. In-service inspection rules for mechanical components of PWR nuclear islands, RSEM. EDF/AFCEN, France, 1990.

177. White paper on reactor vessel integrity requirements for level A and B conditions. Report EPRI TR-100251, Electric Power Research Institute (EPRI), 1993.

178. Cipolla, R. C. Section XI Flaw Acceptance Criteria and Evaluation Using Code Procedure. Chapter 29 in: Companion Guide to the ASME Boiler & Pressure Vessel Code, Criteria and Commentary on Select Aspects of the Boiler & Pressure Vessel and Piping Codes. Rao, K. R. (Ed.). Third Edition, Vol. 2. American Society of Mechanical Engineers (ASME), New York, U.S.A., 2009.

179. Wei, R. P., Landes, J. D. Journal of Materials Research, ASTM, 1969, Vol. 7, p. 25.

180. Lynch, S. P. Metal Science Journal, Vol. 9, 1975, p. 401–410.

181. Beachem, C. D. A. New Model for Hydrogen-Assisted Cracking (Hydrogen "Embrittlement"). Metallurgical Transactions, 1972, Vol. 3, p. 437–451.

182. Lynch, S. P. Fatigue Mechanisms, ASTM-STP-675. In: Fong, J. T. (Eds.). ASTM, Philadelphia, PA, 1979, p. 174.

183. Lynch, S. P. Hydrogen effects in metals. In: Thompson, A. W., Bernstein, I. M. (Eds.). AIME, New York, U.S.A., 1981. P. 863.

184. Chopra, O. K., Shack, W. J. Effect of LWR coolant environments on the fatigue life of reactor materials. Report NUREG/CR-6909, U.S. Nuclear Regulatory Commission (USNRC), Washington, DC, U.S.A., 2007. 115 p.

185. Codes for nuclear power generation facilities – Environmental fatigue evaluation method for nuclear power plants – Explanation. The Japan Society of Mechanical Engineers, JSME S NF1, 2009. 52 p.

186. Codes for nuclear power generation facilities – Environmental fatigue evaluation method for nuclear power plants – Body text. The Japan Society of Mechanical Engineers, JSME S NF1, 2009. 17 p.

187. Code Case N-792. Fatigue evaluations including environmental effects. ASME Boiler and Pressure Vessel Code. American Society of Mechanical Engineers (ASME), New York, September 2010.

188. Taira, S. Lifetime of structures subjected to varying load and temperature. In: Creep in structures. Hoff, N. J. (Ed.). Academic Press, 1962. Pp. 96–124.

189. Majumdar, S., Maiya, P. S. Creep-fatigue interactions in an austenitic stainless steel. Can. Met. Qtrly. Vol. 18, 1979, pp. 57–64.

190. Majumdar, S., Maiya, P. S. A damage equation for creep-fatigue interaction. In: ASME-MPC Symposium on Creep-Fatigue Interaction. MPC-3, Metal Properties Council, New York, U.S.A., 1976. P. 323.

191. Majumdar, S., Maiya, P. S. In: Proceedings of the Second International Conference on Mechanical Behavior of Materials, ICM2, 1976. Pp. 924–928.

192. Majumdar, S., Maiya, P. S. ASME-CSME Pressure Vessel and Piping Conference, PVP-PB 028, 1978.

193. Majumdar, S., Maiya, P. S. In: Proceedings of the Third International Conference on Mechanical Behavior of Materials. ICM3, 1976, Vol. 12. Pp. 101–109.

194. Priest, R. V., Ellison, E. G. An assessment for life analysis techniques for fatigue/creep interaction. Res. Mech., Vol. 4, 1982, pp. 127–150.

195. Winstone, M. R., Nikbin, K. M., Webster, G. A. Modes of failure under creep/fatigue loading of a nickel-based superalloy. Journal of Material Science, Vol. 20, No. 20, 1985, pp. 2471–2476.

196. Dogan, B. Comparison of the defect assessment procedures. European Commission, Plant Life Assessment Network (PLAN). Document No.: PLAN.CT C2 DOC 01.05 Version I, 18.05.2001. 41 p.

197. SINTAP. Structural integrity assessment procedures for European industry, Final procedure. European Union, Project No. BE95-1426, 1999.

198. HIDA. High Temperature Defect Assessment Project, EC Project BE 1702.

199. FKM Guideline fracture mechanics proof of strength for engineering components. 2nd Revised Edition, 2004.

200. R6 Method. Assessment of the integrity of structures containing defects. Revision 4. 2004 update of 2001 edition. British Energy (BE).

201. R6 Method. Assessment of the integrity of structures containing defects. Revision 3. 1986 edition. British Energy (BE).

202. British Standard Institute. BSI PD6493. Guidance on methods for assessing the acceptability of flaws in fusion welded structures, 1981.

203. Dillström, P. et al. a combined deterministic and probabilistic procedure for safety assessment of components with cracks – Handbook. SSM Research Report 2008:01, Swedish Radiation Safety Authority (Strålsäkerhetsmyndigheten, SSM). Stockholm, Sweden, 2008. 27 p. + app. 196 p.

204. Fitness-for-Service Guide. EXXON Chemical, 1995.

205. Fitness-for-Service evaluation procedures for operating pressure vessels, tanks and piping in refinery and chemical service. Draft No. 5. The Materials Properties Council, Consultants Report, 1995.

206. Recommended practice for fitness-for-service. API 579. American Petroleum Institute (API), Washington, DC, American Petroleum Institute, 2000.

207. Kumar, V., German, M. D., Shih, C. F. An engineering approach for elastic-plastic fracture analysis. General Electric Company, NP-1931, Research Project 1237-1, Topical Report, Schenectady, New York, 1981.

208. Zahoor, A. Ductile fracture handbook. Novotech Corporation and Electric Power Research Institute (EPRI), Research Project 1757-69, 1990.

209. Schwalbe, K.-H., Zerbst, U., Brocks, W., Cornec, A., Heerens, J., Amstutz, H. The Engineering Treatment Model for assessing the significance of crack-like defects in engineering structures (EFAM ETM 95). GKSS- Forschungszentrum, 1996.

210. Schwalbe, K.-H., Kim, Y.-J., Hao, S., Cornec, A., Koçak, M. The Engineering Treatment Model for Assessing the significance of crack-like defects in joints with mechanical heterogeneity (strength mis-match) (EFAM ETM-MM 96). GKSS- Forschungszentrum, 1996.

211. RSE-M. In service inspection rules for the mechanical components of PWR nuclear power islands. AFCEN, France, 1997 Edition.

212. Safety standards of the nuclear safety standards commission (KTA). Parts 3201.1, 3201.2, 3201.3, 3201.4 and 3211.4. Germany.

213. ASME boiler and pressure vessel code. Case N-47 (29), Class 1 components in elevated temperature service, Section III, Division I. ASME, New York, 1991.

214. RCC-MR. Technical Appendix A3. Section 1, Subsection Z, Materials design and construction rules for mechanical components of FBR nuclear test islands. AFCEN, Paris, 1985.

215. British Energy, R5. Assessment procedure for the high temperature response of structures. Issue 2, Revision 2, British Energy, Gloucester, 2001.

216. British Standards PD 6539. Guide to methods for the assessment of the influence of the crack growth on the significance of defects in components operating at high temperatures. BSI, London, 1994. Pp. 1–37.

217. Simola, K. Probabilistic methods in nuclear power plant component ageing analysis. VTT Publications 94, VTT Technical Research Centre of Finland, Finland, 1992. 82 p.

218. Barlow, R. E., Proschan, F. Statistical theory of reliability and life testing probability models. Rinehart and Winston Inc., New York, 1975. 290 p.

219. Singpurwalla, N. D. Foundational issues in reliability and risk analysis. In: SIAM Review 30, 2. 1988. Pp. 264–282.

220. Cox, D. R. Renewal Theory. John Wiley & Sons, New York, 1962. 142 p.

221. Vesely, W. E. Risk evaluations of aging phenomena: the linear aging reliability model and its extensions. NUREG/CR-4769, U.S. Nuclear Regulatory Commission. Washington D.C., U.S.A., 1987. 34 p. + app.

222. Cox, D. R. Regression models and life tables. J. Royal Statistical Soc., B, 34, 1972, pp. 187–220.

223. Vesely, W. E. Approaches for age-dependent probabilistic safety assessments with emphasis on priorization and sensitivity studies. Report NUREG/CR-5587, U.S. Nuclear Regulatory Commission (USNRC). Washington D.C., U.S, 1992.

224. Wolford, A. J. et al. Aging data analysis and risk assessment-development and demonstration study. Report NUREG/CR-5378, U.S. Nuclear Regulatory Commission (USNRC). Washington D.C., U.S, 1992.

225. Mann, N. R. et al. Methods for statistical analysis of reliability and life data. John Wiley & Sons, Inc., New York, 1994.

226. Kapur, K. C., Lamberson, L. R. Reliability in engineering design. John Wiley & Sons, New York, 1977. 586 p.

227. Lydersen, S. Reliability testing based on deterioration measurements. Norges Tekniske hogskole, Institutt for matematiske fag, Doktor ingenioravhandling. Trondheim, 1988. 219 p.

228. Rau, J. G. Optimization and probability in systems engineering. Van Nostrand Reinhold Company, New York, 1970. 403 p.

229. Abramowitz, M., Stegun, A. Handbook of mathematical functions with formulas, graphs and mathematical tables. Dover Publications Inc., New York, 1970. 375 p.

230. Bogdanoff, J. L., Kozin, F. Probabilistic models for cumulative damage. John Wiley & Sons, New York, 1985. 341 p.

231. Status report on nuclear power plant life management. Nuclear Energy Agency, Committee for Technical and Economic Studies on Nuclear Energy Development and Fule Cycle, The Expert Group on Nuclear Power Plant Life Management. U.S.A., 2000. 136 p.

232. DuCharme, A. R. et al. United States Department of Energy Nuclear Plant Life Extension Program. In: Proceedings of Safety aspects of the Ageing and Maintenance of Nuclear Power Plants, Vienna, June 29 – July 3, 1987. Pp. 27–38.

233. Mishima, Y. Light water reactor power plant life extension programme in Japan. In: Proceedings of the Safety aspects of the ageing and maintenance of nuclear power plants, Vienna, June 29 – July 3, 1987. Pp. 289–294.

234. Noël, R. et al. Durée de vie des centrales REP, le projet E.D.F. In: Proceedings of an NEA symposium Nuclear Power Plant Life Extension, Paris 24–27 February, 1987. Pp. 190–203.

235. Methodology for the management of ageing of nuclear power plant components important to safety. International Atomic Energy Agency (IAEA), Technical Reports Series No. 338. Vienna, 1992. 62 p.

236. Safety goals for the operations of nuclear power plants. Policy Statement. U.S. Nuclear Regulatory Commission (USNRC), Federal Register, Vol. 51, p. 30028 (51 FR 30028), August 4, 1986.

237. Chapman O. J. V., Gandossi, L., Mengolini, A., Simola, K., Eyre, T., Walker, A. E. (Eds.). European framework document for risk informed in-service inspection. ENIQ Report No. 23, JRC-Petten, EUR 21581 EN, 2005.

238. Balkey et al. Developments on implementation of USNRC-approved WOG risk-informed inservice inspection methodology. Proceedings of ICONE 8, Eighth International Conference on Nuclear Engineering, April 2–6, 2000, Baltimore, U.S.A.

239. American Society of Mechanical Engineers. Code Case N-577, Risk-Informed Requirements for Class 1, 2, and 3 Piping, Method A, Section XI, Division 1, September 2, 1997.

240. ASME Boiler and Pressure Vessel Code, Section XI, Division 1, Nonmandatory Appendix R. 2007 Edition.

241. American Society of Mechanical Engineers. Code Case N-578, Risk-Informed Requirements for Class 1, 2, and 3 Piping, Method B, Section XI, Division 1. March 28, 2000.

242. WCAP-14572 Revision 1-NP-A Supplement 1, Westinghouse Structural Reliability and Risk Assessment (SRRA) Model for Piping Risk-Informed Inservice Inspection. 1999.

243. Risk-informed in-service inspection of piping systems of nuclear power plants: process, status, issues and development. Report No. NP-T-3.1, IAEA Nuclear Energy Series, International Atomic Energy Agency (IAEA), Vienna, Austria, 2010. 42 p.

244. Cronvall, O., Männistö, I., Simola, K. Development and testing of VTT approach to risk-informed in-service inspection methodology – Final report of SAFIR INTELI INPUT Project RI-ISI. VTT Research Notes 2382, Technical Research Centre of Finland (VTT). April 2007, Espoo. 43 p. http://www.vtt.fi/inf/pdf/tiedotteet/2007/T2382.pdf.

245. Cronvall, O., Holmberg, J., Männistö, I., Pulkkinen, U. Continuation of the RI-ISI pilot study of the Shut-down cooling system of the Olkiluoto 1/2 NPP units. VTT Research report TUO72-056667, Technical Research Centre of Finland (VTT), Espoo, Finland, 2006. 60 p.

246. Cronvall, O., Männistö, I. Combining discrete-time Markov processes and probabilistic fracture mechanics in RI-ISI risk estimates. International Journal of Pressure Vessels and Piping, Vol. 86, No. 11, 2009, pp. 732–737.

247. Simola, K., Cronvall, O., Männistö, I., Gunnars, J., Alverling, L., Dillström, P., Gandossi, L. Studies on the effect of flaw detection probability assumptions on risk reduction at inspection. Report of the NKS/PODRIS-Project, Report No. NKS-208, Nordic nuclear safety research (NKS). NKS Secretariat, Roskilde, Denmark, 2009. 69 p.

248. Bergman, M., Brickstad, B. A Procedure for analysis of leak before break in pipes subjected to fatigue or IGSCC accounting for complex crack shapes. Fatigue & Fracture of Engineering Materials & Structures, Vol. 18, 1995, pp. 1173–1188.

249. Bergman, M., Brickstad, B., Nilsson, F. A Procedure for estimation of pipe break probabilities due to IGSCC. International Journal of Pressure Vessels and Piping, Vol. 74, 1997, pp. 239–248.

250. Brickstad, B. Appendix D1, A Short description of the NURBIT piping reliability program for stress corrosion cracking analyses. NURBIM Project, WP-4, Review and benchmarking of SRMs and associated software, May 2004. 17 p.

251. EC-JRC/OECD-NEA Benchmark Study on Risk Informed In Service Inspection Methodologies (RISMET). Report NEA/CSNI/R(2010)13. CSNI Integrity and Ageing Working Group (IAGE), January 2011. 152 p.

252. Gandossi, L., Simola, K. Sensitivity of risk reduction to probability of detection curves (POD) level and detail. Scientific and Technical Research Series; EUR 21902 EN, ISSN 1018-5593, Luxembourg: Office for Official Publications of the European Communities, European Communities, 2007. 30 p.

253. Cronvall, O., Simola, K., Vepsä, A., Alhainen, J. RI-ISI pilot study of the Auxiliary feed water system of the Olkiluoto OL1 NPP unit. VTT, Espoo, 2008. Research Report VTT-R-01414-08. 61 p.

254. Gandossi, L., Annis, C. Probability of Detection Curves: Statistical Best-Practices. ENIQ TGR Technical document. European Network for Inspection and Qualification (ENIQ), EU, Joint Research Centre (JRC), Institute for Energy, Petten, the Netherlands. 68 p.

255. SKI, The Swedish Nuclear Power Inspectorate's regulations concerning structural components in nuclear installations, SKIFS 1994:1. SKI, Stockholm, Sweden, 1994.

256. American Society of Mechanical Engineers. Alternative piping classification and examination requirements. ASME Section XI Division 1, Code Case N-716, New York, U.S.A., April 2006.

257. Gandossi, L. et al. A Benchmark study on Risk-Informed In-Service Inspection Methodologies (RISMET). International Journal for Nuclear Power, No. 7, July 2010, pp. 450–457.

258. Demonstration of reliability centered maintenance. Vol. 1. Project description, EPRI NP-6152. Electric Power Research Institute (EPRI), Palo Alto, 1989. 53 p.

259. Harris, D. O. et al. Fracture mechanics models developed for piping reliability assessment in light water reactors. Report NUREG/CR-2301. U.S. Nuclear Regulatory Commission (USNRC), Washington D.C., 1981.

260. Harris, D. O., Dedhia, D. WinPRAISE 07 – Expanded PRAISE code in windows. Structural Integrity Associates Inc., California, U.S.A., July 2009. 224 p.

261. Internet page http://www.nea.fr/abs/html/ests0071.html. Organisation for Economic Co-operation and Development (OECD), Nuclear Energy Agency (NEA), 2.12.2002.

262. Rudland, D., L, Xu, H., Wilkowski, G., Scott, P., Ghadiali, N., Brust, F. Development of a new generation computer code (PRO-LOCA) for the prediction of break probabilities for commercial nuclear power plants loss-of-coolant-accidents. In:

Proceedings of the ASME Pressure Vessels and Piping Conference, July 23–27, 2006, Vancouver, British Columbia, Canada.

263. Scott, P., Kurth, R, Cox, A., Olson, R., Rudland, D. Development of the PRO-LOCA probabilistic fracture mechanics code. MERIT Final Report. SSM Research Report 2010:46, Swedish Radiation Safety Authority (Strålsäkerhetsmyndigheten, SSM). Stockholm, Sweden, December 2010. 194 p.

264. Simola, K., Sarkimo, M. Review of models for quantification of pipe degradation probabilities for RI-ISI applications. VTT Report TAU A013, VTT Technological Research Centre of Finland (VTT), Espoo, Finland, 2001. 28 p.

265. Brickstad, B. The use of risk based methods for establishing ISI-priorities for piping components at Oskarshamn 1 Nuclear power station. SKI report 00:48. Swedish Nuclear Power Inspectorate (SKI), Sweden, 2000.

266. Nilsson, F. et al. Failure probability of nuclear piping due to IGSCC. International Journal of Pressure Vessels and Piping, 43(1990)205–219.

267. Strategies for reactor safety. Nordic Nuclear Safety Research (NKS), NKS Report NKS(97)FR1, 1998. 88 p.

268. Dillström, P. Appendix G. A Short description of ProSACC. NURBIM Project, WP-4, Review and benchmarking of SRMs and associated software, September 2003. 9 p.

269. Vepsä, A. Verification of the stress intensity factors calculated with the VTTBESIT software. Technical Research Centre of Finland (VTT), research report TUO72-044578. 40 p. + app. 2 p.

270. Varfolomeyev, I. et al. BESIF 1.0: Stress intensity factors for surface cracks under 2D stress gradients. IWM-Report T 14/96. Fraunhofer-Institut für Werkstoffmechanik (IWM), July 1996. 42 p.

271. Busch, M. et al. KI-Factors and polynomial influence functions for axial and circumferential surface cracks in cylinders. IWM-Report T 18/94. Fraunhofer-Institut für Werkstoffmechanik (IWM), October 1994. 41 p.

272. Busch, M. et al. Polynomial influence functions for surface cracks in pressure vessel components. IWM-Report Z 11/95. Fraunhofer-Institut für Werkstoffmechanik (IWM), January 1995. 88 p.

273. Reliability Consulting Programs GmbH (RCP). University of Munich, Germany. 6.12.2002, from: http://www.strurel.de.

274. Das, P. K., Chryssanthopoulos, M. K. Joint-Industry project on a benchmark study of various structural reliability analysis software. October 2000.

275. Dillstrom, P. ProSINTAP – A Probabilistic program implementing the SINTAP assessment procedure. Engineering Fracture Mechanics, 67(2000)647–688.

276. ProSINTAP Version 1.2.11: A probabilistic software for safety evaluation.

277. Liu, P. L., Lin, H. Z., Der Kiureghian, A. Calrel user manual. Department of Civil Engineering, University of California, Berkeley, U.S.A., 1989.

278. Wilson, R. A User's guide to the probabilistic fracture mechanics computer code: STAR 6 – Version 2.2. Memorandum TEM/MEM/0005/95. Nuclear Electric, Engineering Division, 1995. 75 p.

279. Southwest Research Institute (SwRI). Probabilistic Structural Analysis Methods (PSAM) for Select Space Propulsion System Components. Final Report, NASA Contract NAS3-24389. National Aeronautics and Space Administration (NASA), Lewis Research Center, Cleveland, U.S.A., 1995.

280. Riha, D. S. et al. Probabilistic engineering analysis using the NESSUS software. Structural Dynamics and Materials Conference, Paper 2000-1512, Atlanta, Georgia, April 2000.

281. Southwest Research Institute (SwRI). 6.12.2002, from: http://www.swri.edu/.

282. National Aeronautics and Space Administration (NASA). 6.12.2002, from: http://www.nasatech.com/Briefs/Apr02/MSC23082.html.

283. Ardillon, E., Villain, B., Bouchacourt, M. Probabilistic analysis of flow-accelerated corrosion in French PWR: the Probabilistic module of BRT-CICERO. Version 2. ICOSSAR'97. 1997.

284. Dillström, P. Probabilistic safety evaluation – Development of procedures with applications on components used in nuclear power plants. SKI Report 00:58. Swedish Nuclear Power Inspectorate, Stockholm, Sweden, December 2000.

285. Bishop, B. A. An Updated structural reliability model for piping risk-informed ISI. In: ASME PVP Vol. 346. Fatigue and Fracture – Volume 2, 1997. Pp. 245–252.

286. Simonen, F. A. et al. VISA-II – A computer code for predicting the probability of reactor pressure vessel failure. Report NUREG/CR-4486. U.S. Nuclear Regulatory Commission (USNRC), Washington D.C., 1986.

287. Simonen, F., Chapman, O. J. V. A Model for simulating flaws in vessel welds and comparisons with empirical data. 2nd International Conference on NDE in Relation to Structural Integrity for Nuclear and Pressurized Components, New Orleans, Louisiana U.S.A., May 24–26, 2000.

288. Chapman, O. J. V., Simonen, F. A. RR-PRODIGAL – A model for estimating the probabilities of defects in reactor pressure vessel welds. Report NUREG/CR-5505. U.S. Nuclear Regulatory Commission (USNRC), Washington D.C., U.S.A., 1998.

289. Russel, K. D. et al. Systems Analysis Programs for Hands-on Integrated Reliability Evaluations (SAPHIRE) Version 6.0, System Overview Manual. Report NUREG/CR-6532. U.S. Nuclear Regulatory Commission (USNRC), Washington D.C., U.S.A., 1998.

290. Scientech Inc. Internet pages, 25.4.2011, from: http://winnupra.scientech.us.

291. Relcon Scandpower Inc. Internet pages, 25.4.2011, from: http://www.riskspectrum.com/en/risk/Meny_2/RiskSpectrum_PSA/.

292. Data Systems & Solutions Inc. Internet pages, 25.4.2011, from: http://www.ds-s.com.

293. FaultTree+ V11.2. Technical specification. Isograph Reliability Software, 25.4.2011. 10 p.

294. AvSim+ V9. Technical specification. Isograph Reliability Software, 25.4.2011. 10 p.

295. Reliass Inc. Internet pages, 25.4.2011, from: http://www.reliability-safety-software.com/index.html.

296. ReliaSoft's Weibull++ 7 Software Training Guide. ReliaSoft Corporation, Tucson, Arizona, U.S.A., 2011. 98 p.

297. ExproSoft Internet pages, 25.4.2011, from: http://www.exprosoft.com.

298. Item Software Inc. Internet pages, 25.4.2011, from: http://www.itemsoft.com/.

299. Chapman, O. J. V. 2003. Appendix F, Description of PRODIGAL. NURBIM Project, WP-4, Review and benchmarking of SRMs and associated software, July 2003.

300. Schimpfke, T. Appendix C. A short description of the piping reliability code PROST. NURBIM Project, WP-4, Review and benchmarking of SRMs and associated software, January 2003.

301. FinPSA – tool for professional living PSA, 25.5.2011, from: http://www.stuk.fi/ydinturvallisuus/ydinvoimalaitokset/en_GB/finpsa/.

302. Brickstad, B. Appendix A. SCC benchmark study. NURBIM Project, WP-4, Review and benchmarking of SRMs and associated software, May 2004.

303. Schimpfke, T. Appendix B. Fatigue benchmark study. NURBIM Project, WP-4, Review and benchmarking of SRMs and associated software, May 2004.

304. Brickstad, B. The use of risk based methods for establishing ISI-priorities for piping components at Oskarhamn 1 Nuclear power station. SAQ/FoU-Report 99/05, SAQ Kontroll AB, 1999. 83 p.

305. ASME Boiler and Pressure Vessel Code, Section II. 2001.

306. Roark, R. Young, W. Formulas for stress and strain. Fifth Edition. McGraw-Hill Book Company, U.S.A., 1975. 624 p.

307. Kuuluvainen, O. Email sent to Cronvall, O. Teollisuuden Voima Oyj (TVO), 24.1.2008. 1 p.

308. Jansson, C., Morin, U. Assessment of crack growth rates in austenitic stainless steels in operating BWRs. In: Proc. of Eighth International Symposium on Environmental Degradation of Materials in Nuclear Power Systems – Water Reactors. August 10–14, 1997. Amelia Island, Florida, U.S.A. Pp. 667–674.

309. Section XI Task Group for Piping Flaw Evaluation, ASME Code. Evaluation of Flaws in Austenitic Steel Piping. Journal of Pressure Vessel Technology, Vol. 108, 1986, pp. 352–366.

310. Shack, W. J. et al. Environmentally assisted cracking in light water reactors: Annual report, October 1981 – September 1982. Report NUREG/CR-3292, Washington D.C., U.S. Nuclear Regulatory Commission (USNRC), June 1983.

311. SINTAP. Structural integrity assessment procedures for European industry. Final Procedure: November 1999. Project funded by the European Union (EU) under the Brite-Euram Programme: Project No. BE95-1426, Contract No. BRPR-CT95-0024.

312. Barthelemy, J. Y., Janosch, J. J. Structural integrity assessment procedures for European industry. SINTAP; Task 4; Compendium of Residual Stress Profiles; Final Report: 18.5.1999. Project funded by the European Union (EU) under the Brite-Euram Programme: Project No. BE95-1426, Contract No. BRPR-CT95-0024. 40 p. + app. 18 p.

313. Khaleel, M. A., Simonen, F. A. Effects of alternative inspection strategies on piping reliability. Nuclear Engineering and Design 197, 2000, pp. 115–140.

314. Hazelton, W. S., Koo, W. H. Technical report on material selection and processing guidelines for BWR coolant pressure boundary piping: Final report. Report NUREG-0313, Rev. 2-F, Final Technical Report. U.S. Nuclear Regulatory Commission (USNRC), January 1988. 47 p.

315. Bergman, M. et al. A procedure for estimation of pipe break probabilities due to IGSCC. SAQ/FoU-Report 97/06, SAQ Kontroll AB, Stockholm, Sweden, 1997.

316. YVL Guide 3.8. Nuclear power plant pressure equipment. In-service inspection with non-destructive testing methods. Säteilyturvakeskus (STUK, Radiation and Nuclear Safety Authority), Helsinki, Finland, 22 September 2003. 30 p.

317. ENIQ Report No. 30, ENIQ recommended practice 9: Verification and validation of structural reliability models and associated software to be used in risk-informed in-service inspection programmes. EU Joint Research Centre (JRC), Institute for Energy, Petten, the Netherlands. 12 p.

318. OECD-NEA piping failure data exchange project (OPDE). Workshop on database applications. OPDE/SEC(2004)4, 2005. Nuclear Energy Agency, Issy-les-Moulineaux, France.

319. OPDE 2006:1. Coding guideline (OPDECG) & OPDE User instruction. PR01 Version 02, Restricted Distribution. Nuclear Energy Agency, Issy-les-Moulineaux, France, 2006.

Series title, number and
report code of publication

VTT Publications 775
VTT-PUBS-775

Author(s)
Otso Cronvall

Title

Structural lifetime, reliability and risk analysis approaches for power plant components and systems

Abstract

Lifetime, reliability and risk analysis methods and applications for structural systems and components of power plants are discussed in this thesis. These analyses involve many fields of science, such as structural mechanics, fracture mechanics, probability mathematics, material science and fluid mechanics.

An overview of power plant environments and a description of the various degradation mechanisms damaging the power plant systems and components are presented first. This is followed with a description of deterministic structural analysis methods, covering e.g. structural mechanics and fracture mechanics based analysis methods as well as the disadvantages of the deterministic analysis approach. Often, physical probabilistic methods are based on deterministic analysis methods with the modification that one or more of the model parameters are considered as probabilistically distributed. Several probabilistic analysis procedures are presented, e.g. Monte Carlo Simulation (MCS) and importance sampling. Description of probabilistic analysis methods covers both physical and statistical approaches. When the system/component failure probabilities are combined with knowledge of failure consequences, it is possible to assess system/component risks. Several risk analysis methods are presented as well as some limitations and shortcomings concerning to them.

Modelling methods for various degradation (or ageing) mechanisms are presented. These methods are needed in the lifetime analyses of structural systems and components of power plants. In general, the lifetime analyses in question necessitate a thorough knowledge of structural properties, loads, the relevant degradation mechanisms and prevailing environmental conditions. The nature of degradation models of structural systems/components can be deterministic, probabilistic or a combination of these two types. Degradation models of all these kinds are presented here. Some important risk analysis applications are described. These include probabilistic risk/safety assessment (PRA/PSA) and risk informed in-service inspections (RI-ISI).

In practise, lifetime and risk analyses are usually performed with a suitable analysis tool, i.e. with analysis software. A selection of probabilistic system/component degradation and risk analysis software tools is presented in the latter part of this thesis. Computational application of probabilistic failure and lifetime analyses to a representative set of NPP piping components with probabilistic codes VTTBESIT and PIFRAP are presented after that.

The thesis ends with a summary and suggestions for future research.

ISBN
978-951-38-7760-6 (soft back ed.)
978-951-38-7761-3 (URL: http://www.vtt.fi/publications/index.jsp)

Series title and ISSN	Project number
VTT Publications 1235-0621 (soft back ed.) 1455-0849 (URL: http://www.vtt.fi/publications/index.jsp)	

Date	Language	Pages
December 2011	English, Finnish abstr.	264 p.

Keywords	Publisher
Structural mechanics, fracture mechanics, risk analysis, reliability, PFM, RI-ISI	VTT Technical Research Centre of Finland P.O. Box 1000, FI-02044 VTT, Finland Phone internat. +358 20 722 4520 Fax +358 20 722 4374

Julkaisun sarja, numero ja raporttikoodi

VTT Publications 775
VTT-PUBS-775

Tekijä(t)
Otso Cronvall

Rakenteellisen eliniän, varmuuden ja riskien analysoimisen lähestymistapoja voimalaitosten komponenteille ja järjestelmille

Tiivistelmä

Tämän lisensiaattityön aiheina ovat voimalaitosten rakennejärjestelmien ja -komponenttien käyttöiän, luotettavuuden ja riskitarkastelujen analyysimenetelmät ja sovellukset. Näihin analyysimenetelmiin liittyy usea tieteen ala, kuten lujuusoppi, murtumismekaniikka, todennäköisyysmatematiikka, materiaalitiede ja virtausmekaniikka.

Ensin esitetään yleiskatsaus voimalaitosympäristöistä sekä kuvaukset erilaisista voimalaitosten rakennejärjestelmiä ja -komponentteja koskevista vaurioitumismekanismeista. Sitten käsitellään deterministiset rakenneanalyysimenetelmät, kuten lujuusopin ja murtumismekaniikan menetelmät, sekä erittelyä deterministisen lähestymistavan puutteista. Usein fysikaaliset probabilistiset menetelmät perustuvat deterministisiin vastaaviin sillä muunnelmalla, että yksi tai useampi malliparametri on asetettu probabilistisesti jakaantuneeksi. Työssä esitetään useita probabilistisia analyysimenetelmiä, kuten Monte Carlo -simulaatio ja tärkeysperusteinen otanta. Todennäköisyysperusteisia analyysimenetelmiä koskeva kuvaus kattaa sekä fysikaaliset että tilastolliset lähestymistavat. Kun rakennejärjestelmien/-komponenttien todennäköisyydet yhdistetään tietämykseen seurausvaikutuksista, voidaan arvioida vastaavat riskit. Työssä esitetään useita riskianalyysimenetelmiä, sekä eräitä niitä koskevia rajoituksia ja puutteellisuuksia.

Työssä esitetään valikoima erilaisia vaurioitumismekanismeja koskevia mallinnusmenetelmiä. Näitä menetelmiä tarvitaan rakennejärjestelmien ja -komponenttien käyttöikäanalyyseissa. Yleisesti ottaen kyseiset käyttöikäanalyysit edellyttävät perusteellisia tietoja rakenteellisista ominaisuuksista, kuormista, merkittävistä vaurioitumismekanismeista sekä vallitsevista olosuhteista. Rakennejärjestelmien/-komponenttien vaurioitumista kuvaavat mallit voivat olla tyypiltään deterministisiä, probabilistisia tai näiden yhdistelmä. Työssä esitetään kaikkiin näihin tyyppeihin lukeutuvia vaurioitumismalleja. Esitetään muutamia merkittäviä riskianalyysin sovelluksia. Näihin lukeutuu todennäköisyyspohjaiset turvallisuus- ja riskianalyysit (PSA ja PRA) ja riskitietoiset tarkastusohjelmat (RI-ISI).

Käytännössä käyttöikä- ja riskianalyysit tehdään yleensä jollakin sopivalla analyysityökalulla, eli sovellusohjelmalla. Työn jälkipuoliskolla esitetään valikoima rakennejärjestelmien/-komponenttien vaurioitumisen ja riskien analyysisovelluksia. Sen jälkeen edustavalle valikoimalle ydinvoimalan putkistokomponentteja esitetään analyysiohjelmilla VTTBESIT ja PIFRAP tehdyt todennäköisyysperusteiset vikaantumis- ja käyttöikäanalyysit.

Työn lopuksi esitetään yhteenveto sekä jatkotutkimusaiheita koskevia ehdotuksia.

ISBN
978-951-38-7760-6 (nid.)
978-951-38-7761-3 (URL: http://www.vtt.fi/publications/index.jsp)

Avainnimeke ja ISSN	Projektinumero
VTT Publications 1235-0621 (nid.) 1455-0849 (URL: http://www.vtt.fi/publications/index.jsp)	

Julkaisuaika	Kieli	Sivuja
Joulukuu 2011	Suomi, engl. tiiv.	264 s.

Avainsanat	Julkaisija
Structural mechanics, fracture mechanics, risk analysis, reliability, PFM, RI-ISI	VTT PL 1000, 02044 VTT Puh. 020 722 4520 Faksi 020 722 4374

Lifetime, reliability and risk analysis methods and applications for structural systems and components of power plants are considered in this thesis. There are various degradation mechanisms to which power plant systems and components are susceptible to. Probabilistic structural analysis procedures can be used to assess their effects. For power plant components, probabilistic fracture mechanics is an often used approach. When the system/component failure probabilities are combined with knowledge of failure consequences, it is possible to assess system/component risks. Examples of important risk analysis applications for power plants include probabilistic risk/safety assessment (PRA/PSA) and risk informed in-service inspections (RI-ISI). In general, the lifetime analyses of power plant systems/components necessitate a thorough knowledge of structural properties, loads, the relevant degradation mechanisms and prevailing environmental conditions.

Several objectives were set for this thesis. One objective is to collect both the methods and background theories for evaluation of operational lifetime, reliability and risk of structural systems and components of power plants. This was pursued by making an extensive literature survey. Another objective is to collect information concerning the relevant existing probabilistic degradation and risk analysis tools, with which one can assess the remaining lifetime and structural integrity of systems/components of power plants. The scope and characteristics of such tools are described. The last objective is to provide an application example. This was carried out by making a failure probability analysis to a representative set of nuclear power plant piping components.

ISBN 978-951-38-7760-6 (soft back ed.)
ISSN 1235-0621 (soft back ed.)

ISBN 978-951-38-7761-3 (URL: http://www.vtt.fi/publications/index.jsp)
ISSN 1455-0849 (URL: http://www.vtt.fi/publications/index.jsp)